

3D Dynamic Rupture Modeling and an Introduction to SeisSol

An abstract visualization of seismic wave propagation and fault rupture. It features several intersecting, semi-transparent planes in teal and orange-yellow. Overlaid on these planes are concentric, glowing orange-yellow rings that represent seismic wave fronts. The background is a dark, textured grey.

Alice-Agnes Gabriel & Duo Li
LMU Munich

3D Dynamic Rupture Modeling and an Introduction to SeisSol

- ◎ **3D dynamic rupture modeling in the ‘ideal’ and ‘real’ world**
- ◎ **How to constrain initial conditions for large-scale earthquake scenarios - the 2016, Mw7.8 Kaikōura, NZ, rupture cascade**
- ◎ **Under the hood: SeisSol - a discontinuous Galerkin (DG) software for modern supercomputers**
- ◎ **Two training examples: A 3D SCEC community benchmark and the 2018, Palu, Sulawesi supershear earthquake generating a “surprise” tsunami**

HIGH-PERFORMANCE-COMPUTING FOR **COMPUTATIONAL (PHYSICS-BASED) EARTHQUAKE SEISMOLOGY**



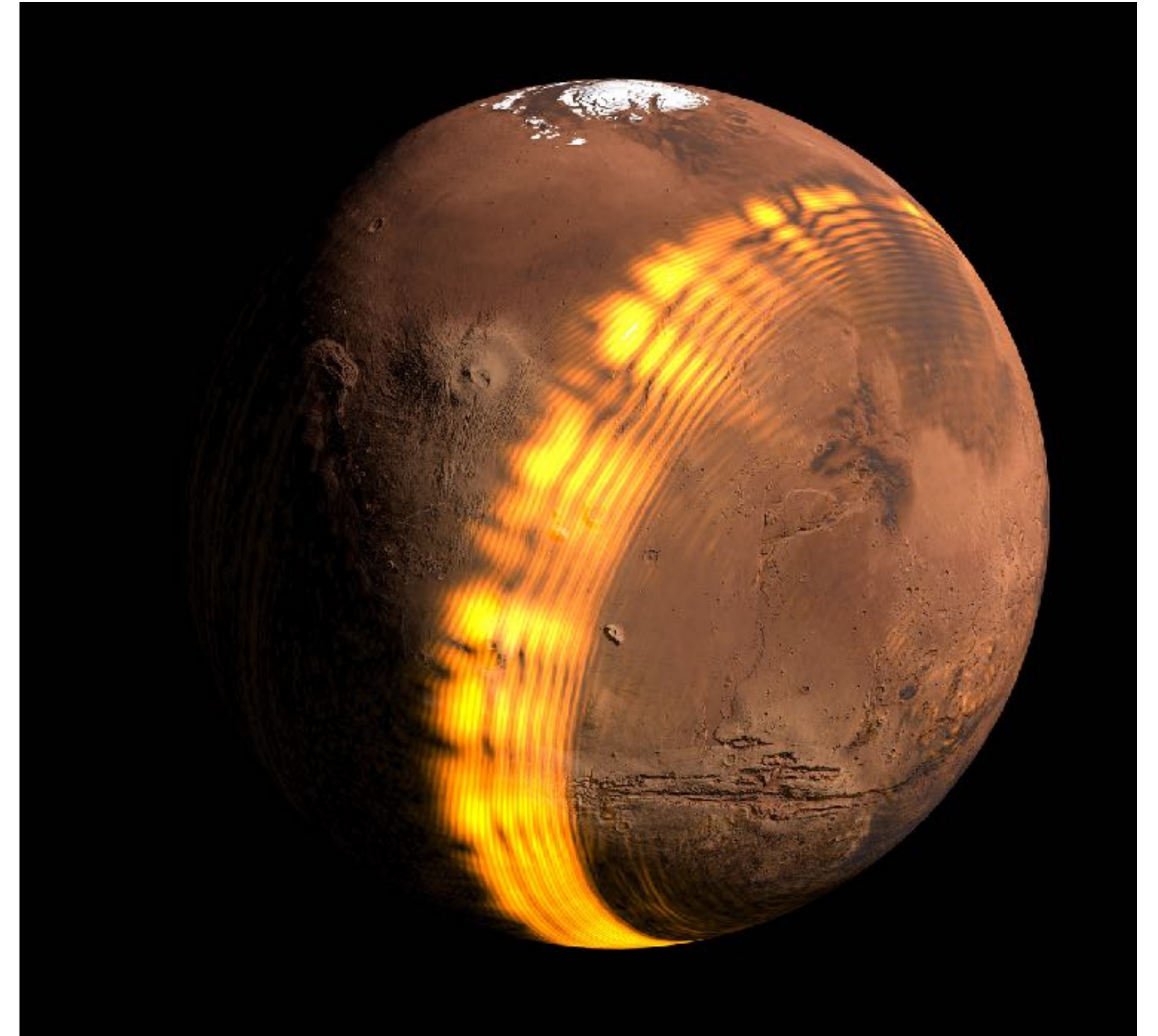
Wave simulations of the 2009 L'Aquila earthquake
using SeisSol, Igel 2017, Wenk et al., 2009



Schematic view of on-going seismic rupture of the Parkfield
segment of Sand Andreas Fault, Caltech/Tim Pyle

COMPUTATIONAL SEISMOLOGY

- Computational seismology has been a pioneering field and has been pioneered by **HPC**
- Seismology is **data-rich** and can often be treated as **linear system**
- **Key activities:** Calculation of synthetic seismograms in 3D Earth and solving seismic inverse problems
- **Key achievements:** Imaging Earth's interior, understanding the dynamics of the mantle, tracking down energy resources
- **Common approach:** time-domain solutions of space-dependent seismic wavefield solved by domain decomposition
- **On-going challenges:** 3D (elastic, anisotropic, poroelastic, ...) Earth structure, computational efficiency (resolving high frequencies), meshing (irregular geometries), and the need for community solutions (cf. SpecFEM)



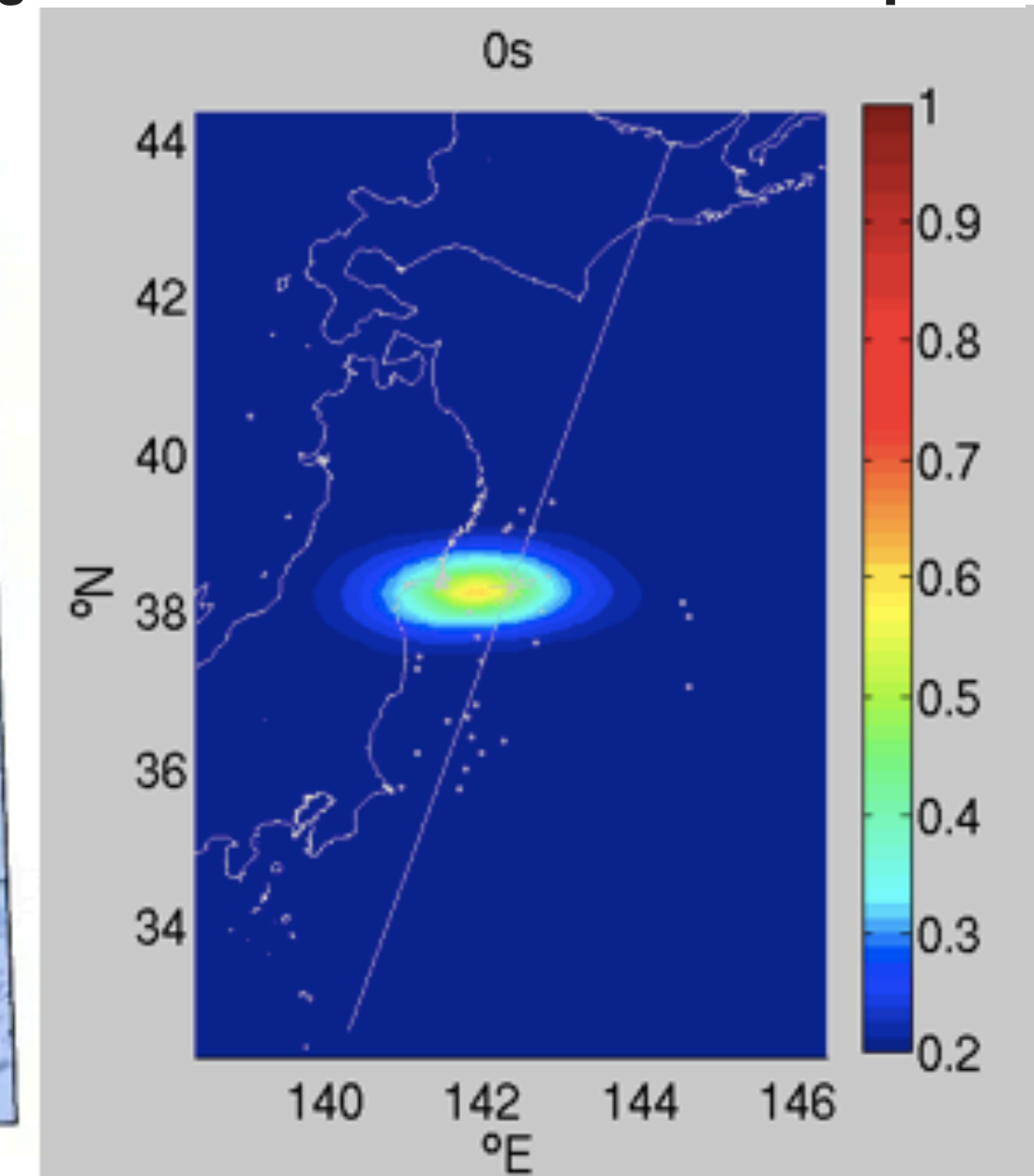
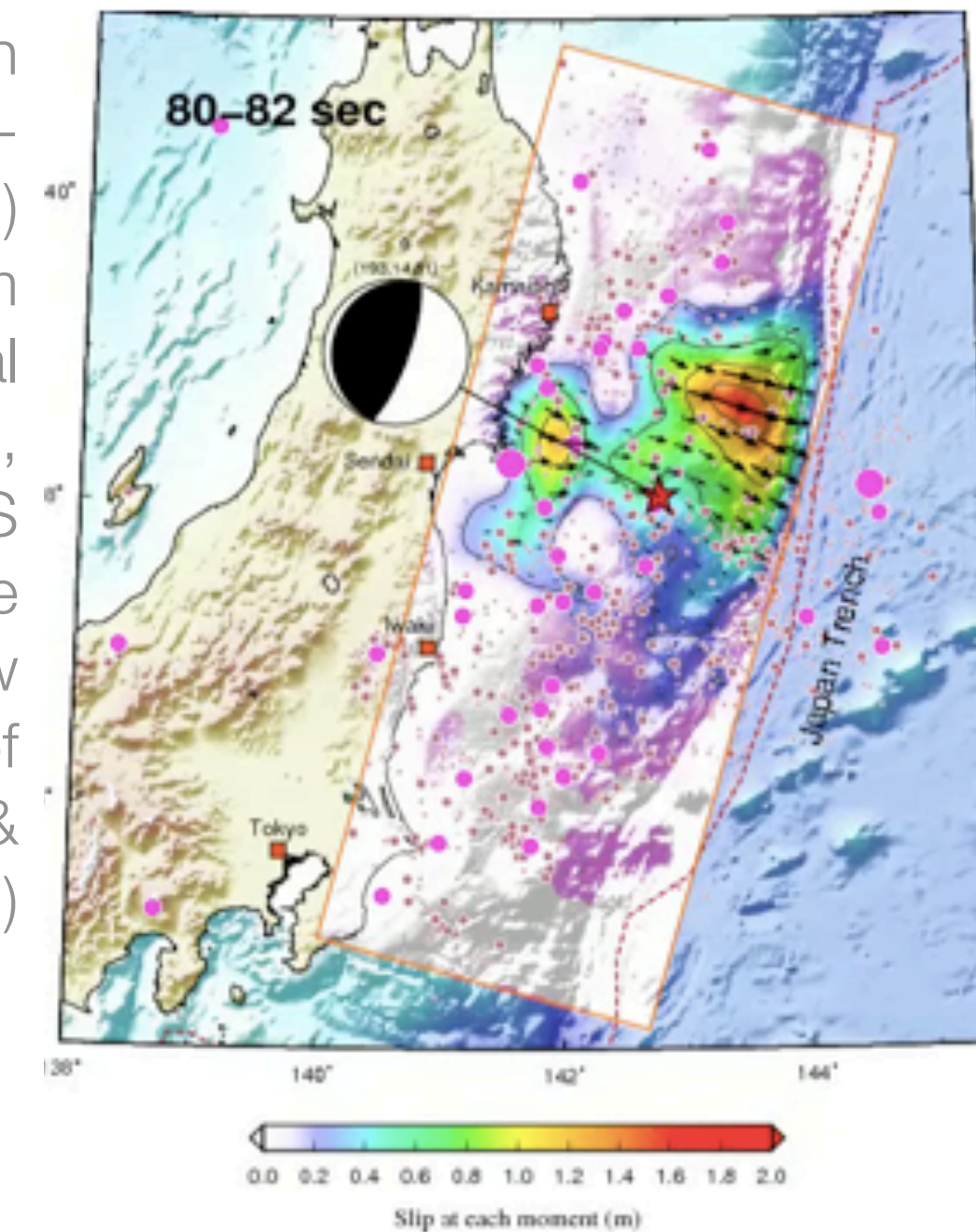
On May 5th, the NASA “InSight”-lander set off to investigate the internal structure of Mars carrying a seismometer. Forward simulations of seismic waves travelling through Mars have been performed on “Piz Daint” in real time solving 10 billion degrees of freedom and 300,000 time steps (Bozdag et al., 2017)

Earthquake source dynamics

- Recent well-recorded earthquakes and laboratory experiments reveal **striking variability** in terms of source dynamics

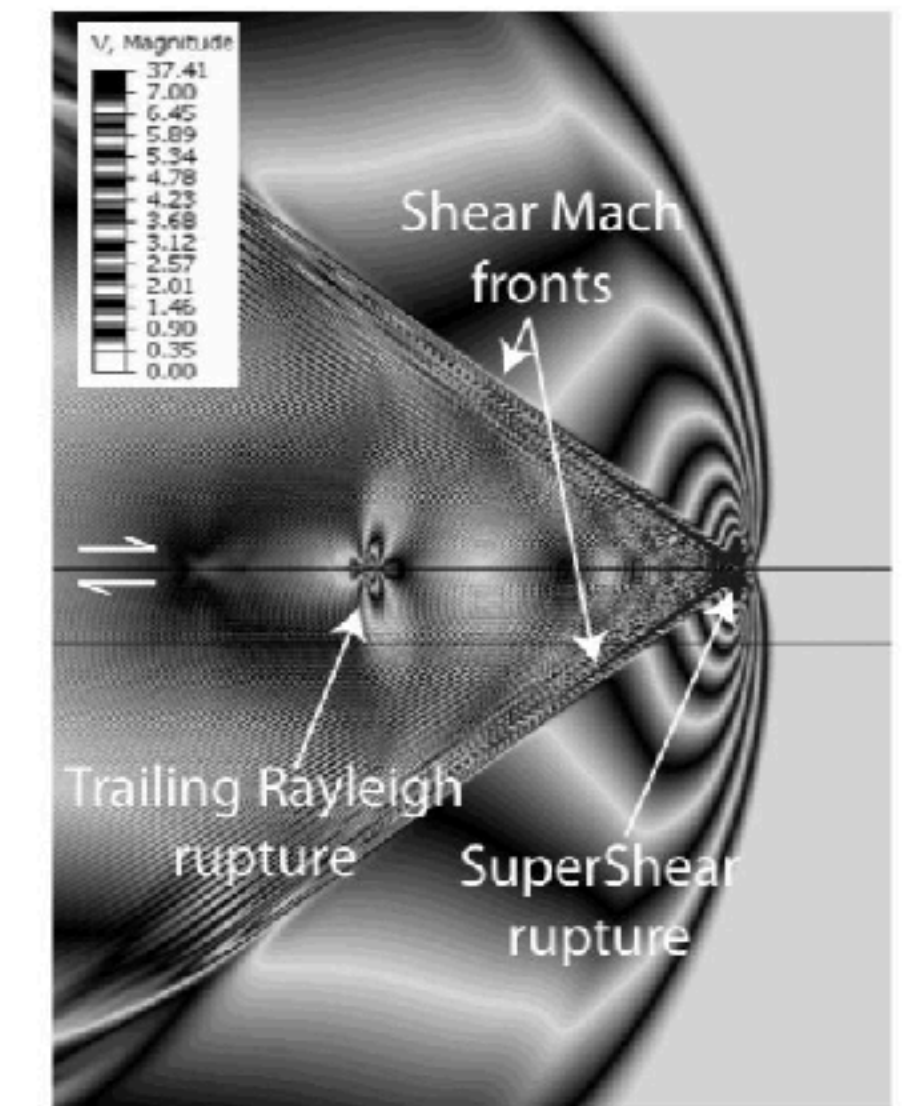
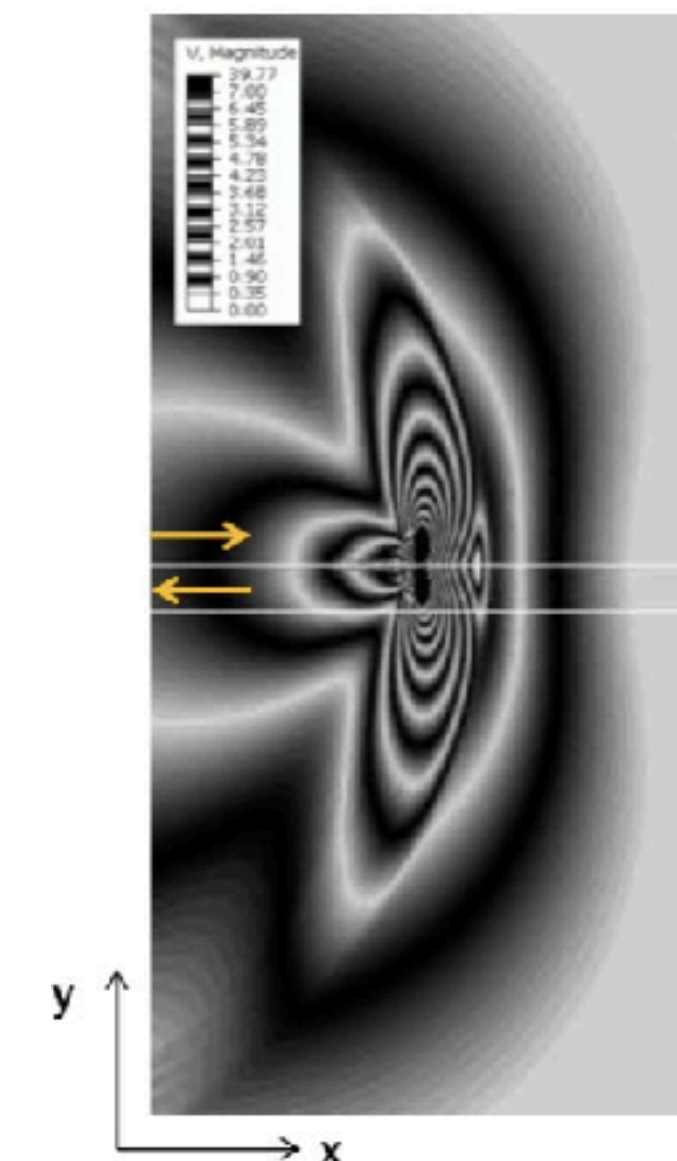
- Slip-reactivation
- Nucleation with/without slow-slip pre-cursors
- Variability of rupture style (pulses vs cracks)
- Rupture cascading and “jumping”
- Propagation along both locked and creeping fault sections during the same earthquake
- Super-shear propagation

Source inversion model of Tohoku-Oki event (Japan) 2011, from combined local ground motion, teleseismics, GPS & multiple time window parametrization of slip rate. (Lee & Wang, 2011)



Back projection: Indicating major areas of high-frequency radiation on the fault (Meng et al., 2012)

Sub-Rayleigh vs **supershear** rupture in the laboratory. Mach cone emanating from rupture tip (courtesy of L. Bruhat)

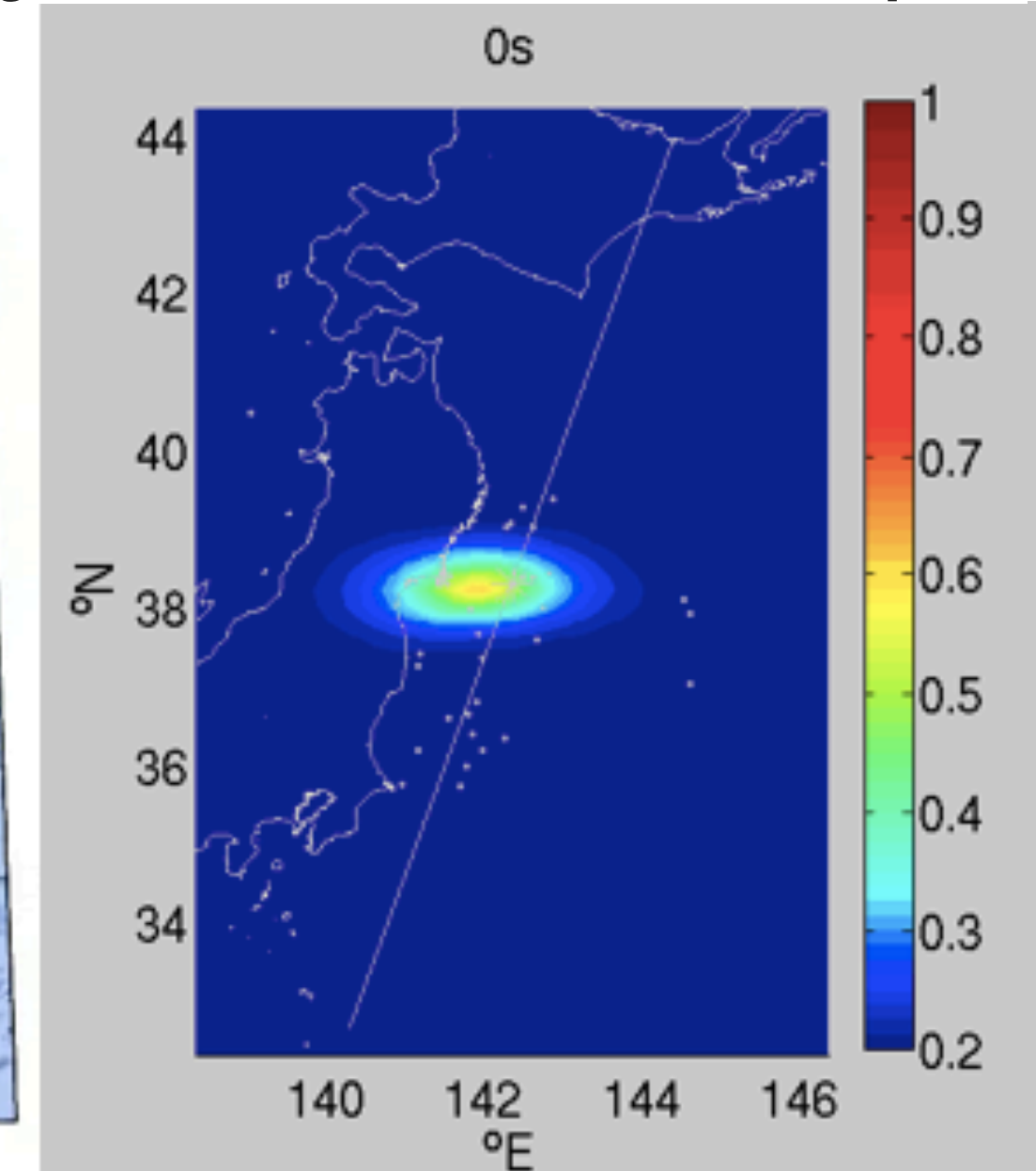
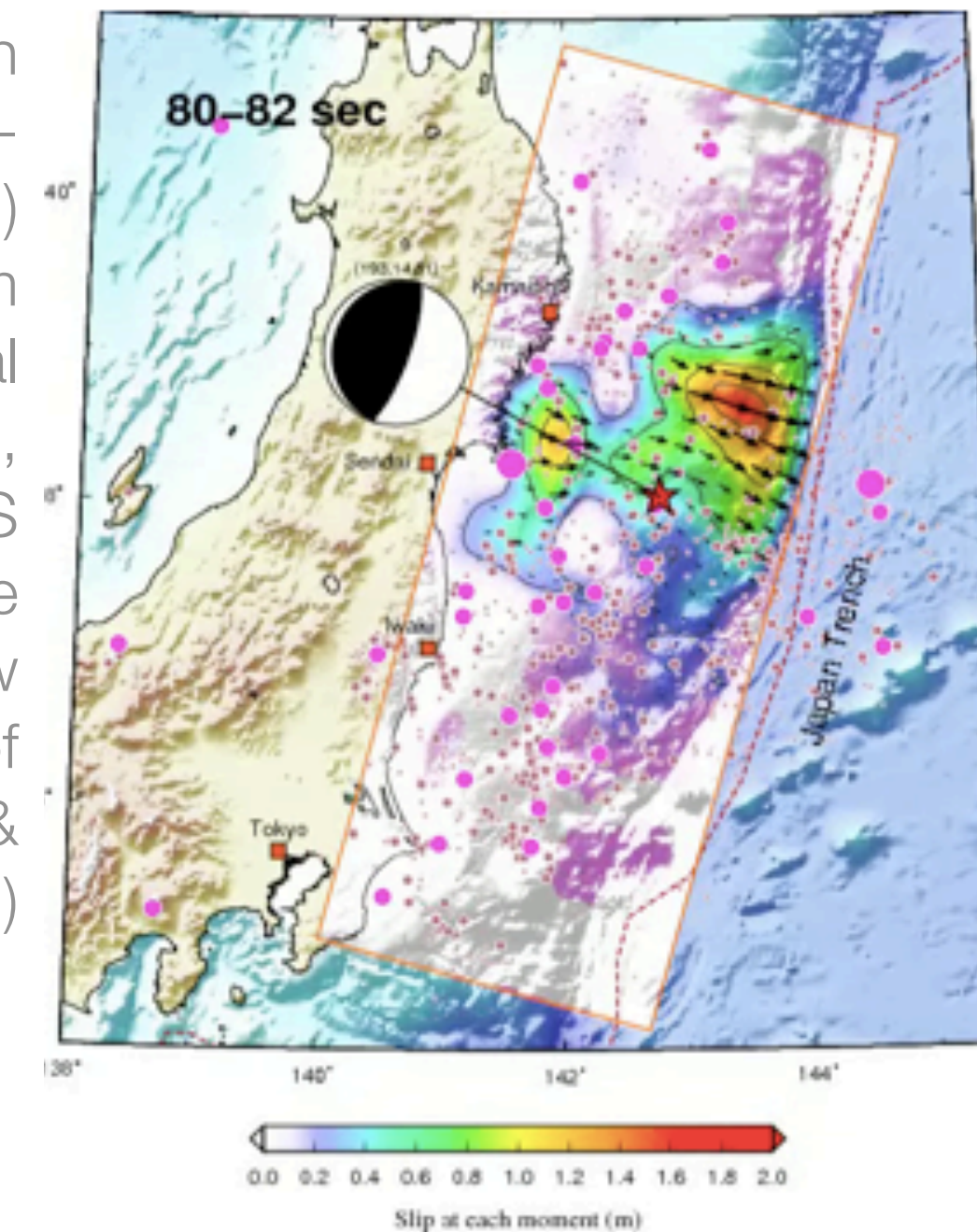


Earthquake source dynamics

- Recent well-recorded earthquakes and laboratory experiments reveal **striking variability** in terms of source dynamics

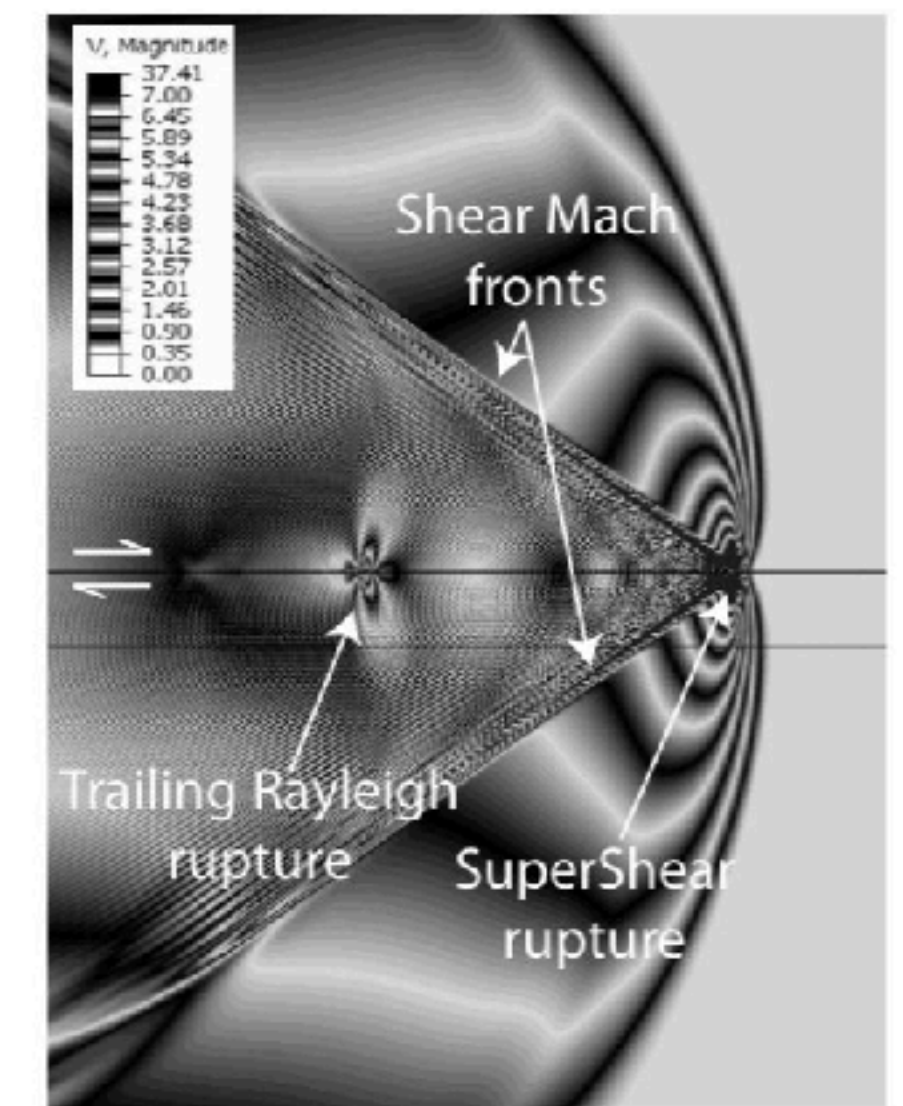
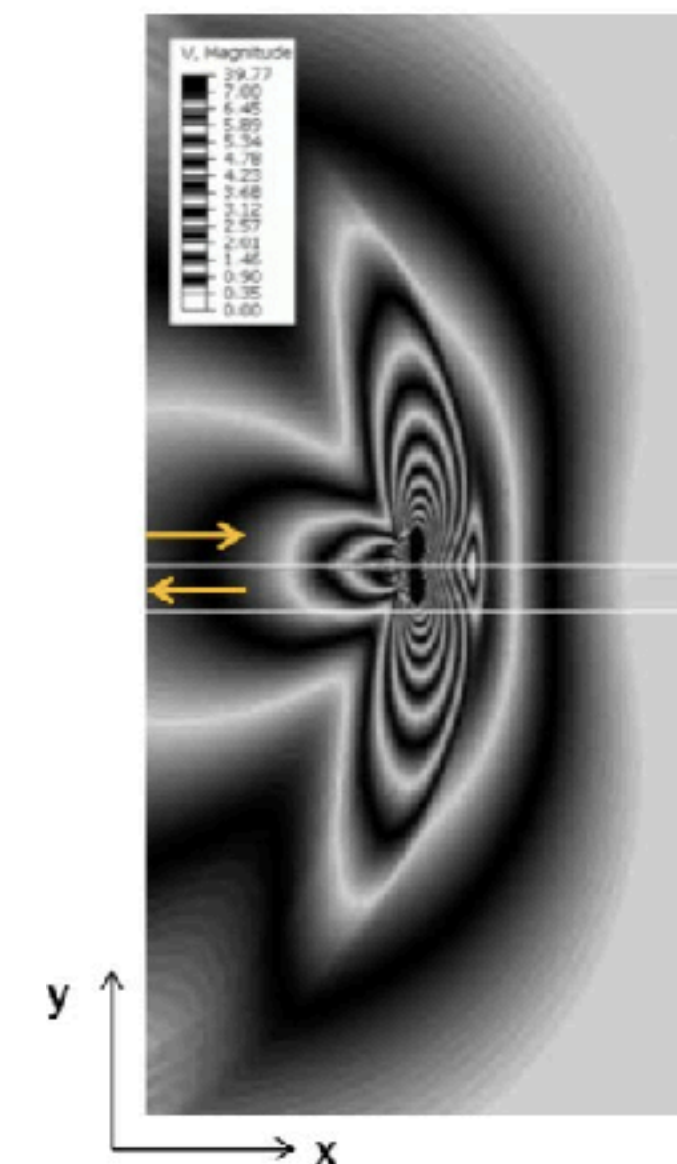
- Challenge 1: Earthquake source processes are (very) **ill-constrained** and **highly non-linear**.
- Challenge 2: Which **physical processes** are **dominant and relevant** at a given spatio-temporal scale (and in real earthquakes)? Can we justify the “cost” of their inclusion?
- Challenge 3: How to **assimilate all available knowledge** in a suitable manner for **software** (numerical discretisation, solvers, equations solved) and **hardware** (heterogeneous HPC systems, energy concerns)?

Source inversion model of Tohoku-Oki event (Japan) 2011, from combined local ground motion, teleseismics, GPS & multiple time window parametrization of slip rate. (Lee & Wang, 2011)



Back projection: Indicating major areas of high-frequency radiation on the fault (Meng et al., 2012)

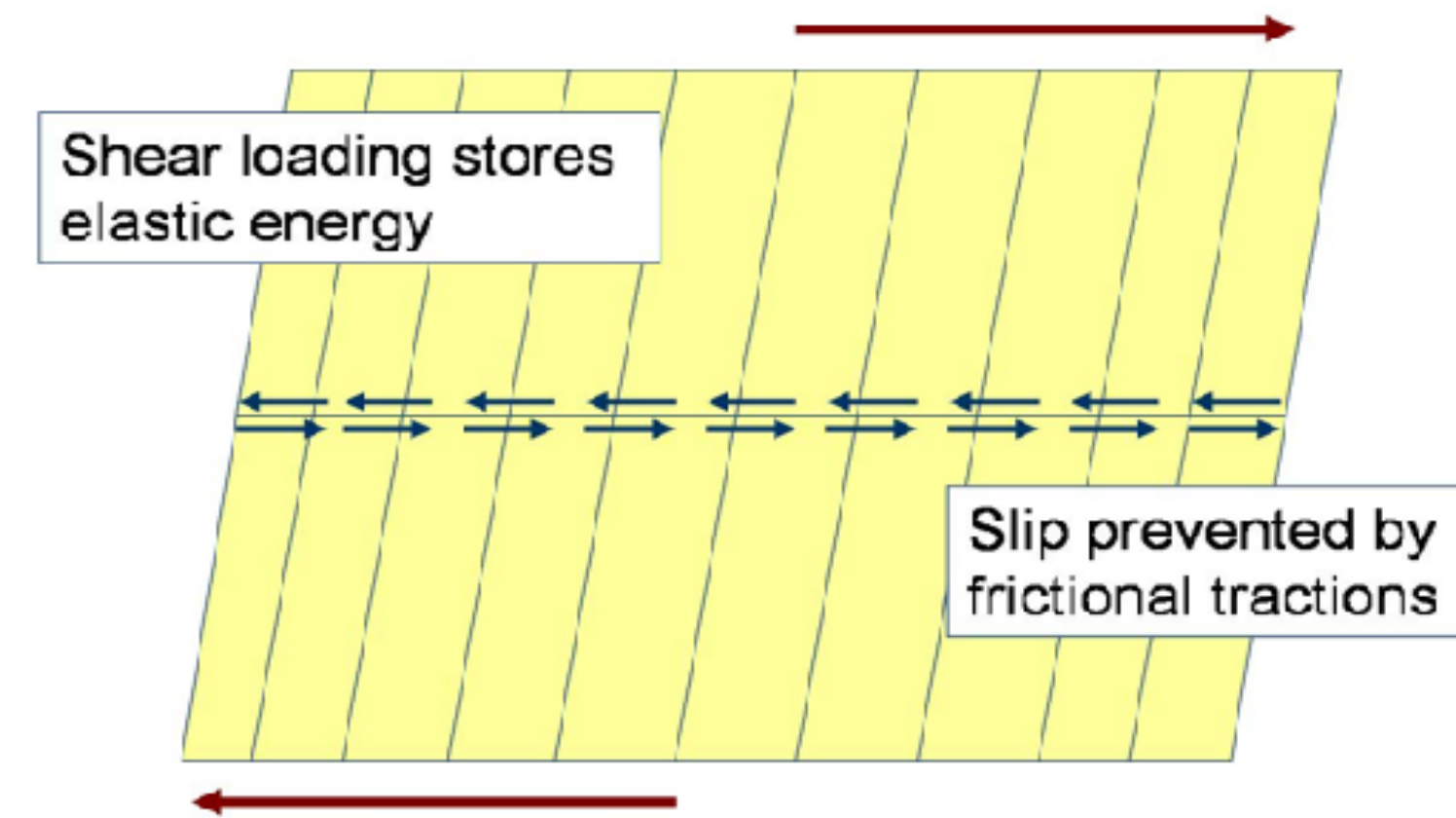
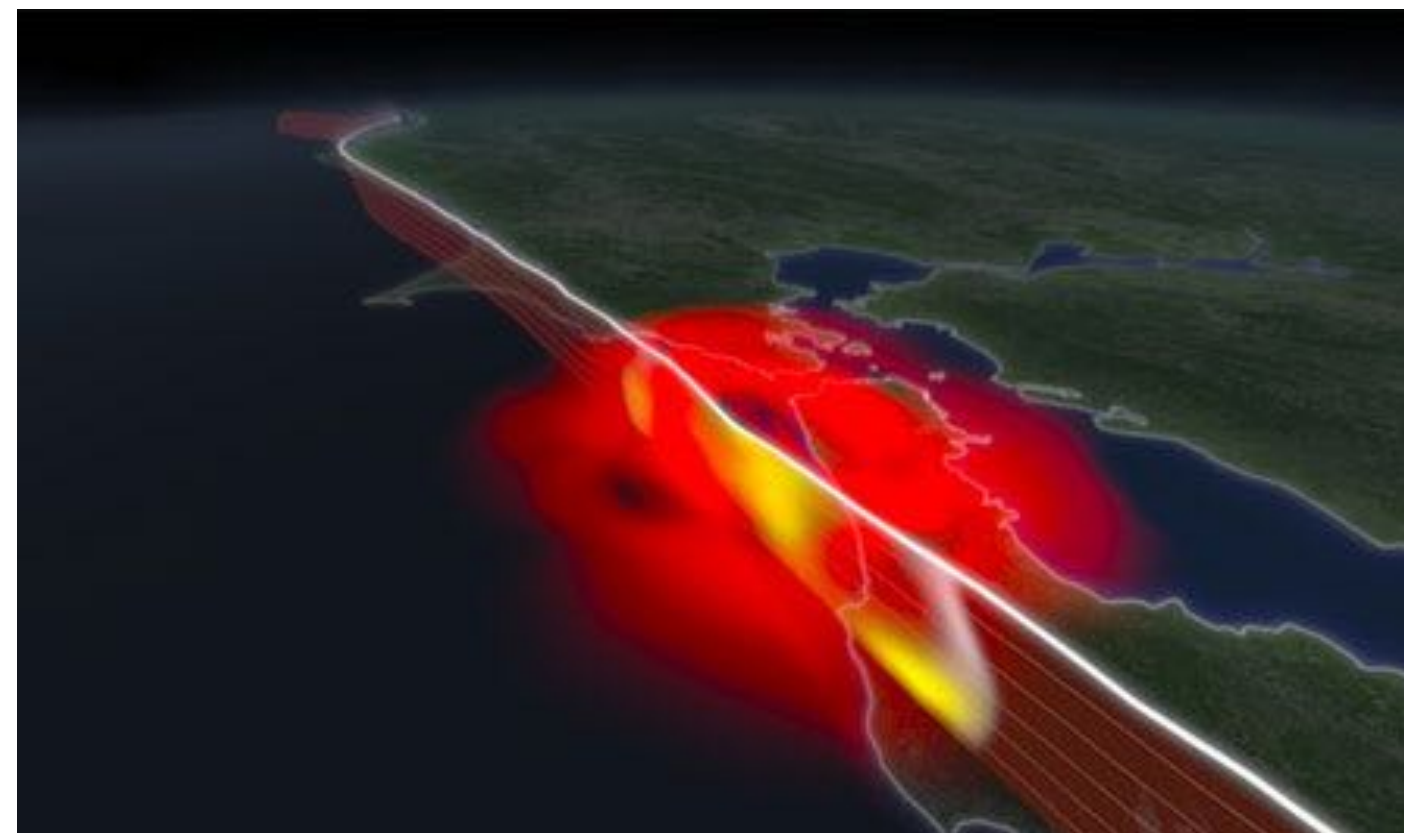
Sub-Rayleigh vs **supershear** rupture in the laboratory. Mach cone emanating from rupture tip (courtesy of L. Bruhat)



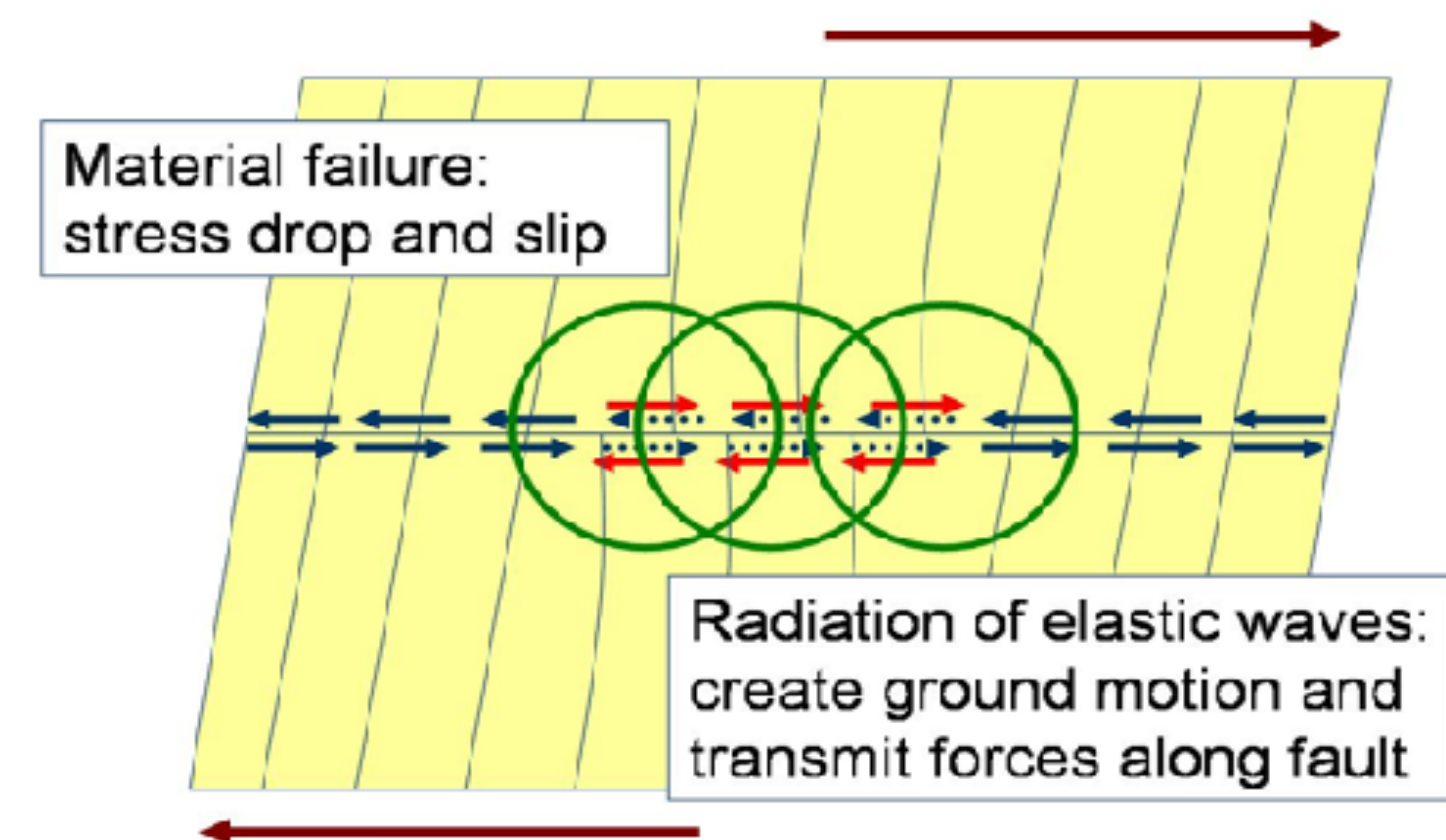
MODELLING

EARTHQUAKE SOURCE DYNAMICS

- **“Bootstrapping” on methods from computational seismology even if originally not developed for earthquake source modelling**
- **Definition: Earthquake = Frictional shear failure of brittle solids under compression along preexisting weak interfaces**



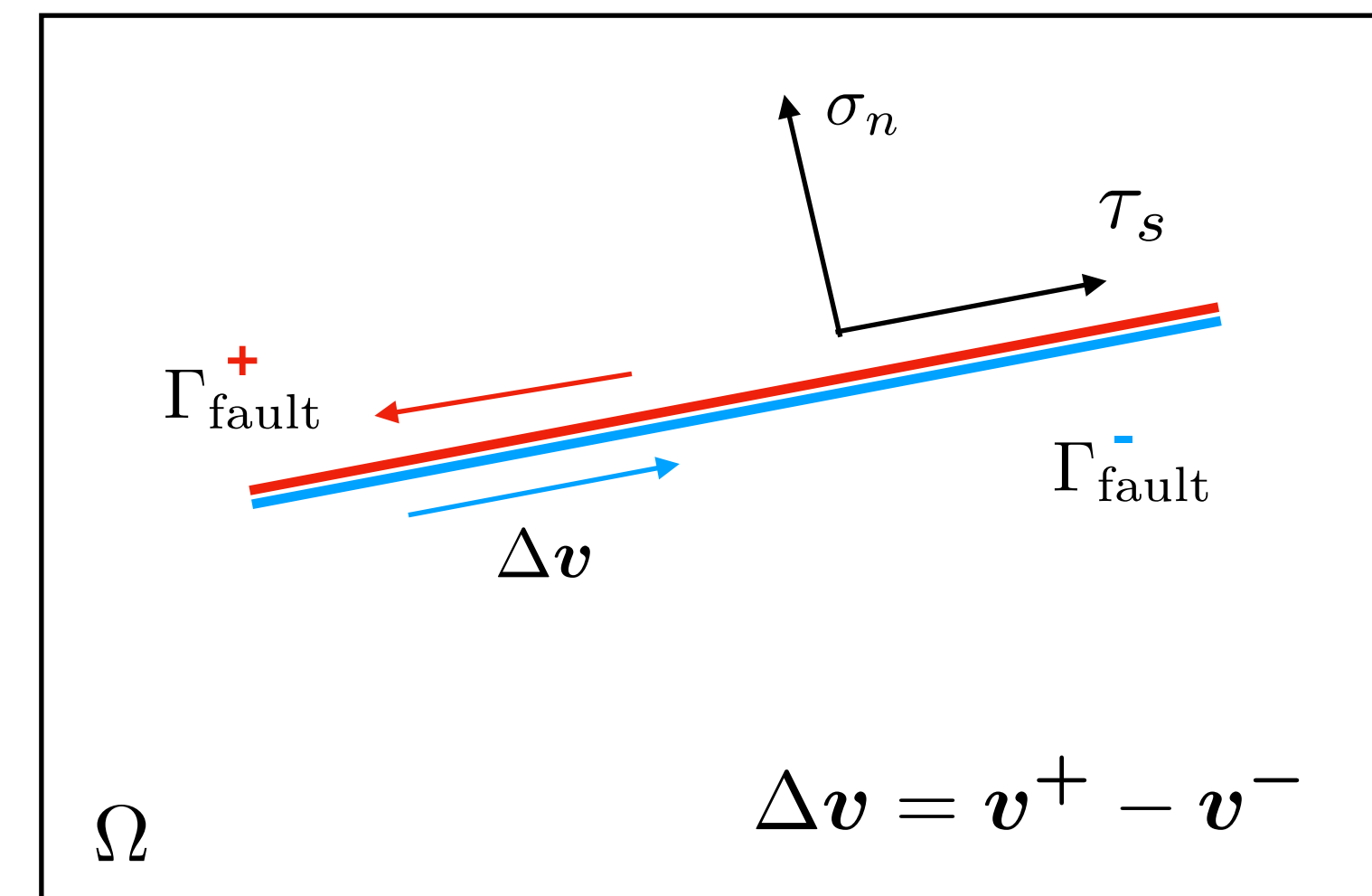
The fault is the horizontal line through the center, with the blue arrows representing frictional forces that keep the sides of the fault locked. The slanted vertical lines indicate the shear displacements created by tectonic loading.



Material in the fault zone fails (or static friction is exceeded) and the fault begins to slip. Physically, we can view this process as the application of shear forces on the fault that negate the static friction, as represented by the red arrows. This releases elastic waves, indicated by the expanding green circles.

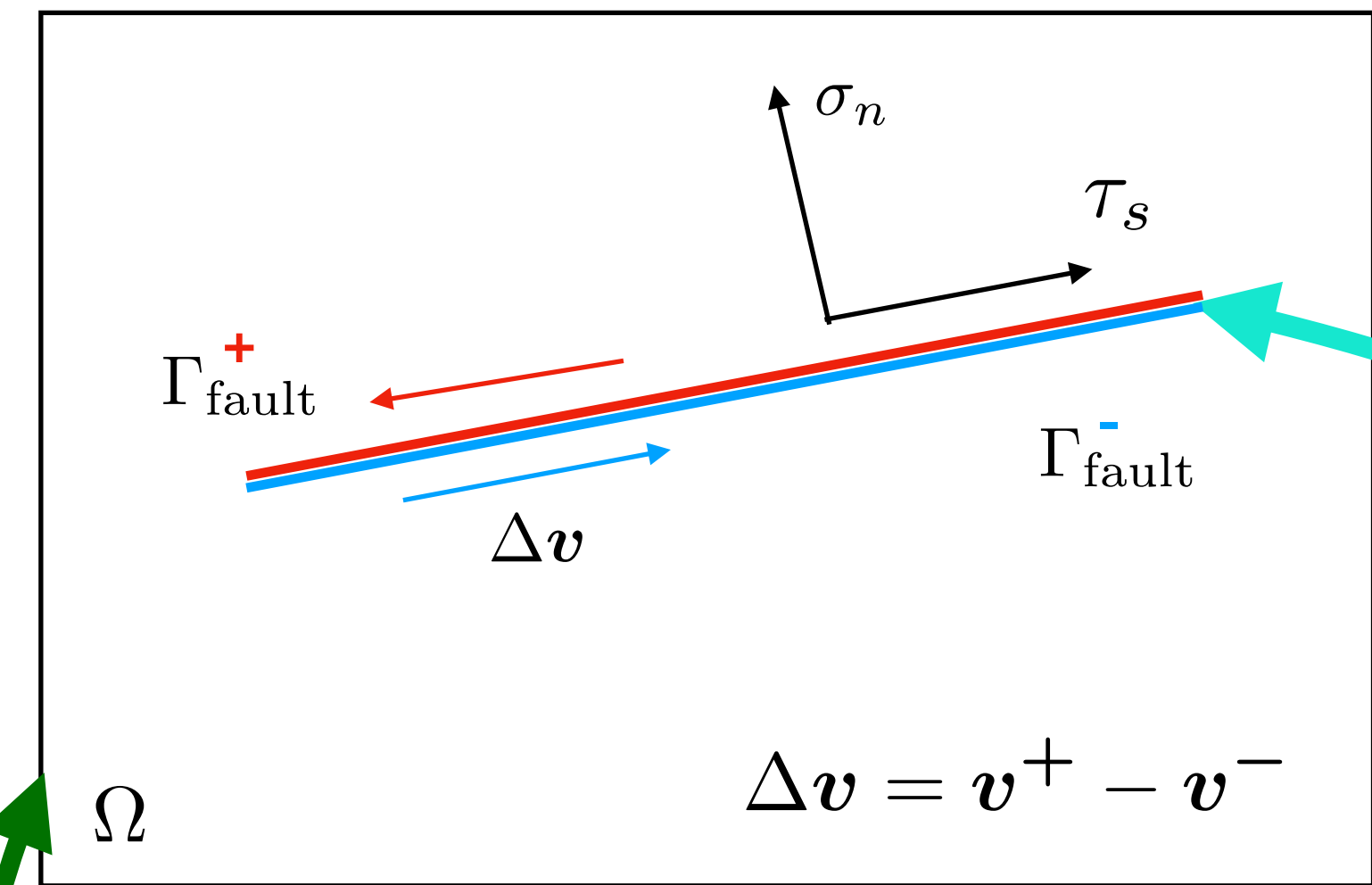
ELASTODYNAMICS WITH EMBEDDED FRICTIONAL INTERFACES

- Earthquake dynamic rupture is typically treated as a boundary condition in terms of **contact and friction**
- **Thin fault without ‘opening’** - two matching fault surfaces are in unilateral contact
- **Displacement discontinuity** across the fault = **slip**
- Much complexity lives in the definition of **friction** (shear traction is bounded by the fault strength), and **fault geometry** and **intersections**
- Typically implemented by **splitting the fault interface**



ELASTODYNAMICS WITH EMBEDDED FRICTIONAL INTERFACES

- Earthquake dynamic rupture is typically treated as a boundary condition in terms of **contact and friction**
- **Thin fault without ‘opening’** - two matching fault surfaces are in unilateral contact
- **Displacement discontinuity** across the fault = **slip**
- Much complexity lives in the definition of **friction** (shear traction is bounded by the fault strength), and **fault geometry** and **intersections**
- Typically implemented by **splitting the fault interface**



constitutive law
(volume)

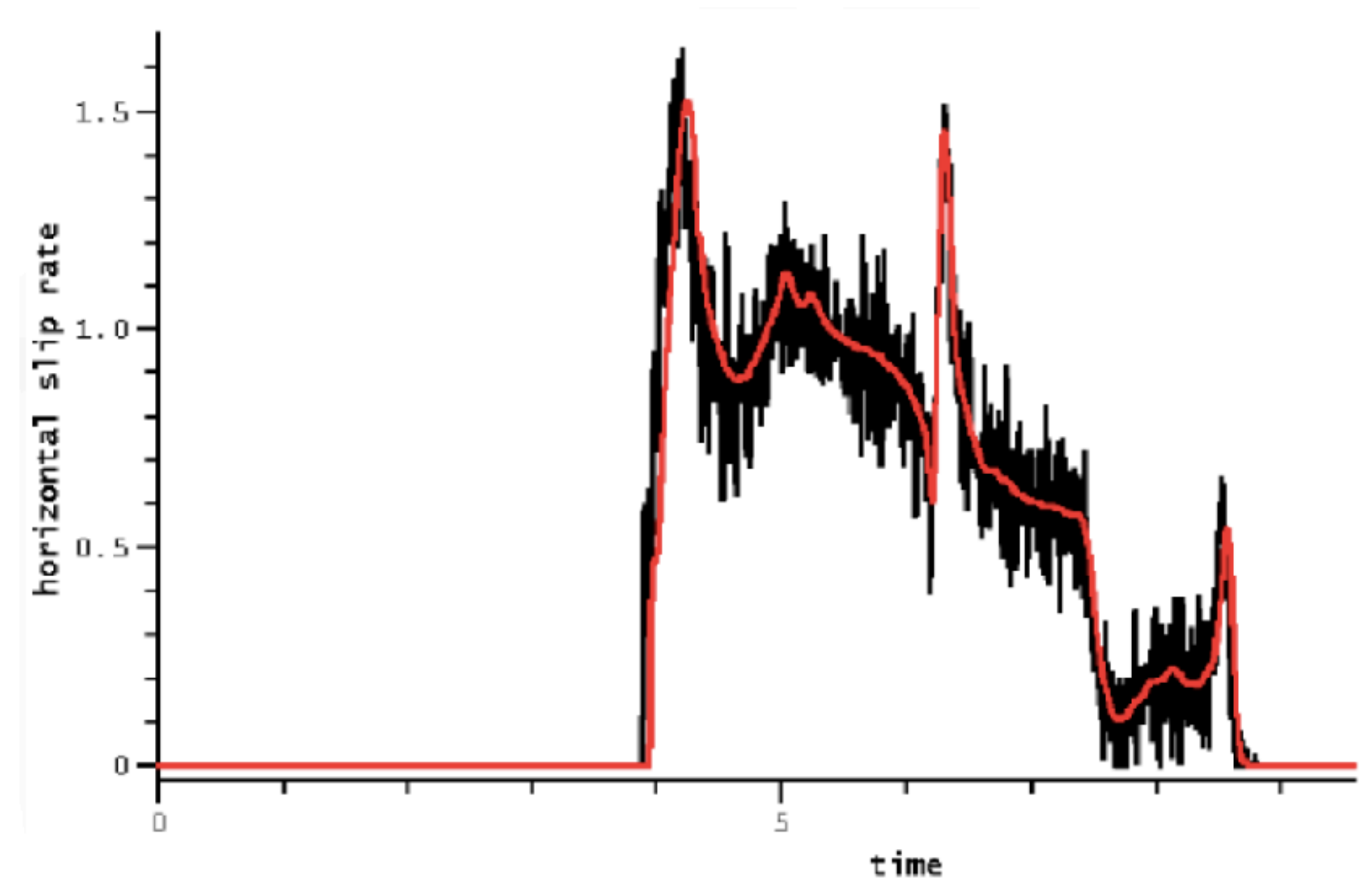
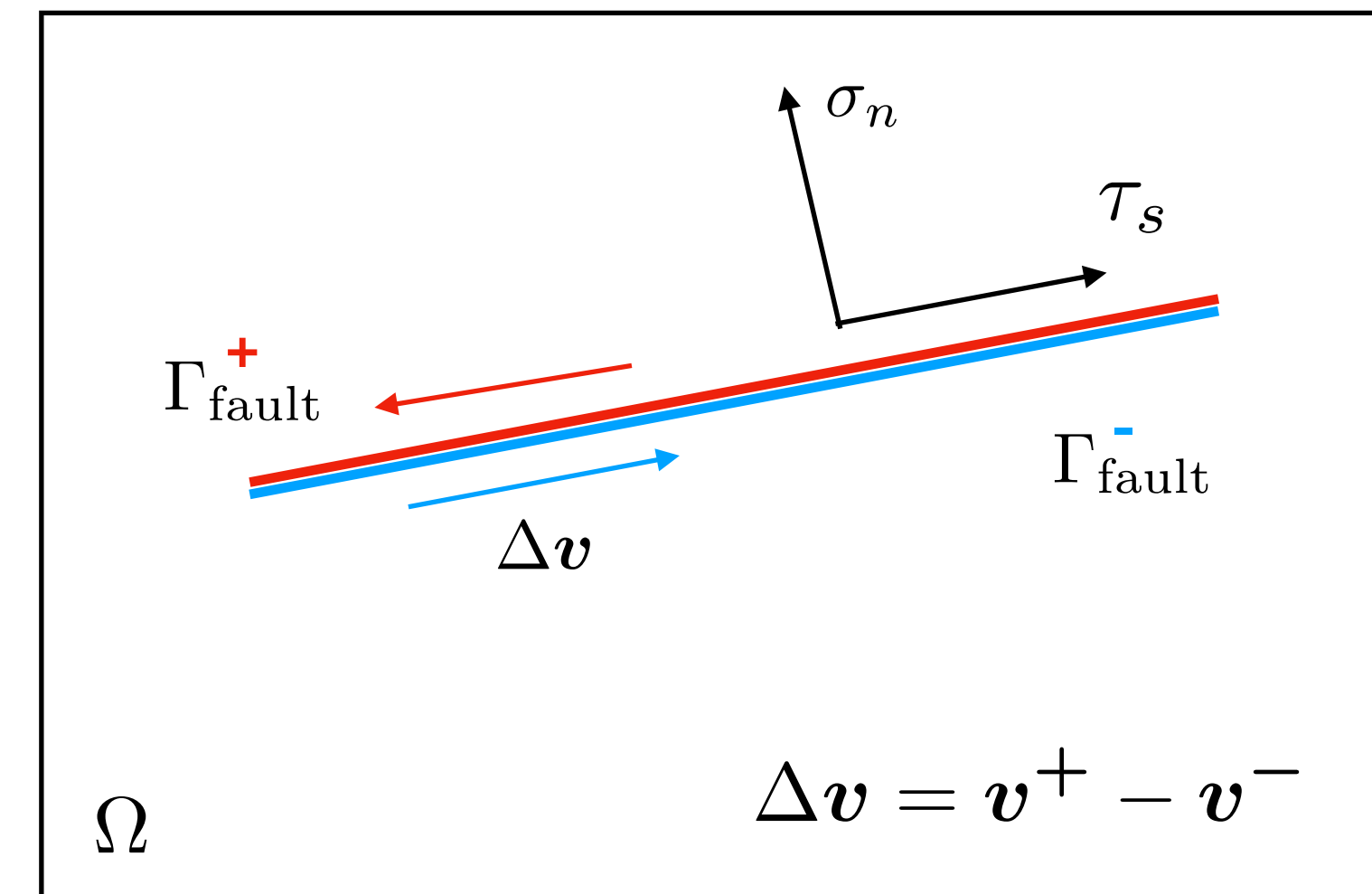
$$\begin{aligned} \frac{\partial}{\partial t} \sigma_{xx} - (\lambda + 2\mu) \frac{\partial}{\partial x} u - \lambda \frac{\partial}{\partial y} v - \lambda \frac{\partial}{\partial z} w &= 0, \\ \frac{\partial}{\partial t} \sigma_{yy} - \lambda \frac{\partial}{\partial x} u - (\lambda + 2\mu) \frac{\partial}{\partial y} v - \lambda \frac{\partial}{\partial z} w &= 0, \\ \frac{\partial}{\partial t} \sigma_{zz} - \lambda \frac{\partial}{\partial x} u - \lambda \frac{\partial}{\partial y} v - (\lambda + 2\mu) \frac{\partial}{\partial z} w &= 0, \end{aligned}$$

constitutive law
(surfaces)

$$\begin{aligned} \tau_s &= \mu_f \sigma_n, \\ |\boldsymbol{\tau}| &\leq \tau_s, \\ (|\boldsymbol{\tau}| - \tau_s) |\Delta \mathbf{v}| &= 0, \\ \Delta \mathbf{v} |\boldsymbol{\tau}| + |\Delta \mathbf{v}| \boldsymbol{\tau} &= 0. \end{aligned}$$

ELASTODYNAMICS WITH EMBEDDED FRICTIONAL INTERFACES

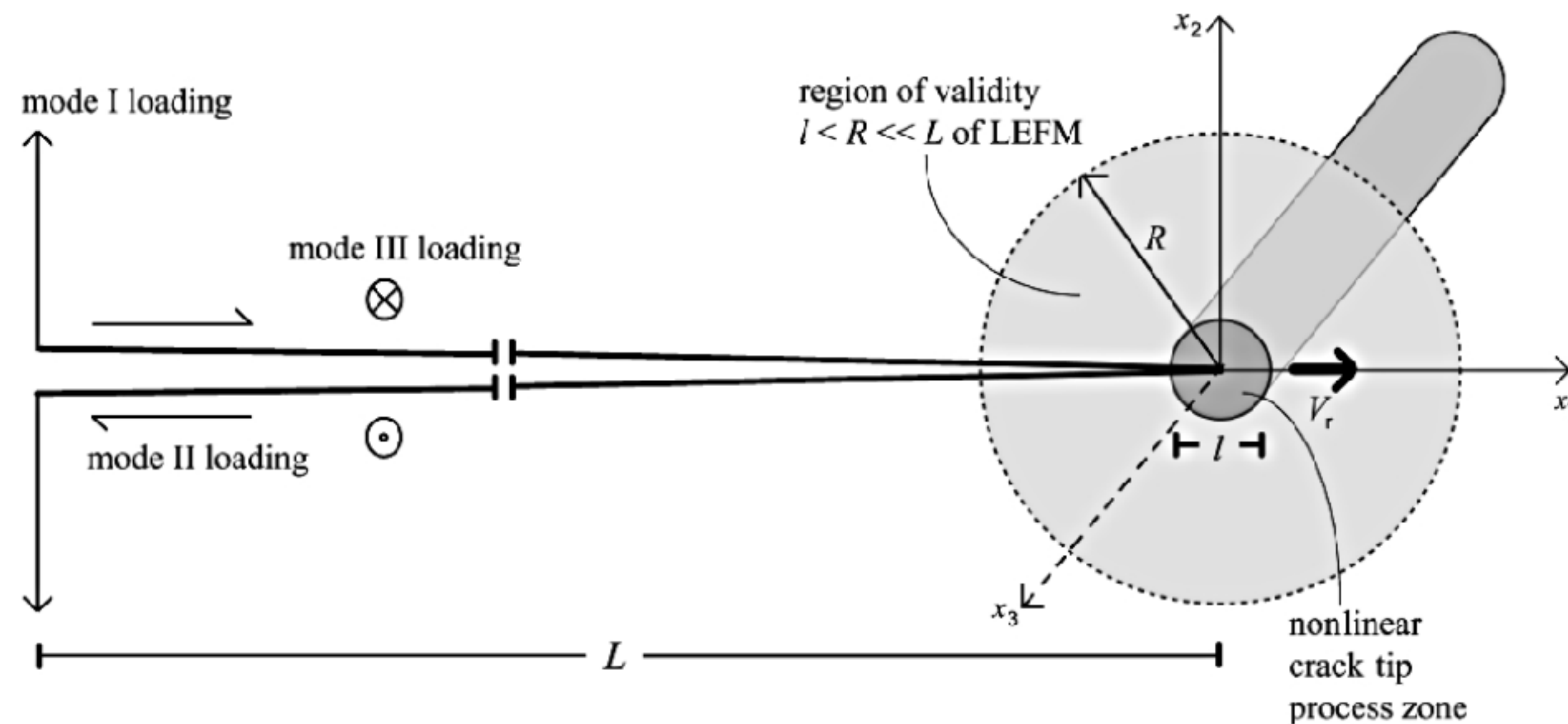
- Earthquake dynamic rupture is typically treated as a boundary condition in terms of **contact and friction**
- **Thin fault without ‘opening’** - two matching fault surfaces are in unilateral contact
- **Displacement discontinuity** across the fault = **slip**
- Much complexity lives in the definition of **friction** (shear traction is bounded by the fault strength), and **fault geometry** and **intersections**
- Typically implemented by **splitting the fault interface**
- **FD, FEM, SEM methods suffer from spurious oscillations - which have to be damped (e.g., by a thin layer of Kelvin-Voigt-Damping cells, Day et al., 2005)**
- **Inherent length scale: cohesive zone**



Dynamic rupture

earthquake simulation

- **Physics-based approach:** Solving for spontaneous dynamic earthquake rupture as non-linear interaction of frictional failure and seismic wave propagation

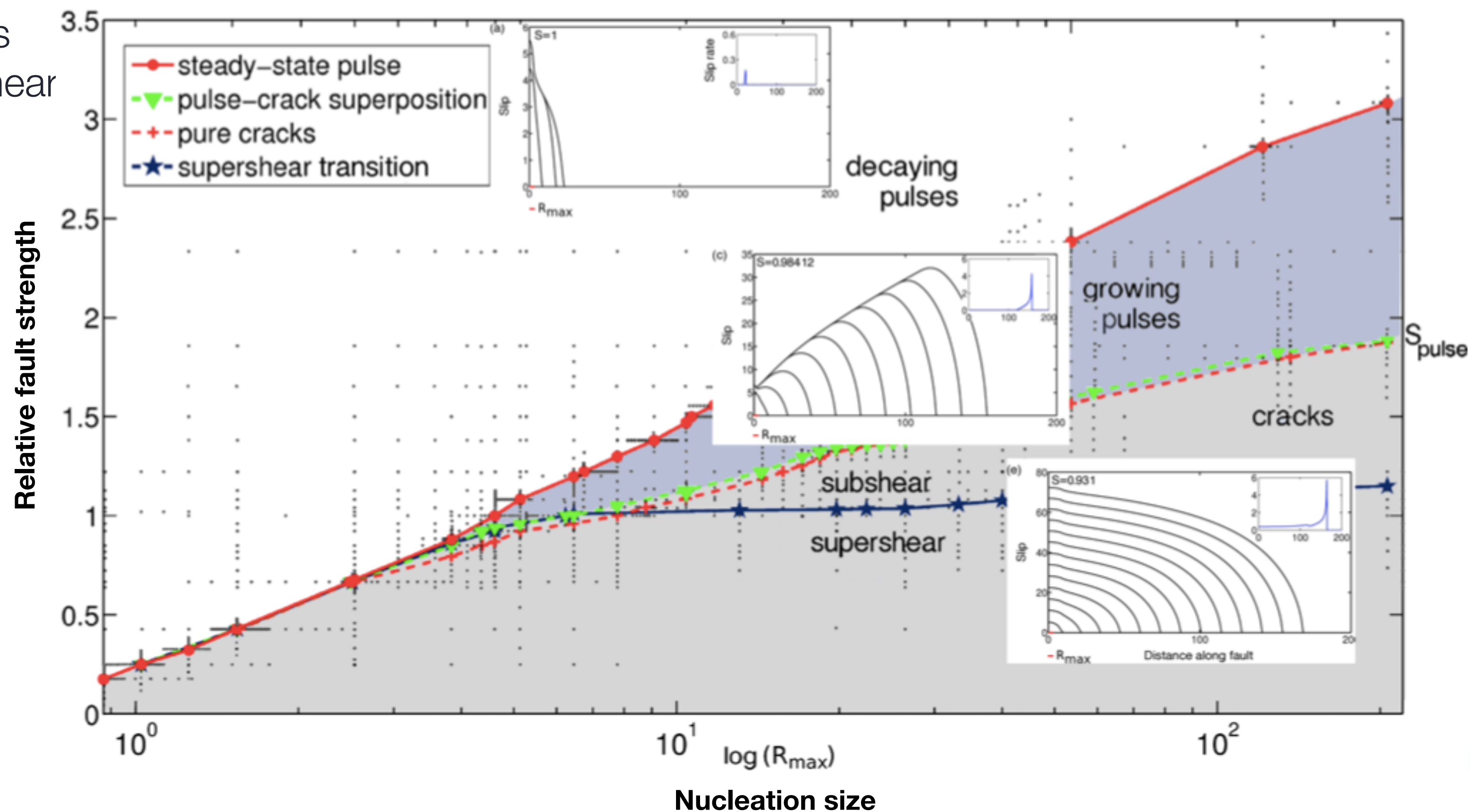


A schematic of a 2D crack illustrating the region of validity for linear elastic fracture mechanics and modes I, II and III of rupture extending along the x_1 axis with velocity v_r (Ben-Zion, 2003).

Dynamic rupture earthquake simulation

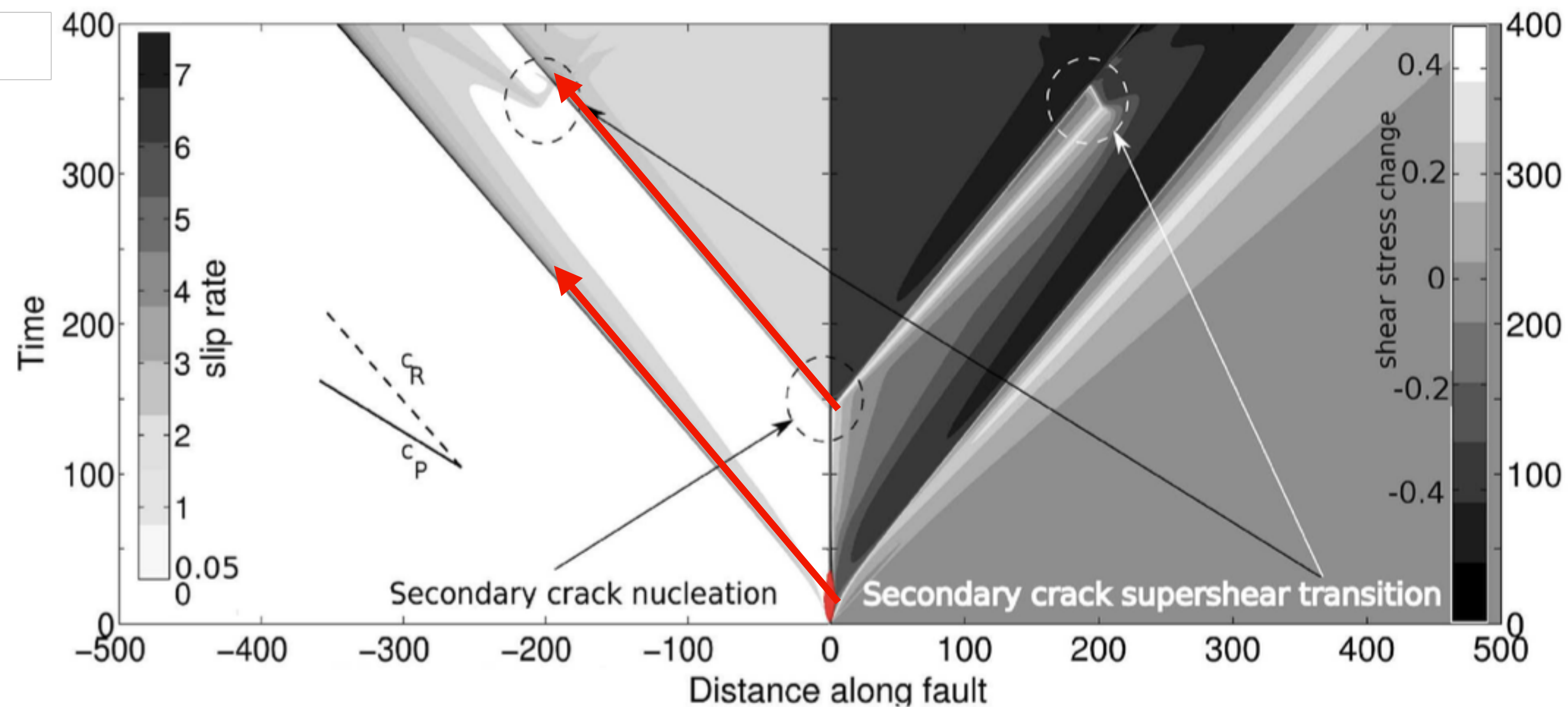
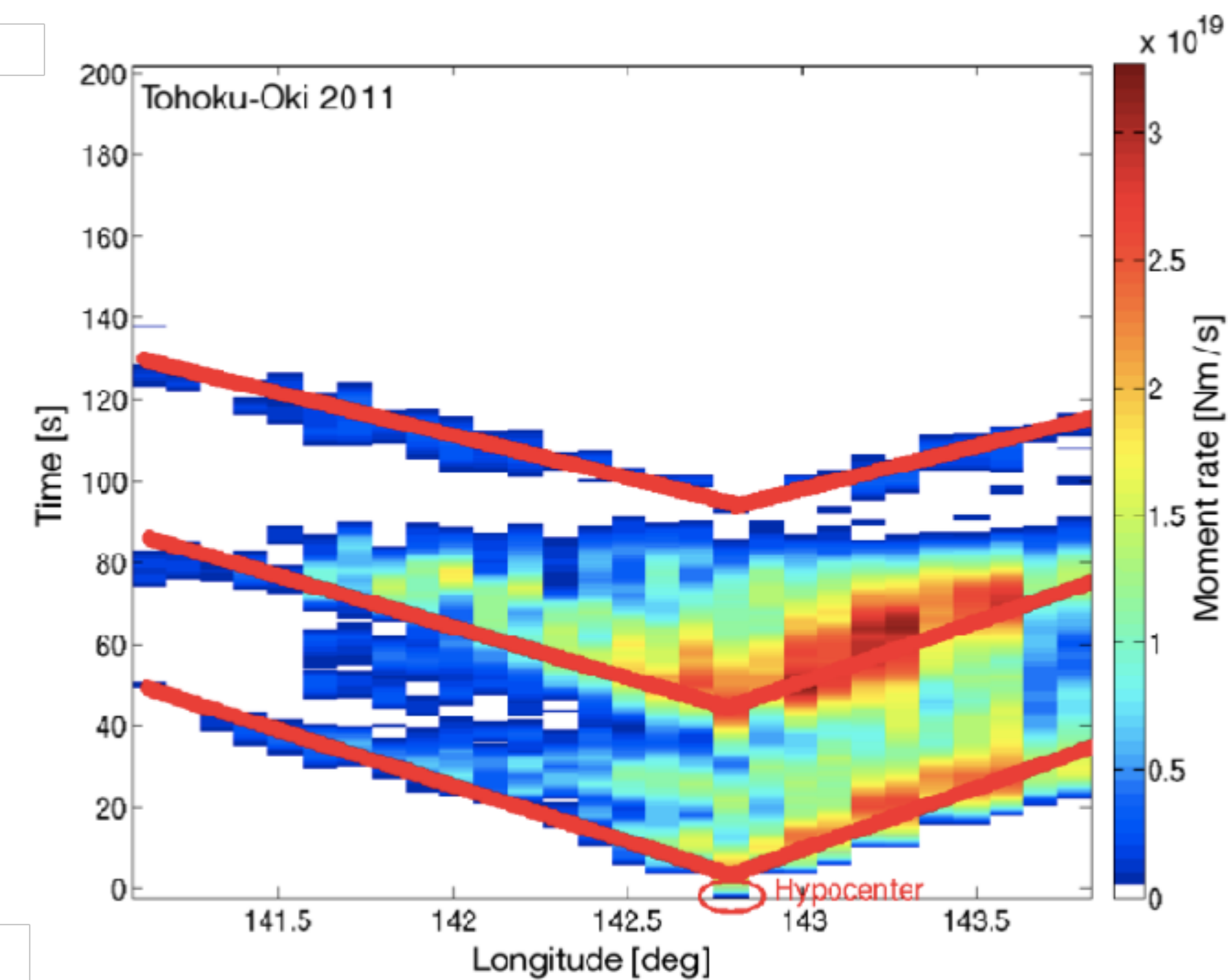
- **Earthquake dynamics are not predetermined:**
but evolve as a consequence of the model's initial conditions and the way the fault yields and slides controlled by an assigned friction law relating shear and normal traction on frictional interfaces

the ideal
world



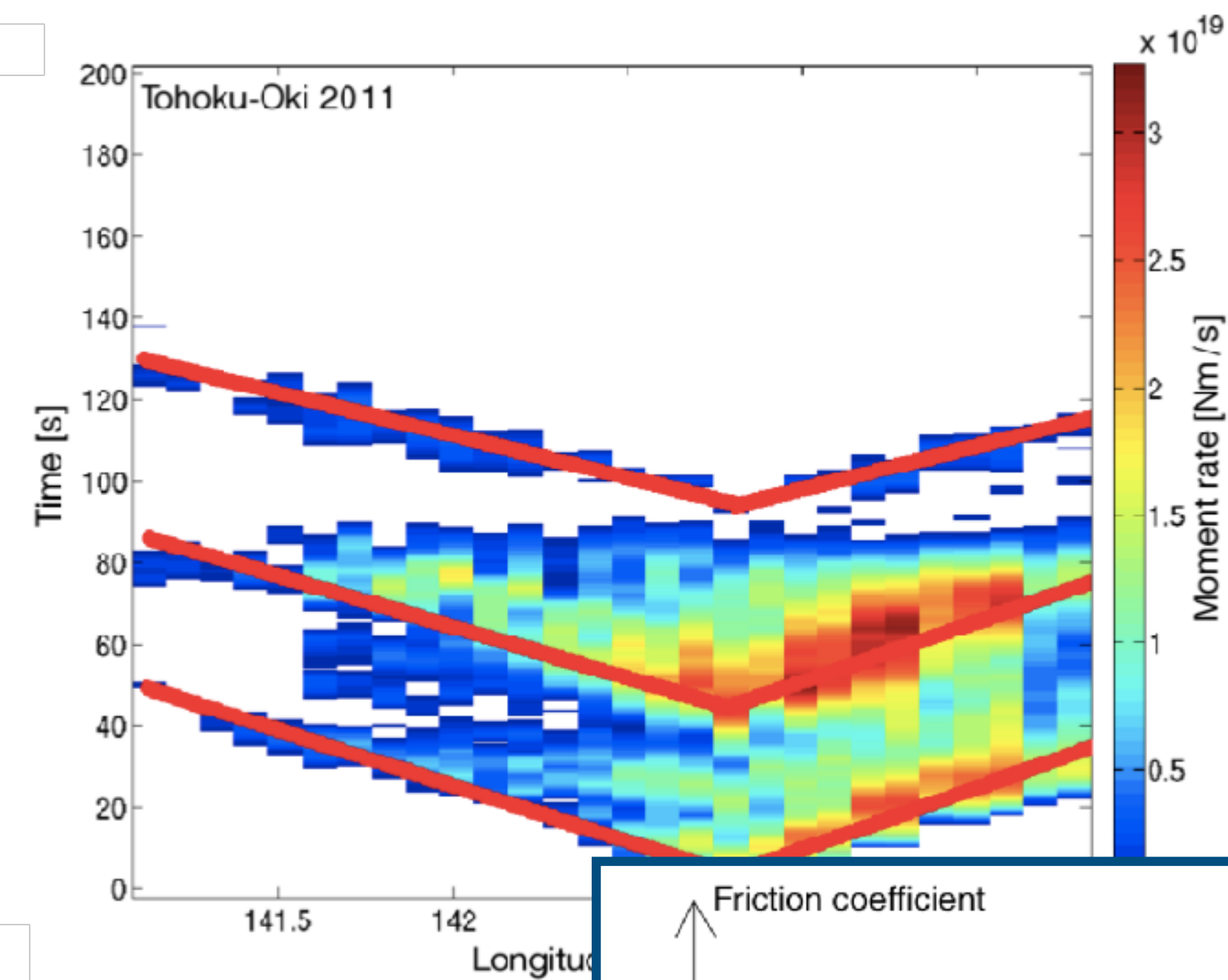
Simple 2D models + analytics reveal a 'zoo of rupture styles'

- **Slip re-activation:** Growing pulses gradually concentrate stress in their hypo-central region, as analytically predicted (Nielsen & Madariaga, 2003) \Rightarrow may trigger secondary rupture



Simple 2D models + analytics reveal a ‘zoo of rupture styles’

- **Slip re-activation:** Growing pulses gradually concentrate stress in their hypo-central region, as analytically predicted (Nielsen & Madariaga, 2003) \Rightarrow may trigger secondary rupture



Bulletin of the Seismological Society of America, Vol. 106, No. 3, pp. 819–831, June 2016, doi: 10.1785/0120150153

Rupture Reactivation during the 2011 M_w 9.0 Tohoku Earthquake: Dynamic Rupture and Ground-Motion Simulations

by Percy Galvez,* Luis A. Dalguer, Jean-Paul Ampuero, and Domenico Giardini

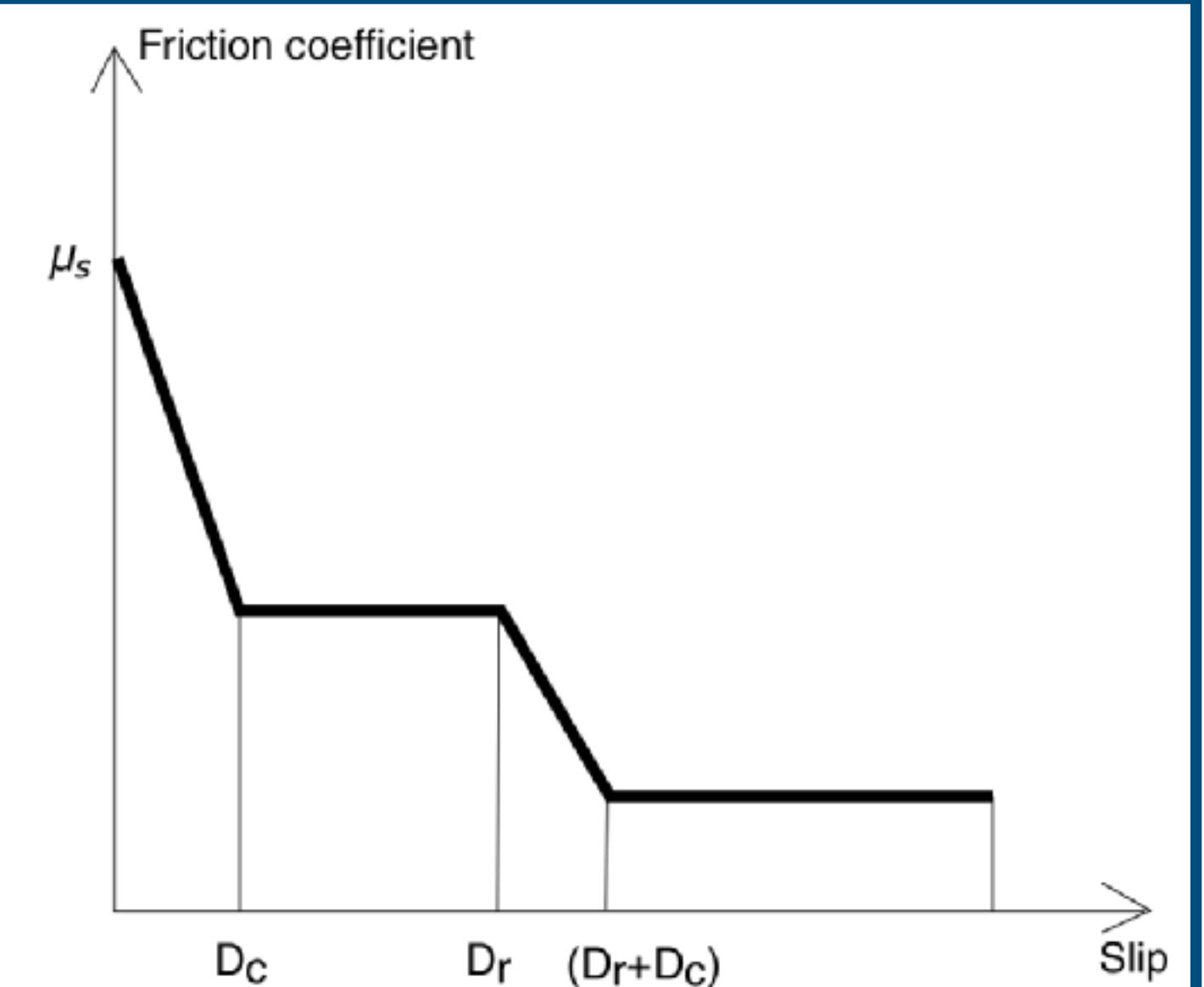
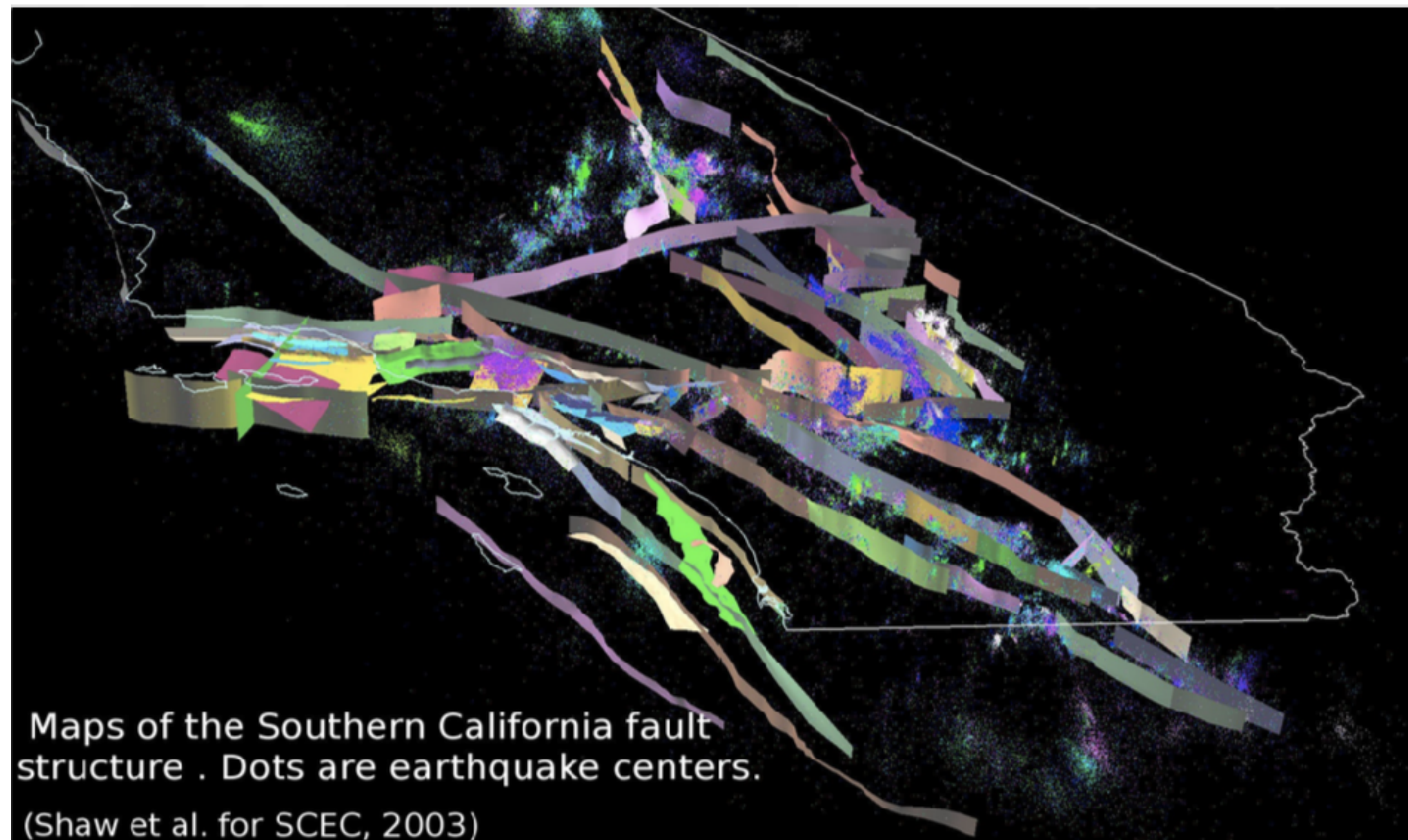


Figure 3. Slip-weakening friction model with two sequential strength drops. The second weakening phase is activated at a large slip D_r by thermally activated physicochemical processes such as fault-zone fluid pressurization due to dehydration or decomposition reactions.

3D dynamic rupture earthquake simulation

➔ Few methods support all modelling requirements



Multitude of spatio-temporal scales: fault geometry spans hundreds of km; frictional process zone size is m (or even cm) scale, tectonic loading (seismic cycle) 10-10000 years; rise time on second scale

the real
world

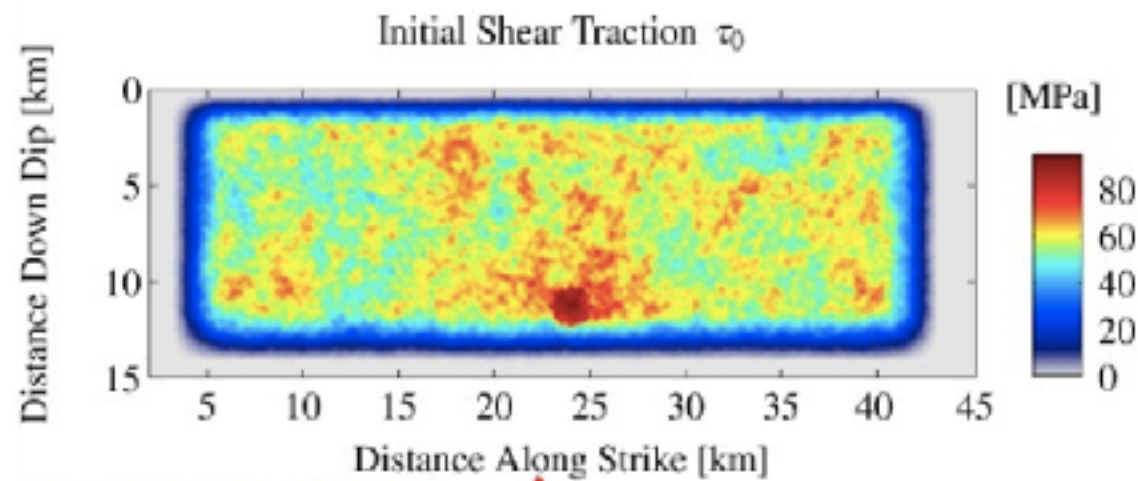
- Non-planar, intersecting faults
- Non-linear friction
- Heterogeneities in stress and strength
- Dynamic damage around the fault
- Fault roughness and segmentation on all scales
- Bi-material effects
- Low velocity zones surrounding faults
- Thermal pressurization of fault zone fluids
- Thermal decomposition
- Dilatancy of the fault gouge
- Flash heating, melting, lubrication
- Feedback mechanisms across time scales

... this list grows continuously

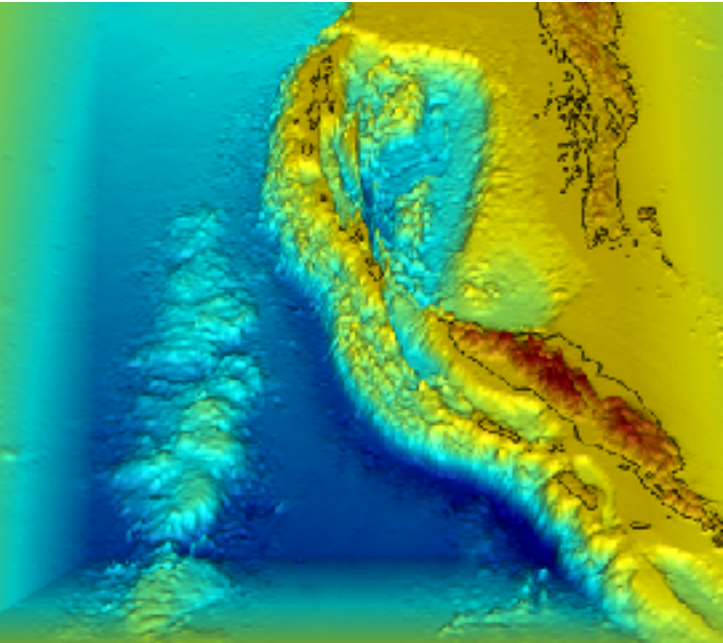
3D dynamic rupture earthquake simulation

- **Physics-based approach:** Solving for spontaneous dynamic earthquake rupture as non-linear interaction of frictional failure and seismic wave propagation

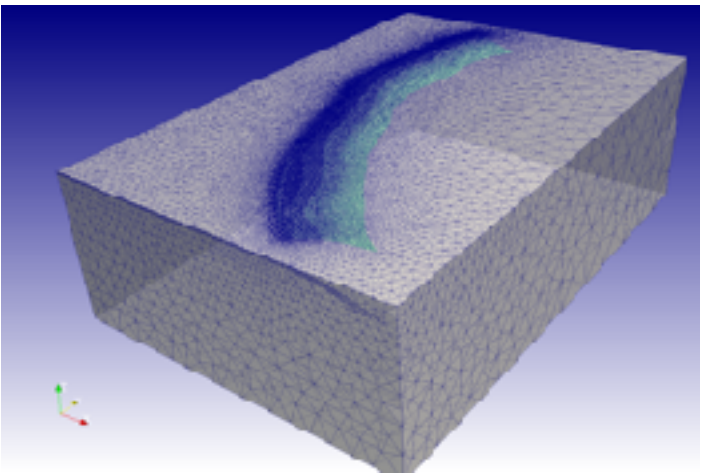
“Input”



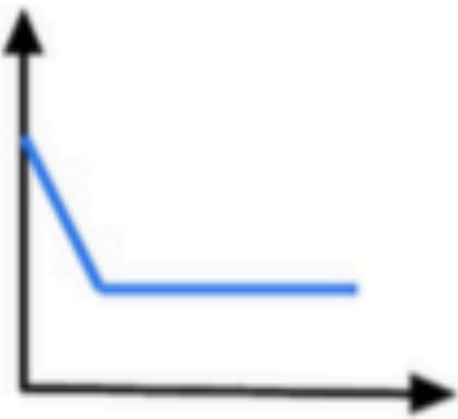
Initial fault stresses



Geological structure



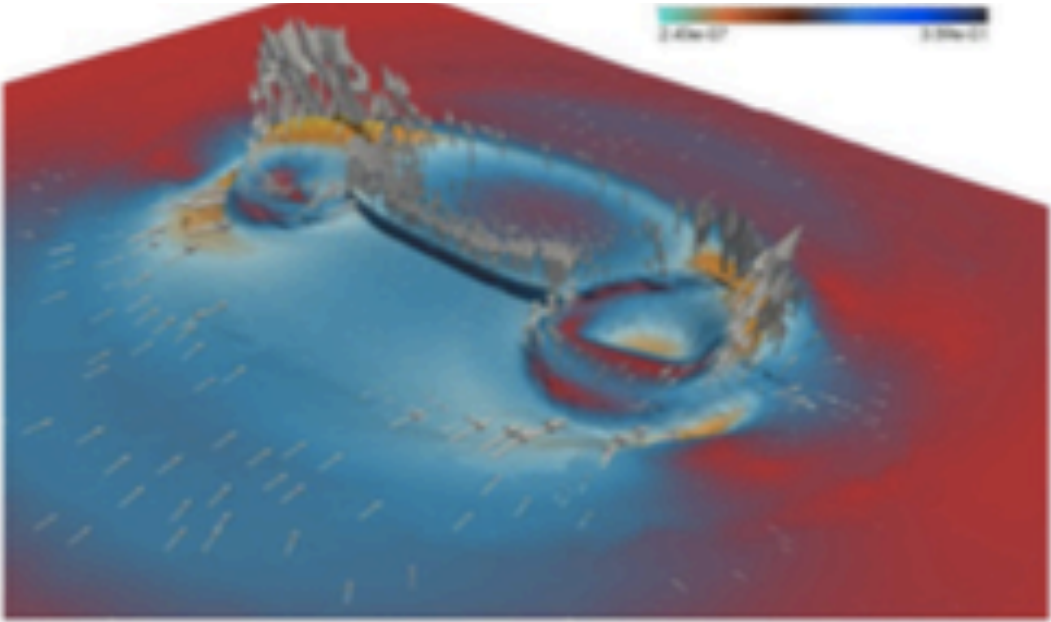
CAD & mesh generation



Failure Criterion

SOLVER

Ground motion



“Output”

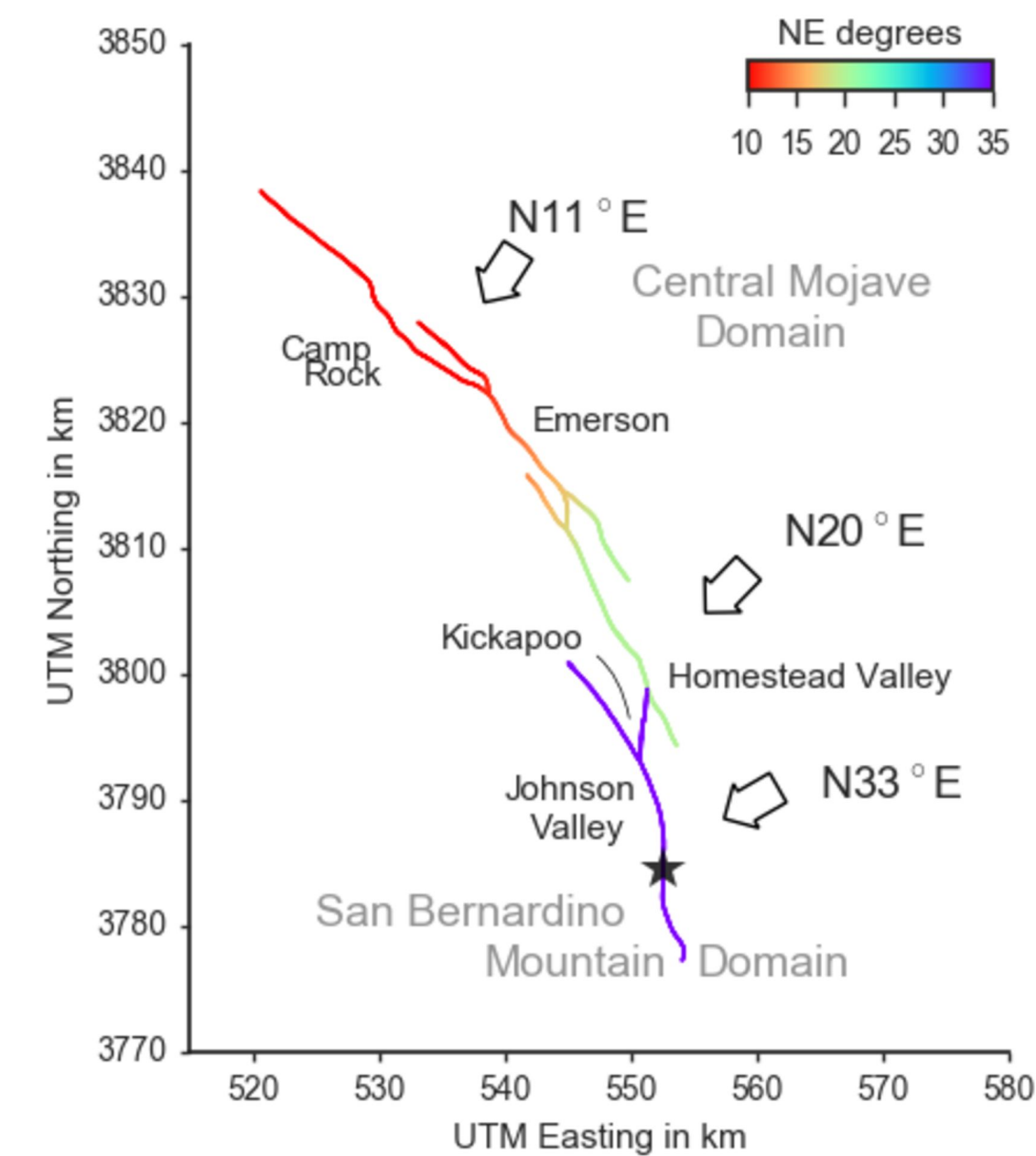
Synthetic seismograms



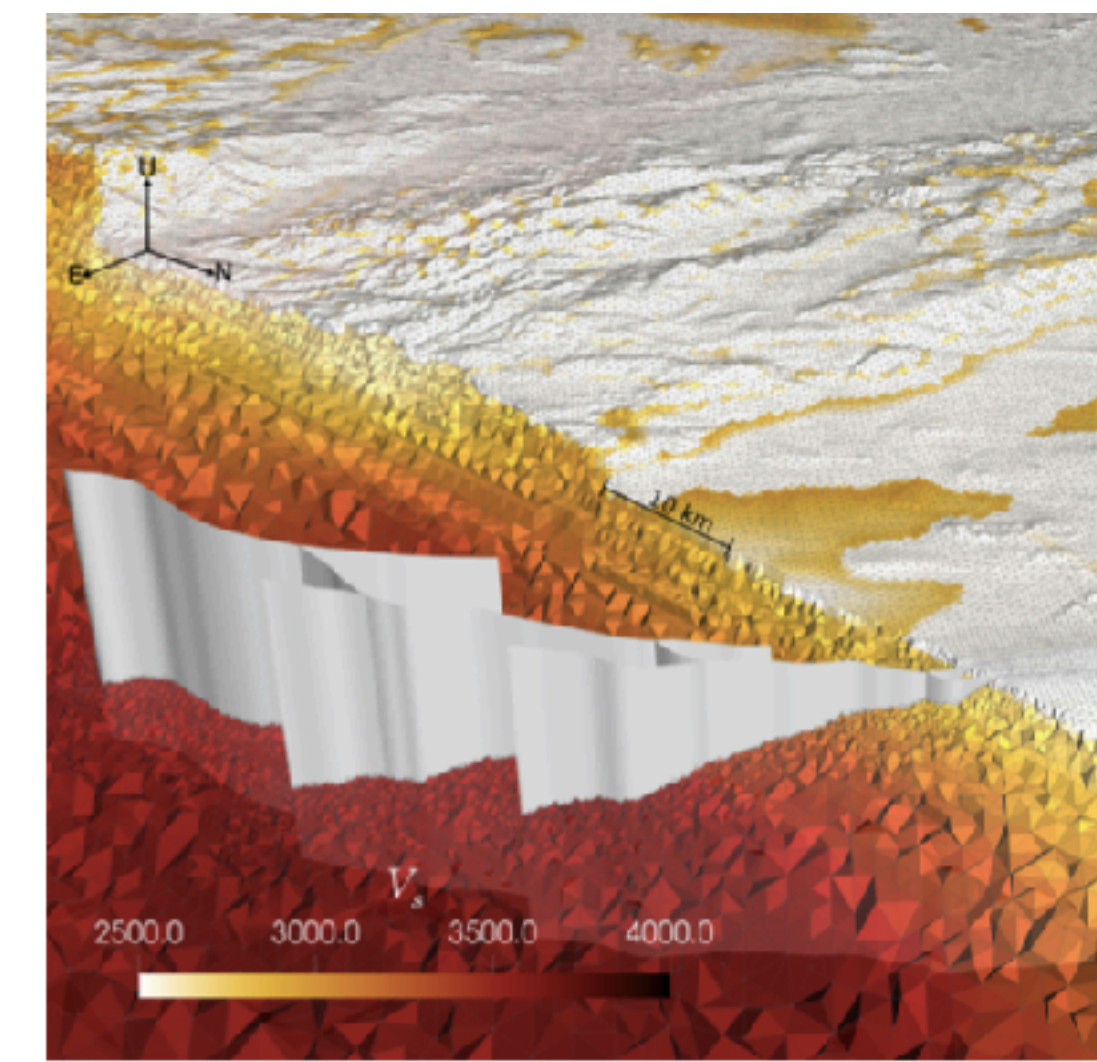
The 1992 Mw 7.3 Landers earthquake “reloaded” (Wollherr et al., JGR 2019)

➔ Geometry (fault morphology) matters!

- **Large-scale dynamic rupture simulation** aiming to understand on “natural-scale” which of the earthquake source “complexities” provides **first order influences**
- **A high degree of realism** leads in turn to a **high degree of uniqueness**



Mapped fault traces (Fleming et al., 1998) and assumed orientation of maximum compressional principal stress.



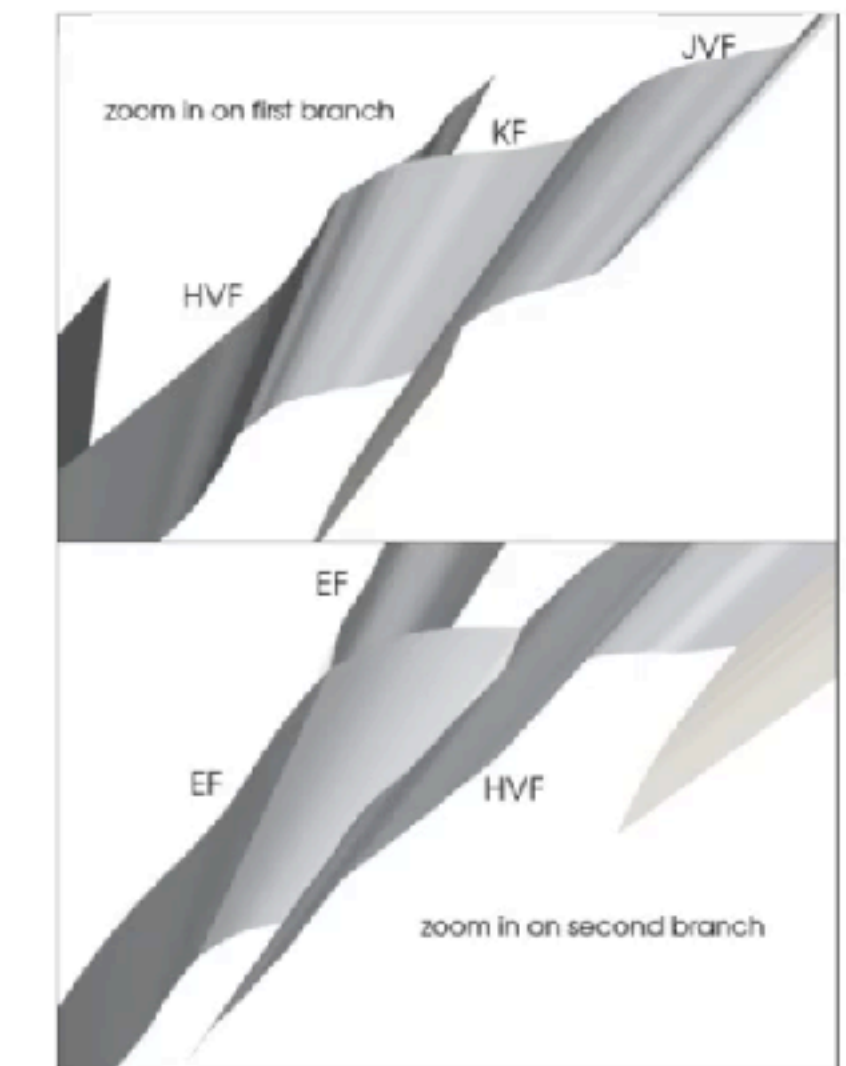
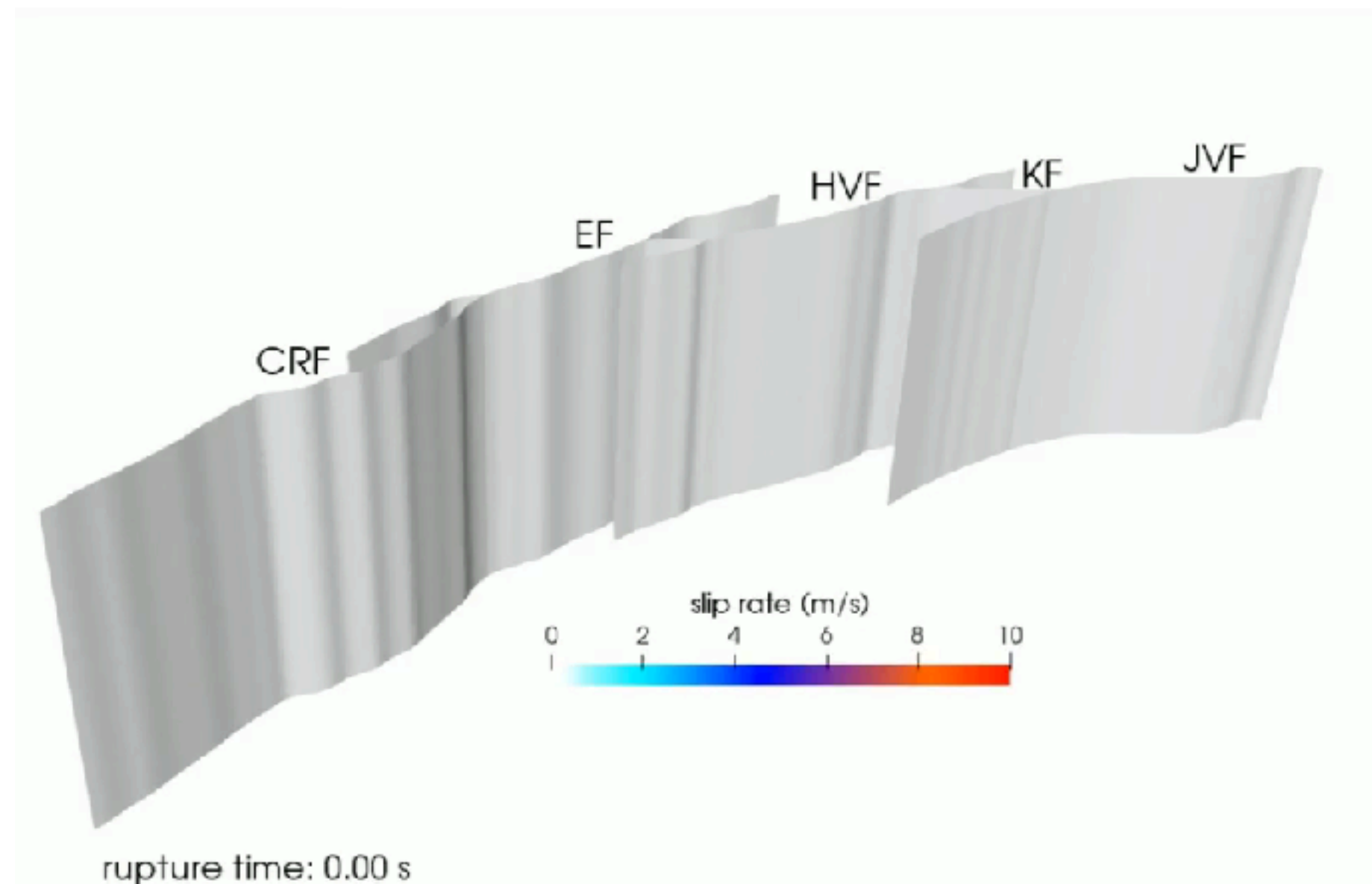
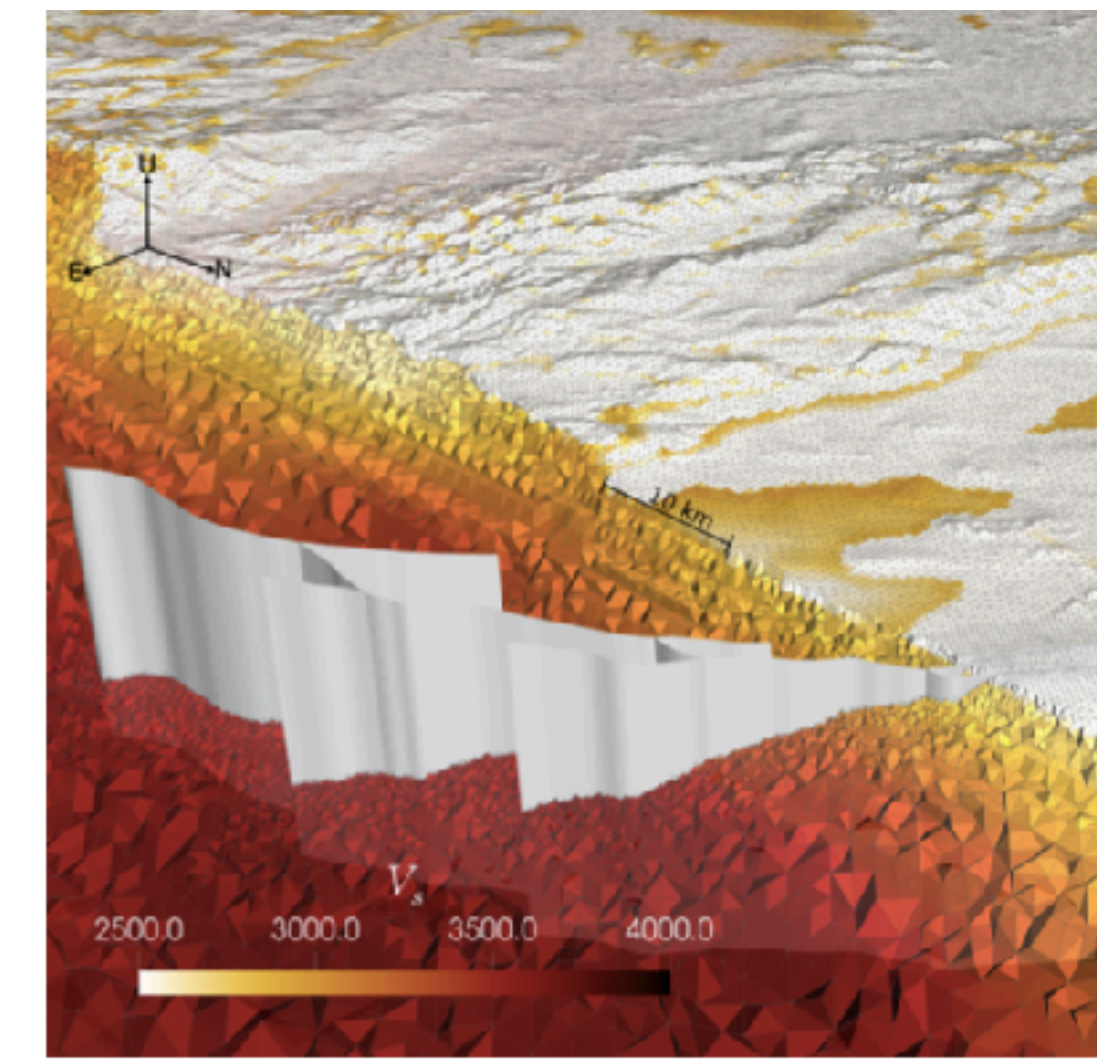
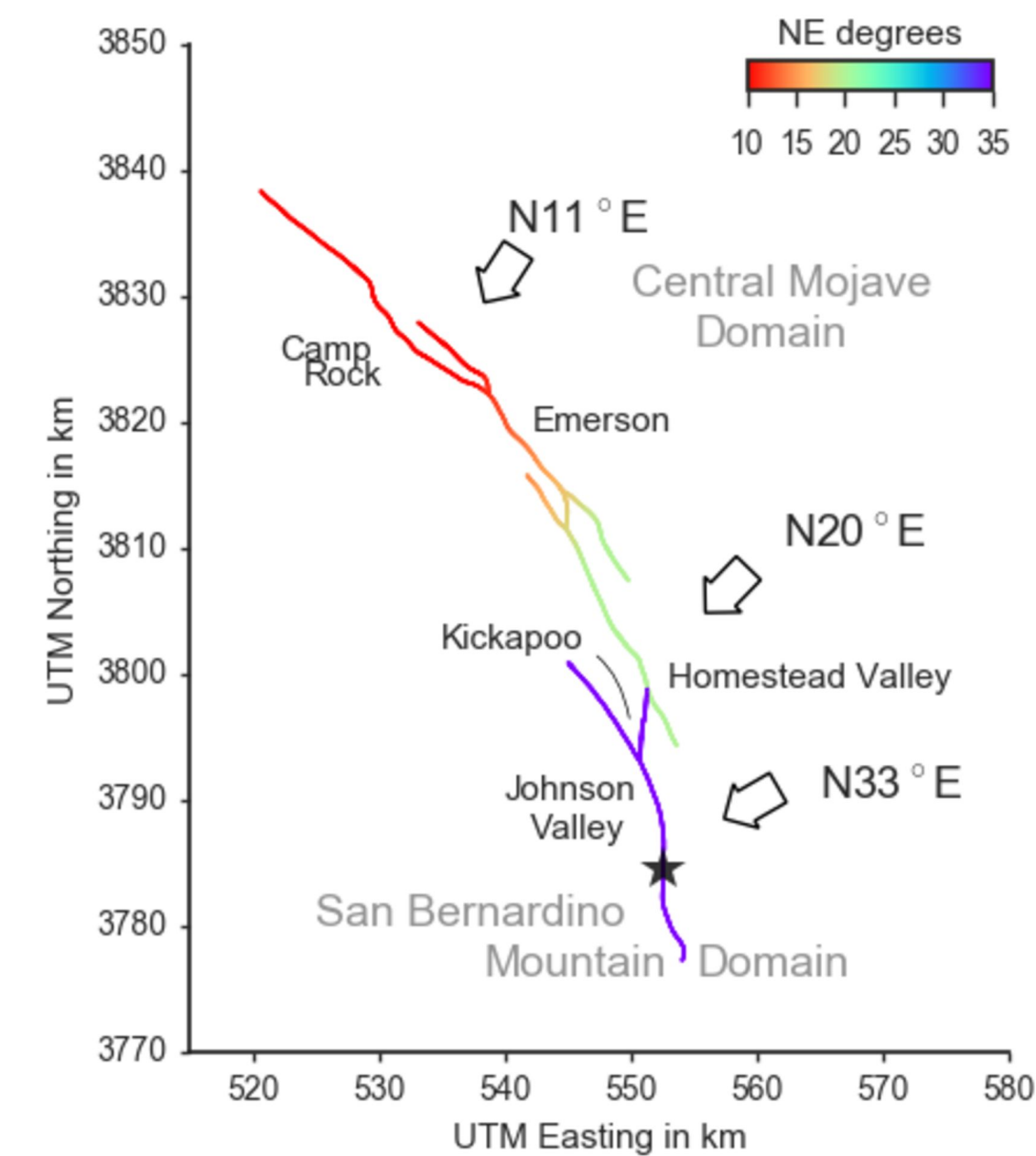
Computational model feat. 3D Community Velocity Model-Harvard (CVM-H, Shaw et al., 2015). Local refinement is applied in the vicinity of the faults (200 m) and the Earth's topography (500 m) (Farr et al., 2007)

The 1992 Mw 7.3 Landers earthquake

“reloaded” (Wollherr et al., JGR 2019)

➔ Geometry (fault morphology) matters!

- Large-scale dynamic rupture simulation aiming to understand on “natural-scale” which of the earthquake source “complexities” provides first order influences
- A high degree of realism leads in turn to a high degree of uniqueness
- **Sustained** dynamic rupture interconnecting fault segments **constraints pre-stress and fault strength**
- Complex rupture transfers as combination of direct branching and dynamic triggering over **large distances** due to simultaneous failure of segments and **affected by viscoelastic wave attenuation**

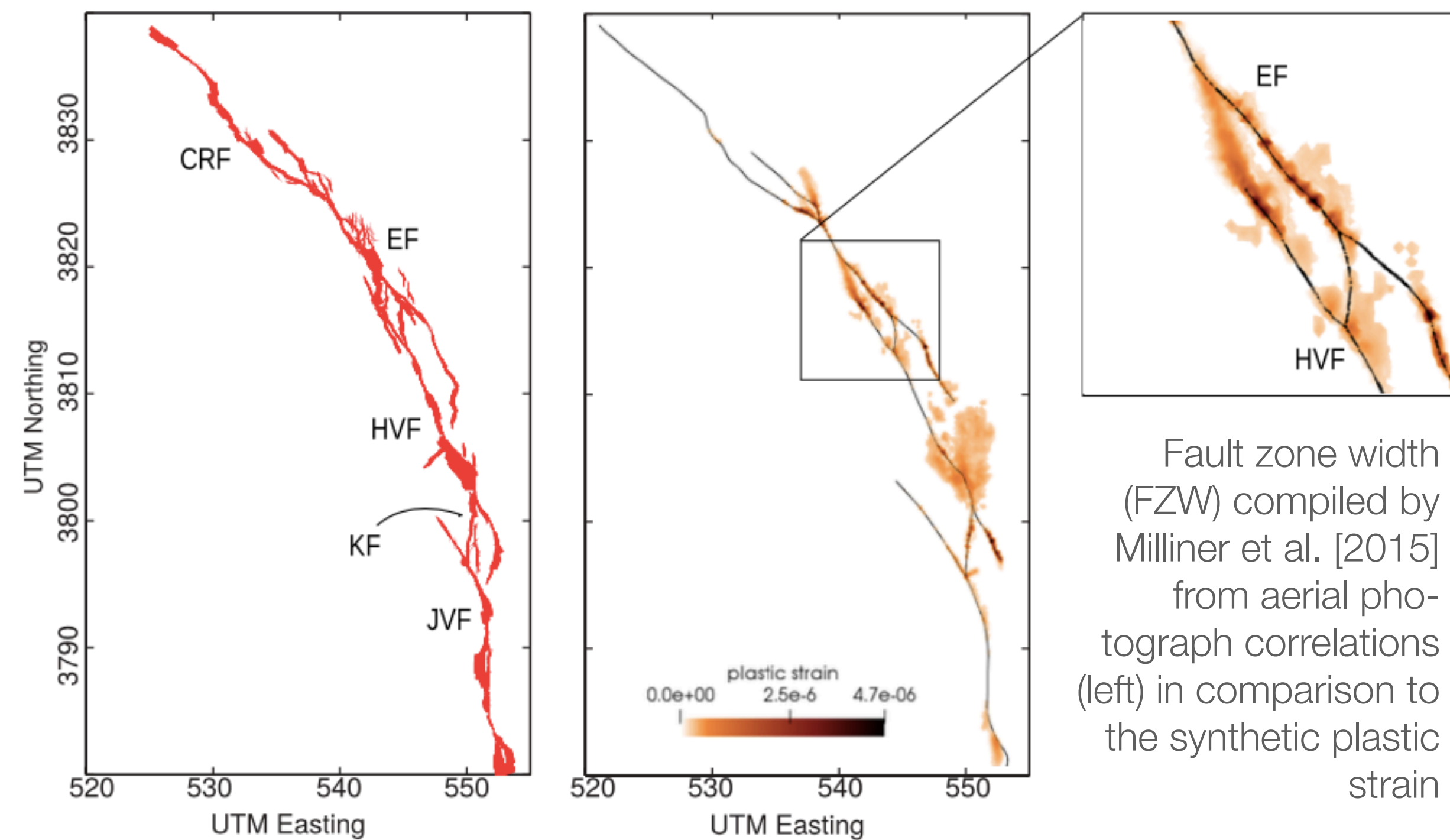


Slip rate across the fault system of dynamic rupture simulation with SeisSol of frictional failure on-fault coupled to seismic wave propagation accounting for off-fault plasticity (Wollherr et al., 2018) and viscoelastic attenuation (Uphoff & Bader, 2016).

The 1992 Mw 7.3 Landers earthquake “reloaded” (Wollherr et al., JGR 2019)

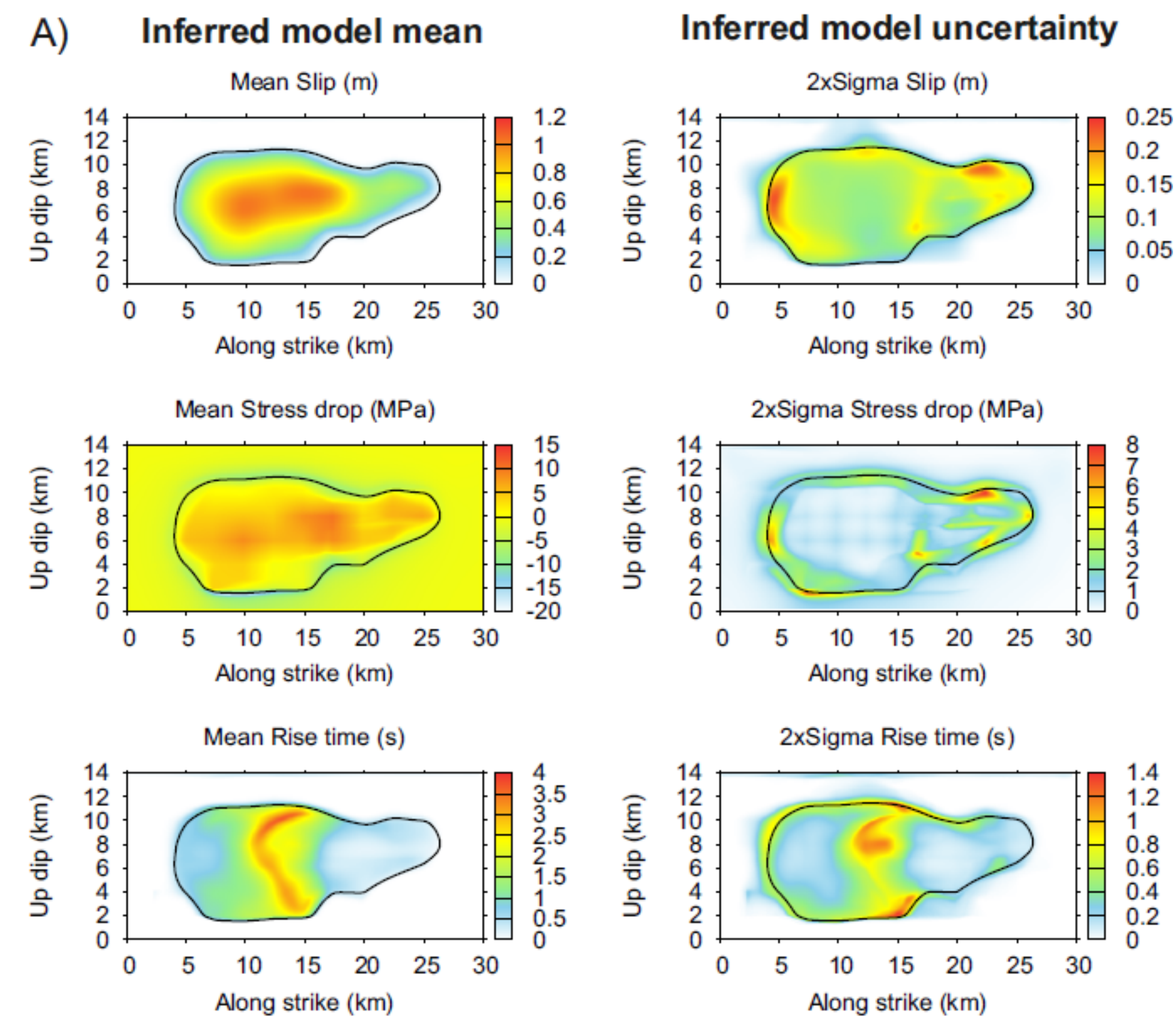
➡ **Multi-physics, such as off-fault plasticity, matters!**

- **Drastic increase of off-fault deformation in geometrically complex fault regions** enhancing geometric barriers, hindering rupture transfers and matching newly available mapping
- **Strain localisation** forming non-prescribed ‘faults’

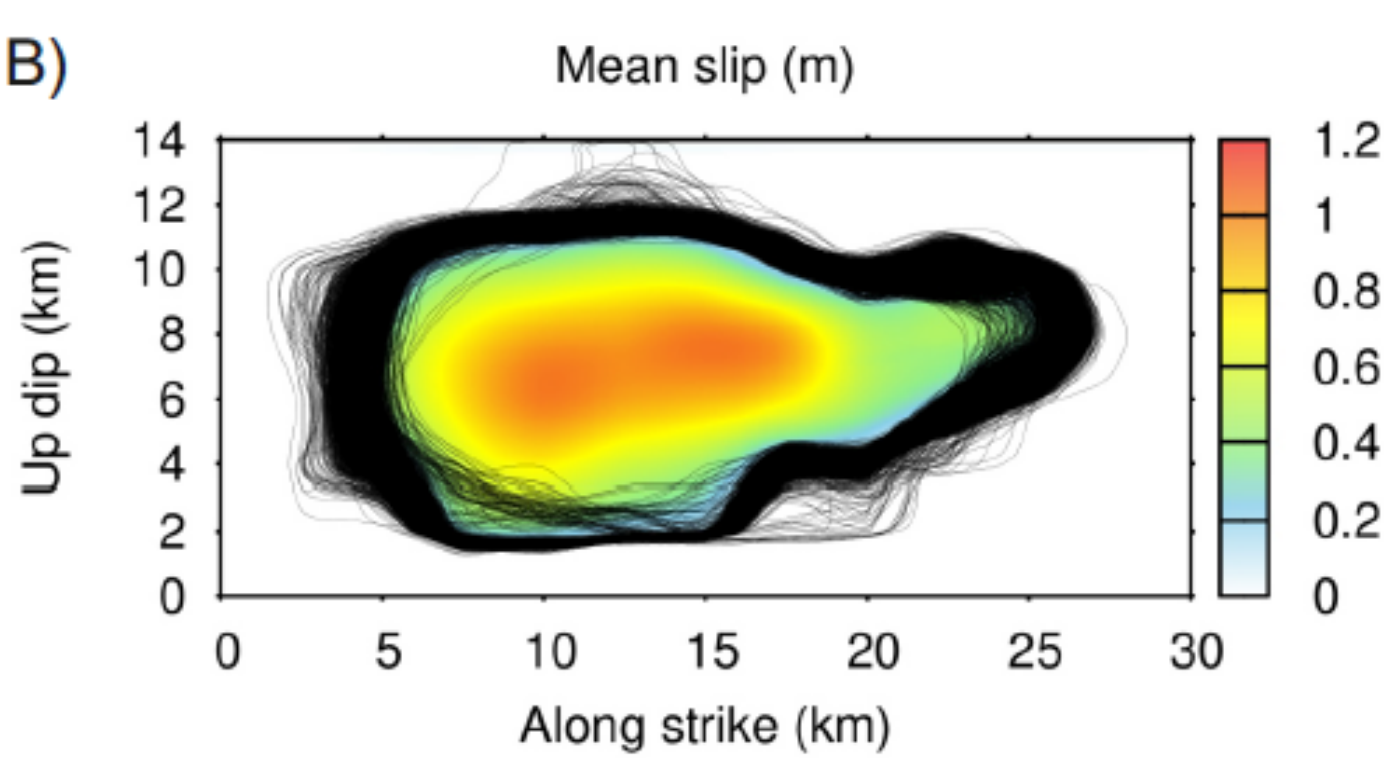


The 2016 Amatrice earthquake

- Dynamic source inversion visiting >1 million of dynamic rupture simulations to constrain initial conditions



Gallovic et al., 2019a,b

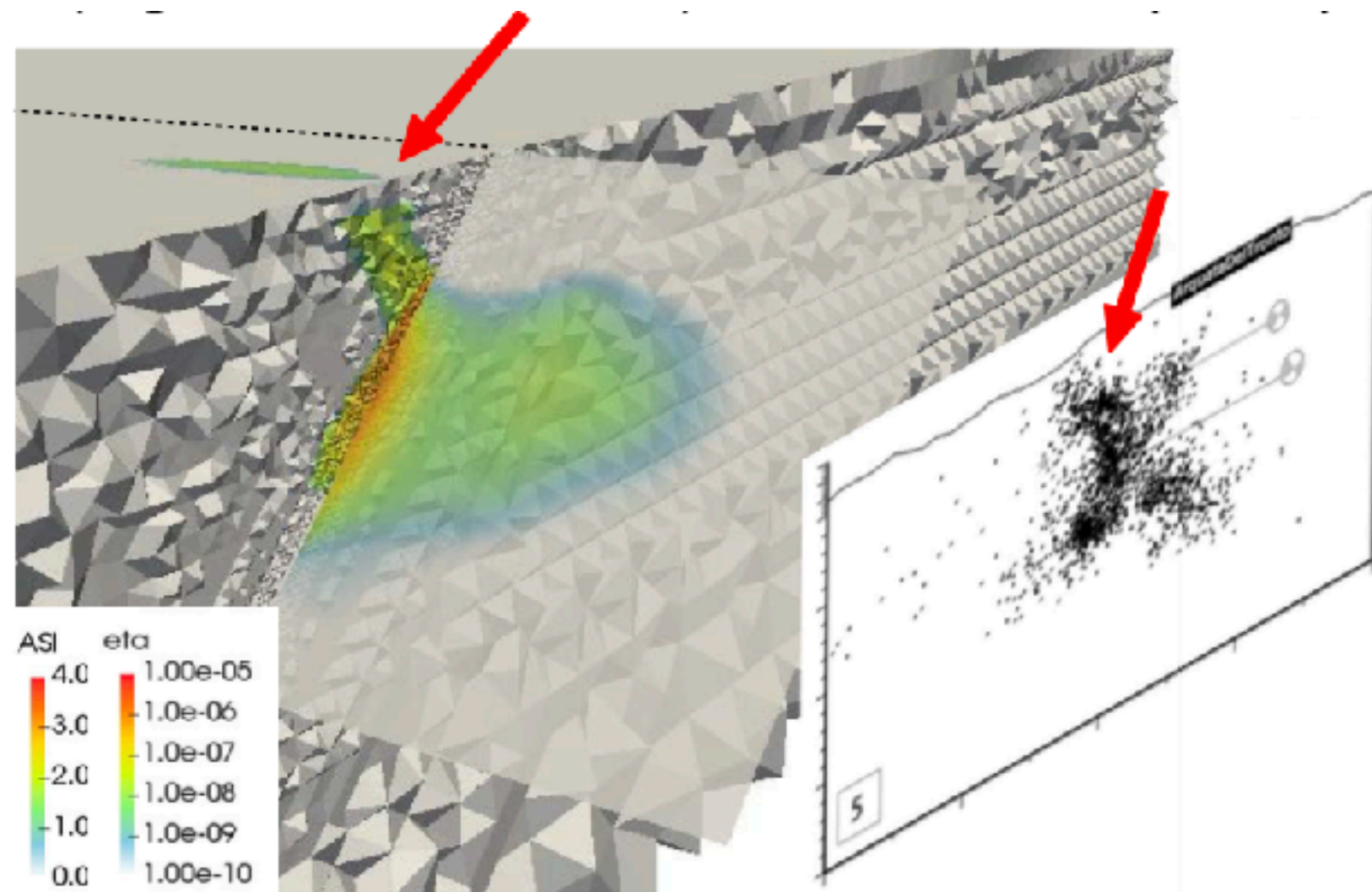
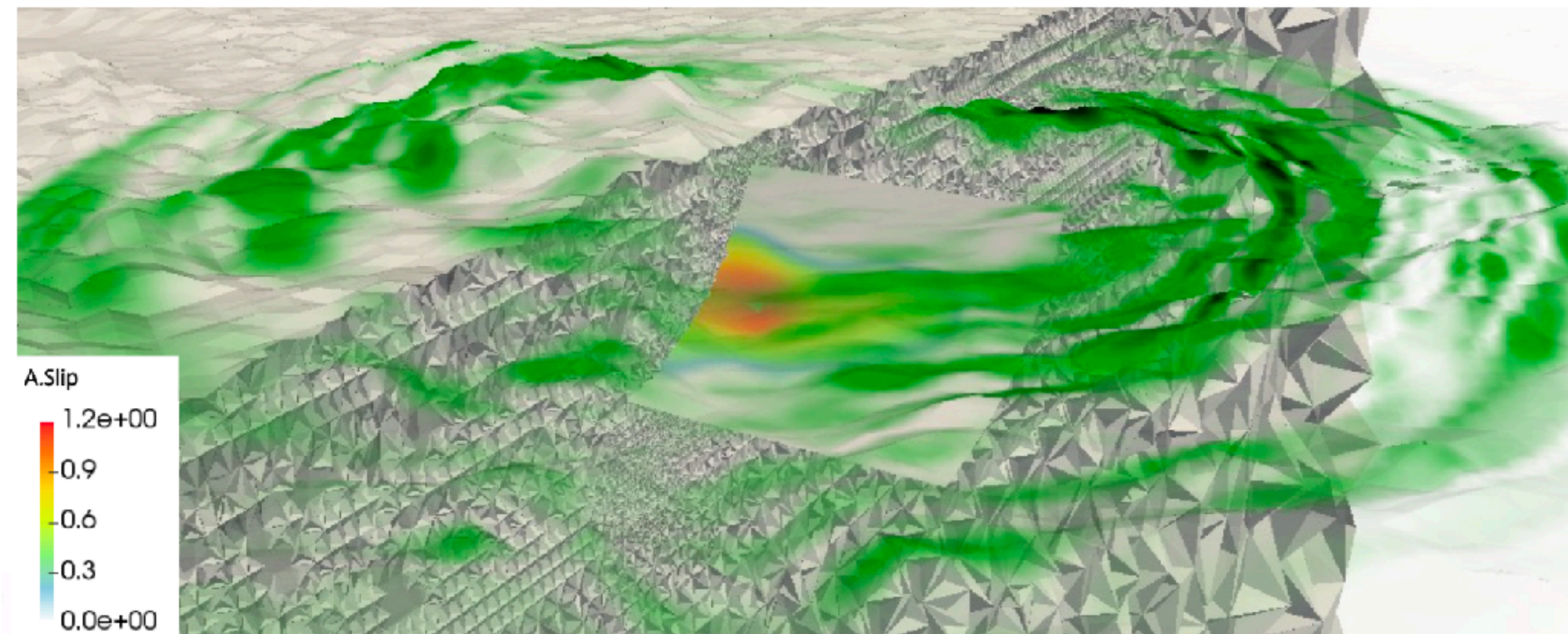


A) Rupture parameters inferred by the Bayesian dynamic inversion averaged over posterior samples (left) and the model parameters' uncertainty in terms of two sigma (right). B) Averaged model of slip (color-coded) with slip contours of all accepted posterior model samples displaying the uncertainty of the inferred spatial rupture extent.

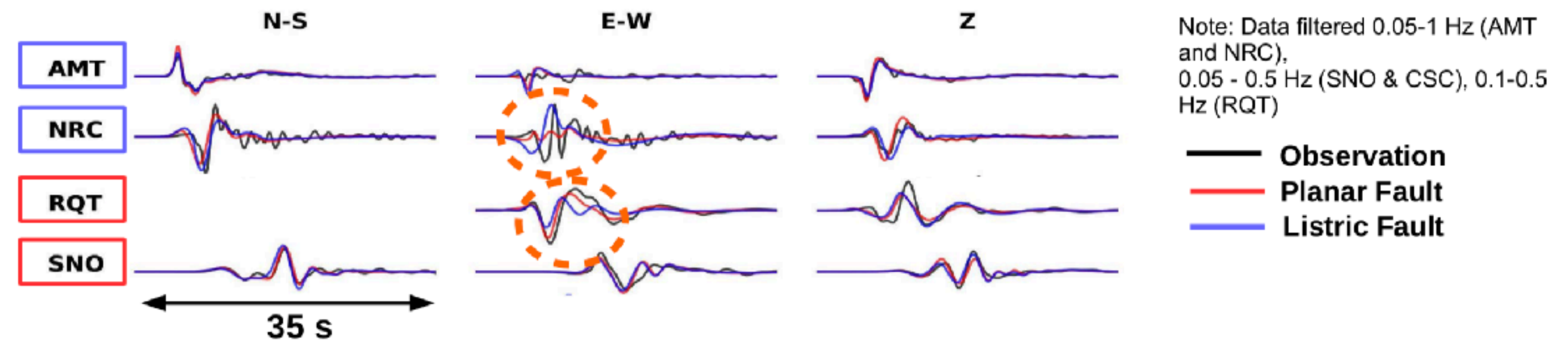
The 2016 Amatrice earthquake

(Taufiqurrahman et al., in prep.)

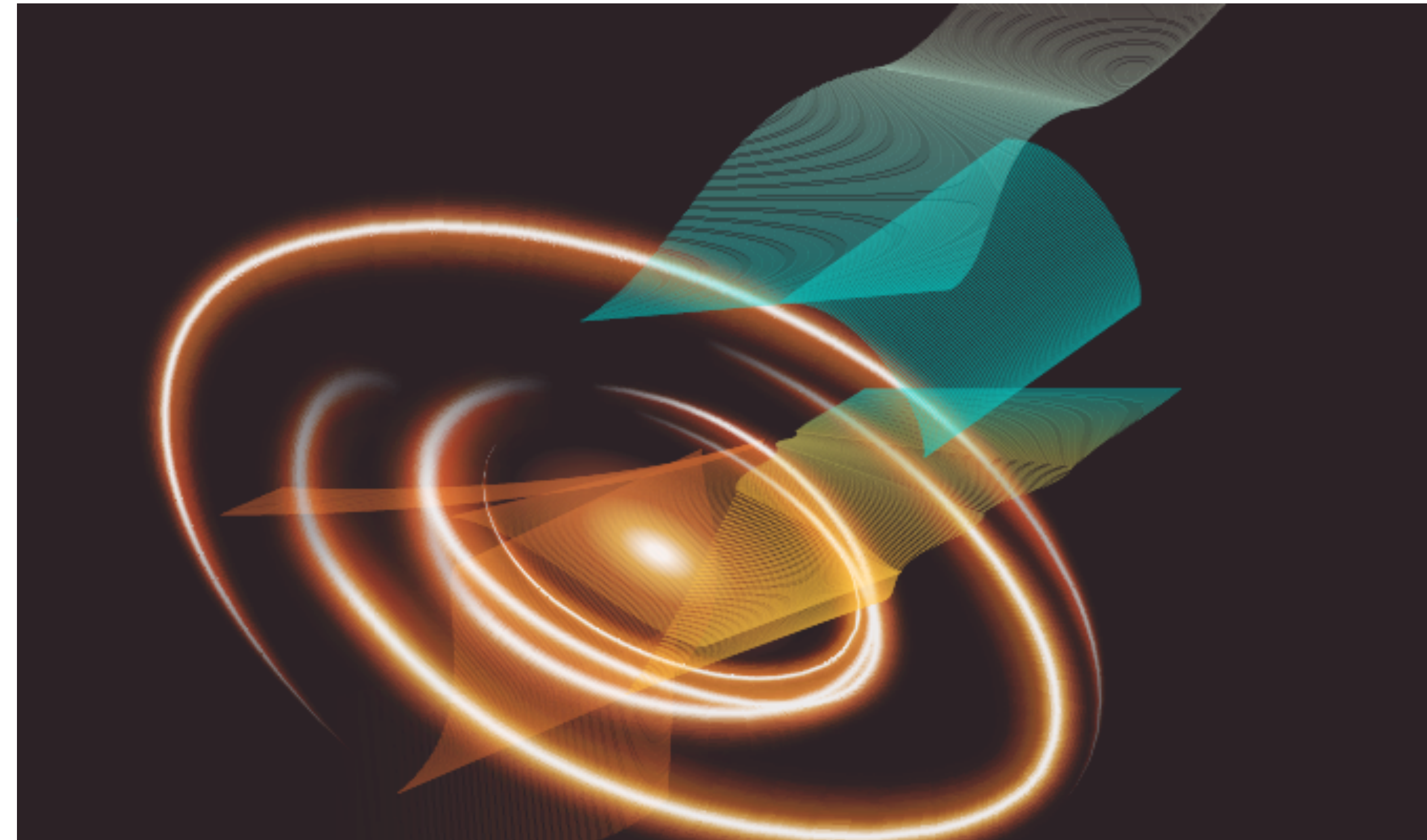
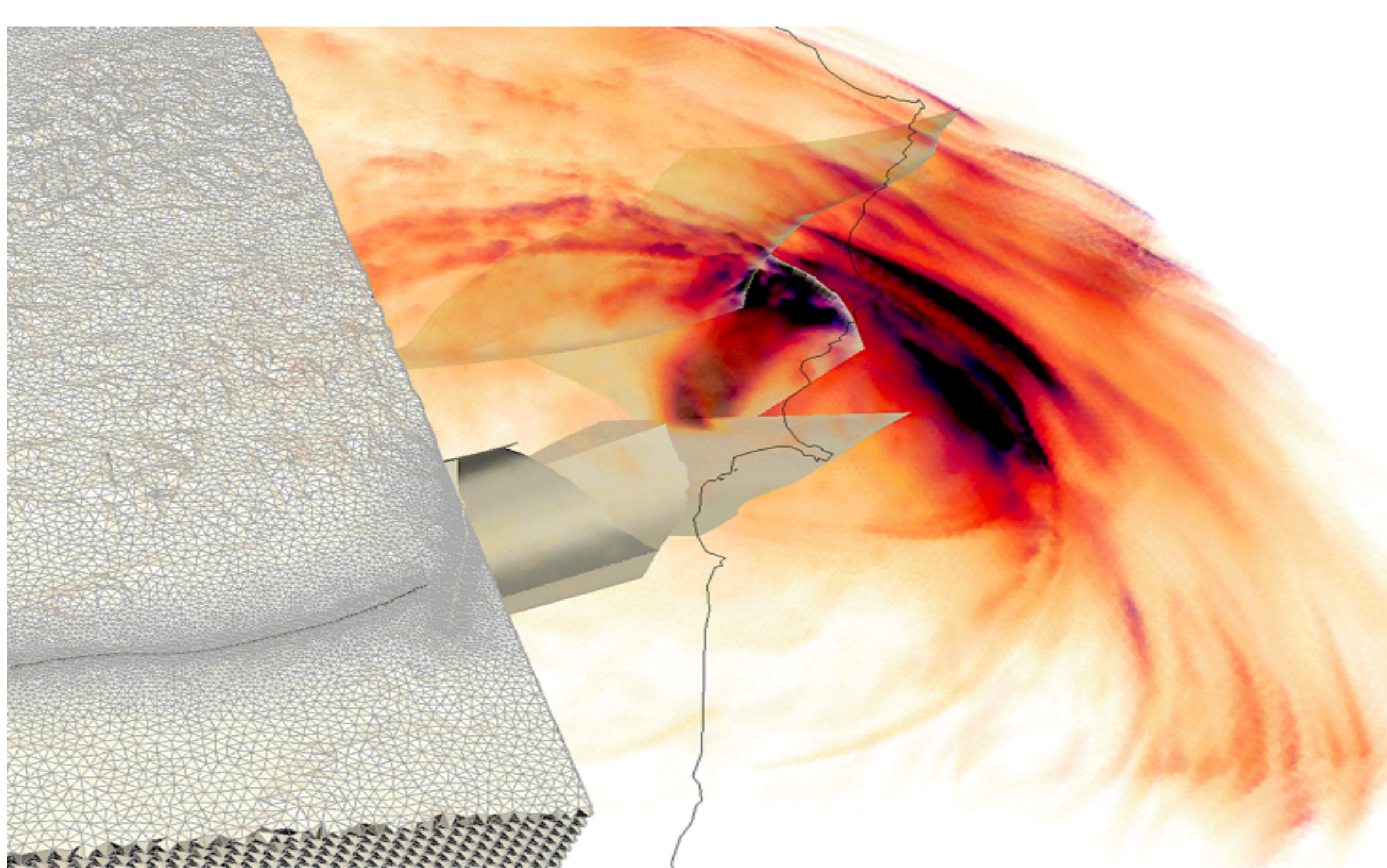
- **Dynamic source inversion visiting >1 million of dynamic rupture simulations to constrain initial conditions**
- **Adding listric fault geometry improves match with strong motion data**
- **Off-fault plasticity aligns with aftershock distribution (antithetic fault, Chiaraluce et al., 2017)**



• Seismograms of N-S, E-W, and Z for selected receivers



How to constrain initial conditions?



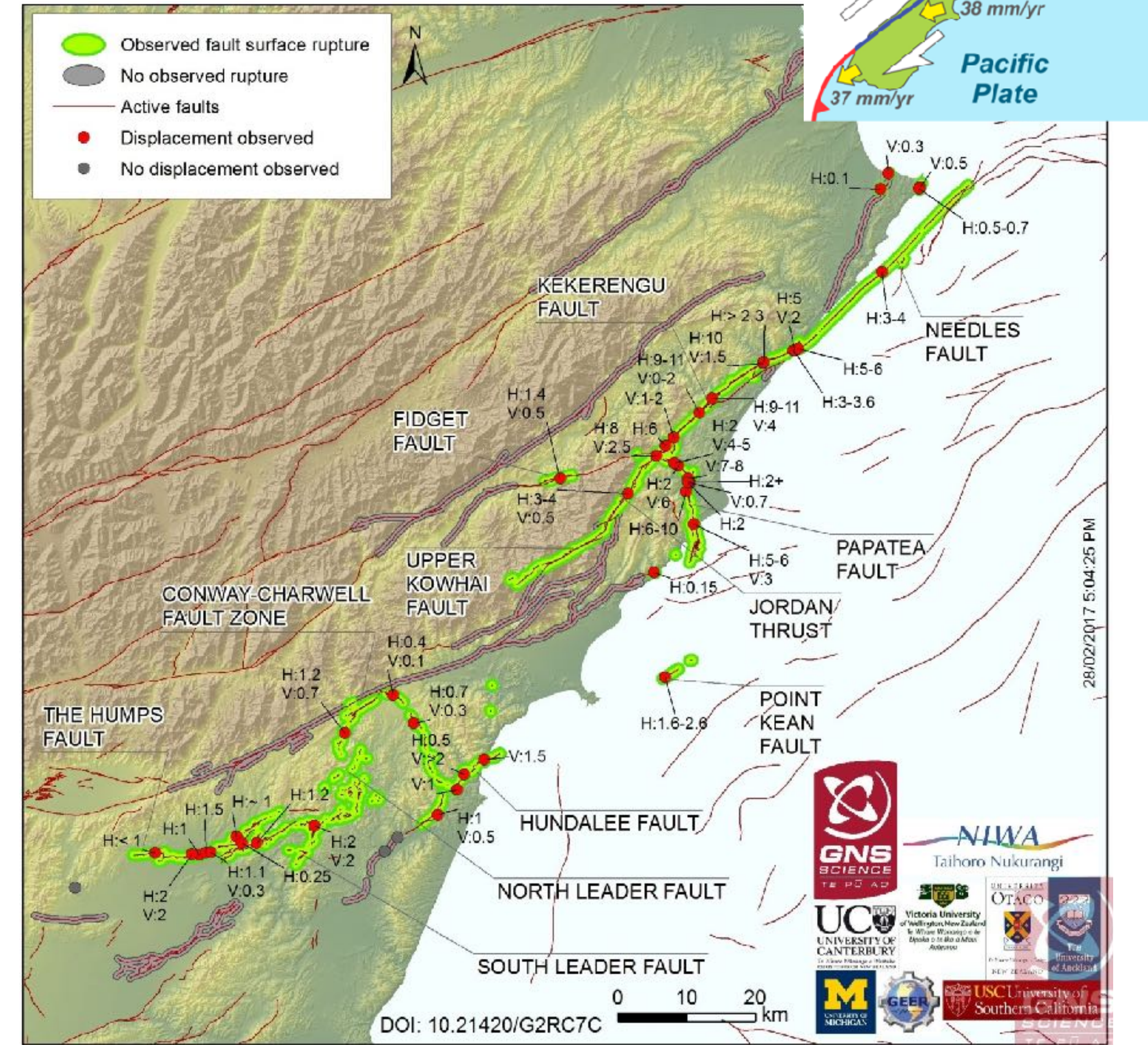
Impressions of a complex dynamic rupture scenario of the 2016, Kaikōura Earthquake (Ulrich et al., 2019, Nature Comm.)

The 2016, Mw7.8 Kaikōura earthquake - a rupture cascade on weak crustal faults

- Rupture propagation across highly segmented fault system with **diverse orientations and faulting mechanisms (strike-slip, thrusting)**
- Duration of ~100s, 200km of rupture, triggered landslides, local tsunami
- 2 deaths, 57 injured, damaged infrastructure, e.g. bridges, road subsidence
- High-quality, but **puzzling observations**



Kekerengu Fault
rupture displacement
by ~10 meters

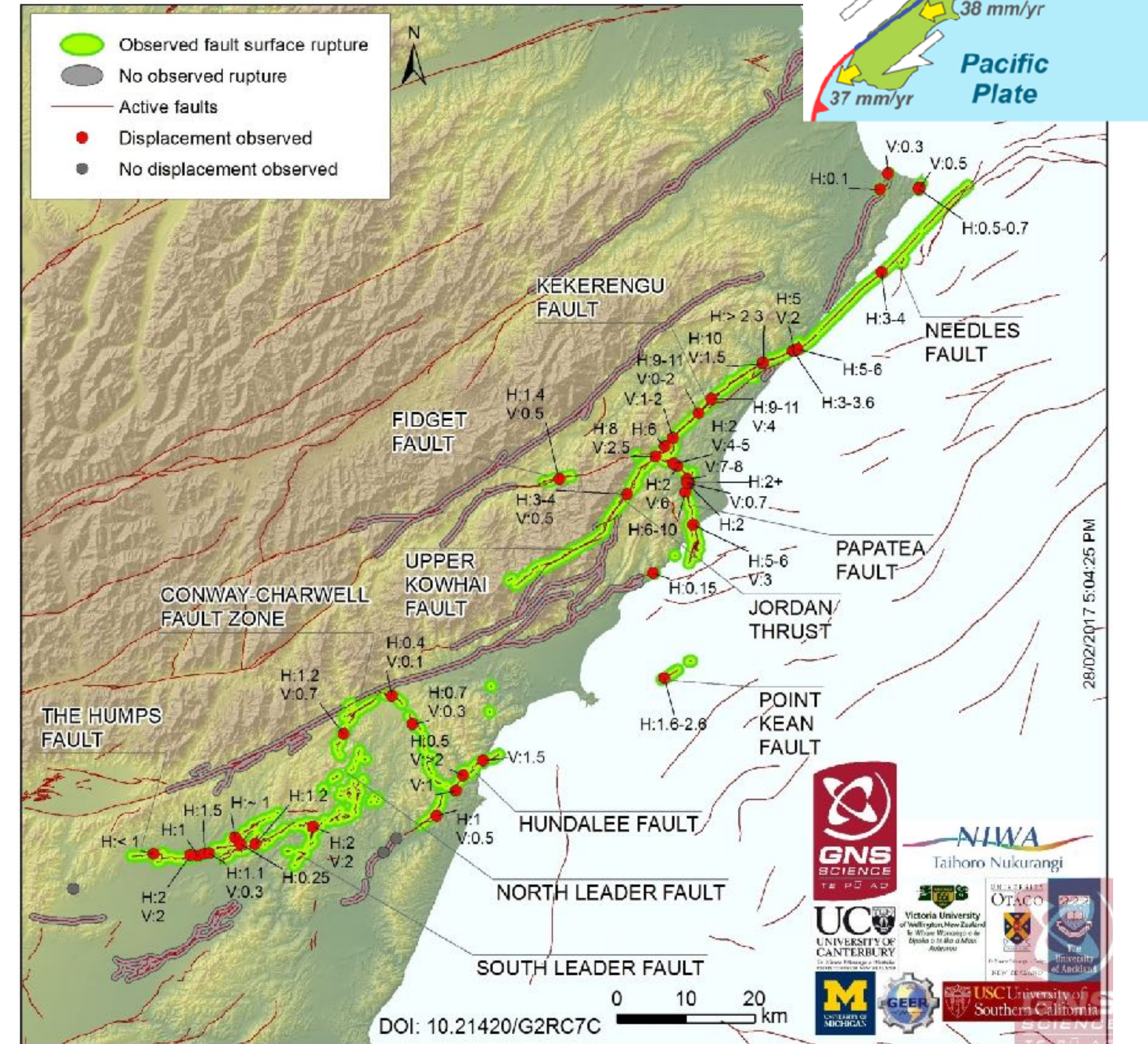


The 2016, Mw7.8 Kaikōura earthquake - a rupture cascade on weak crustal faults

Open questions:

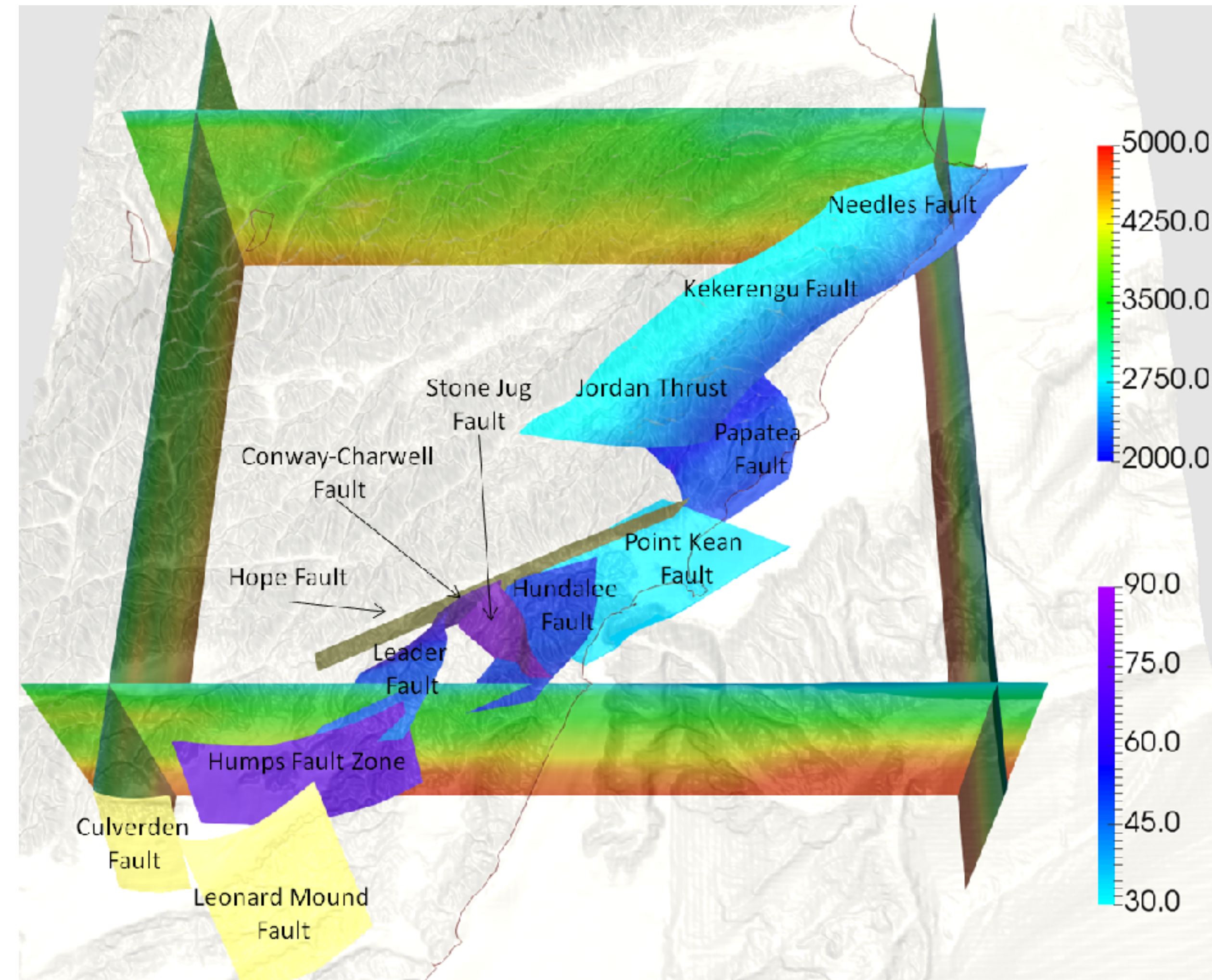
- Did the rupture of multiple crustal faults **connect via slip on a subduction interface?**
- A 15 km large gap separating the surface ruptures of the Hundalee and Upper Kowhai faults - **Can earthquake ruptures jump across wider fault gaps than previously thought?**
- Why was this earthquake **anomalously slow?**
- Why did the **Hope Fault not rupture?**
- How can such a complex cascade occur on faults that have **low apparent friction?**

Physics-based dynamic rupture simulations can help constraining those competing views and provide a self-consistent earthquake source description



The 2016, Mw7.8 Kaikōura earthquake - a rupture cascade on weak crustal faults

➡ Unraveling the event's riddles in a physics-based manner at a new degree of realism

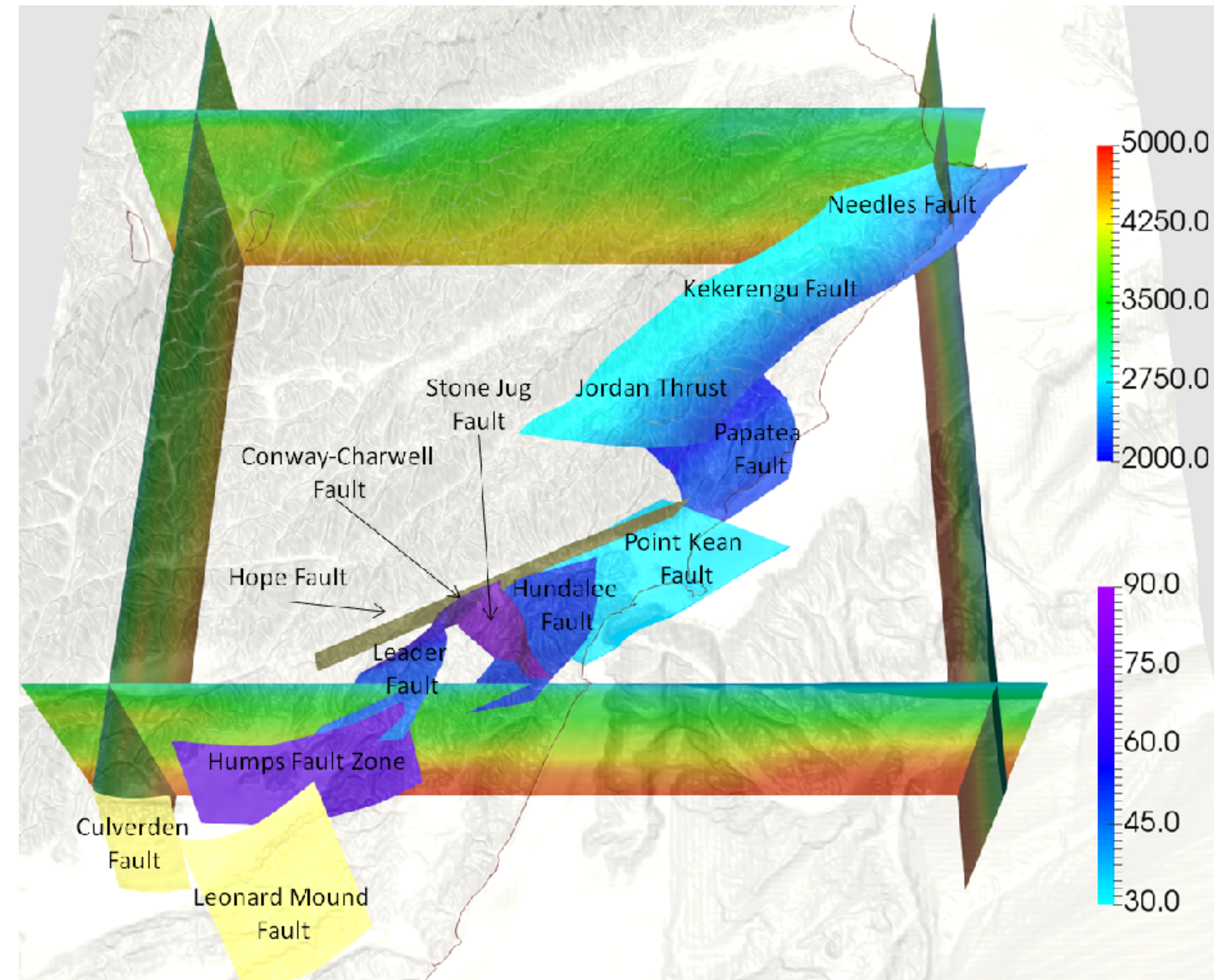


Model fault network coloured by **dipping angle**. The Hope, Culverden and Leonard Mound faults are included but do not rupture. Faults are embedded in high-resolution topography and bathymetry (Mitchell et al., 2012) and 3D subsurface structure (Eberhart-Phillips et al., 2010).

The 2016, Mw7.8 Kaikōura earthquake - a rupture cascade on weak crustal faults

➔ **Unraveling the event's riddles in a physics-based manner at a new degree of realism**

- High-resolution topography and bathymetry
- Severe velocity-weakening friction
- 3D subsurface structure
- Off-fault plasticity
- Viscoelastic attenuation
- Crustal fault network geometry inferred from seismic and geodetic data
- Including a linking, off-shore, low-dipping shallow thrust fault (Point Kean Fault)
- Including faults that did not break (Hope, Culverden, Leonard Mound)

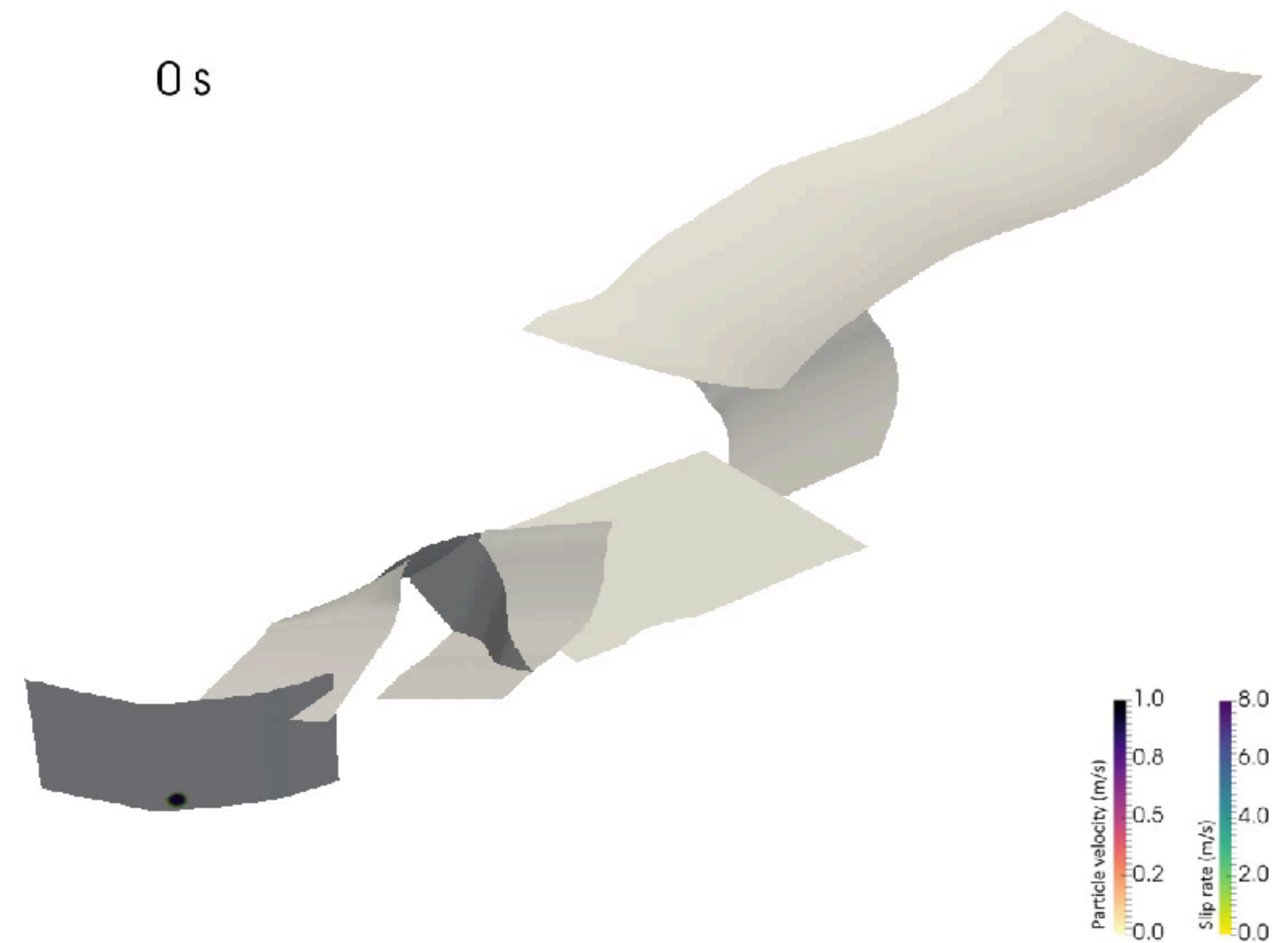


Model fault network coloured by **dipping angle**. The Hope, Culverden and Leonard Mound faults are included but do not rupture. Faults are embedded in high-resolution topography and bathymetry (Mitchell et al., 2012) and 3D subsurface structure (Eberhart-Phillips et al., 2010).

The 2016, Mw7.8 Kaikōura earthquake - a rupture cascade on weak crustal faults

➔ **Reproducing observations and
constraining competing views**

- Rupture propagation across fault segments with diverse orientations and faulting mechanisms does **not require slip on the underlying subduction interface**
- **Slow** apparent rupture velocity from **zigzagging rupture** path
- **Point Kean fault** (Clark et al., 2017) acted as a **crucial link** between the Hundalee fault and the Northern faults
- **Non-rupture of the Hope fault** due to unfavourable dynamic stresses on the restraining step-over formed by the Conway-Charwell and Hope faults

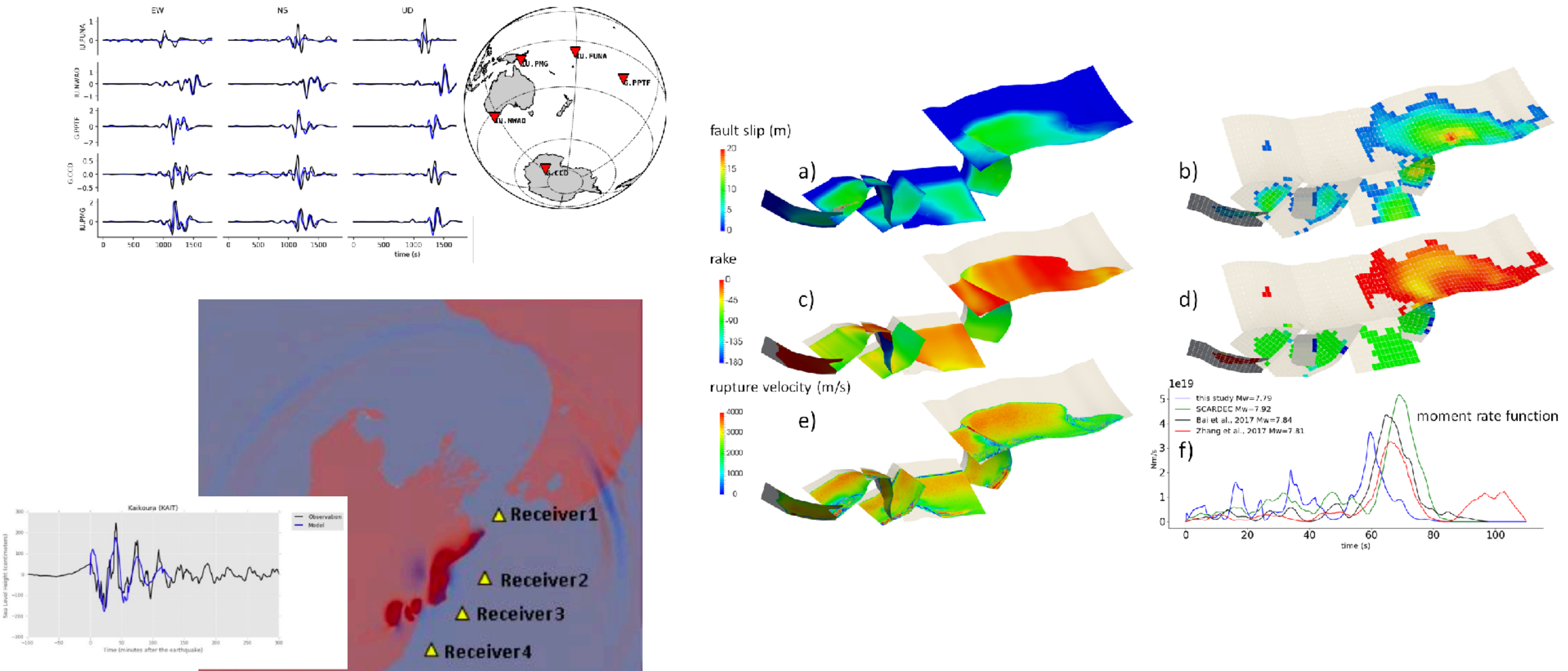


On-fault slip rate and wave speed. Multiple rupture fronts, Point Kean, Papatea and Kekerengu segments slip more than once.

The 2016, Mw7.8 Kaikōura earthquake

- a rupture cascade on weak crustal faults

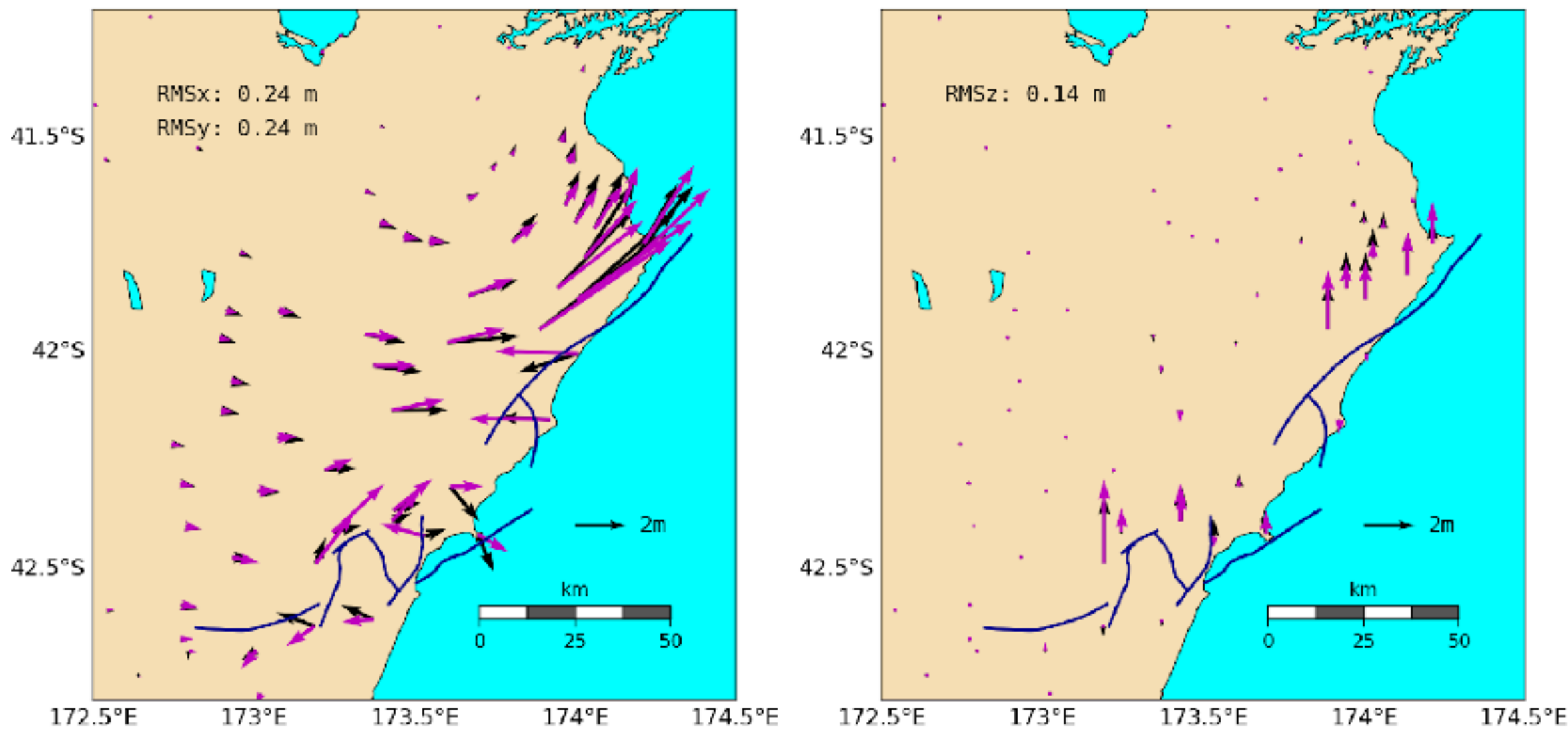
➡ **Constrained by observations**



The 2016, Mw7.8 Kaikōura earthquake

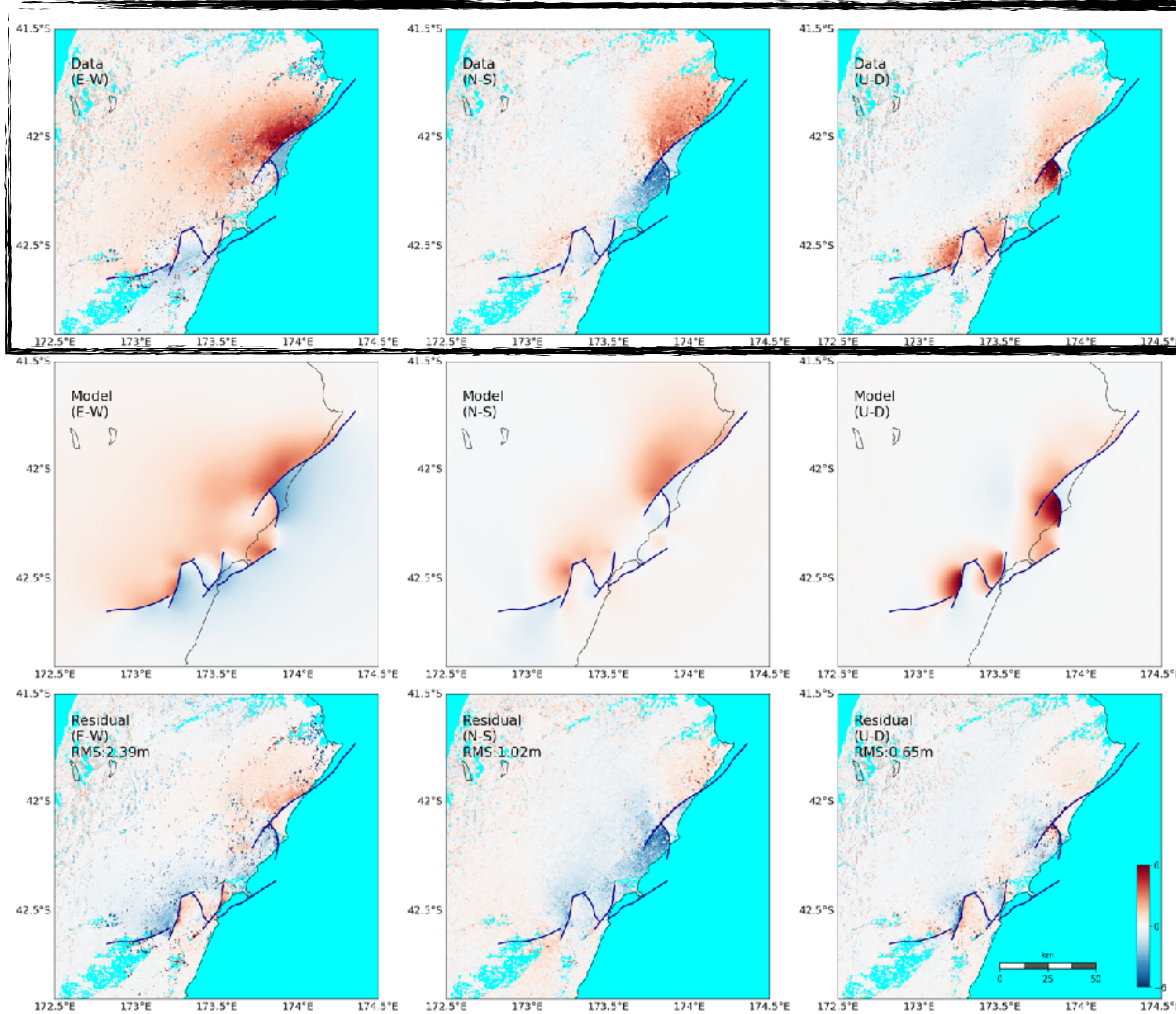
- constrained by observation

- Ground deformation



Comparison of observed (black, Hamling et al. 2017) and modeled (magenta) horizontal (left) and vertical (right) ground displacement at GPS stations. Root-mean-square (RMS) misfits are provided for each component.

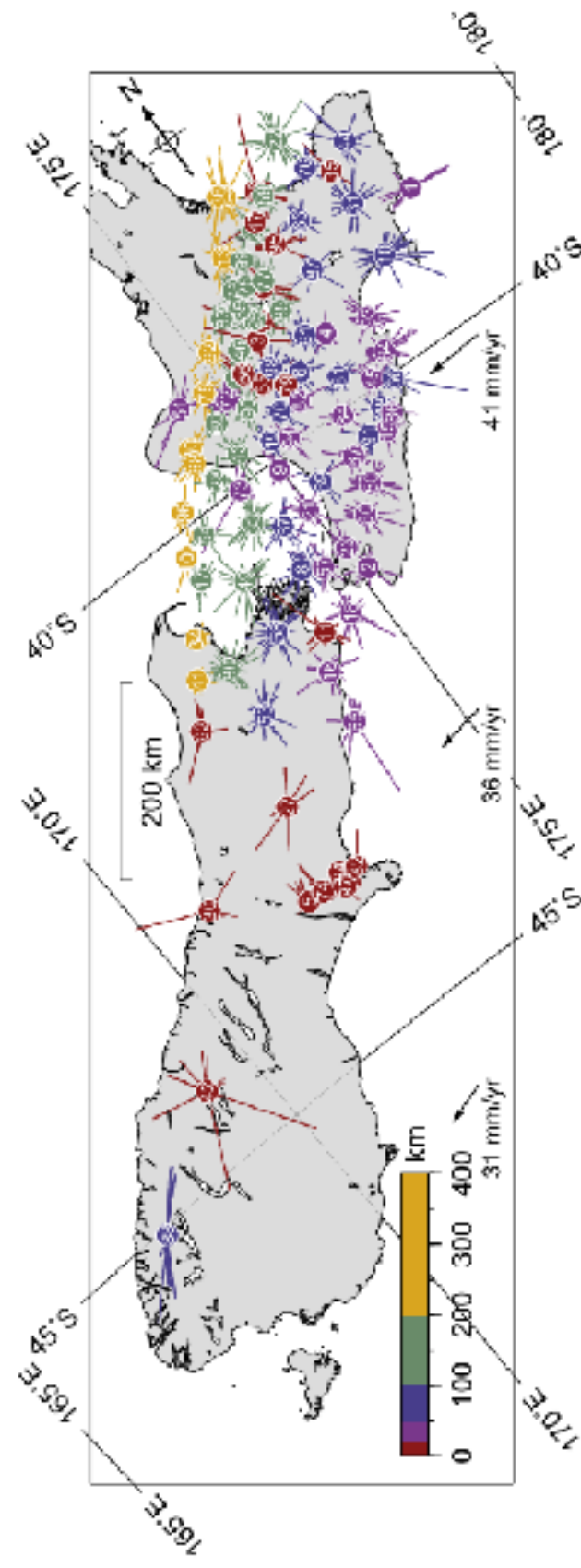
Geodetic data (Xu et al., 2018)



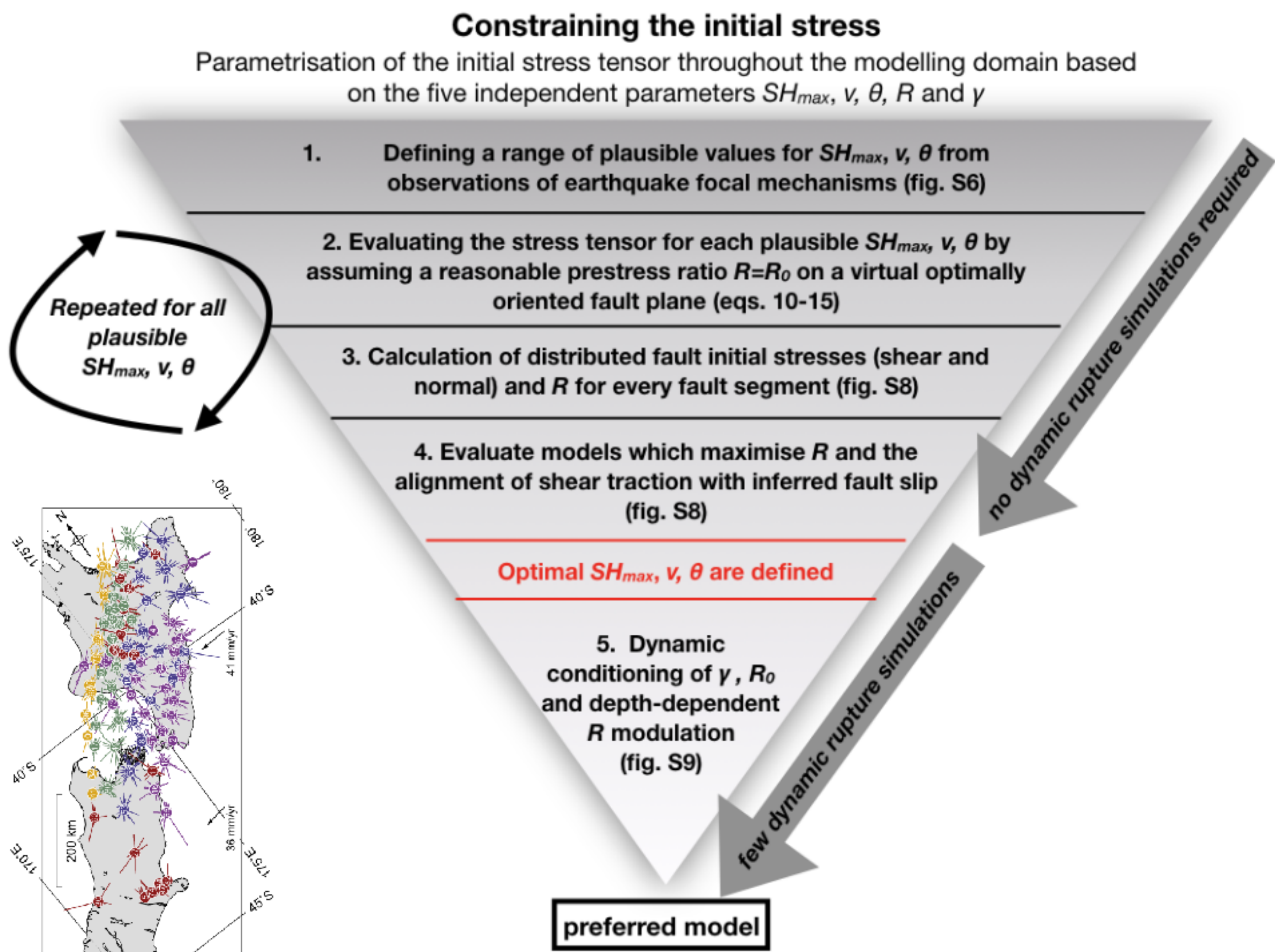
Comparison of observed and modeled coseismic surface displacements. 3D ground displacement (first row) inferred by space geodetic data (Xu et al. 2018), (second row) generated by the dynamic rupture model and (third row) their difference, all in meters. Columns from left to right are EW, NS and UD components. Root-mean-square (RMS) misfits are provided in the third row for each component.

Initial fault stress and strength

We systematically search for a **smoothly varying regional stress** parametrised by:



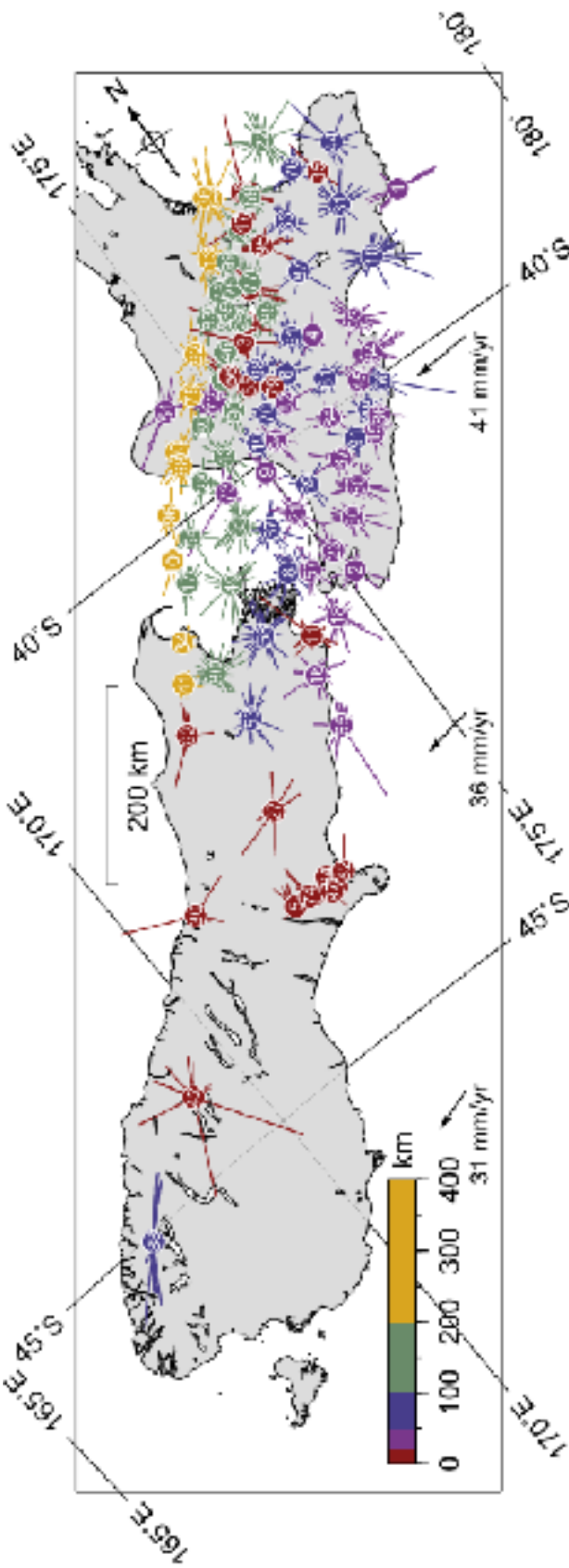
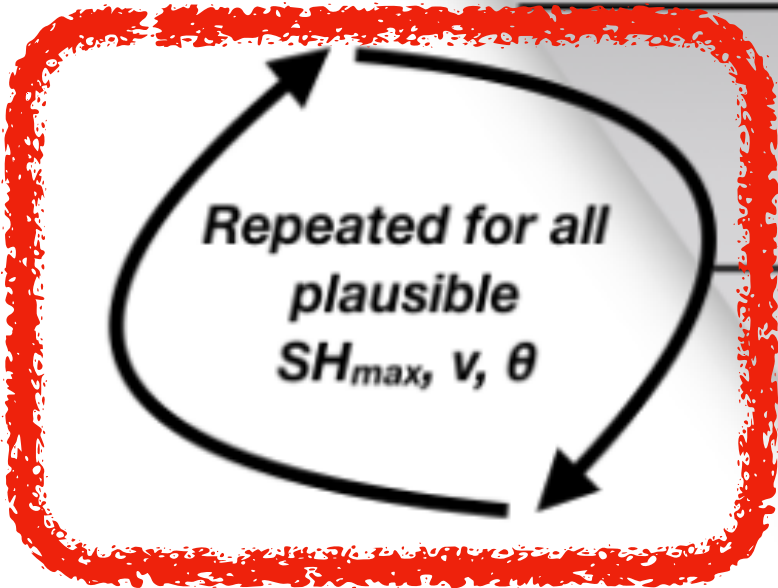
Townend et al., 2012



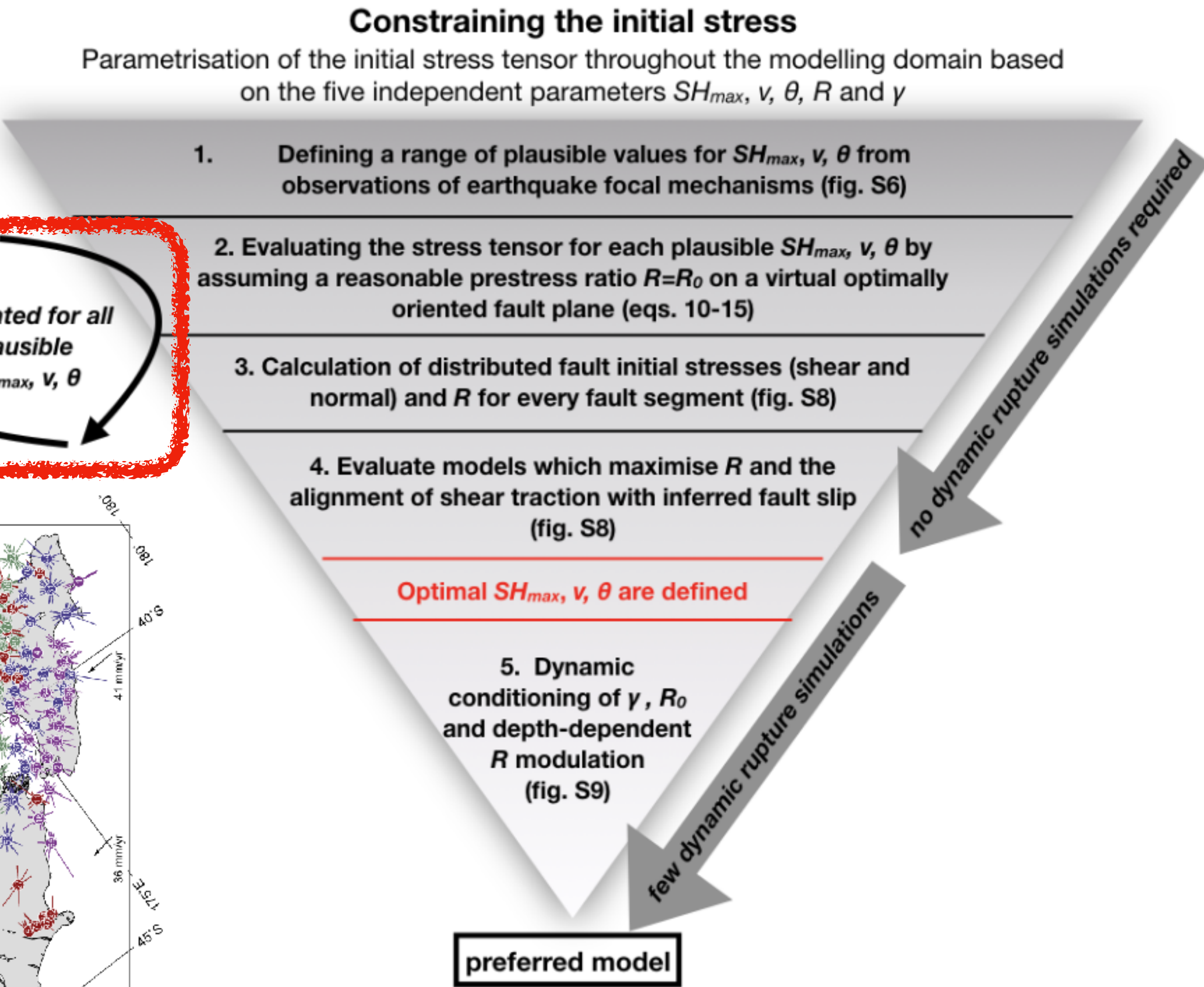
Initial fault stress and strength

We systematically search for a **smoothly varying regional stress** parametrised by:

- In practice: few parameters, **3 unknown**: background shear stress (here **Andersonian**) and the stress shape ratio balancing the principal stress amplitudes (here: **transpressional**) and **fluid pressure** (here: **elevated** but well below lithostatic)

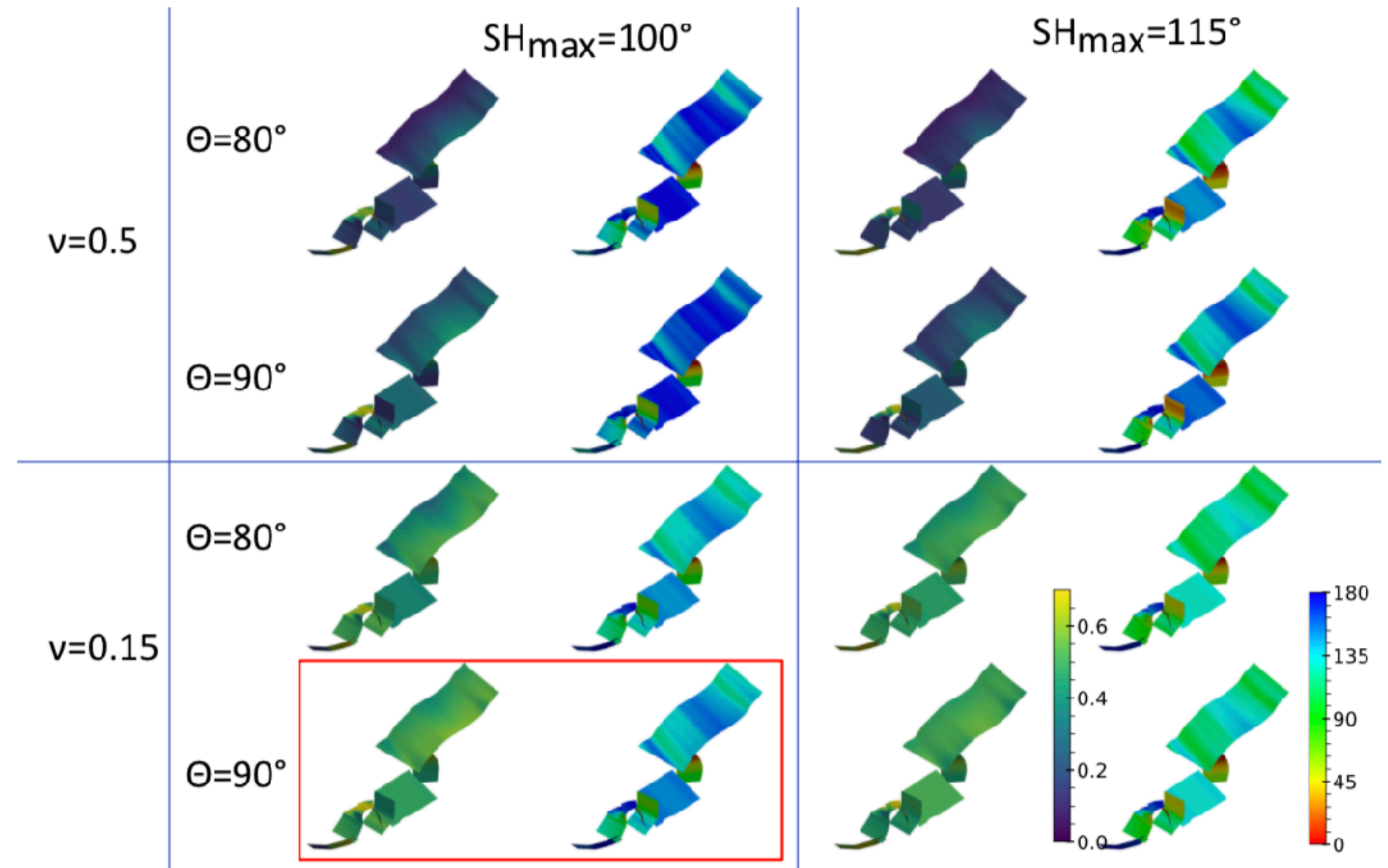


Townend et al., 2012



Initial fault stress and strength

- **Purely statically:** constraining optimal stress parameters within their identified uncertainties **maximising the ratio of shear to normal stress and the alignment between fault shear tractions and inferred slip**
- Few **dynamic rupture simulations** to constrain depth-dependences (intensity of **deep stress concentration**) and dynamic viability



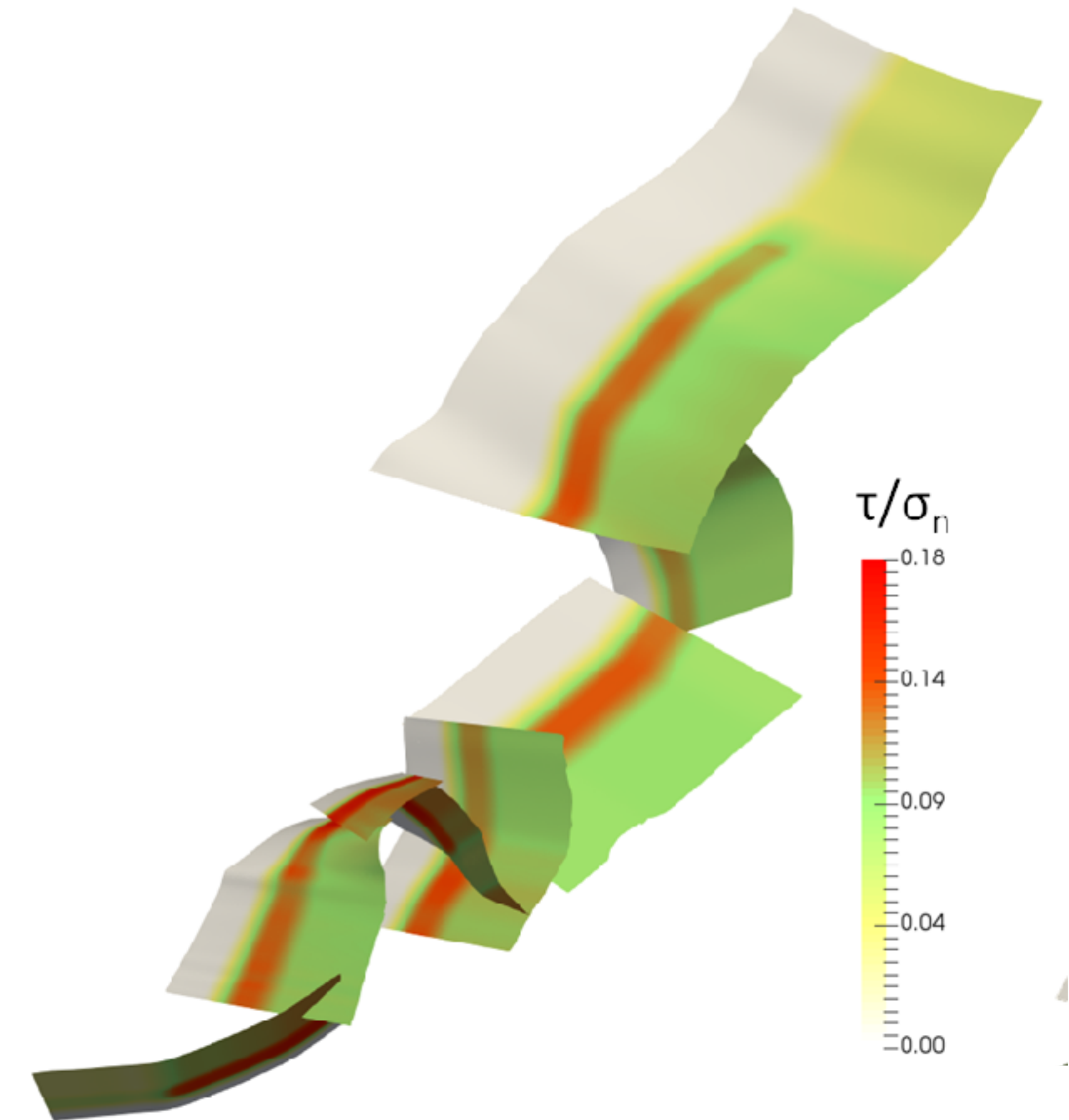
Supplementary Figure 9: A representative sample of initial stress models tested. We show 8 examples that correspond to all permutations involving the two values indicated in the labels for each stress parameter, SH_{\max} , ν and θ . For each example, two plots show the spatial distribution on the fault surfaces of (left) the pre-stress ratio and (right) the rake angle of the shear traction. Here we assume a uniform $R_{\text{opt}}(z) = 0.7$ on the optimal plane.

The 2016, Mw7.8 Kaikōura earthquake

- a rupture cascade on **weak crustal faults**

➡ **Fault weakness across time scales restores dynamic triggering potential**

- Fault weakness (I) - **low dynamic friction**
- Fault weakness (II) - **overpressurized fluids**
- Fault weakness (III) - **deep stress concentration induced by deep fault creep**
- However, faults are overall well oriented - thus not weak in the Andersonian sense



“Optimal stress algorithm” - all faults are overall stressed well below failure and yet break spontaneously.

The 2016, Mw7.8 Kaikōura earthquake

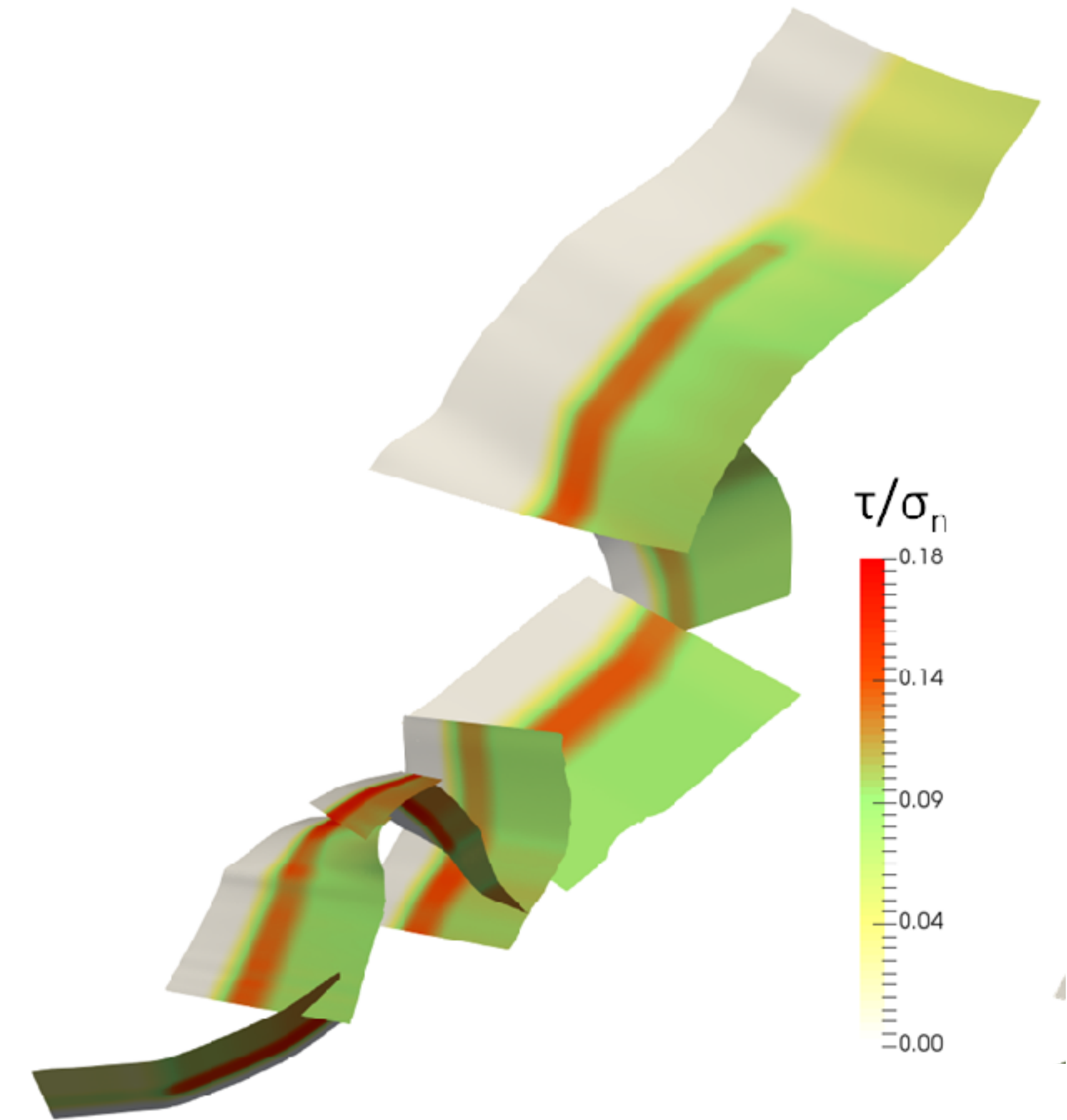
- a rupture cascade on **weak crustal faults**

➔ **Fault weakness across time scales restores dynamic triggering potential**

- Fault weakness (I) - **low dynamic friction**
- Fault weakness (II) - **overpressurized fluids**
- Fault weakness (III) - **deep stress concentration induced by deep fault creep**
- However, faults are overall well oriented - thus not weak in the Andersonian sense

Touching on a major corundum in Earth Sciences:

- **Hypothesis:** mature plate boundary faults are apparently weak (e.g., Zoback, 1987) - BUT: incompatible with Byerlee's high static friction of rock
- **Dynamic weakening** allows faults to operate at low average shear stress - BUT: unfavourable for cascading



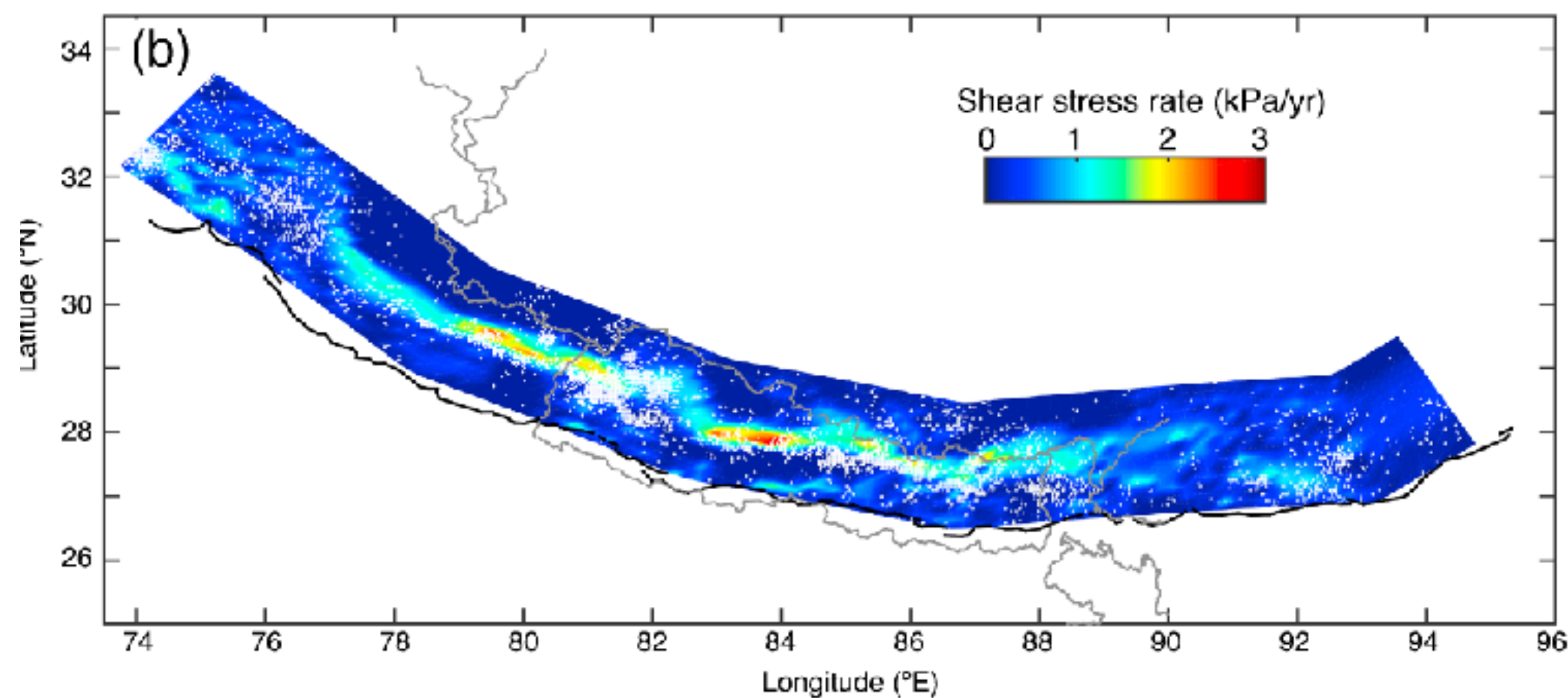
“Optimal stress algorithm” - all faults are overall stressed well below failure and yet break spontaneously.

The 2016, Mw7.8 Kaikōura earthquake

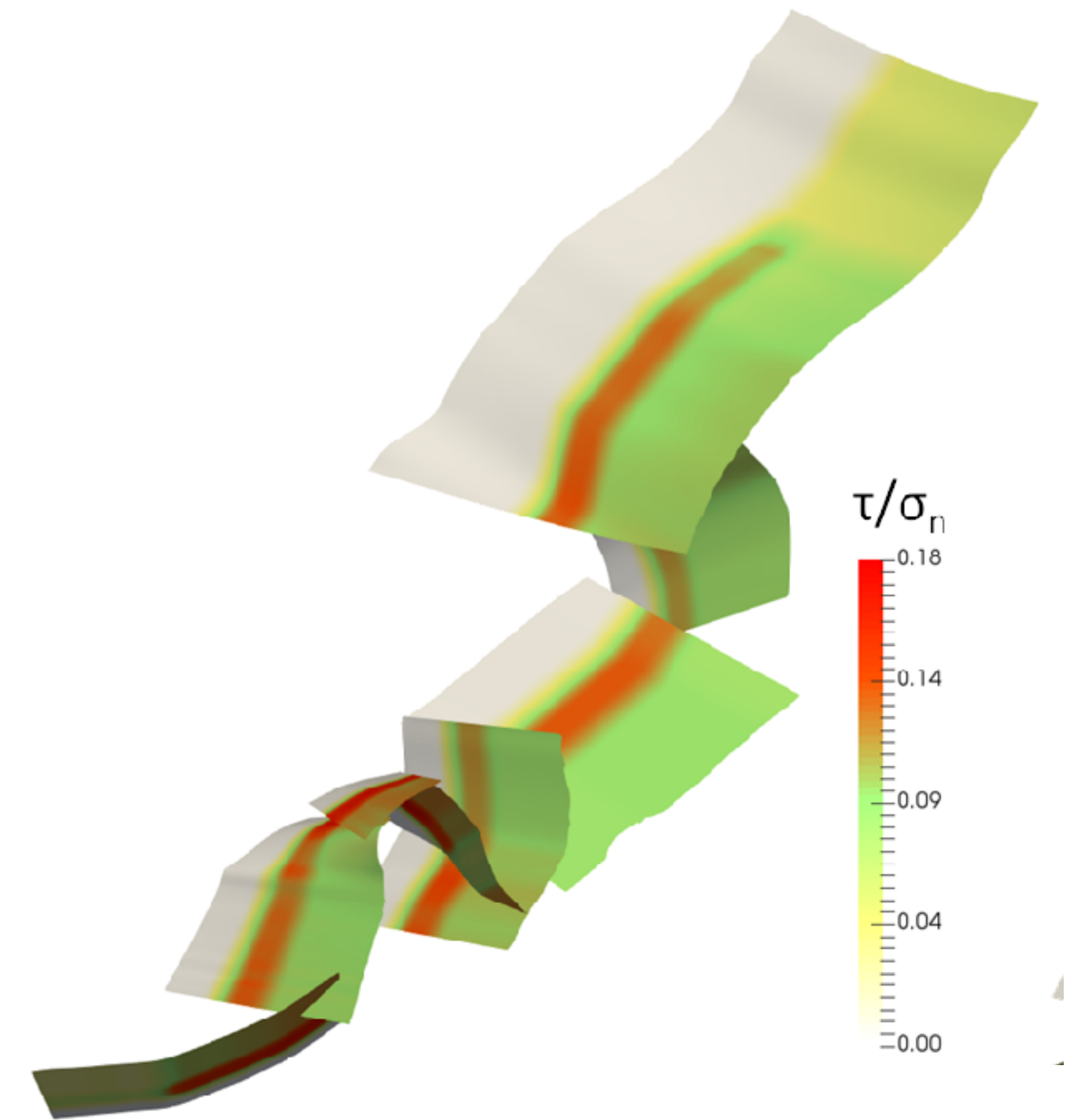
- a rupture cascade on **weak crustal faults**

➔ **Fault weakness across time scales restores dynamic triggering potential**

- Fault weakness (I) - **low dynamic friction**
- Fault weakness (II) - **overpressurized fluids**
- Fault weakness (III) - **deep stress concentration induced by deep fault creep**

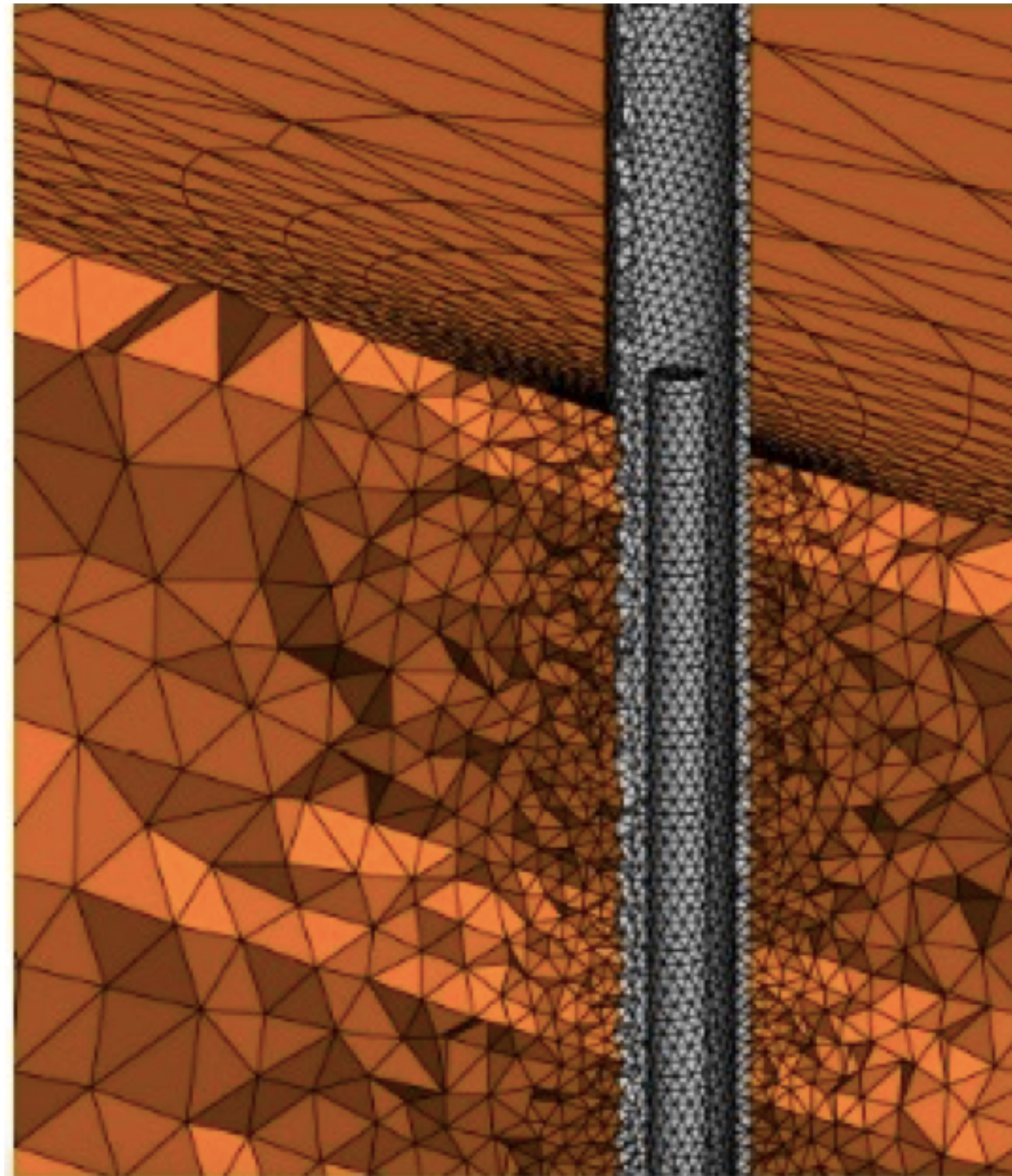


Shear stress accumulation rate on the Main Himalayan Thrust, Stevens and Avouac (2016)



“Optimal stress algorithm” - all faults are overall stressed well below failure and yet break spontaneously.

SEISSOL - A 3D DYNAMIC RUPTURE TOOL USING THE ADER-DG



www.seissol.org

github.com/SeisSol



Extreme Scale Multi-Physics Simulations of the Tsunamigenic 2004 Sumatra Megathrust Earthquake

Carsten Uphoff
Sebastian Rettenberger
Michael Bader
uphoff@in.tum.de
rettenbs@in.tum.de
bader@in.tum.de
Technical University of Munich
Boltzmannstr. 3
85748 Garching, Germany

Elizabeth H. Madden
Thomas Ulrich
Stephanie Wollherr
Alice-Agnes Gabriel
madden@geophysik.uni-muenchen.de
ulrich@geophysik.uni-muenchen.de
wollherr@geophysik.uni-muenchen.de
gabriel@geophysik.uni-muenchen.de
Ludwig-Maximilians-Universität München
Theresienstr. 41
80333 Munich, Germany

SC'17

Petascale High Order Dynamic Rupture Earthquake Simulations on Heterogeneous Supercomputers

Alexander Heinecke^{*‡}, Alexander Breuer^{*}, Sebastian Rettenberger^{*}, Michael Bader^{*},
Alice-Agnes Gabriel[†], Christian Pelties[†],
Arndt Bode^{§*}, William Barth[¶], Xiang-Ke Liao^{||},
Karthikeyan Vaidyanathan^{**}, Mikhail Smelyanskiy[‡], Pradeep Dubey[‡]

SC'14

Discontinuous Galerkin methods for wave propagation in poroelastic media

Geophysics, 2008

Josep de la Puente¹, Michael Dumbser², Martin Käser¹, and Heiner Igel¹

Verification of an ADER-DG method for complex dynamic rupture problems

C. Pelties¹, A.-A. Gabriel¹, and J.-P. Ampuero²

GMD, 2014

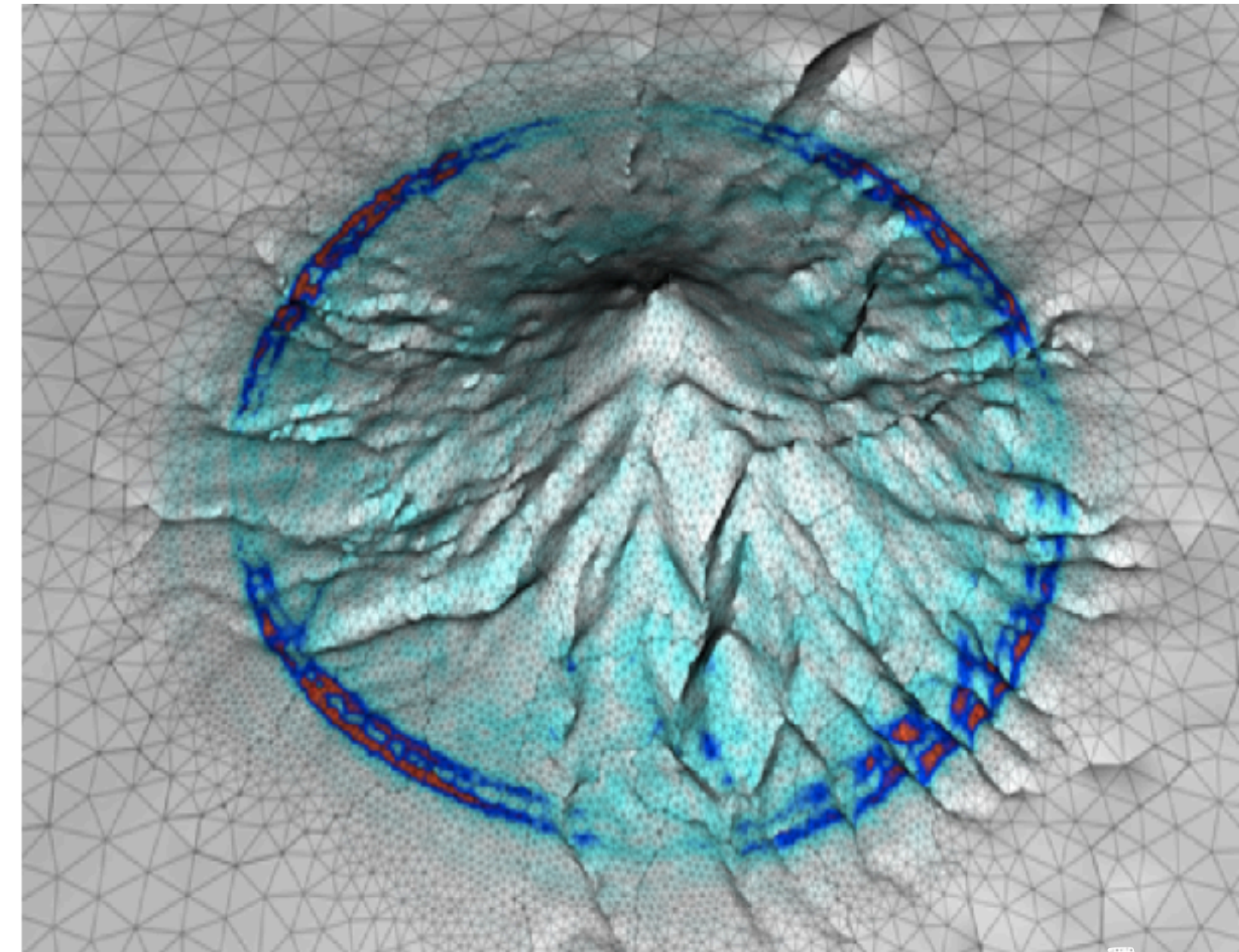
SEISSOL - ADER-DG

A UNIQUE MODELLING FRAMEWORK

We develop and host an open-source Arbitrary high-order DERivative Discontinuous Galerkin (**ADER-DG**) software package. SeisSol solves the seismic wave equations in elastic, viscoelastic, and viscoplastic media on unstructured tetrahedral meshes.

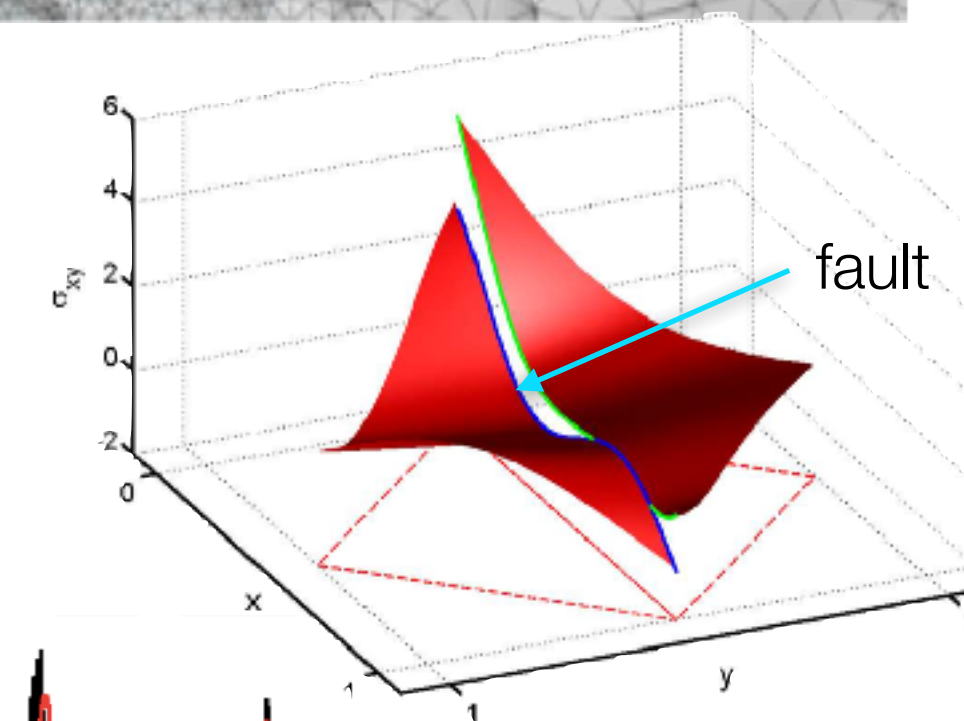
The method, by design, permits:

- representing **complex geometries** - by discretising the volume via a tetrahedral mesh
- modelling **heterogenous media** - elastic, viscoelastic, viscoplastic, anisotropic
- **multi-physics coupling** - flux based formulation is natural for representing physics defined on interfaces
- **high accuracy** - modal flux based formulation allows us to suppress spurious (unresolved) high frequencies
- **high resolution** - suitable for parallel computing environments

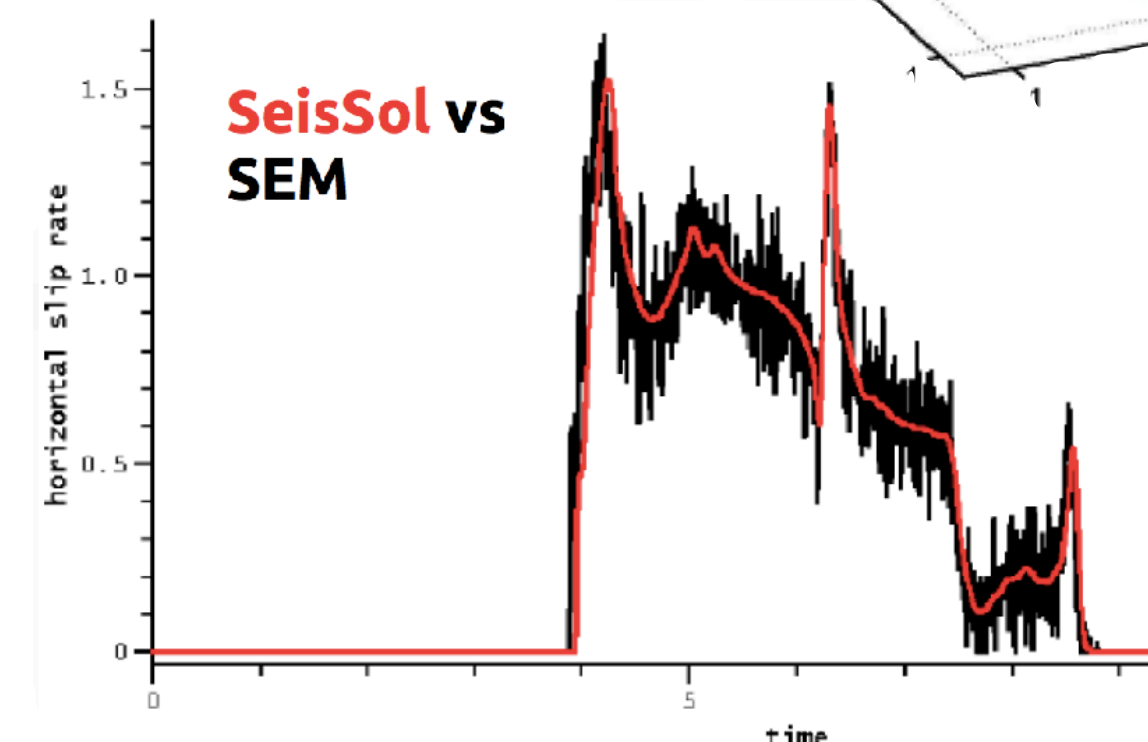


Wave field of a point source interacting with the topography of Mount Merapi Volcano.

PRACE ISC Award for producing the first simulations that obtained the “magical” performance milestone of 1 Peta-flop/s (10^{15} floating point operations per second) at the Munich Supercomputing Centre.



Representation of the shear stress discontinuity across the fault interface. Spontaneous rupture = internal boundary condition of flux term.



Due to the properties of the exact Riemann solver, solutions on the fault remain free of spurious oscillations

SEISSOL - ADER-DG

A UNIQUE MODELLING FRAMEWORK

Why DG? Low numerical dispersion, minor changes for dynamic rupture, intersecting and branching faults/structure

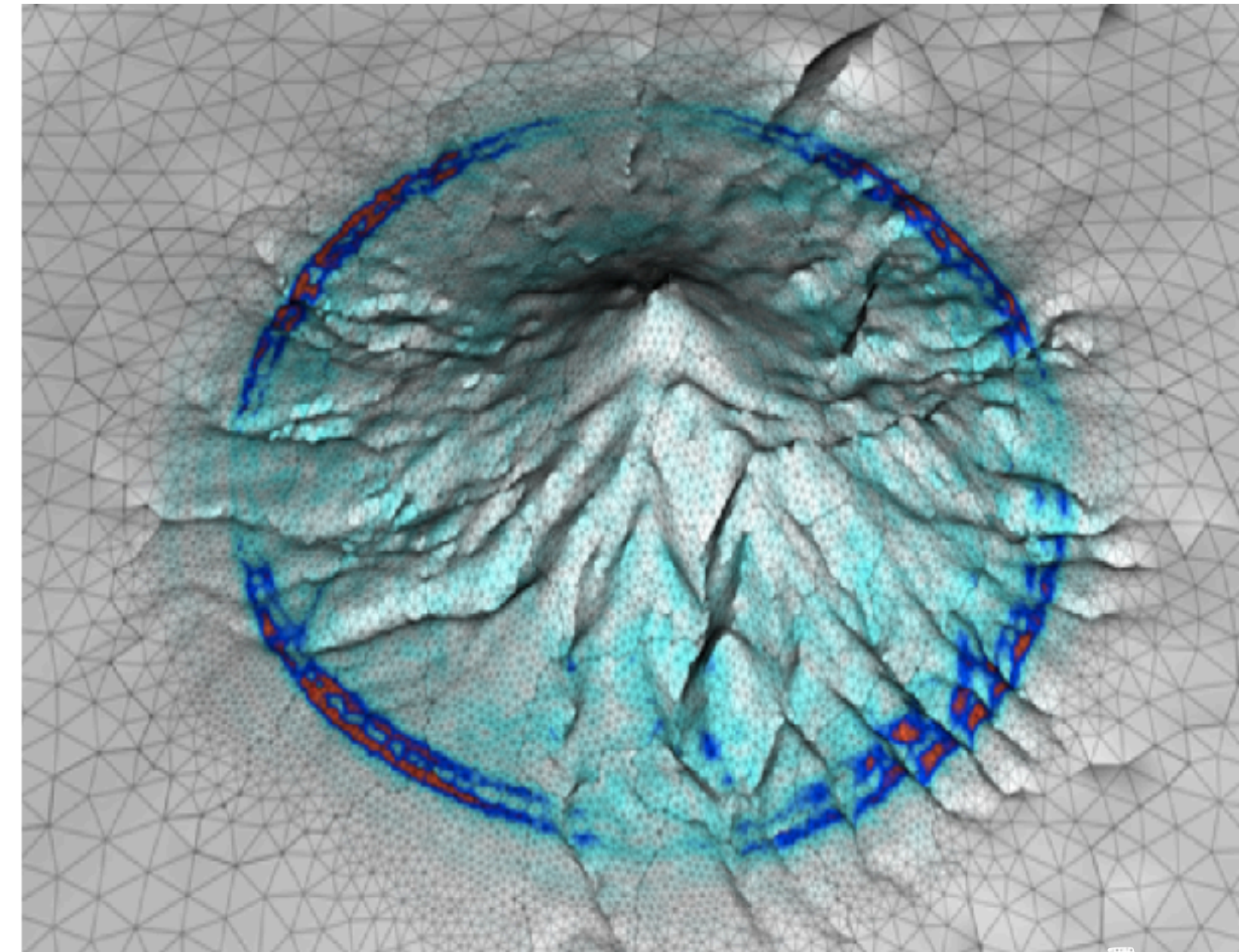
Why ADER? Equivalent high-order accuracy as in space using a single explicit time integration step. Increasing order of accuracy can be 'cheap' if hardware is exploited)

Why tets? Complex realities of geological subsurface, non-planar fault surfaces, intersecting undulating surfaces, static mesh refinement and coarsening

Why modal formulation? Favourable numerical dissipation of the Godunov flux (Hu et al. 1999; Kaeser et al. 2008; Hesthaven & Warburton 2010), easy to build arbitrary high-order basis functions for tets

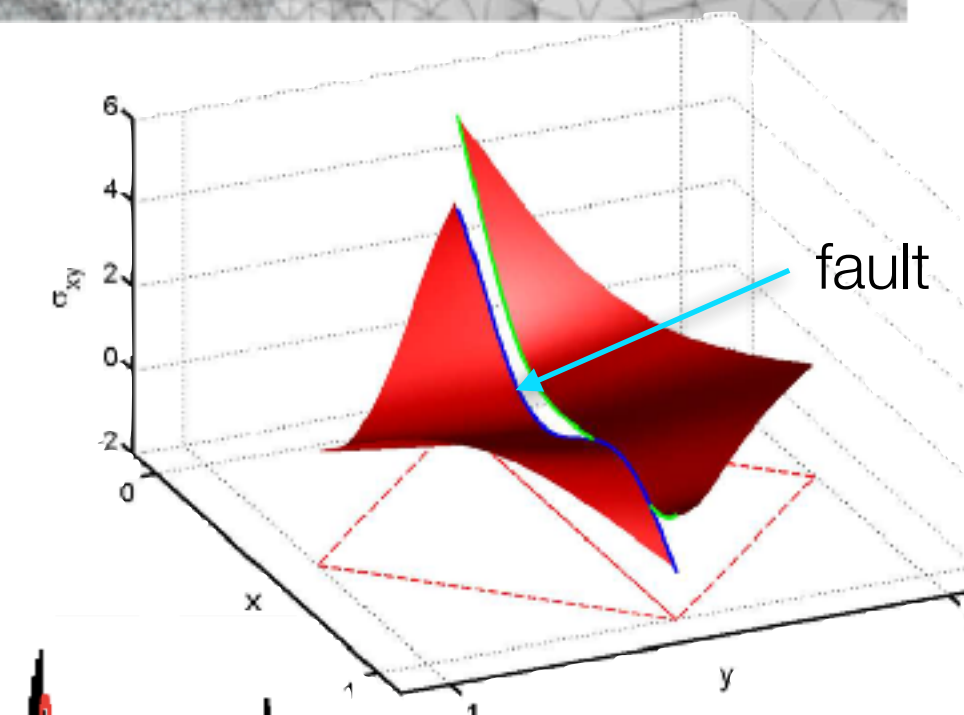
Why orthogonal basis functions? Dubiner's basis functions (Cockburn et al. 2000), leads to diagonal mass matrix, all matrices can then be precalculated analytically leading to a quadrature-free scheme (e.g., Atkins & Shu 1996)

Käser and Dumbser, 2006; de la Puente et al., 2008; Pelties et al., 2014

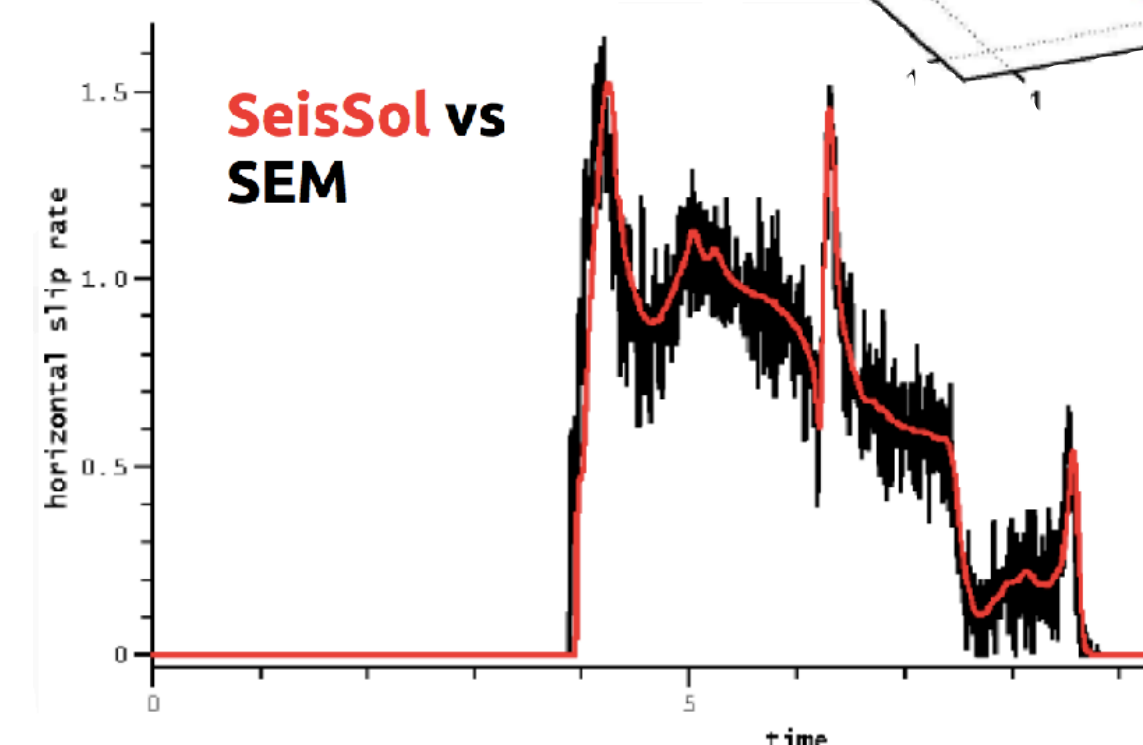


Wave field of a point source interacting with the topography of Mount Merapi Volcano.

PRACE ISC Award for producing the first simulations that obtained the "magical" performance milestone of 1 Peta-flop/s (10^{15} floating point operations per second) at the Munich Supercomputing Centre.



Representation of the shear stress discontinuity across the fault interface. Spontaneous rupture = internal boundary condition of flux term.



Due to the properties of the exact Riemann solver, solutions on the fault remain free of spurious oscillations

SEISSOL - ADER-DG

A UNIQUE MODELLING FRAMEWORK

Why DG? Low numerical dispersion, minor changes for dynamic rupture, intersecting and branching faults/structure

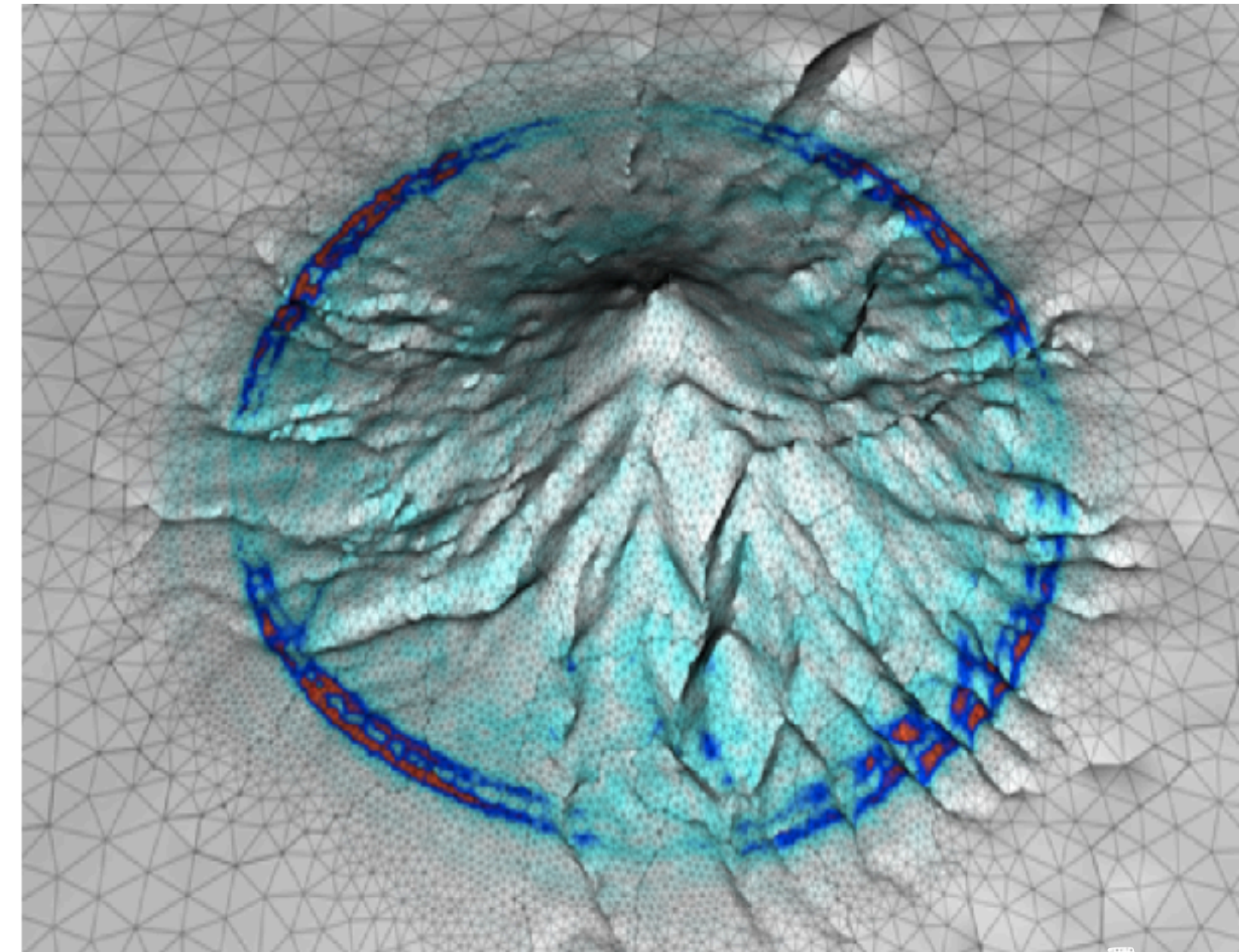
Why ADER? Equivalent high-order accuracy as in space using a single explicit time integration step. Increasing order of accuracy can be 'cheap' if hardware is exploited)

Why tets? Complex realities of geological subsurface, non-planar fault surfaces, intersecting undulating surfaces, static mesh refinement and coarsening

Why of the Hest orde
A software that allows for rapid setup of models with realistic non-planar and intersecting fault systems while exploiting the accuracy of a high-order numerical method

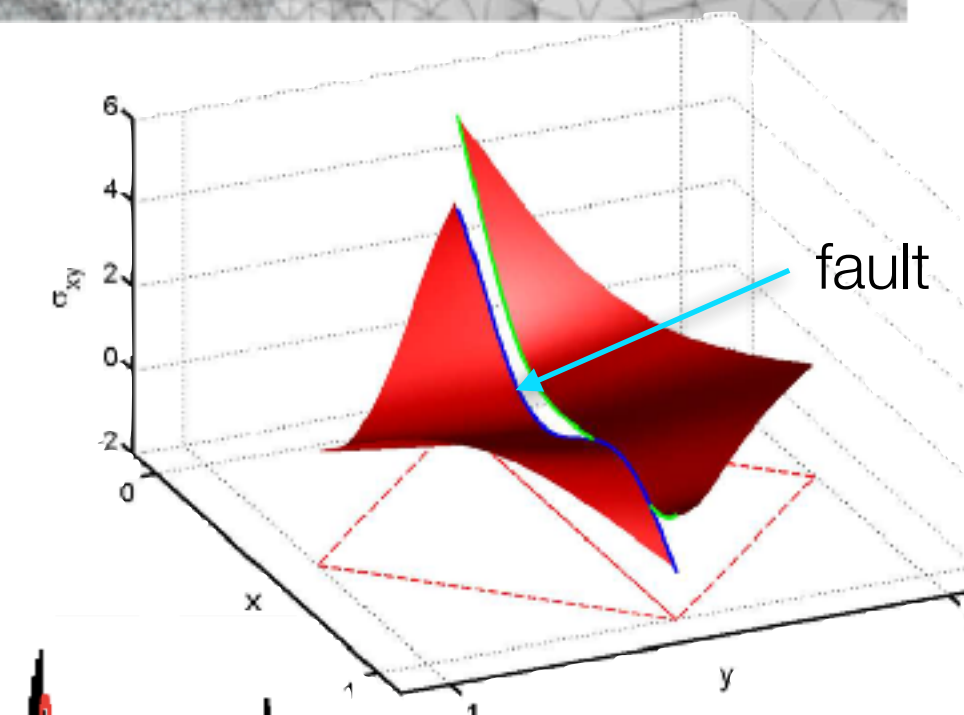
Why orthogonal basis functions? Dubiner's basis functions (Cockburn et al. 2000), leads to diagonal mass matrix, all matrices can then be precalculated analytically leading to a quadrature-free scheme (e.g., Atkins & Shu 1996)

Käser and Dumbser, 2006; de la Puente et al., 2008; Pelties et al., 2014

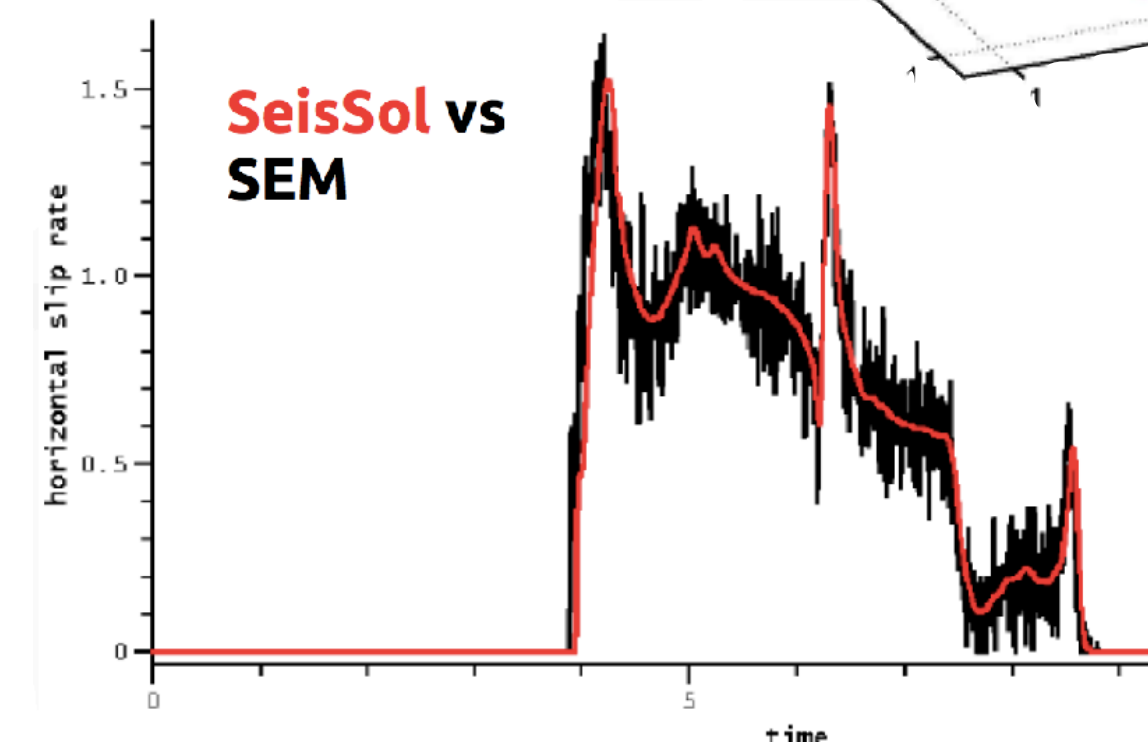


Wave field of a point source interacting with the topography of Mount Merapi Volcano.

PRACE ISC Award for producing the first simulations that obtained the "magical" performance milestone of 1 Peta-flop/s (10^{15} floating point operations per second) at the Munich Supercomputing Centre.



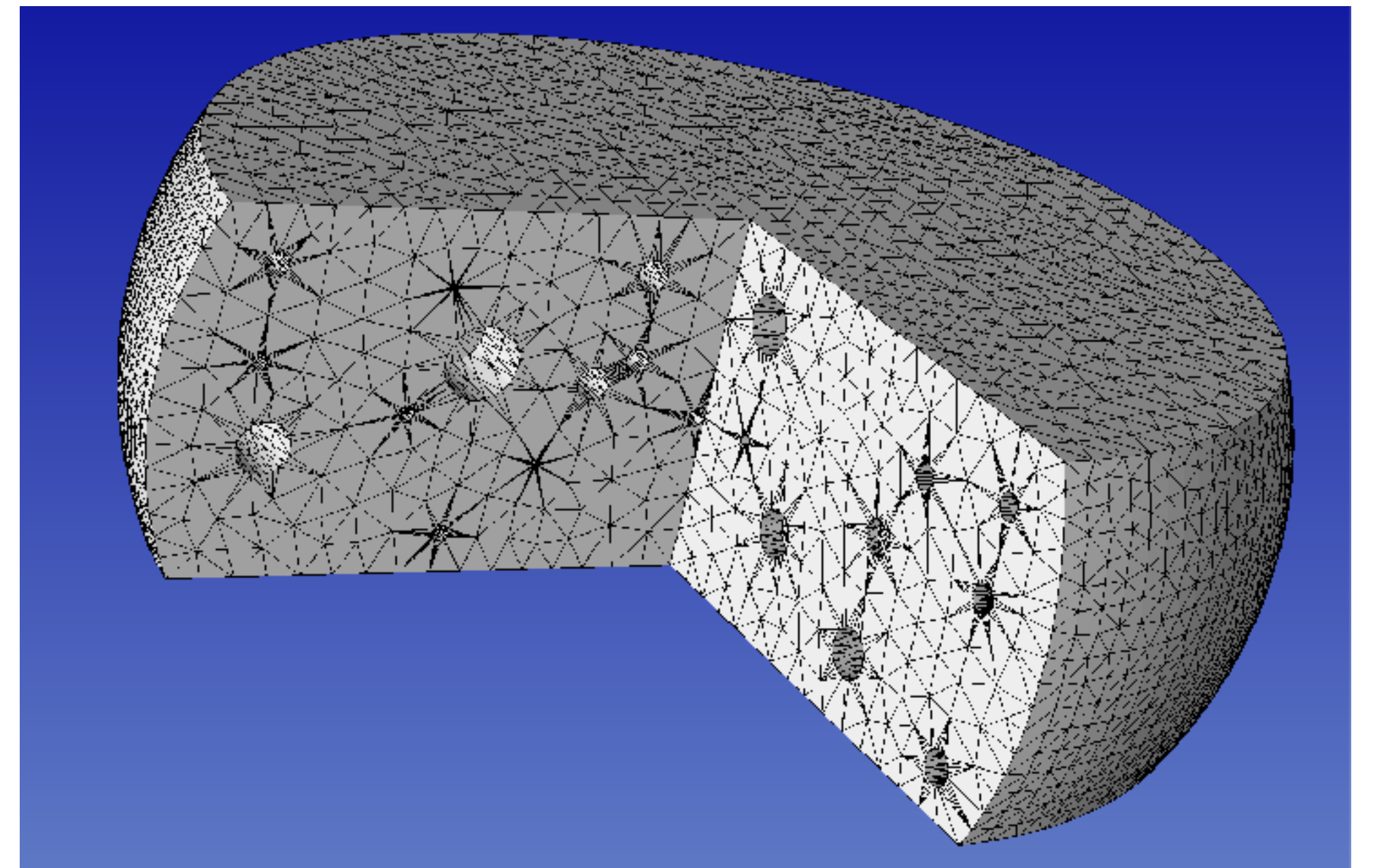
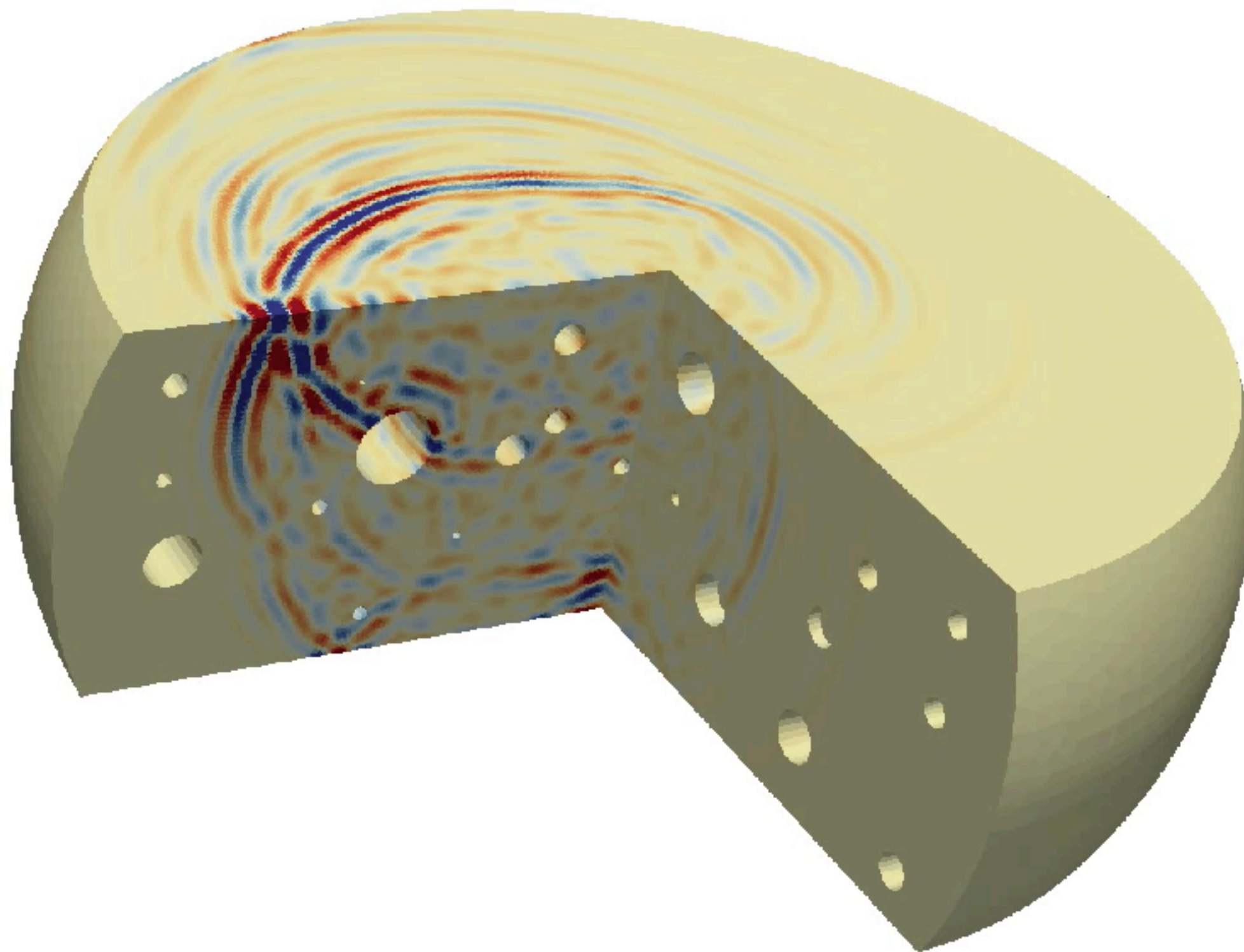
Representation of the shear stress discontinuity across the fault interface. Spontaneous rupture = internal boundary condition of flux term.



Due to the properties of the exact Riemann solver, solutions on the fault remain free of spurious oscillations

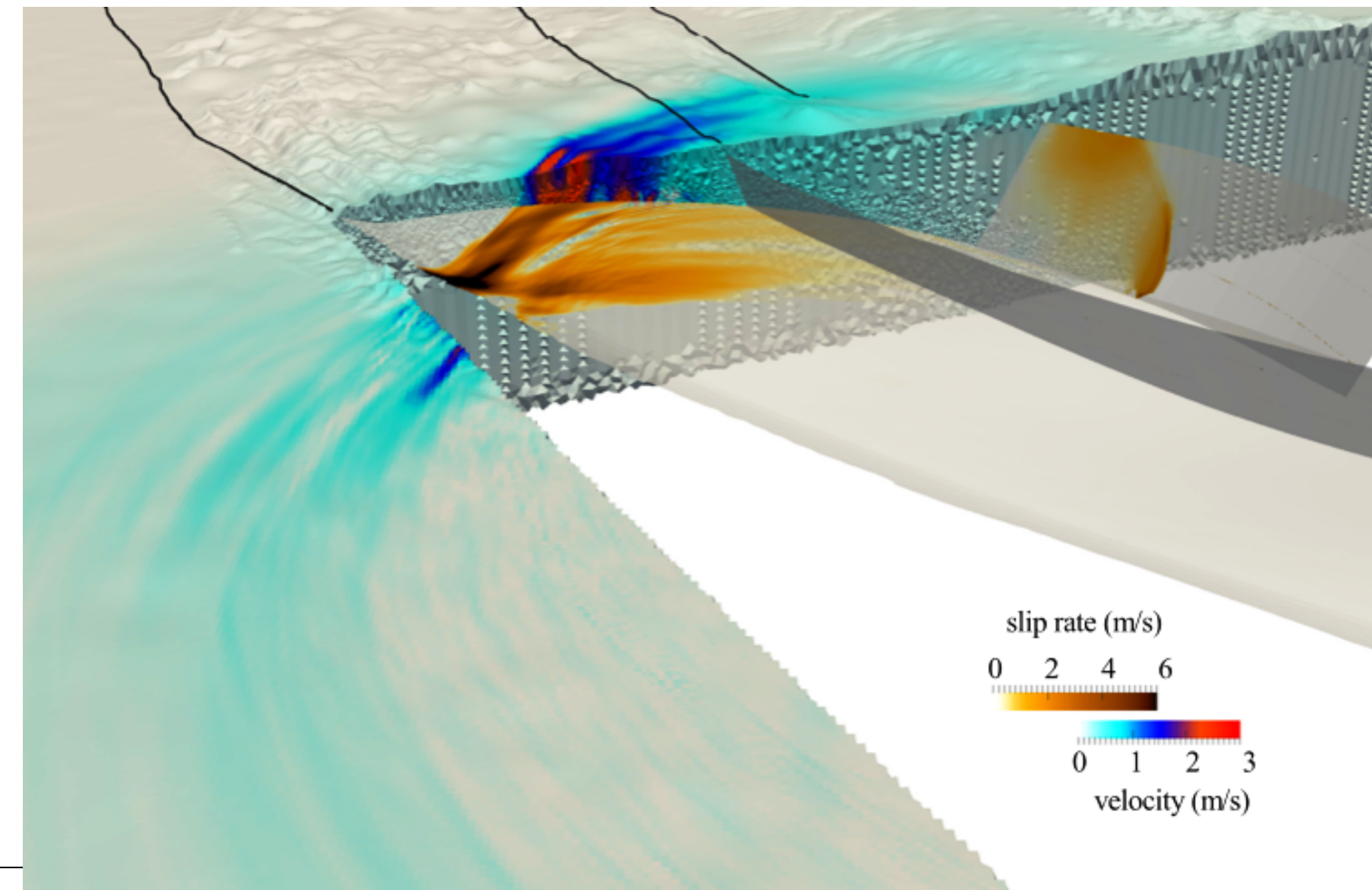
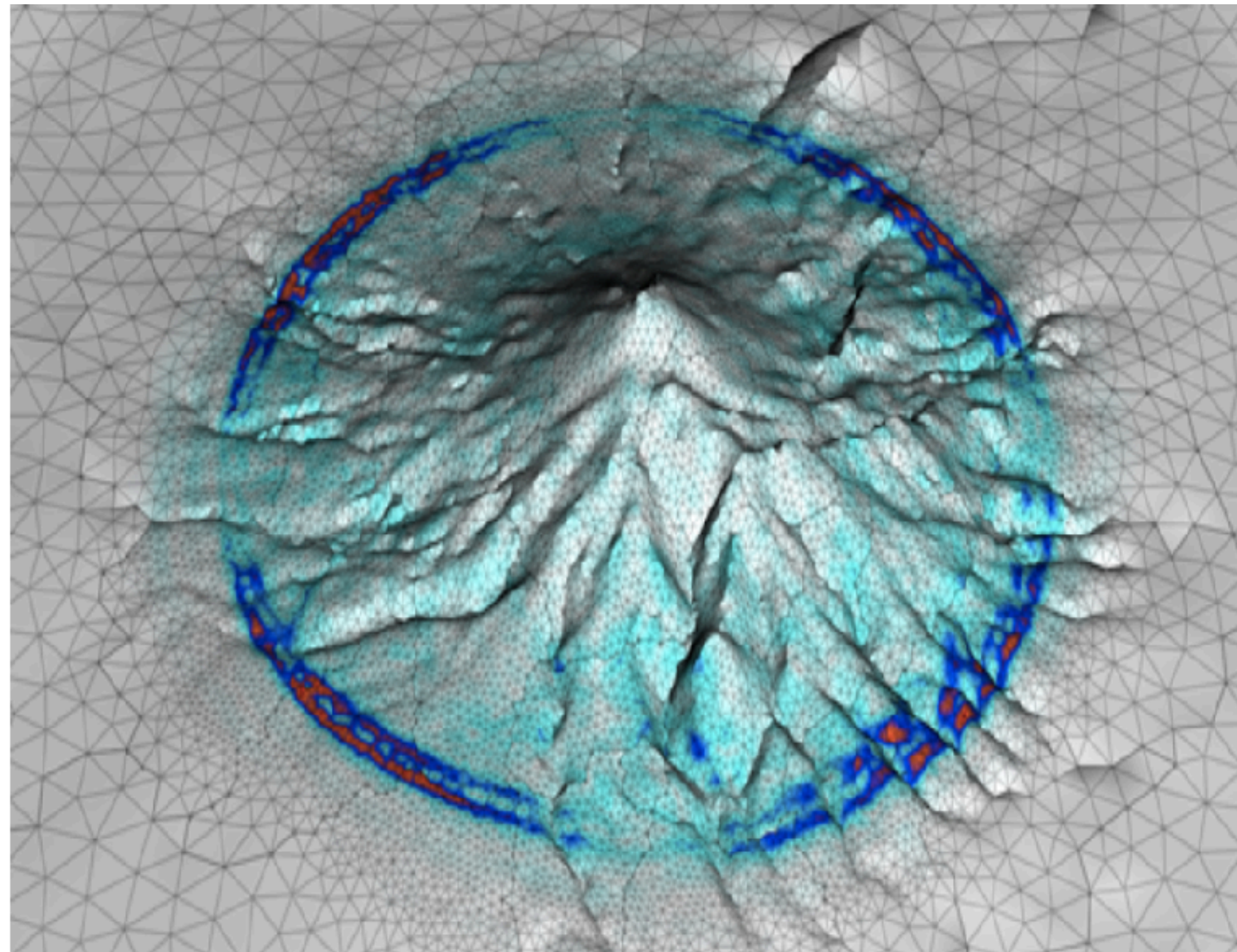
THE “GRAND CHALLENGE” OF MESHING

- Community standard 1) **Hexahedral** meshes - can easily consume **weeks to months**, is **limited** for complex geometries (external / internal boundary conditions)
- Community standard 2) **Unstructured tetrahedral** meshes - allows automatised meshing and complex internal/ external boundary conditions - however are numerically challenging (sliver elements)



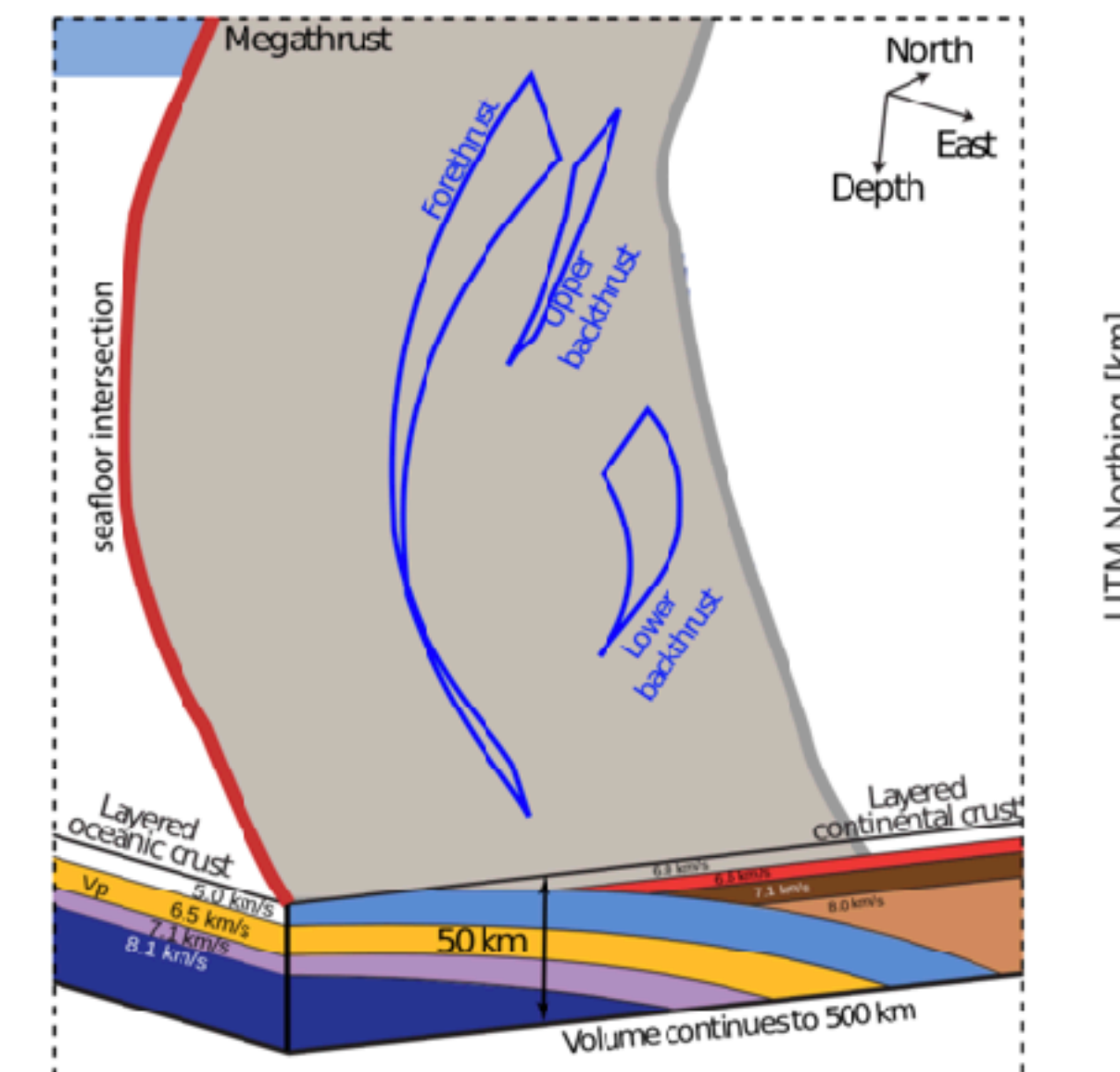
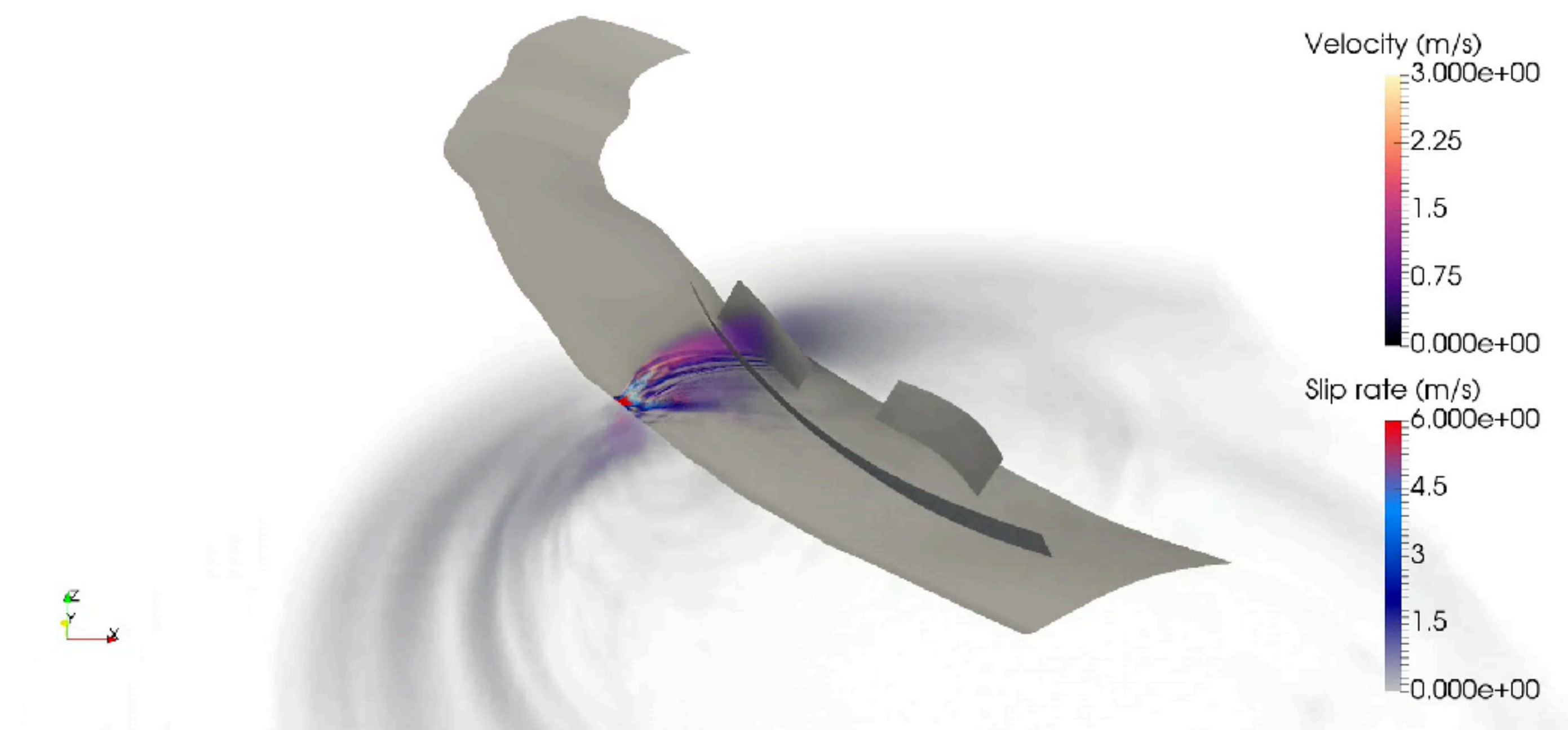
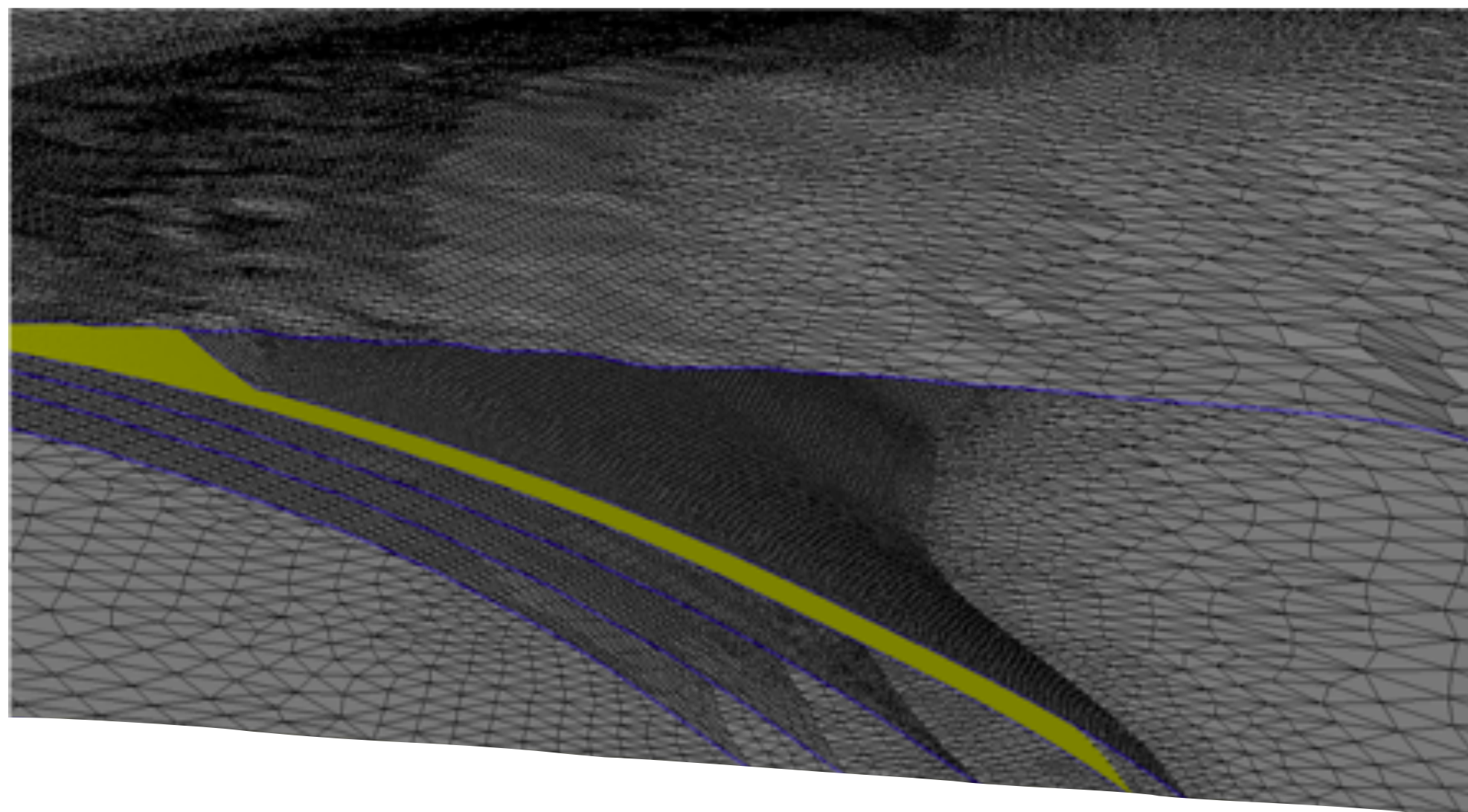
THE “GRAND CHALLENGE” OF MESHING

- Community standard 1) **Hexahedral** meshes - can easily consume **weeks to months**, is **limited** for complex geometries (external / internal boundary conditions)
- Community standard 2) **Unstructured tetrahedral** meshes - allows automatised meshing and complex internal/ external boundary conditions - however are numerically challenging (sliver elements)



Sumatra megathrust & splay faults scenario

- Complex, non-planar **intersections, at shallow angles**
CAD and mesh generation is a bottleneck
- **Small-ish “pop-up” fractures splaying off the curved megathrust that itself merges with the bathymetry in narrow subduction wedges** - requires numerical methods handling geometric complexity and highly varying element sizes



DG vs FEM

Considering one mesh type, say hexahedral, and a nodal DG method:

- Then DG is **considerably more expensive** than a Finite Element method

Requirements for solving conservation laws				
	FVM	FDM	FEM	DGFEM
High-order/Low dispersion	no	yes	yes	yes
Unstructured hybrid meshes	yes	no	yes	yes
High-order meshes	no	no	yes	yes
Stability	yes	no	no	yes

I here define in the context of dynamic rupture the "stability" **for both FDM and FEM** is labeled as "no" which means the solutions are highly oscillatory

What does ‘computationally expensive’ actually mean ?

DG vs FEM

Considering one mesh type, say hexahedral, and a nodal DG method:

- Then DG is **considerably more expensive** than a Finite Element method

1) storage

2) time-to-solution

1a) DG stores **duplicate DoFs** on the cell edges, faces and vertices

1b) best defined using **first-order systems** (FE typically solves second order systems, storing the symmetric stress tensor represents 2x more DOFs compared to the unknowns for velocity)

2a) more DoF's need to be updated each time step

2b) requires to evaluate the flux on each cell face (which can be expensive)

Requirements for solving conservation laws				
	FVM	FDM	FEM	DGFEM
High-order/Low dispersion	no	yes	yes	yes
Unstructured hybrid meshes	yes	no	yes	yes
High-order meshes	no	no	yes	yes
Stability	yes	no	no	yes

I here define in the context of dynamic rupture the "stability" **for both FDM and FEM** is labeled as "no" which means the solutions are highly oscillatory

DG vs FEM

Considering one mesh type, say hexahedral, and a nodal DG method:

- Then DG is **considerably more expensive** than a Finite Element method

- 1) storage
- 2) time-to-solution

- Good news: all these extra flops can be performed **really** fast using Computational Science.
- And: Comparisons are not ‘fair’ if a method is specifically suitable for your problem at hand.

Requirements for solving conservation laws				
	FVM	FDM	FEM	DGFEM
High-order/Low dispersion	no	yes	yes	yes
Unstructured hybrid meshes	yes	no	yes	yes
High-order meshes	no	no	yes	yes
Stability	yes	no	no	yes

I here define in the context of dynamic rupture the "stability" **for both FDM and FEM** is labeled as "no" which means the solutions are highly oscillatory

DG vs FINITE VOLUMES (FV)

- Finite volume methods are barely used for 3D dynamic rupture modeling
- Some reasons are:
 - High-order schemes which reduce numerical dispersion are very hard to be implemented with FV on **unstructured hex or tet meshes** (hard math problem)
 - Optimization is hard since there is no common pattern in the data structures
- DG has all the benefits of a finite volume method but simple data structures since all operations happen in one cell
- DG allows high-order time integration (ADER)



See also the free online course by Heiner Igel [Computers, Waves, Simulations: A Practical Introduction to Numerical Methods using Python](#)

SEISSOL - ADER-DG

NUMERICS IN A NUTSHELL

- **Elastic wave equation** in velocity stress formulation

linear hyperbolic system

$$\frac{\partial Q_p}{\partial t} + A_{pq} \frac{\partial Q_q}{\partial x} + B_{pq} \frac{\partial Q_q}{\partial y} + C_{pq} \frac{\partial Q_q}{\partial z} = S_p$$

$$Q = (\sigma_{xx}, \sigma_{yy}, \sigma_{zz}, \sigma_{xy}, \sigma_{yz}, \sigma_{xz}, u, v, w)^T$$

$$\frac{\partial}{\partial t} \sigma_{xx} - (\lambda + 2\mu) \frac{\partial}{\partial x} u - \lambda \frac{\partial}{\partial y} v - \lambda \frac{\partial}{\partial z} w = 0,$$

$$\frac{\partial}{\partial t} \sigma_{yy} - \lambda \frac{\partial}{\partial x} u - (\lambda + 2\mu) \frac{\partial}{\partial y} v - \lambda \frac{\partial}{\partial z} w = 0,$$

$$\frac{\partial}{\partial t} \sigma_{zz} - \lambda \frac{\partial}{\partial x} u - \lambda \frac{\partial}{\partial y} v - (\lambda + 2\mu) \frac{\partial}{\partial z} w = 0,$$

$$\frac{\partial}{\partial t} \sigma_{xy} - \mu \left(\frac{\partial}{\partial x} v + \frac{\partial}{\partial y} u \right) = 0,$$

$$\frac{\partial}{\partial t} \sigma_{yz} - \mu \left(\frac{\partial}{\partial z} v + \frac{\partial}{\partial y} w \right) = 0,$$

$$\frac{\partial}{\partial t} \sigma_{xz} - \mu \left(\frac{\partial}{\partial z} u + \frac{\partial}{\partial x} w \right) = 0,$$

$$\rho \frac{\partial}{\partial t} u - \frac{\partial}{\partial x} \sigma_{xx} - \frac{\partial}{\partial y} \sigma_{xy} - \frac{\partial}{\partial z} \sigma_{xz} = 0,$$

$$\rho \frac{\partial}{\partial t} v - \frac{\partial}{\partial x} \sigma_{xy} - \frac{\partial}{\partial y} \sigma_{yy} - \frac{\partial}{\partial z} \sigma_{yz} = 0,$$

$$\rho \frac{\partial}{\partial t} w - \frac{\partial}{\partial x} \sigma_{xz} - \frac{\partial}{\partial y} \sigma_{yz} - \frac{\partial}{\partial z} \sigma_{zz} = 0,$$

constitutive relationships in terms of velocity

conservation of momentum

SEISSOL - ADER-DG

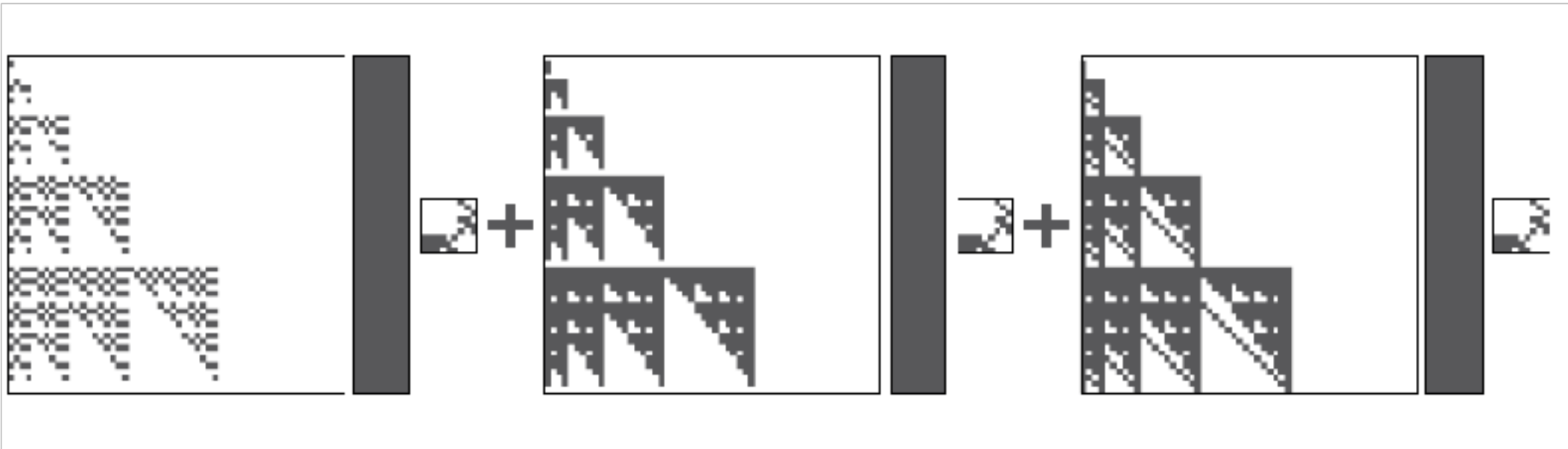
NUMERICS IN A NUTSHELL

- **Elastic wave equation** in velocity stress formulation
- **ADER:** high-order time integration + **DG:** high-order space discretisation
- DG with orthogonal basis functions (**modal**)
- **Exact Riemann-Solver** computes the upwind flux = state at the element interfaces

$$\frac{\partial Q_p}{\partial t} + A_{pq} \frac{\partial Q_q}{\partial x} + B_{pq} \frac{\partial Q_q}{\partial y} + C_{pq} \frac{\partial Q_q}{\partial z} = S_p$$

$$Q = (\sigma_{xx}, \sigma_{yy}, \sigma_{zz}, \sigma_{xy}, \sigma_{yz}, \sigma_{xz}, u, v, w)^T$$

$$\tilde{K}^\xi \left(j_k^{n,n+1} \right) A_k^\star + \tilde{K}^\eta \left(j_k^{n,n+1} \right) B_k^\star + \tilde{K}^\zeta \left(j_k^{n,n+1} \right) C_k^\star$$



DG discrete form

DG operators

SEISSOL - ADER-DG

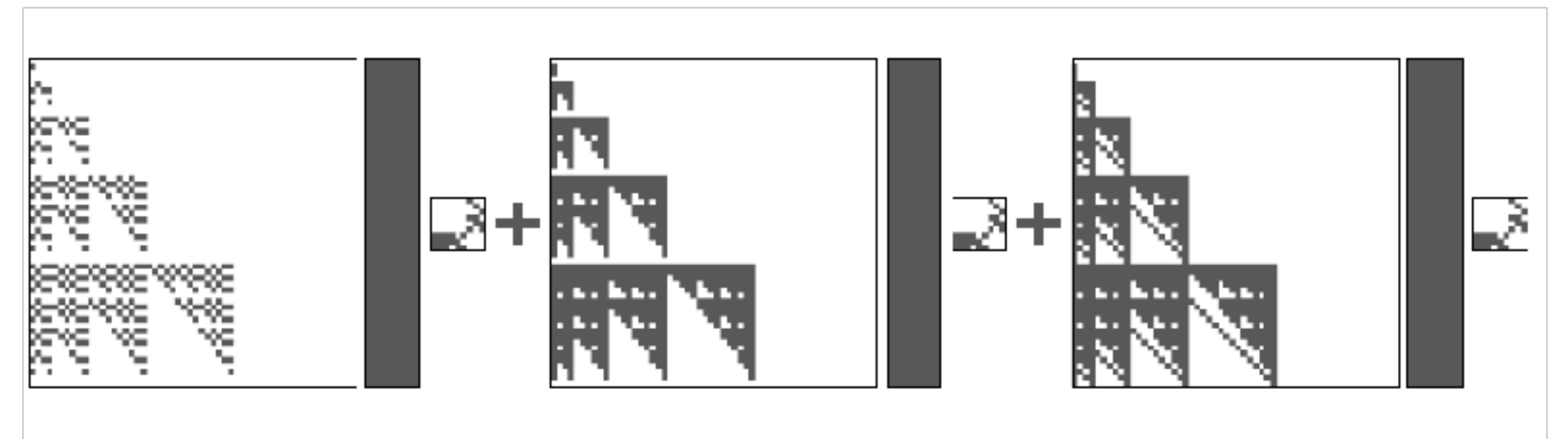
NUMERICS IN A NUTSHELL

- **Elastic wave equation** in velocity stress formulation
 - **ADER:** high-order time integration + **DG:** high-order space discretisation
 - DG with orthogonal basis functions (**modal**)
 - **Exact Riemann-Solver** computes the upwind flux = state at the element interfaces
 - **Locality of the computations:** only neighbouring elements exchange data
- ➔ **ADER-DG boils down to small matrix-matrix multiplications, where the dimension of the matrices depends on the order of the scheme (75 % of runtime consumption).**

$$\frac{\partial Q_p}{\partial t} + A_{pq} \frac{\partial Q_q}{\partial x} + B_{pq} \frac{\partial Q_q}{\partial y} + C_{pq} \frac{\partial Q_q}{\partial z} = S_p$$

$$Q = (\sigma_{xx}, \sigma_{yy}, \sigma_{zz}, \sigma_{xy}, \sigma_{yz}, \sigma_{xz}, u, v, w)^T$$

$$\tilde{K}^\xi \left(J_k^{n,n+1} \right) A_k^* + \tilde{K}^\eta \left(J_k^{n,n+1} \right) B_k^* + \tilde{K}^\zeta \left(J_k^{n,n+1} \right) C_k^*$$



Update scheme

$$Q_k^{n+1} = Q_k - \frac{|S_k|}{|J_k|} M^{-1} \left(\sum_{i=1}^4 F^{-,i} I(t^n, t^{n+1}, Q_k^n) N_{k,i} A_{k,i}^+ N_{k,i}^{-1} + \sum_{i=1}^4 F^{+,i,j,h} I(t^n, t^{n+1}, Q_{k(i)}^n) N_{k,i} A_{k(i)}^- N_{k,i}^{-1} \right) + M^{-1} K^\xi I(t^n, t^{n+1}, Q_k^n) A_k^* + M^{-1} K^\eta I(t^n, t^{n+1}, Q_k^n) B_k^* + M^{-1} K^\zeta I(t^n, t^{n+1}, Q_k^n) C_k^*$$

Cauchy Kovalewski

$$I(t^n, t^{n+1}, Q_k^n) = \sum_{j=0}^J \frac{(t^{n+1} - t^n)^{j+1}}{(j+1)!} \frac{\partial^j}{\partial t^j} Q_k(t^n)$$

$$(Q_k)_t = -M^{-1} \left((K^\xi)^T Q_k A_k^* + (K^\eta)^T Q_k B_k^* + (K^\zeta)^T Q_k C_k^* \right)$$

SEISSOL - **BALANCING HPC AND PHYSICS**

“Geophysics” Version

- Fortran 90
- MPI parallelised
- Ascii based, serial I/O

End-to-end optimization targeting strong scalability on many-core CPUs

Mutual benefits of strong collaborations between domain and computational scientists



TECHNISCHE
UNIVERSITÄT
MÜNCHEN

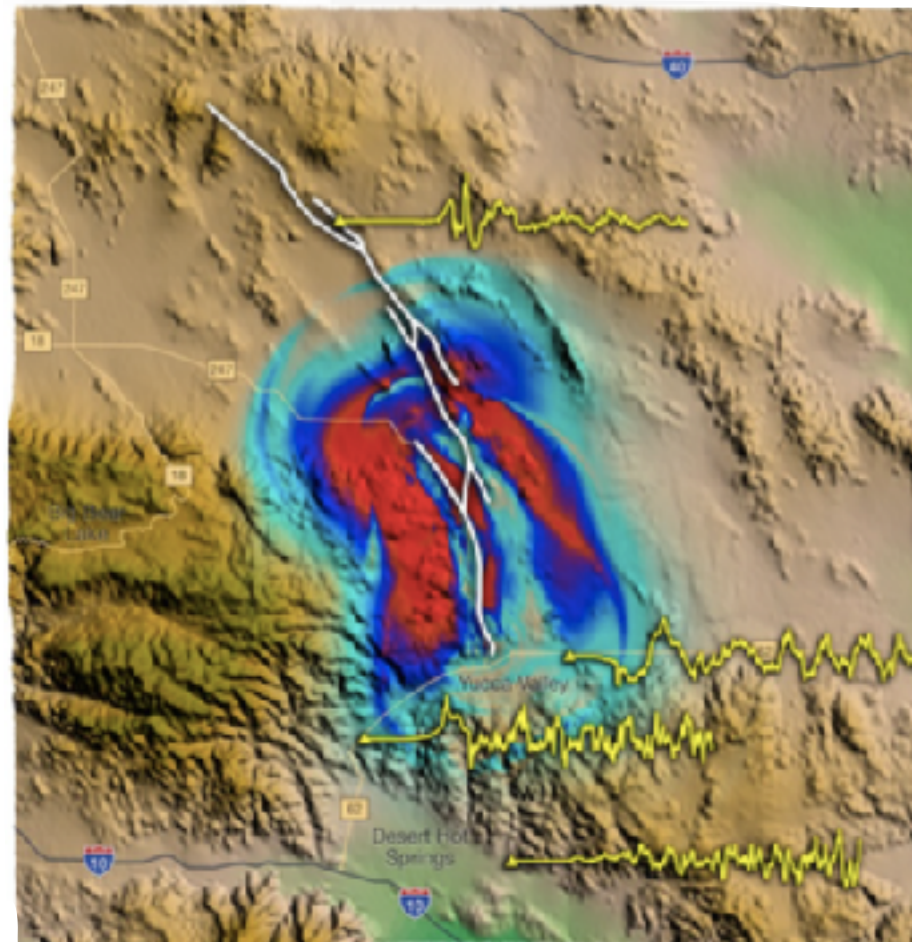


Leibniz-Rechenzentrum
der Bayerischen Akademie der Wissenschaften

Breuer et al.,ISC14, Heinecke et al.,SC14
Breuer et al.,IEEE16, Heinecke et al.,SC16
Rettenberger et al., EASC16
Upphoff & Bader, HPCS'16
Upphoff et al., SC17

SEISSOL - BALANCING HPC AND PHYSICS

Gordon Bell Prize Finalist, SC14



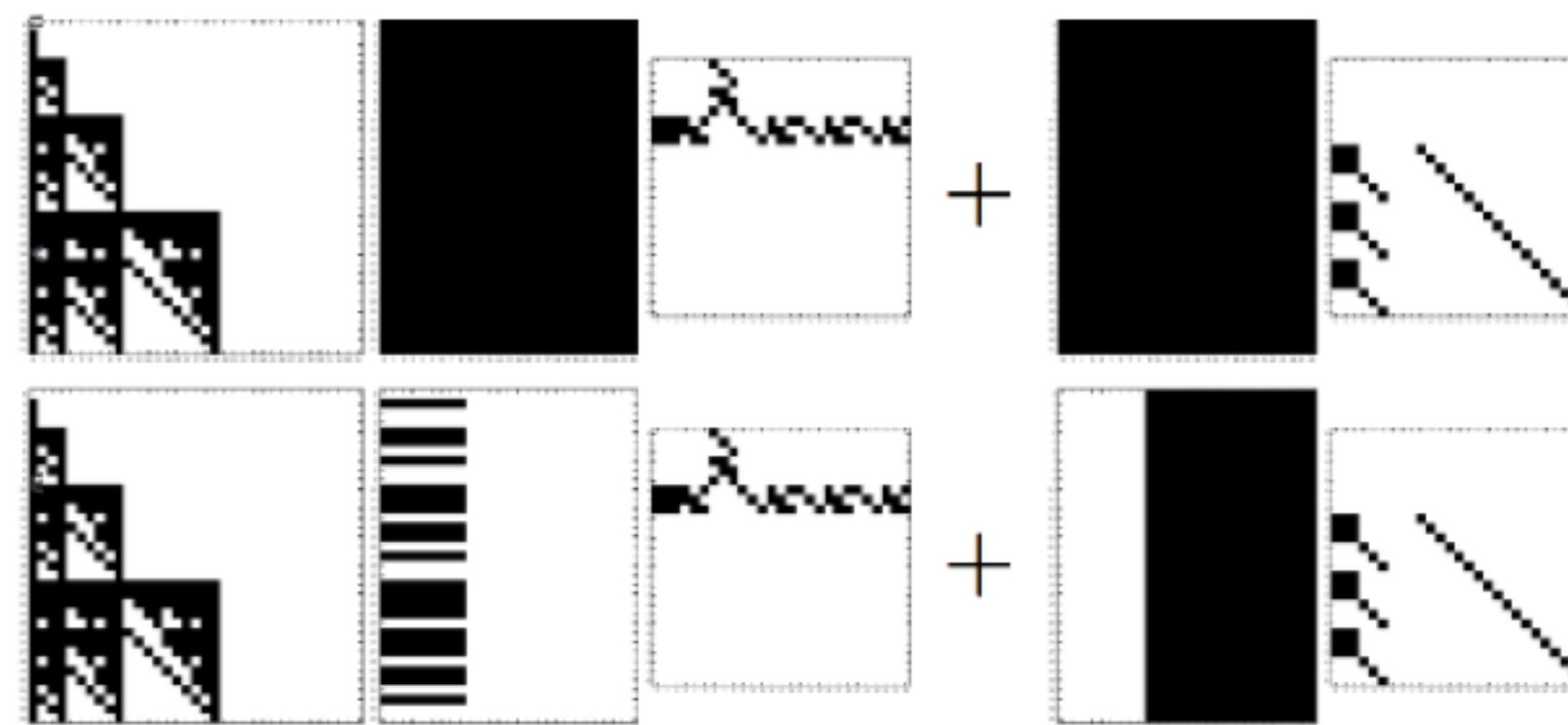
“Geophysics” Version

Landers scenario
(96 billion DoF,
200,000 time steps)

- Fortran 90
- MPI parallelised
- Ascii based, serial I/O
- Hybrid MPI+OpenMP parallelisation
- Parallel I/O (HDF5, inc. mesh init.)
- **Assembler-level DG kernels**
- multi-physics off-load scheme for many-core architectures

Breuer et al.,ISC14, Heinecke et al.,SC14
Breuer et al.,IEEE16, Heinecke et al.,SC16
Rettenberger et al., EASC16
Upphoff & Bader, HPCS'16
Upphoff et al., SC17

- > 1 PFlop/s performance
- 90% parallel efficiency
- 45% of peak performance
- 5x-10x faster time-to-solution
- 10x-100x bigger problems

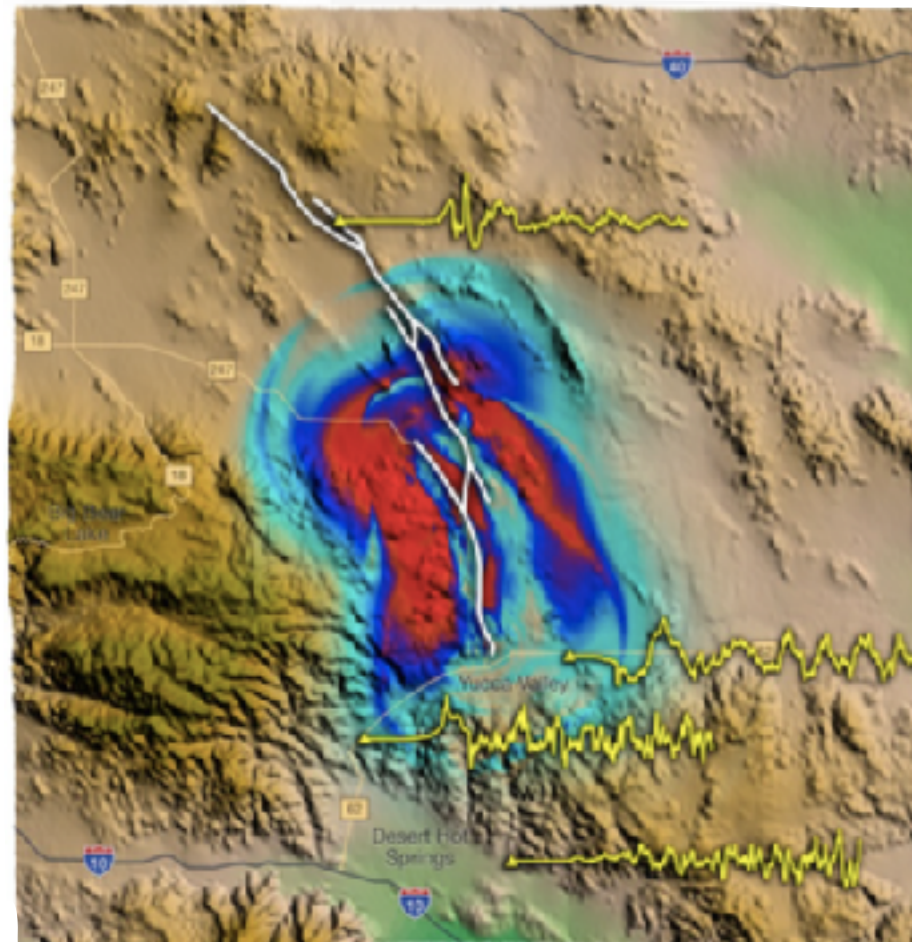


Partial kernel before (top) and after (bottom) removing irrelevant entries in matrix chain products

- ➔ A code generator automatically detects and exploits sparse block patterns
- ➔ Hardware specific full “unrolling” and vectorization of all element operations
- ➔ Customised code for each matrix-matrix multiplication via the libxsmm back-end
- ➔ Efficiently exploits as of 2014 available hardware (AVX, MIC), reaching unto 8.6 PFLOPS on Tianhe-2

SEISSOL - BALANCING HPC AND PHYSICS

Gordon Bell Prize Finalist, SC14



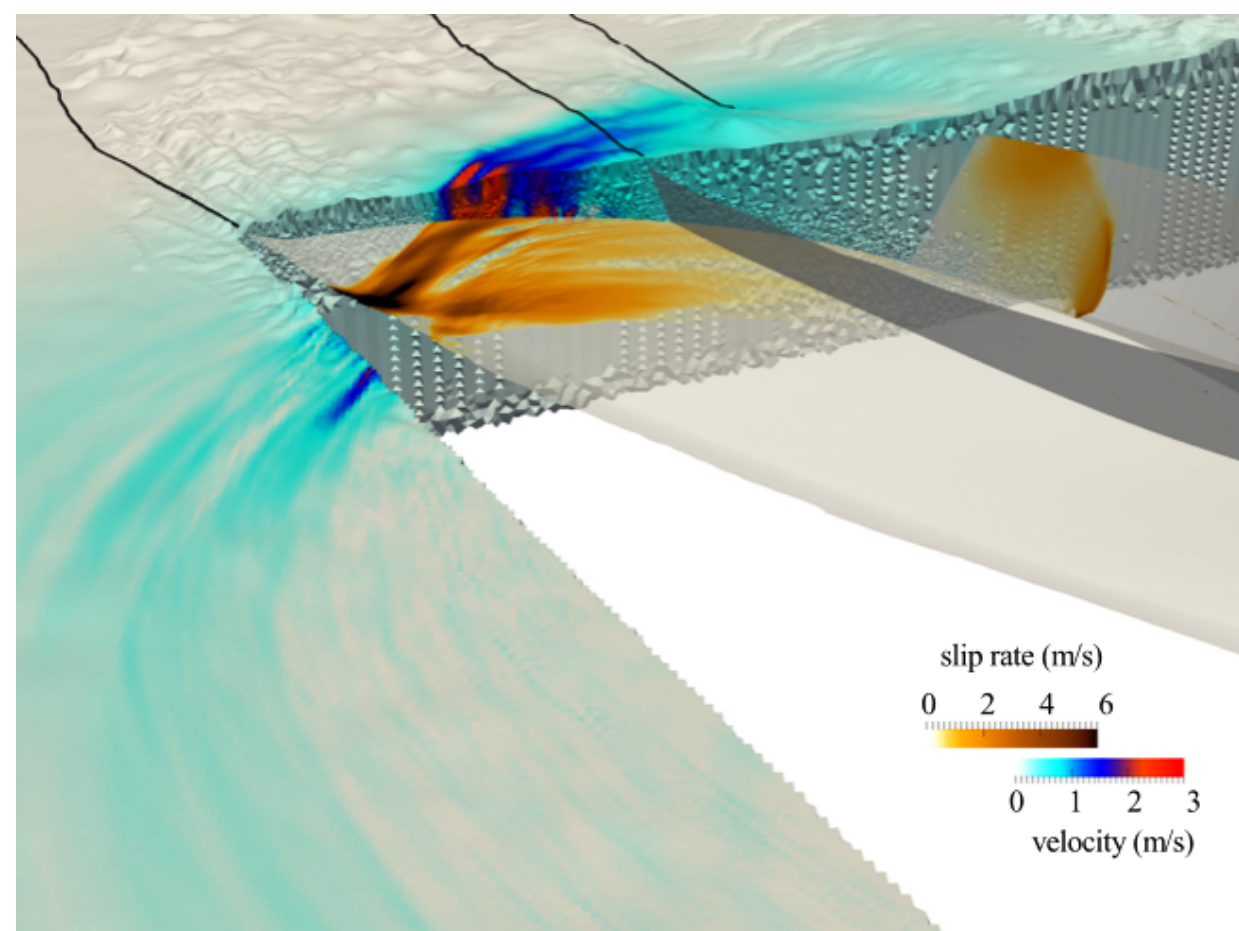
“Geophysics” Version

Landers scenario
(96 billion DoF,
200,000 time steps)

- Fortran 90
- MPI parallelised
- Ascii based, serial I/O

- Hybrid MPI+OpenMP parallelisation
- Parallel I/O (HDF5, inc. mesh init.)
- Assembler-level DG kernels
- multi-physics off-load scheme for many-core architectures

- **> 1 PFlop/s performance**
- **90% parallel efficiency**
- **45% of peak performance**
- **5x-10x faster time-to-solution**
- **10x-100x bigger problems**



Sumatra scenario
(111 billion DoF,
3,300,000 time steps)

- **Cluster-based local time stepping**
- Code generator also for advanced PDE's as viscoelastic attenuation
- Asagi (XDMF)-geoinformation server
- Asynchronous input/output
- Overlapping computation and communication

- **Optimized for Intel KNL**
- **Speed up of 14x**
- **14 hours compared to almost 8 days for Sumatra scenario on SuperMuc2**

Best Paper Award, SC17

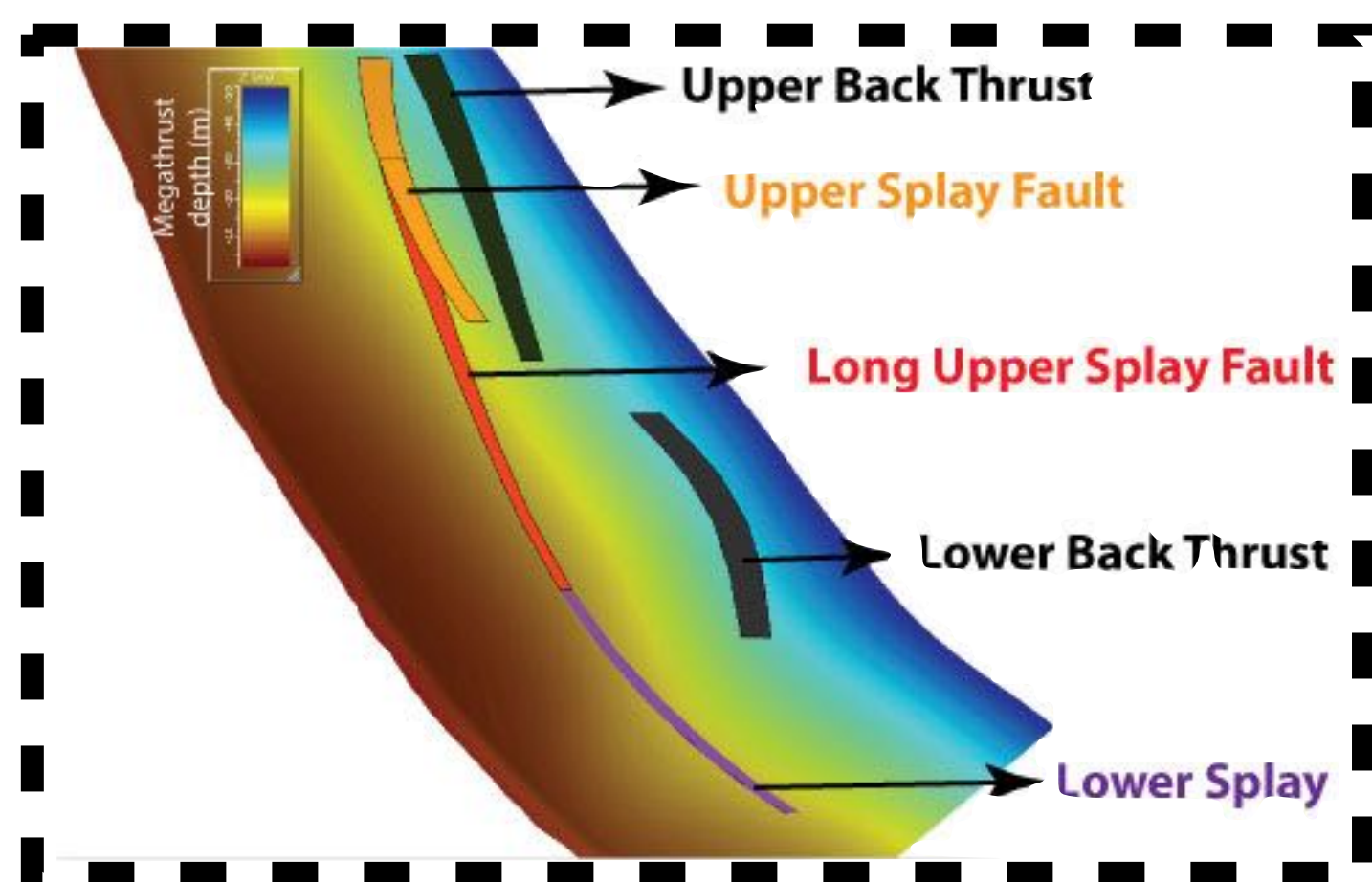
Breuer et al.,ISC14, Heinecke et al.,SC14
Breuer et al.,IEEE16, Heinecke et al.,SC16
Rettenberger et al., EASC16
Upphoff & Bader, HPCS'16
Upphoff et al., SC17

The 2004 Sumatra-Andaman earthquake

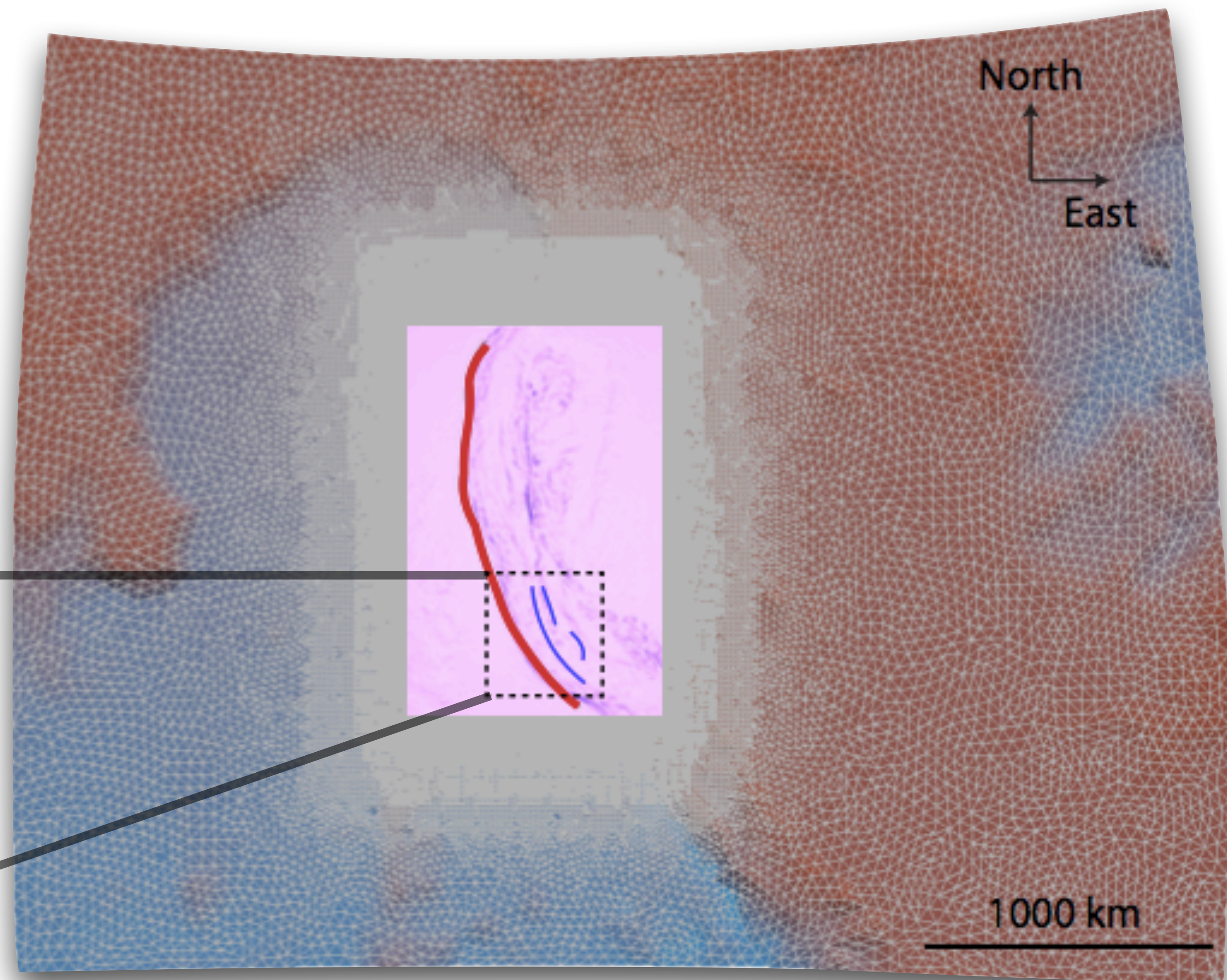
- rise to a modeling challenge!

Uphoff et al., SC17

- Spatial resolution (400m on-fault, O6) and 2.2 Hz wave propagation required mesh with 220 million finite elements ($\sim 111 \times 10^9$ degrees of freedom)
- **Small-ish “pop-up” fractures splaying off the curved megathrust** that itself merges with the bathymetry in narrow subduction wedges - **requires numerical methods handling geometric complexity and highly varying element sizes**



Sibuet et al., 2007;
Singh et al., 2008;
Chauhan et al.,
2009; Lin et al.,
2009



The 2004 Sumatra-Andaman earthquake

- rise to a modeling challenge!

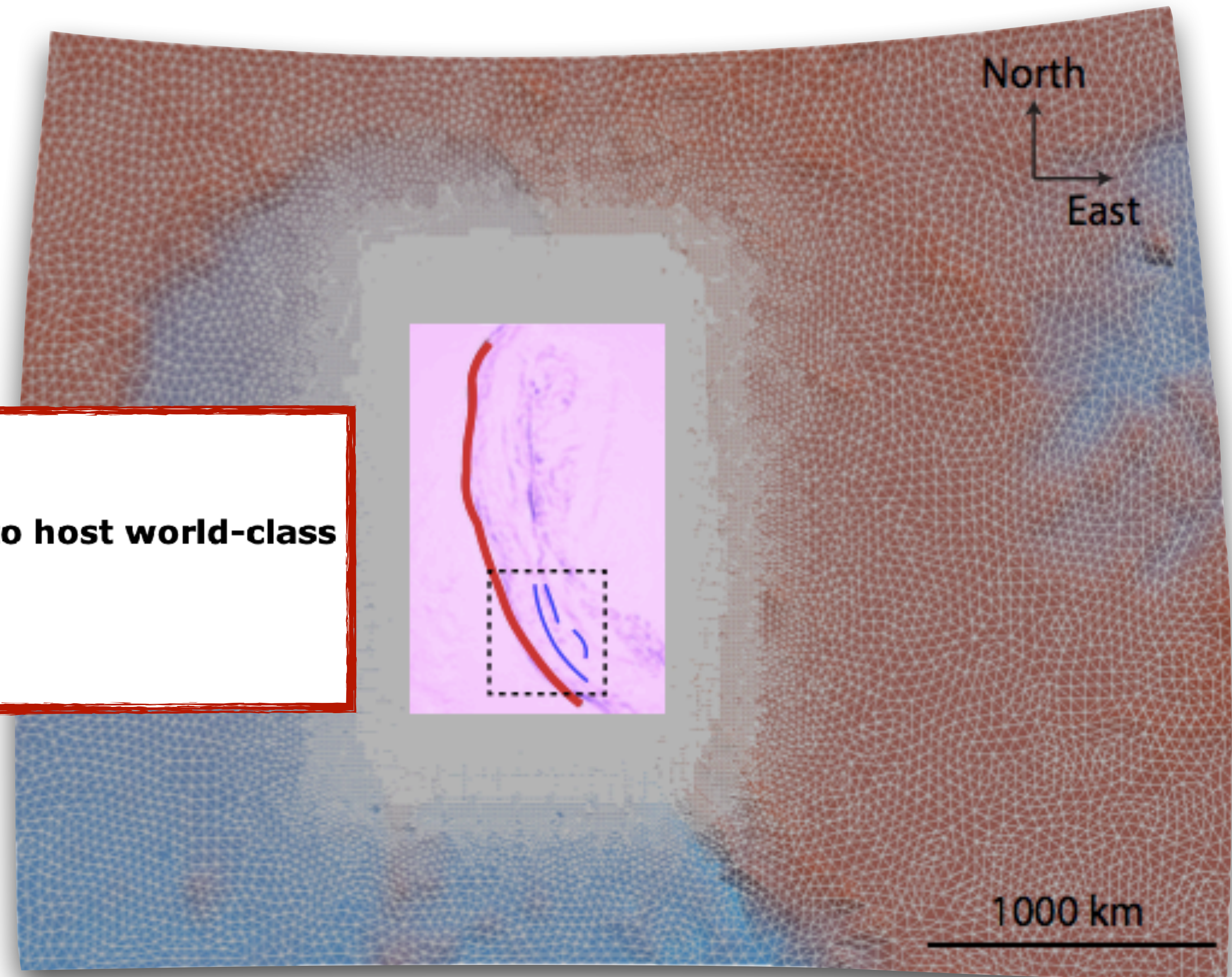
Uphoff et al., SC17

- Spatial resolution (400m on-fault, O6) and 2.2 Hz wave propagation required mesh with 220 million finite elements ($\sim 111 \times 10^9$ degrees of freedom)
- Requires high-performance computing

European Commission - Press release

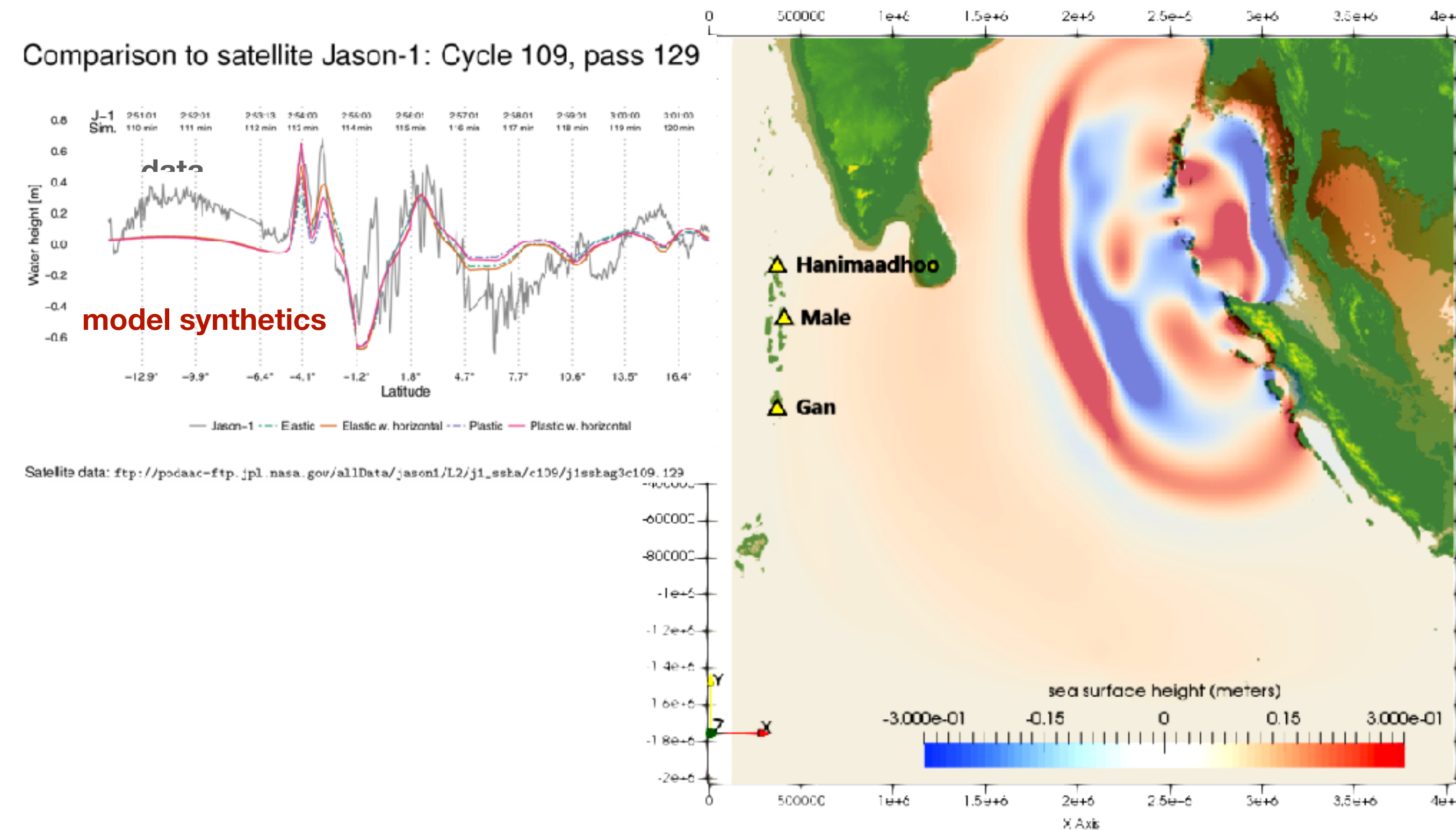
Digital Single Market: Europe announces eight sites to host world-class supercomputers

Luxembourg, 7 June 2019



The 2004 Sumatra-Andaman earthquake - dynamic model vs. observational constraints

- Our parametrization matches current theories: **low stress, low strength drop, high fluid pressure**
- Following Hardebeck (2012), we define a **non-andersonian stress state**, in which the second principal stress is horizontally orientated at 309° in the south and gradually rotates to 330°
- The **plunge** of the maximum and minimum principal stresses is 8° , **confining stress varies linearly with depth**
- **Low velocity layer** around the fault causes **slip pulses** from refracted waves
- Only **back thrust splay faults are activated** in reverse manner.



The 2004 Sumatra-Andaman earthquake

- dynamic model vs. observational constraints

● Replicating observations in near- and far-field to first-order:

● **fault slip**

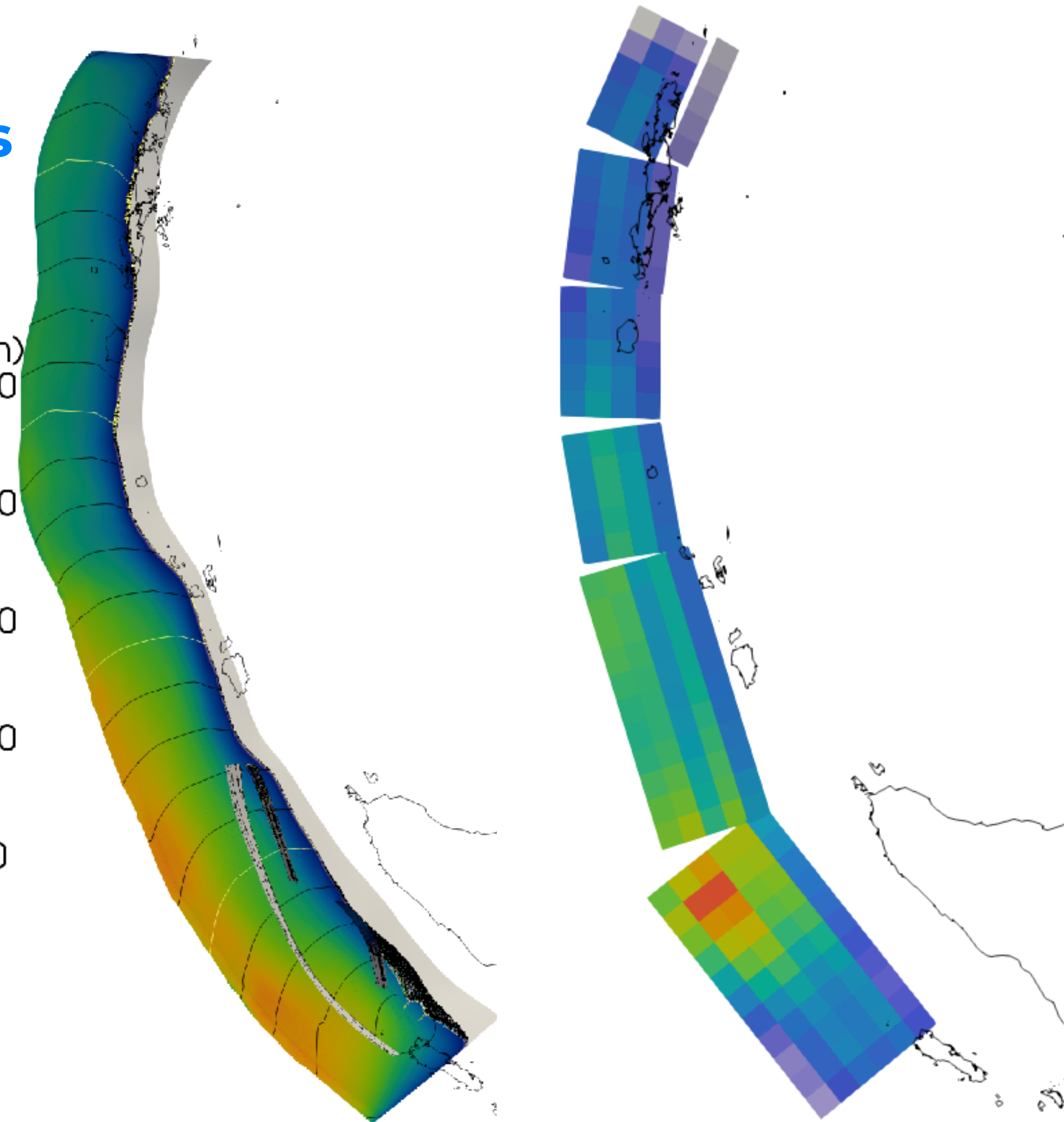


● ground deformation

● teleseismics

● tsunami data

fault slip (m)



Can the geometry of the slab and a smooth regional stress state explain the rupture characteristics to first-order? (Yes!)

Are “pop-up” ruptures splaying off the megathrust crucial for tsunami generation? (Depends!)

Accumulated fault slip of the DR model. Black (resp. yellow) lines show the rupture front position every 20 s (resp. 100 s). The slip inverted by Rhie et al. (2007) from teleseismic and GPS data shown for comparison.

The 2004 Sumatra-Andaman earthquake

- dynamic model vs. observational constraints

● Replicating observations in near- and far-field to first-order:

● **fault slip**

● ground deformation

● teleseismics

● tsunami data

However! Too short overall duration, no slip segmentation, high slip localised at the trench

That does not mean this is what happened:

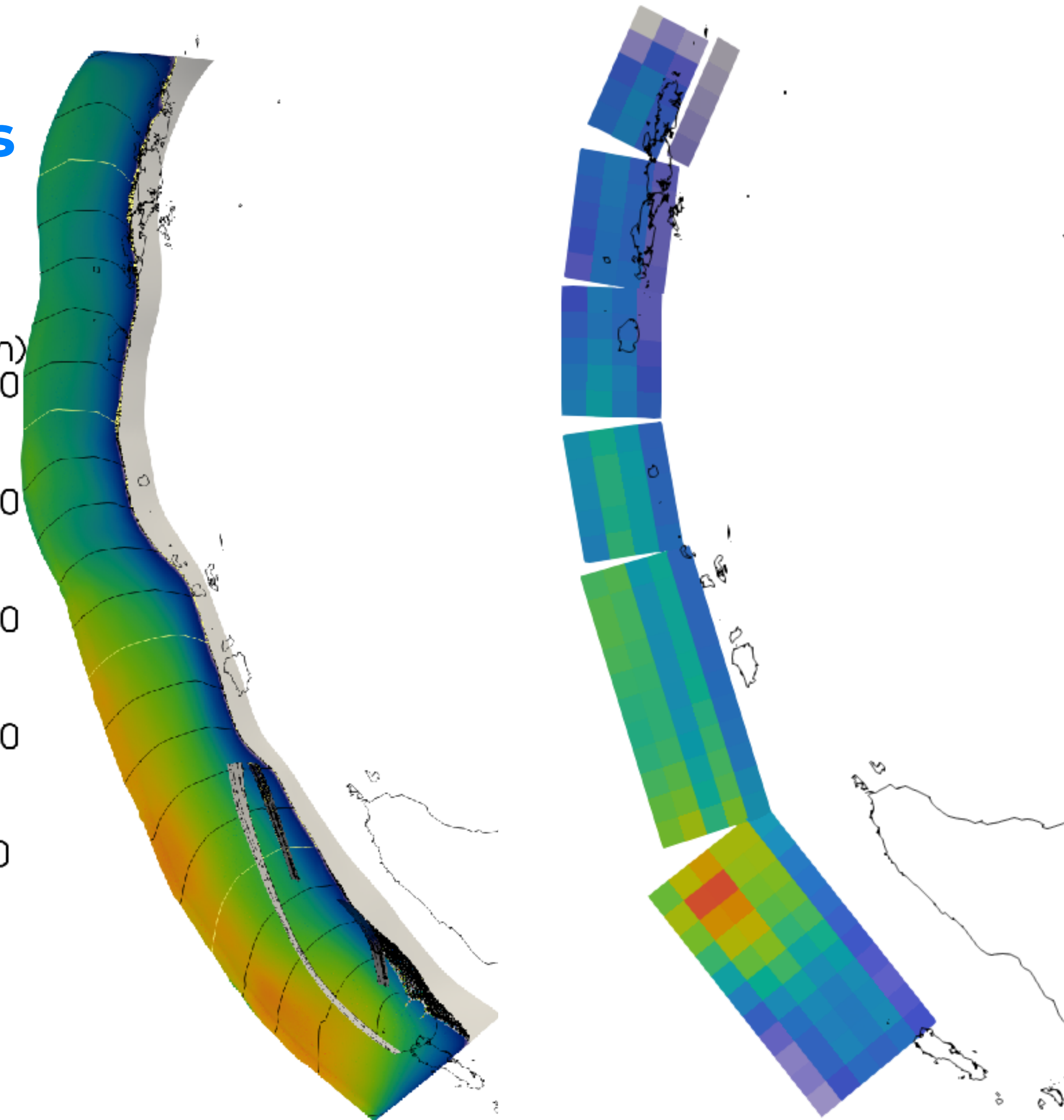
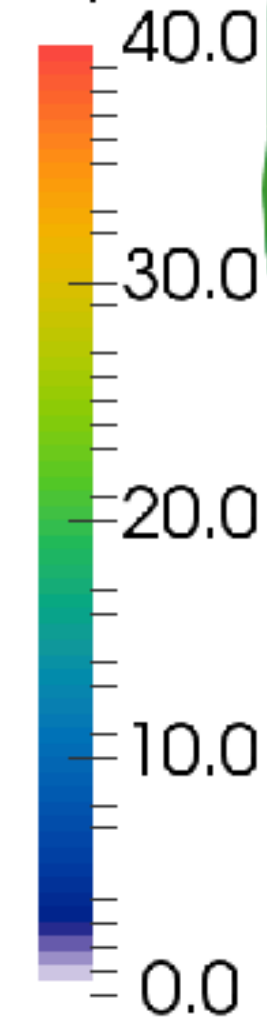
● Slip at the trench?

● Importance of splay-faults?

● Along-arc variations - the role of sediments?

● Rotation of stresses along arc and with depth?

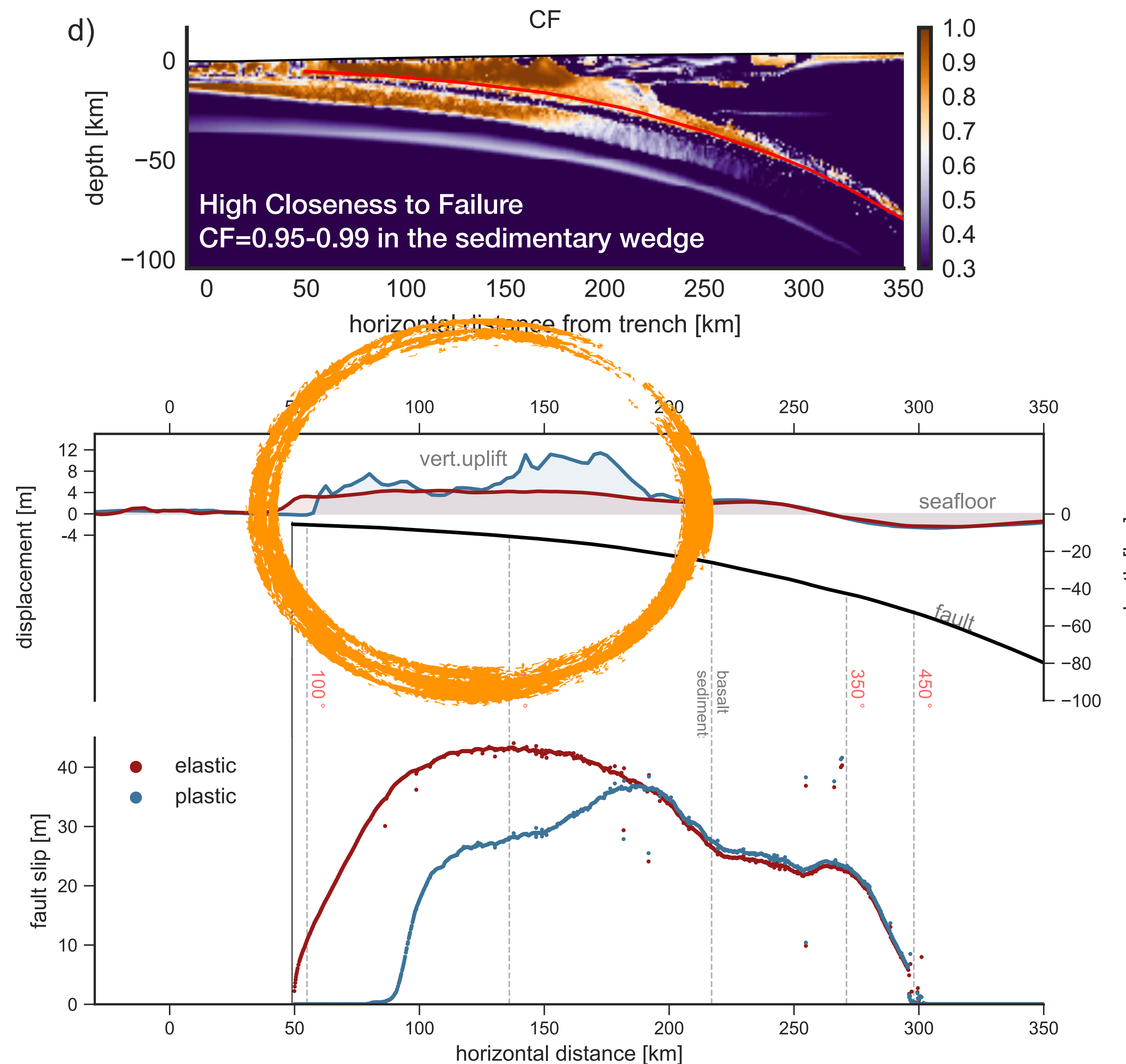
fault slip (m)



Accumulated fault slip of the DR model. Black (resp. yellow) lines show the rupture front position every 20 s (resp. 100 s). The slip inverted by Rhie et al. (2007) from teleseismic and GPS data shown for comparison.

Geodynamics constraints

- **Large presence of sediments (large CF)** and **trapped waves** causes inelastic deformation in the wedge which **reduces fault slip at the trench**, but causes **uplift** efficiently landward from the trench
- Similar effects have been shown by Shuo Ma, SDSU, from critically stressed sedimentary wedges
- For one-way coupling to fully elastic earthquake models see our preprint **van Zelst et al., 2019** eartharxiv.org/f6ng5/



Matching static and (long-term/large-scale) dynamic constraints

Elastic model: no slip
segmentation, high slip
localised at the trench

elastic model

fault slip

plasticity model

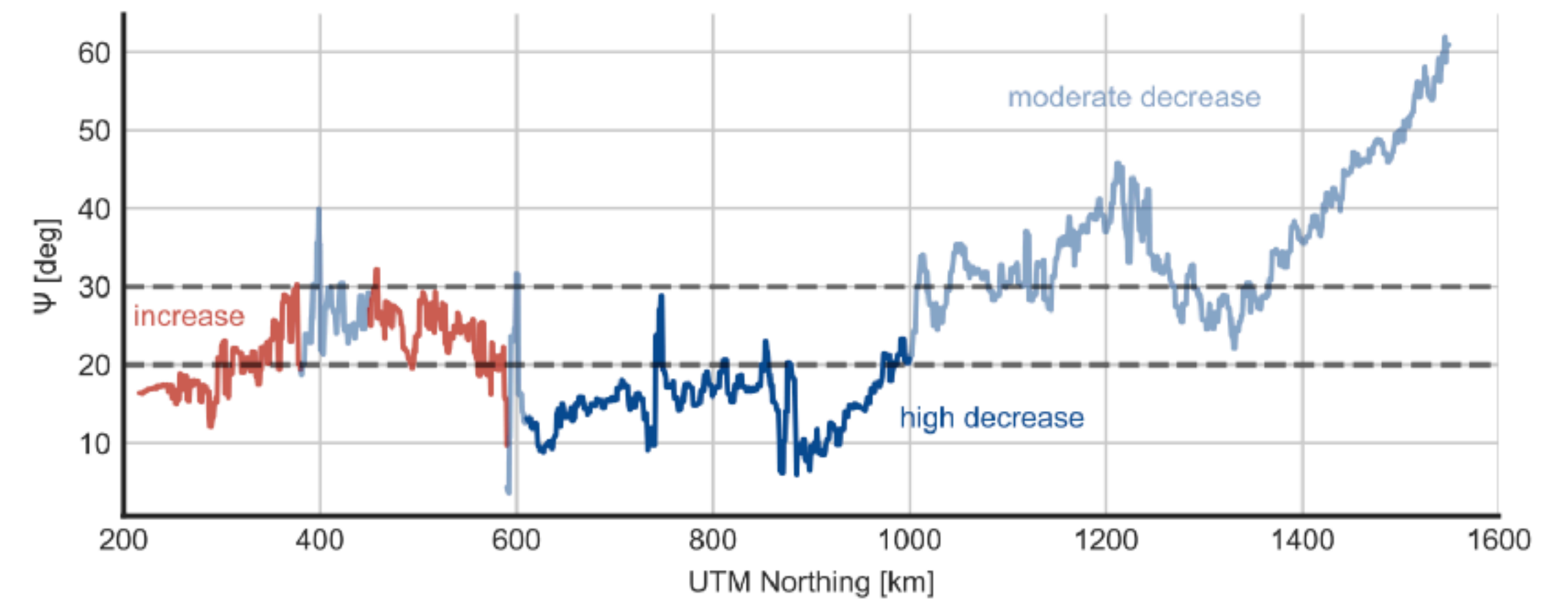
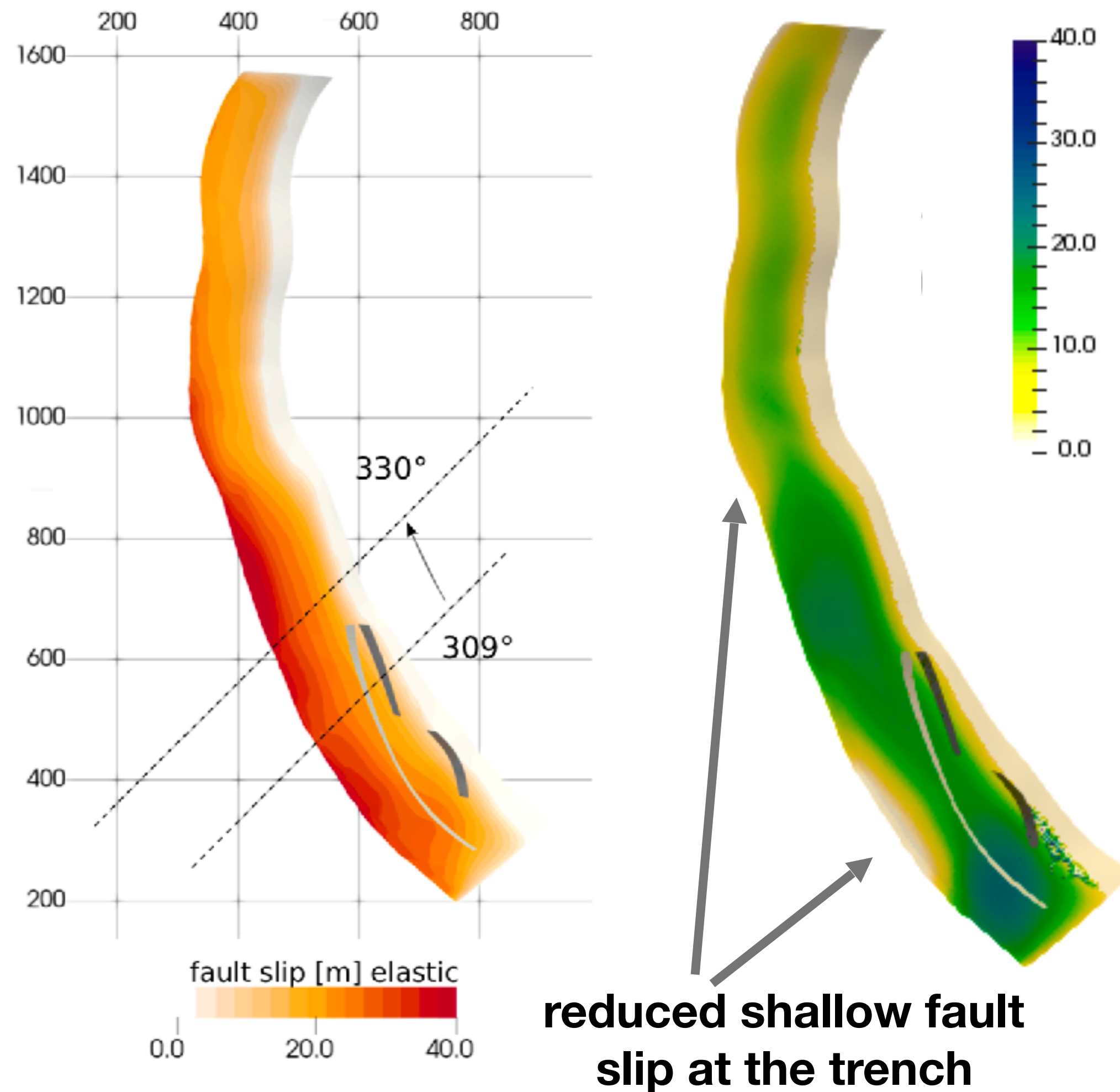


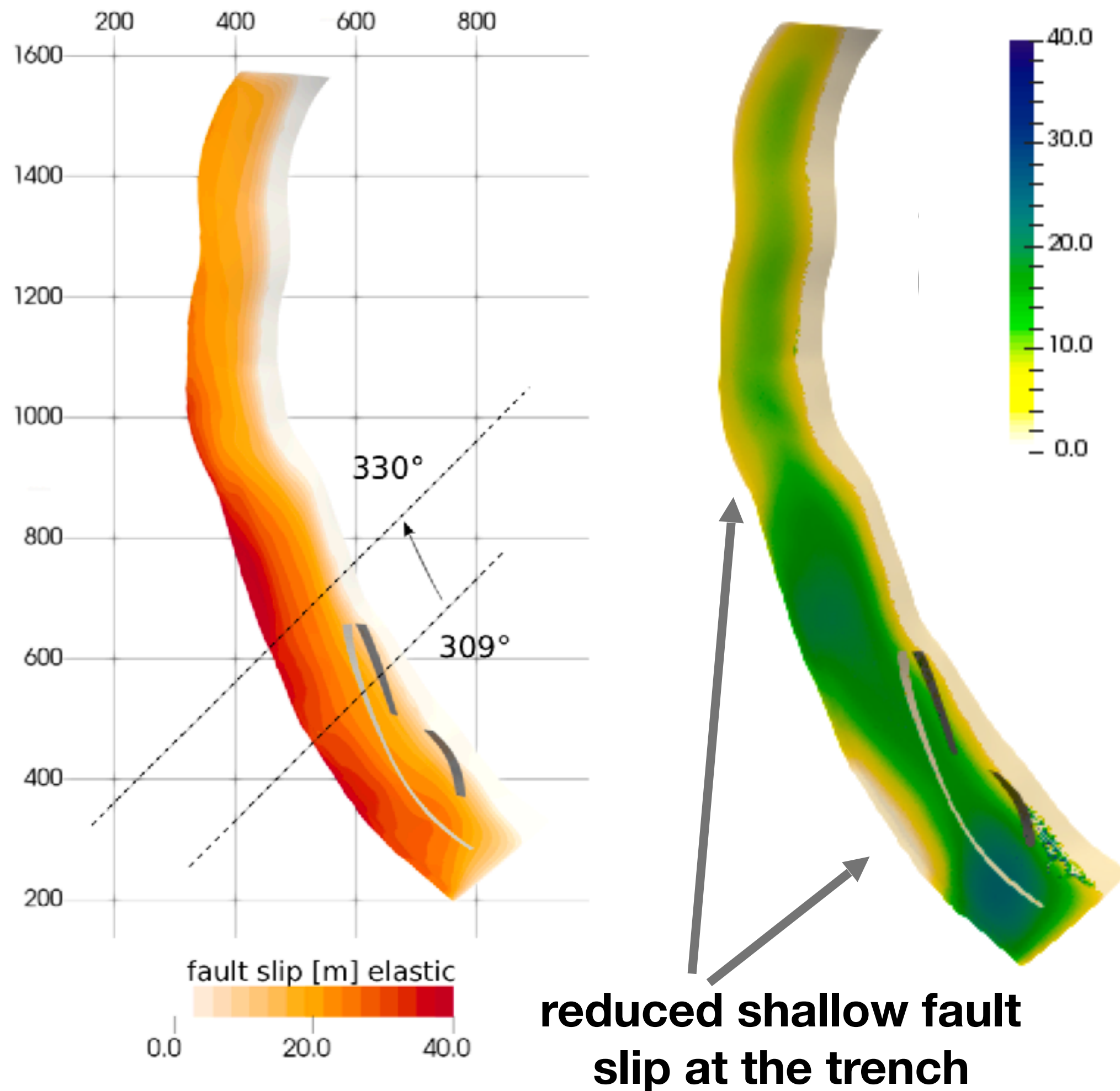
Figure 4.6: Variation of Ψ , the angle between the maximum compressive horizontal stress orientation and fault strike, along UTM Northing coordinates.

Matching static and (long-term/large-scale) dynamic constraints

elastic model

fault slip

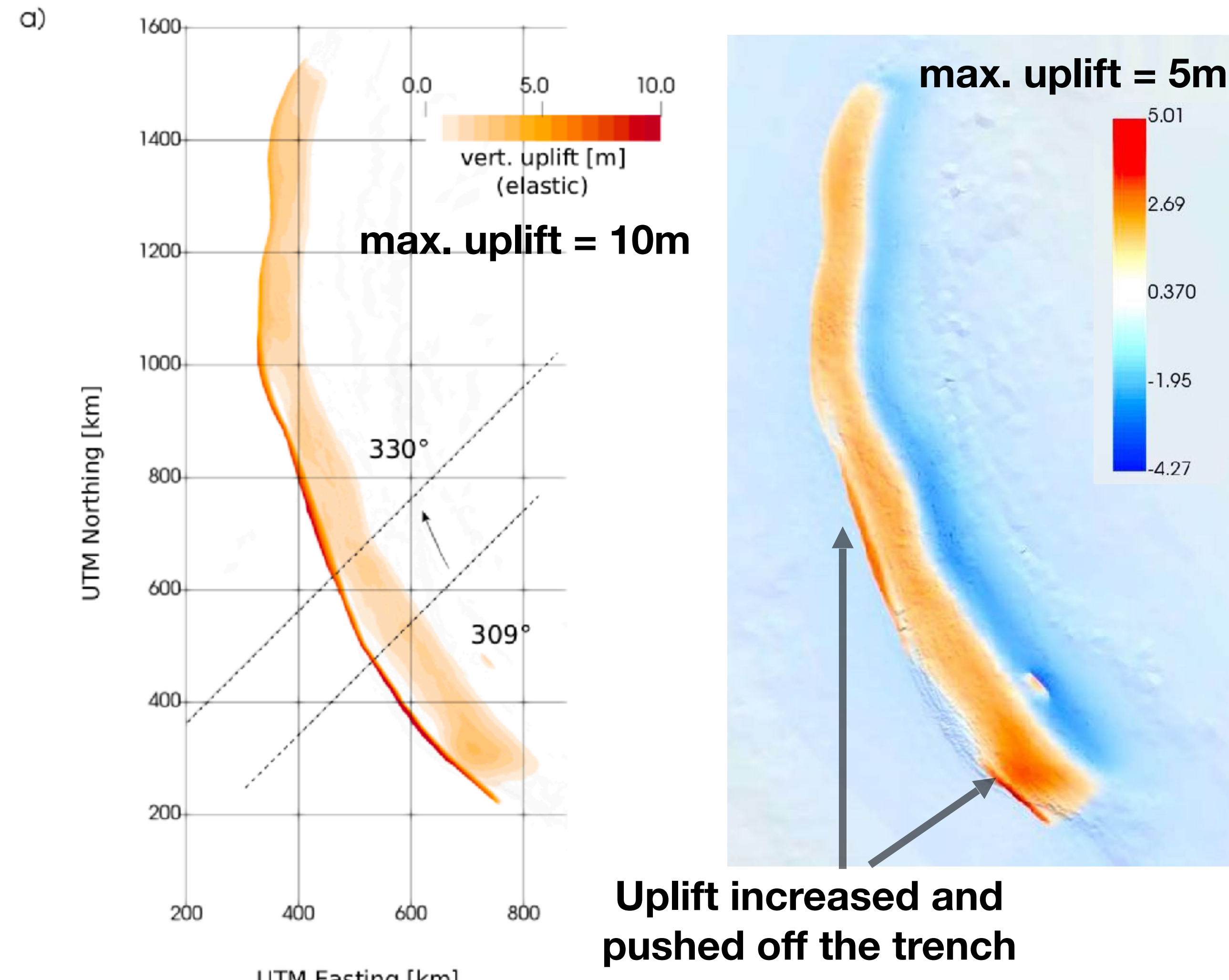
plasticity model



elastic model

vertical uplift

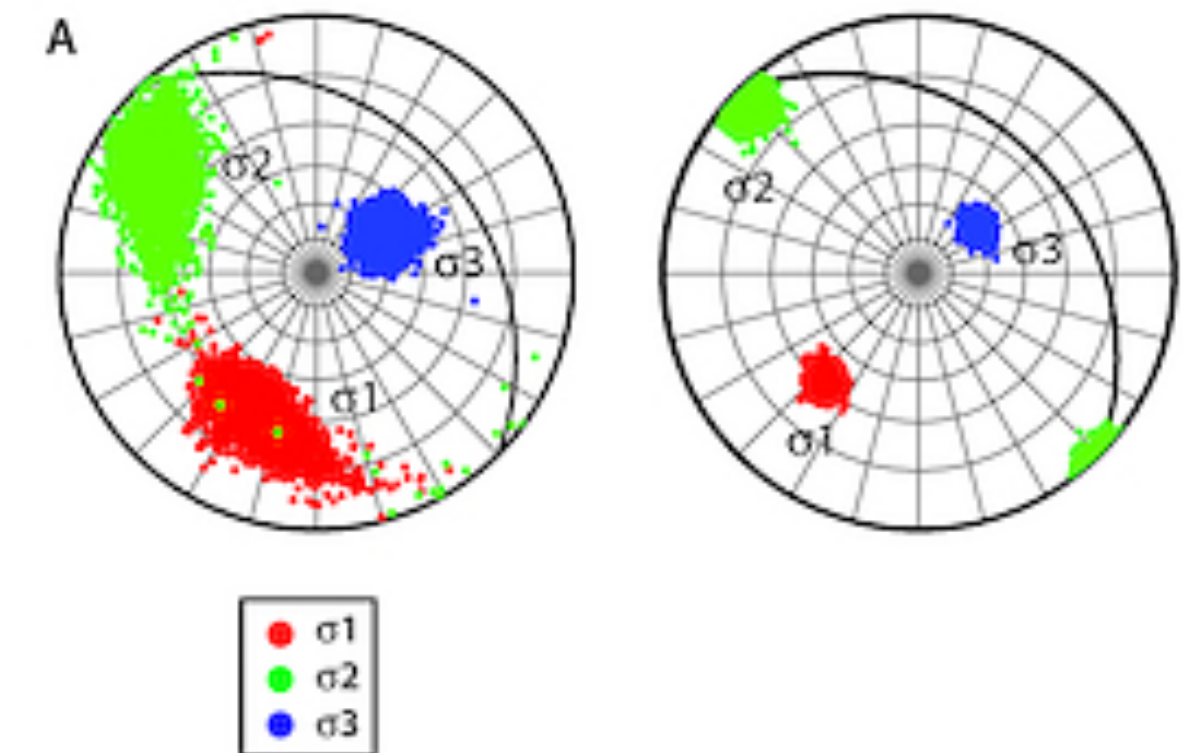
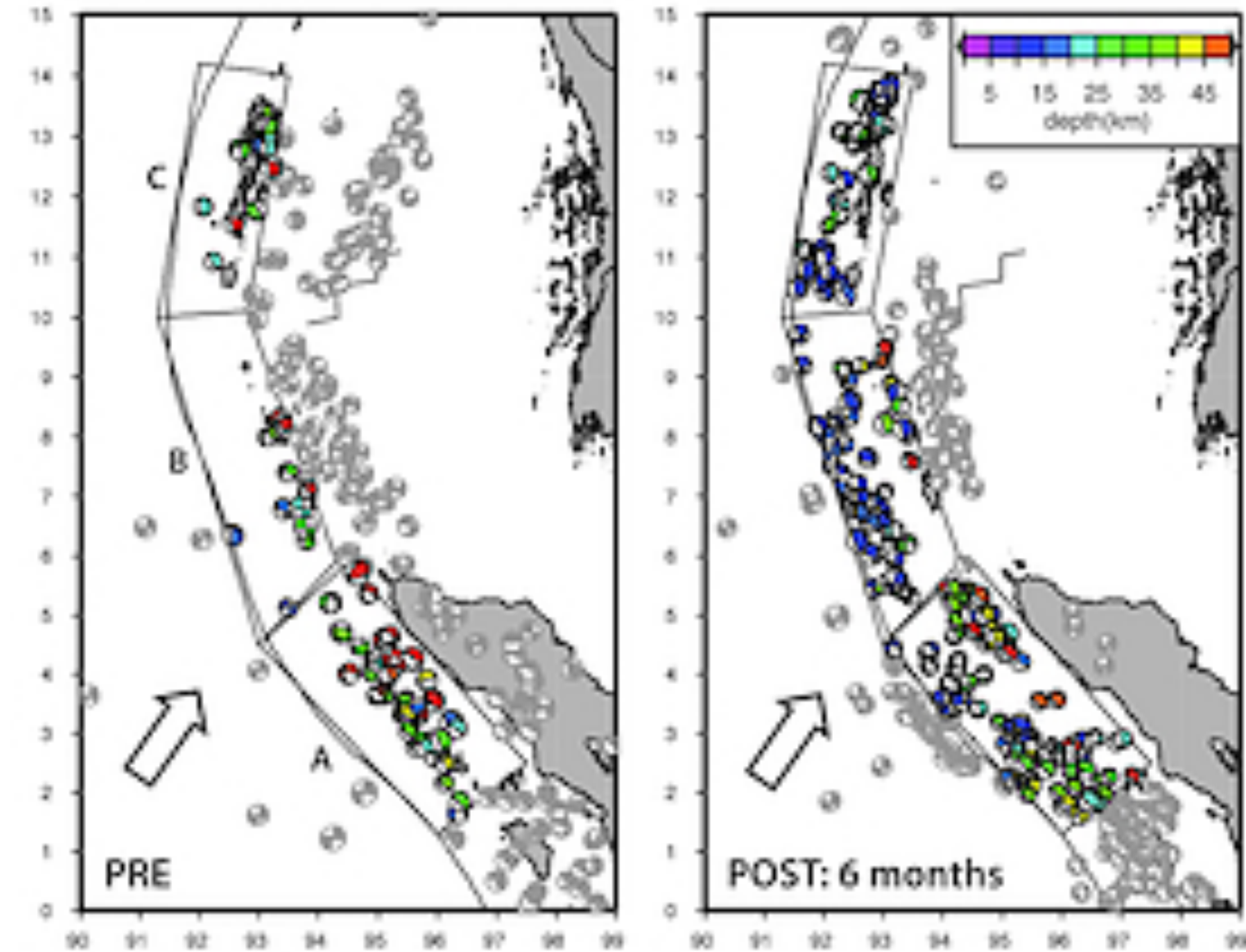
plasticity model



Tectonic constraints - Variations along-Arc

- **Coseismic stress rotation:** constraints the absolute level of initial and residual stress (**dynamic friction coefficient** via inferred ratio of stress drop to residual stress level)

(c) Sumatra-Andaman 2004



Ulrich et al., in preparation

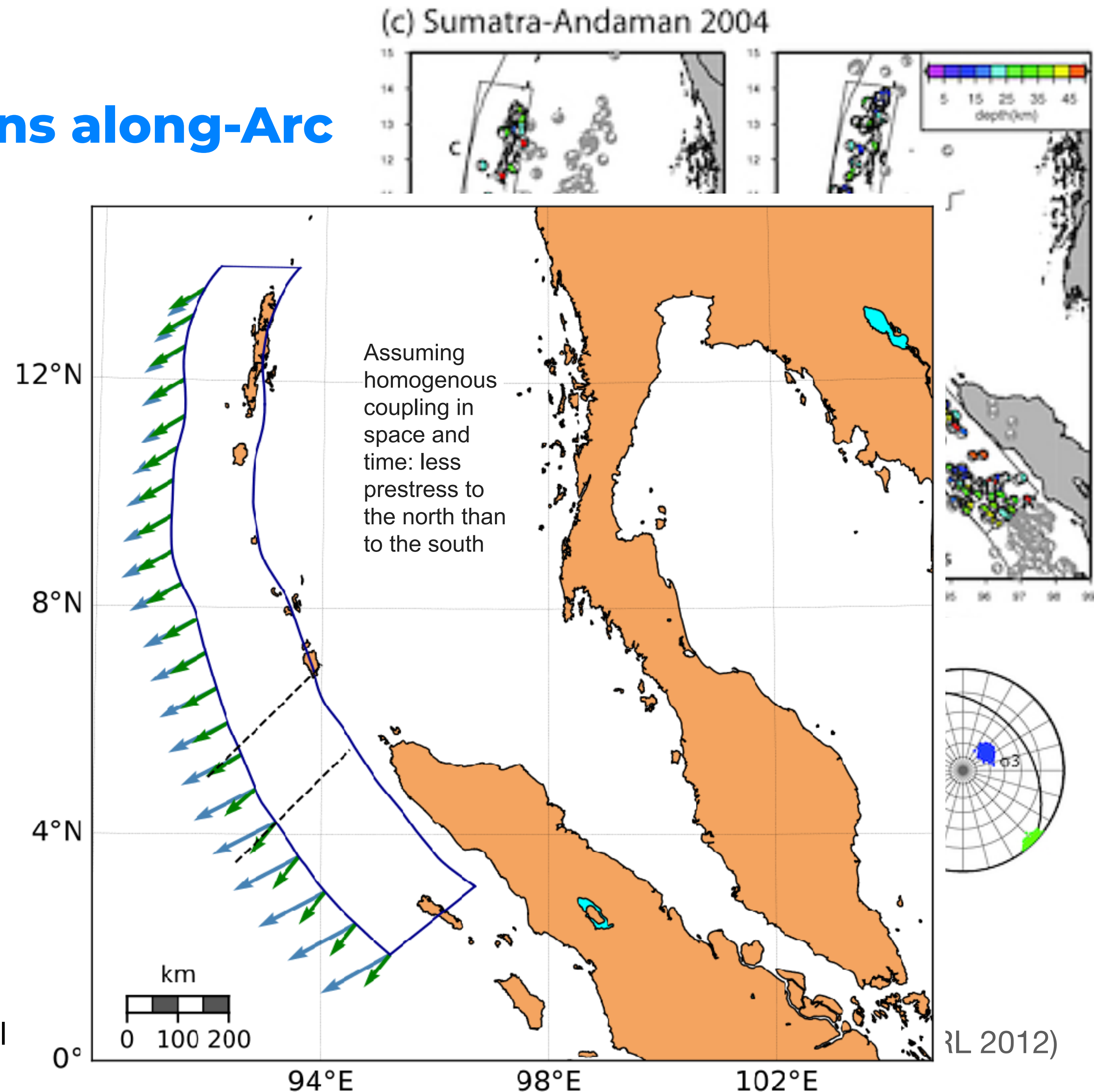
(Hardebeck, GRL 2012)

Tectonic constraints - Variations along-Arc

- **Coseismic stress rotation:** constraints the absolute level of initial and residual stress (**dynamic friction coefficient** via inferred ratio of stress drop to residual stress level)
- Tectonic **convergence rates** (calculated using Euler pole of Indo-Burma plate pair after Gahalaut and Gahalaut, 2007): **magnitudes of deviatoric stresses** (or the S ratio on optimally oriented fault)
- Requires high fluid pressure (96% lithostatic)

Ulrich et al., in preparation

Blue: relative velocities of the Indo-burma pair
Green: orientation of SHmax in the DR model
 To the South, different orientation may suggest internal deformations/segmentation of the Burma plate



SEISSOL - **BALANCING HPC AND PHYSICS**

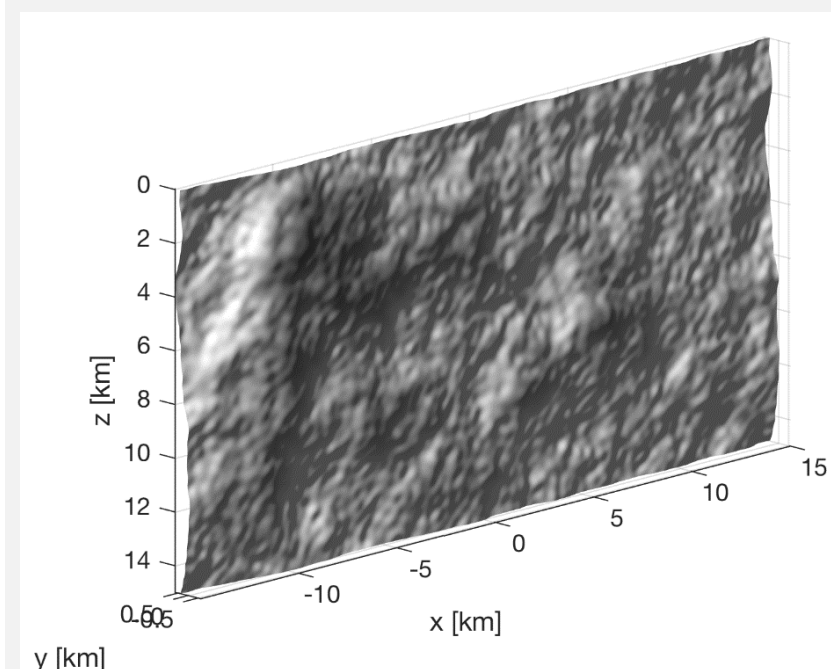
Breuer et al.,ISC14, Heinecke et al.,SC14
Breuer et al.,IEEE16, Heinecke et al.,SC16
Rettenberger et al., EASC16
Upphoff & Bader, HPCS'16
Upphoff et al., SC17

“Geophysics” Version

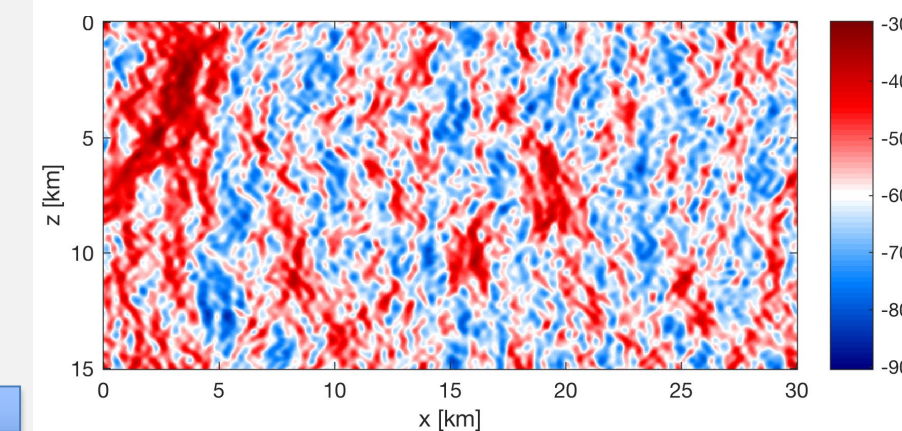
Kaikoura rough fault scenario
(up to 600 Mio elements)

- Fortran 90
- MPI parallelised
- Ascii based, serial I/O
- SuperMUC-NG (friendly user tests)
- Running multiple simulations at once (2-5x speed-up)
- (Work in progress ...)

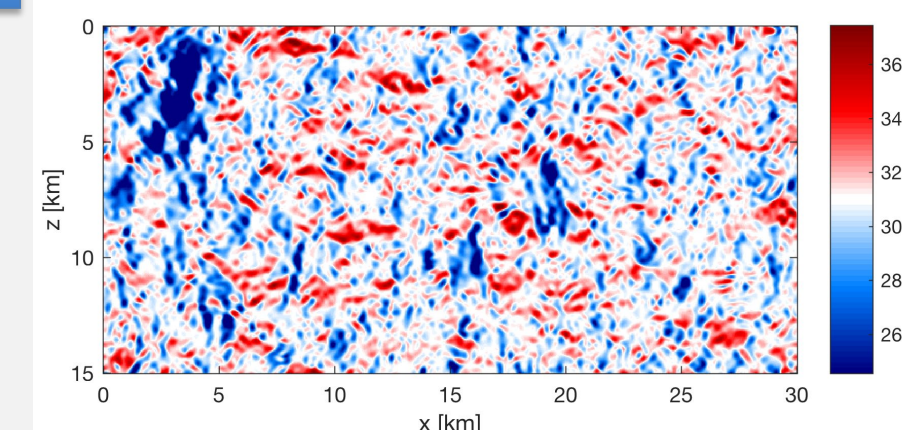
uniform background stress tensor



normal traction



shear traction

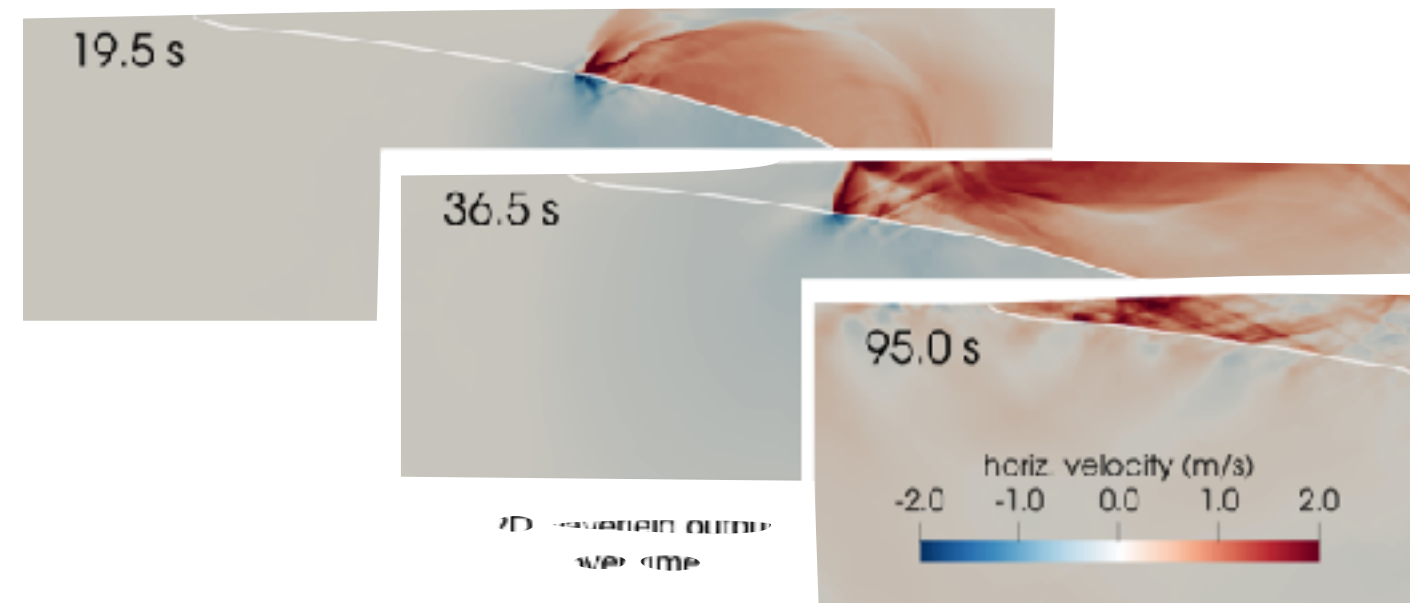


SeisSol

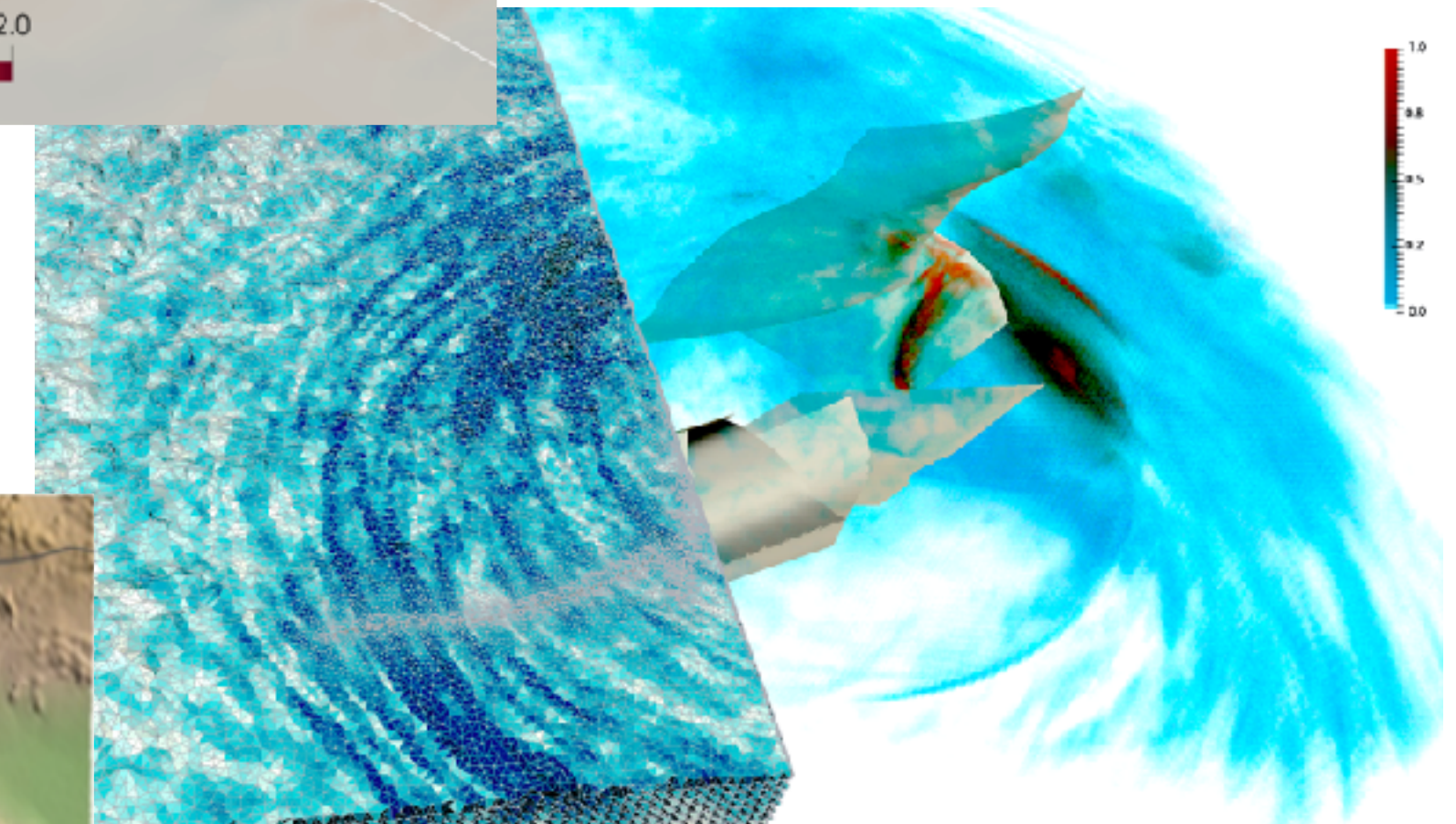
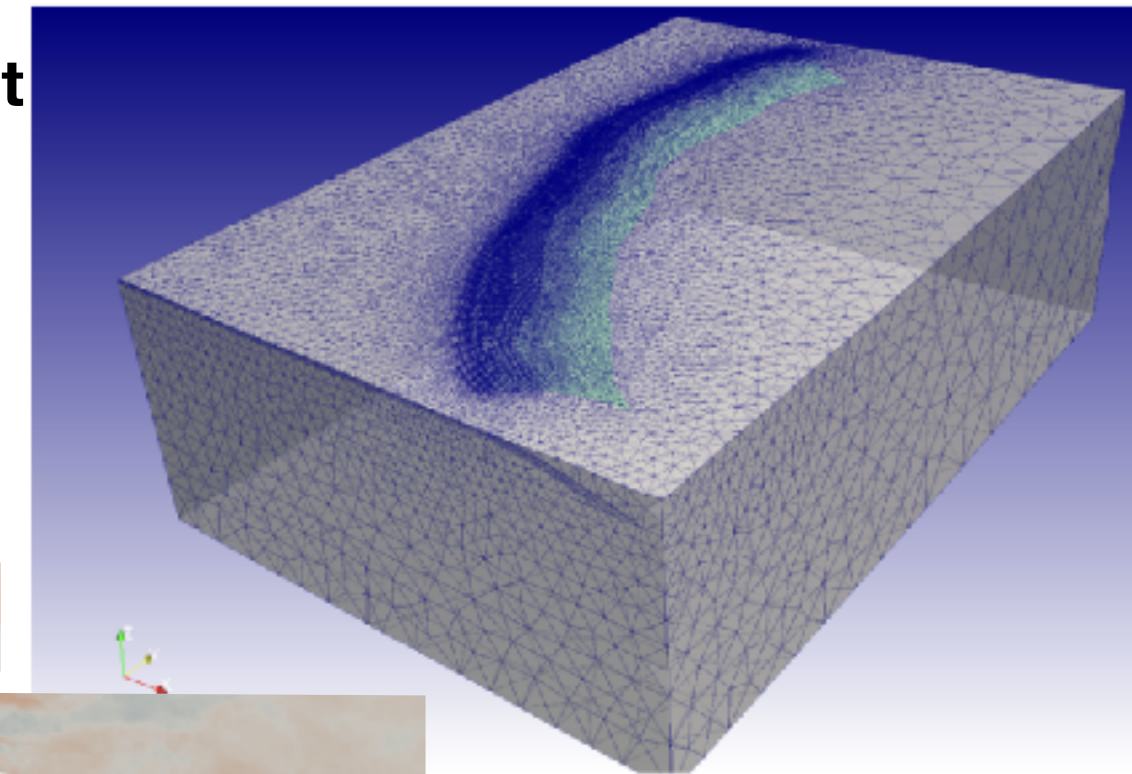
Features and Scales

- Viscoelastic attenuation
- Anisotropy
- Kinematic sources
- Modern friction laws
- Off-fault plasticity
- Fault roughness
- Thermal pressurisation
- Fast loading of 3D datasets with ASAGI
- Adjoint (2D)
- Checkpointing
- Parallel I/O
- Initial parametrization with EASI
- Full local time stepping
- Tested meshing workflow up to 925 million elements
- Tools for pre- and post processing
- overnight builds / code testing. (using Travis, Jenkins, ...)

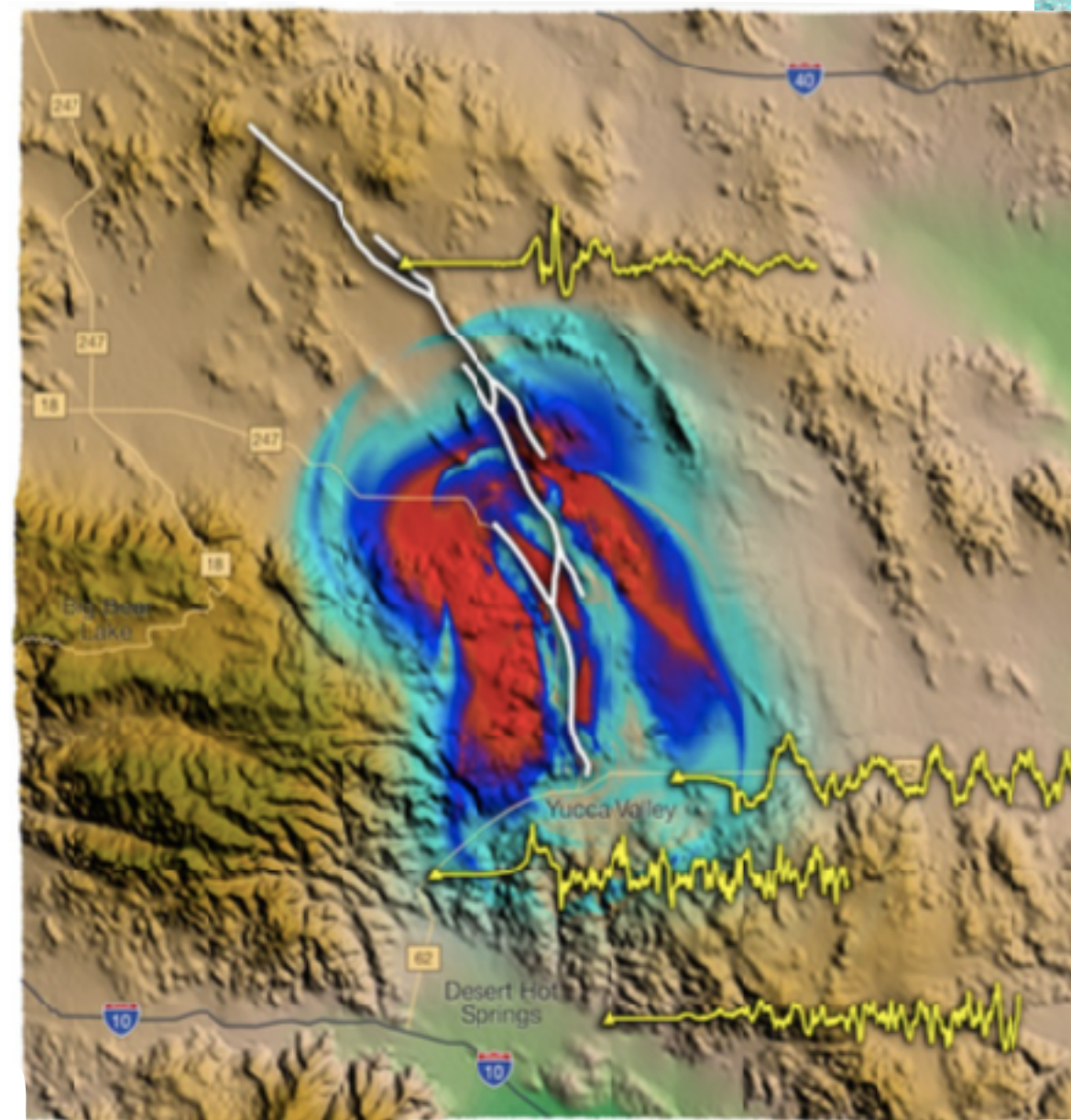
Sumatra: 14 mio element
mesh, 400s: ~2h on 300
nodes



2D SeisSol (Laptop)

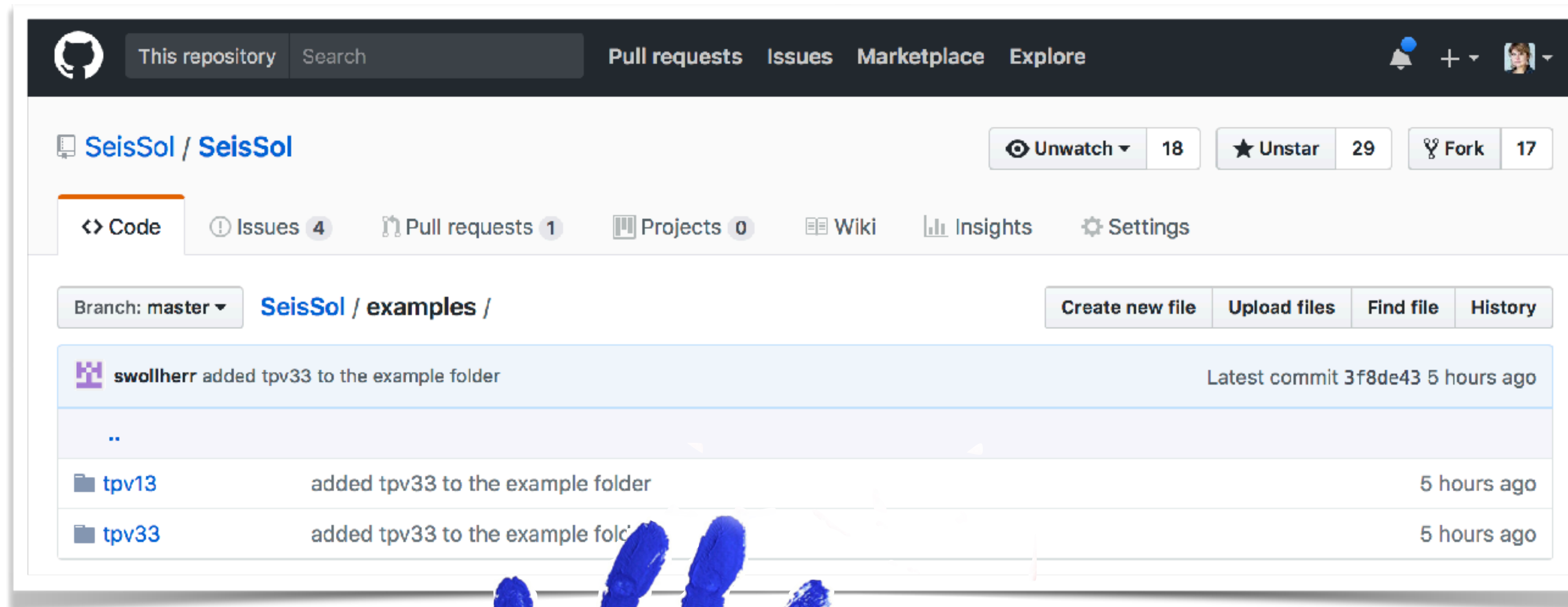


Kaikoura: 29 mio elements, 90 sec., **2 hours**
on 3000 Sandy Bridge cores



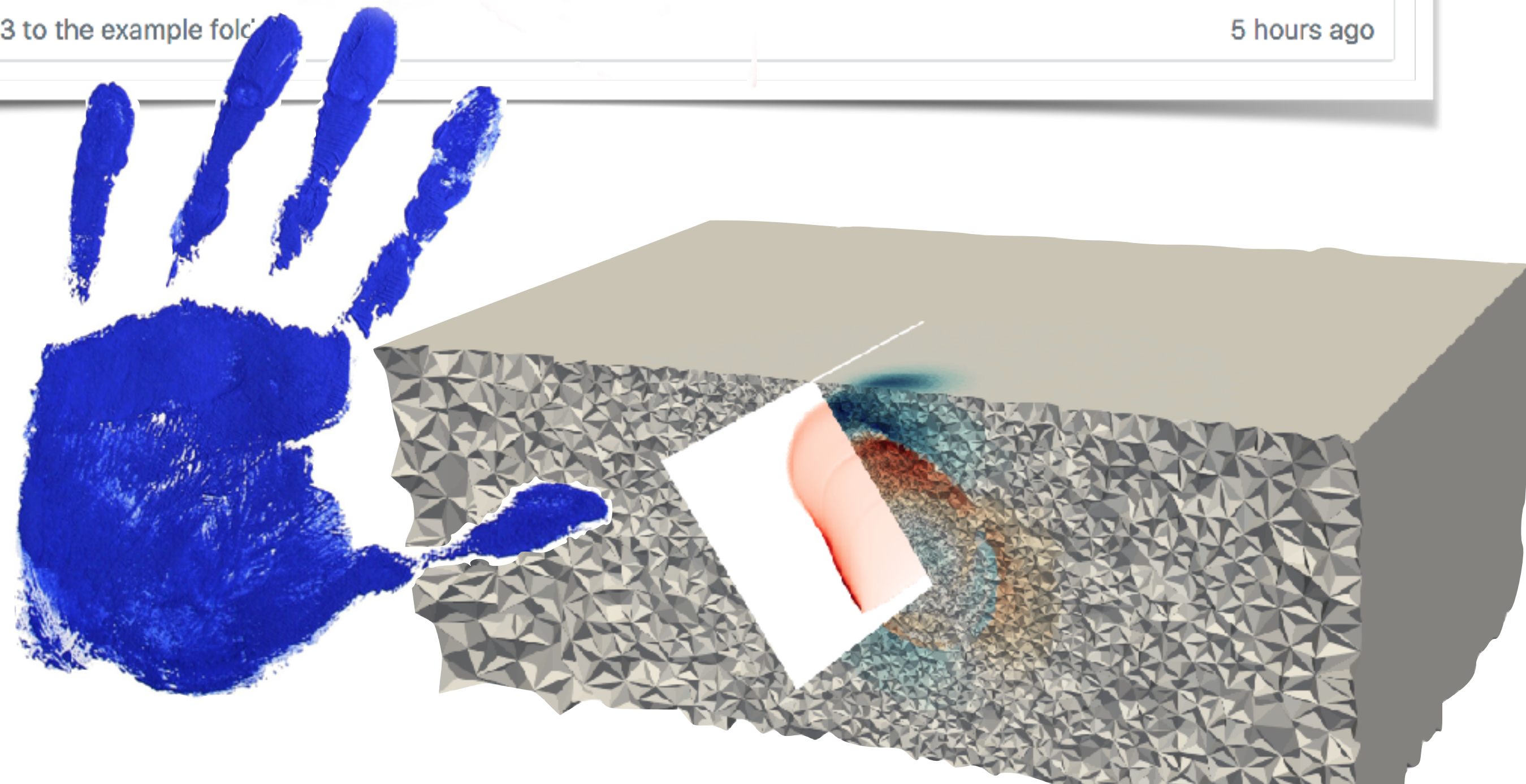
Landers: 10 mio elements, 100s, 200m
fault resolution, 500m topo resolution,
3D velocity model =: ~1h on 100 nodes
(with plasticity 6.2% increase)

Hand's on!



github.com/SeisSol

www.seissol.org




SeisSol

On Github

- Please note the **read the docs** with first steps and lots of material on geometry, meshing, compiling, source formats, ...

<https://seissol.readthedocs.io/>


 SeisSol
latest

Search docs

INTRODUCTION
History
Compilation
A first example
Acknowledgements
Related publications

STRUCTURAL MODELS
CAD models
Meshing with SimModeler
Meshing with PUMGen
Gmsh

INVOKING SEISSOL
Configuration
Parameter File
easi
Fault tagging

 Read the Docs v: latest ▾

Docs » SeisSol

SeisSol

SeisSol is a software package for simulating wave propagation and dynamic rupture based on the arbitrary high-order accurate derivative discontinuous Galerkin method (ADER-DG).

Characteristics of the SeisSol simulation software are:

- use of arbitrarily high approximation order in time and space
- use of tetrahedral meshes to approximate complex 3D model geometries (faults & topography) and rapid model generation
- use of elastic, viscoelastic and viscoplastic material to approximate realistic geological subsurface properties
- parallel geo-information input (ASAGI)
- to produce reliable and sufficiently accurate synthetic seismograms or other seismological data set

Introduction

- [History](#)
- [Compilation](#)
 - [Initial Adjustments to .bashrc](#)
 - [Installing SCons](#)
 - [Installing HDF5](#)
 - [Installing netCDF](#)



SeisSol

On Github

<https://seissol.readthedocs.io/>

- Please note the **read the docs** with first steps and lots of material on geometry, meshing, compiling, source formats, ...

Compilation

In order to run SeisSol, you need to first install:

- Python (≥ 3.5)
- Numpy ($\geq 1.12.0$)
- SCons (≥ 3.0 , for instructions see below)
- hdf5 (≥ 1.8 , for instructions see below)
- netcdf (C-Release) (≥ 4.4 , for instructions see below)
- Intel compiler (≥ 17.0 , icc, icpc, ifort) or GCC (≥ 5.0 , gcc, g++, gfortran)
- Some MPI implementation (e.g. OpenMPI)
- ParMETIS for partitioning
- libxsmm (libxsmm_gemm_generator) for small matrix multiplications
- PSpaMM (pspamm.py) for small sparse matrix multiplications (required only on Knights Landing or Skylake)
- CMake (for compiling submodules ImpalaJIT and yaml-cpp)

- Prerequisites:

SeisSol

Cookbook

<https://seissol.readthedocs.io/>

COOKBOOK

Overview

SCEC TPV5

SCEC TPV6

SCEC TPV12

SCEC TPV13

SCEC TPV16/17

SCEC TPV24

SCEC TPV29

SCEC TPV104

Point Source

Kinematic source example - 1994
Northridge earthquake

[Docs](#) » Overview

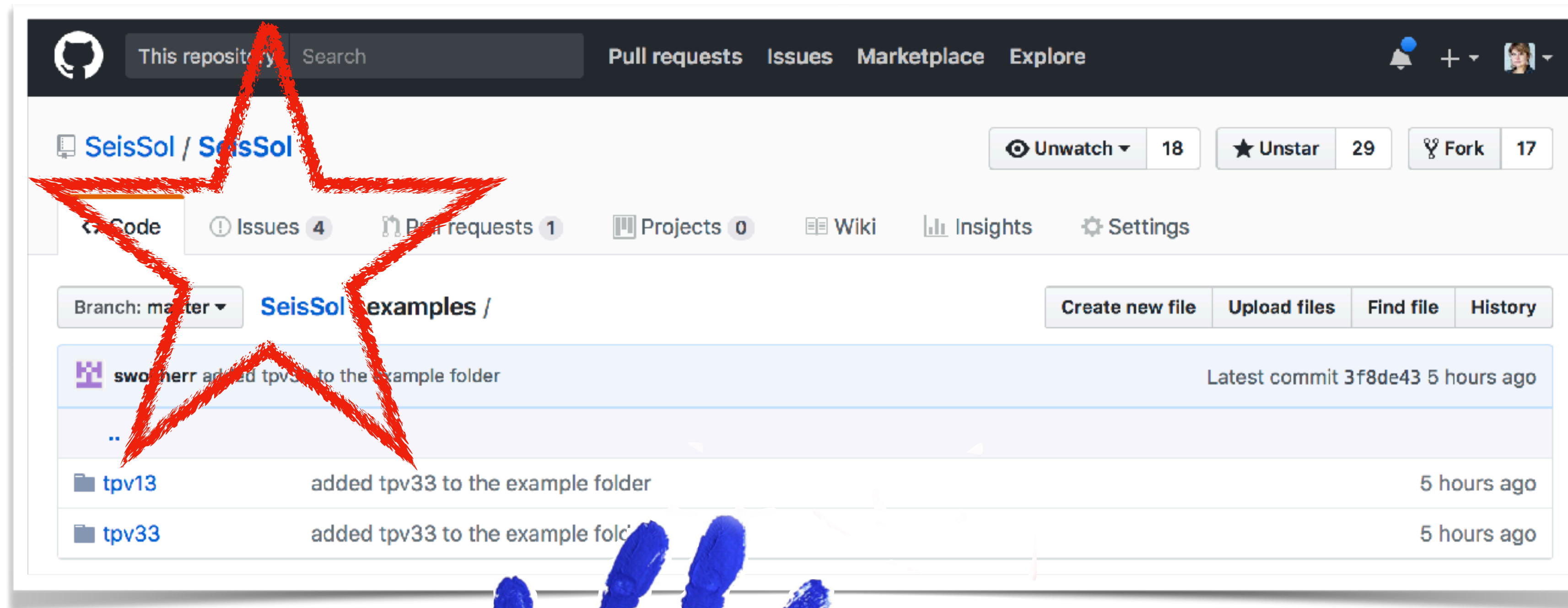
[Edit on GitHub](#)

Overview

This documentation is a collection of useful dynamic simulation examples to help users build models from scratch with little effort. Each example is demonstrated carefully with geometry building, parameter setup and result visualization. Users are suggested to repeat each example in order to get a comprehensive idea of how to set up dynamic simulation models with SeisSol.

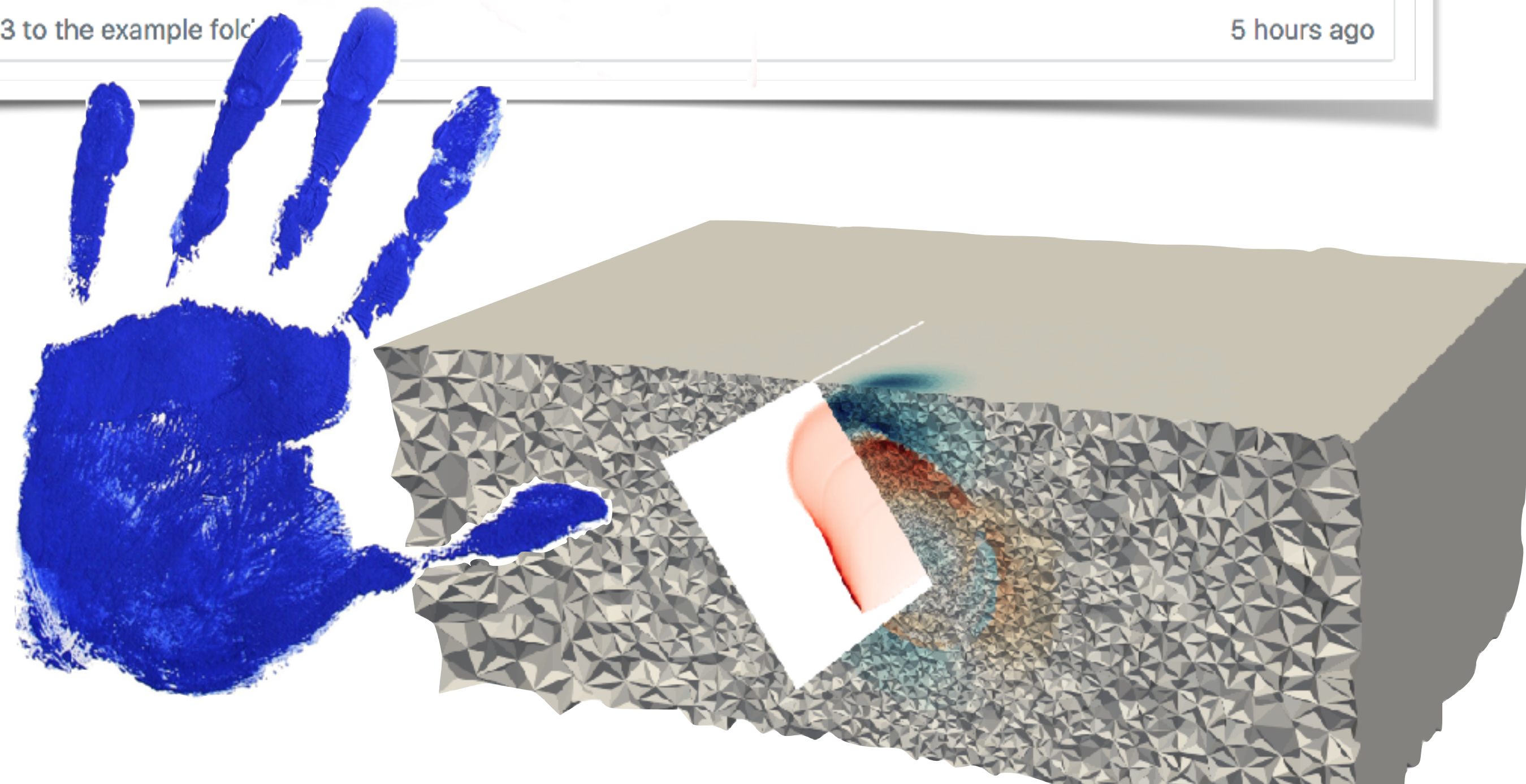
SeisSol is a part of SCEC dynamic code validation project (Harris et al. 2018) (<http://scecddata.usc.edu/cvws/>). Here we show several SCEC benchmarks for beginners to quickly catch up with SeisSol workflow. Each benchmark example is composed of a short problem description, a section of *geometry*, *initial setups* (*stress*, *nucleation*, *friction*, etc.), and *simulation results*.

For all further questions ...



github.com/SeisSol

www.seissol.org



1. Training:

A simple example

- **SCEC benchmark** tpv13: dipping fault, off-fault plastic deformation, supershear rupture, 8s simulation time
- 1.5 mio element mesh with 250m fault discretisation - 9 min, 20 nodes with 16 omp threads).

SeisSol / SeisSol

<> Code

Issues 4

Pull requests 1

Branch: master

SeisSol / examples / tpv13 /

swollherr added tpv33 to the example folder

..

DGPATH

parameters_tpv13.par

parameters_tpv13_easi.par

tpv12_13_example.geo

tpv12_13_fault.yaml

tpv12_13_initial_stress.yaml

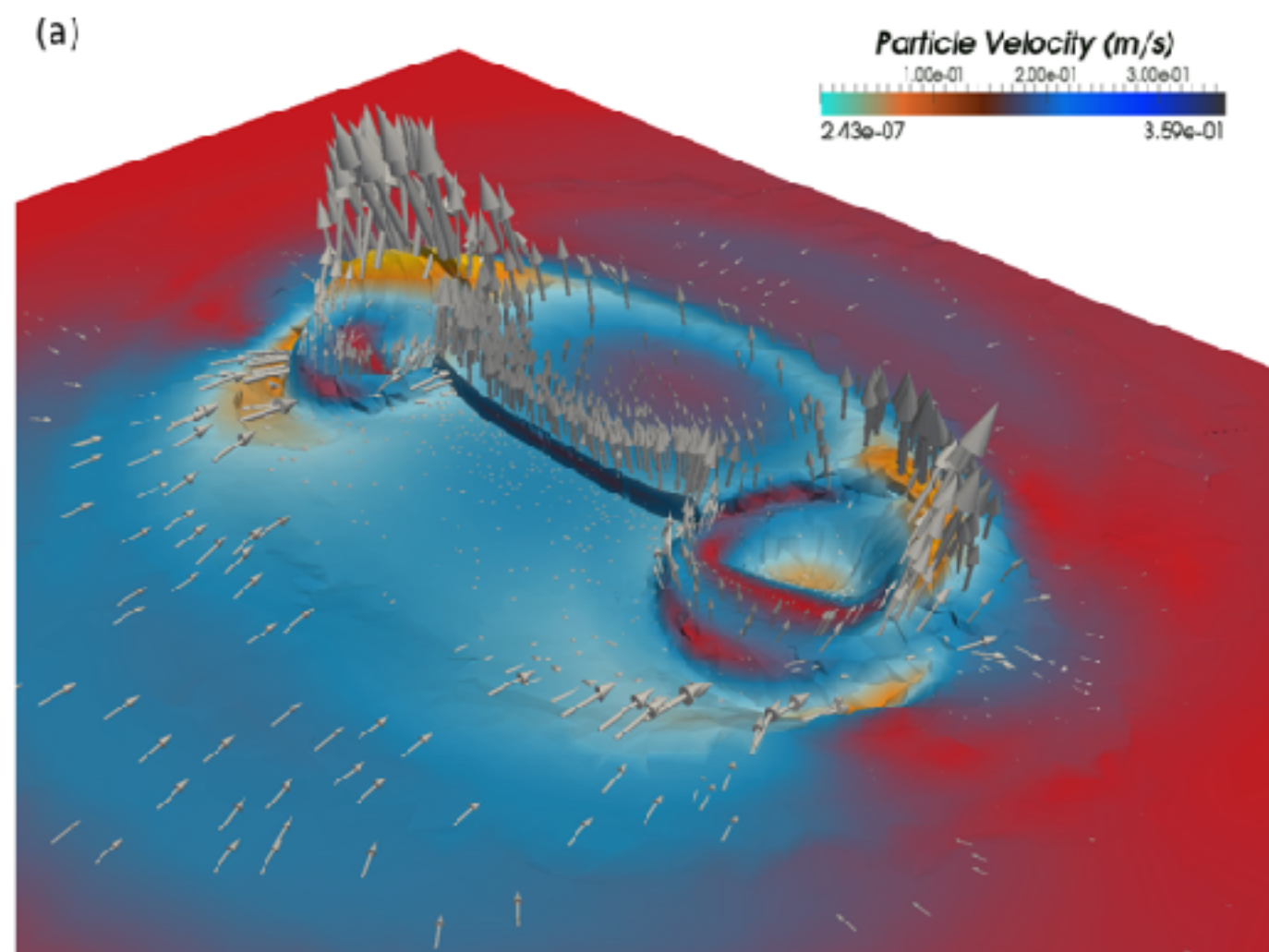
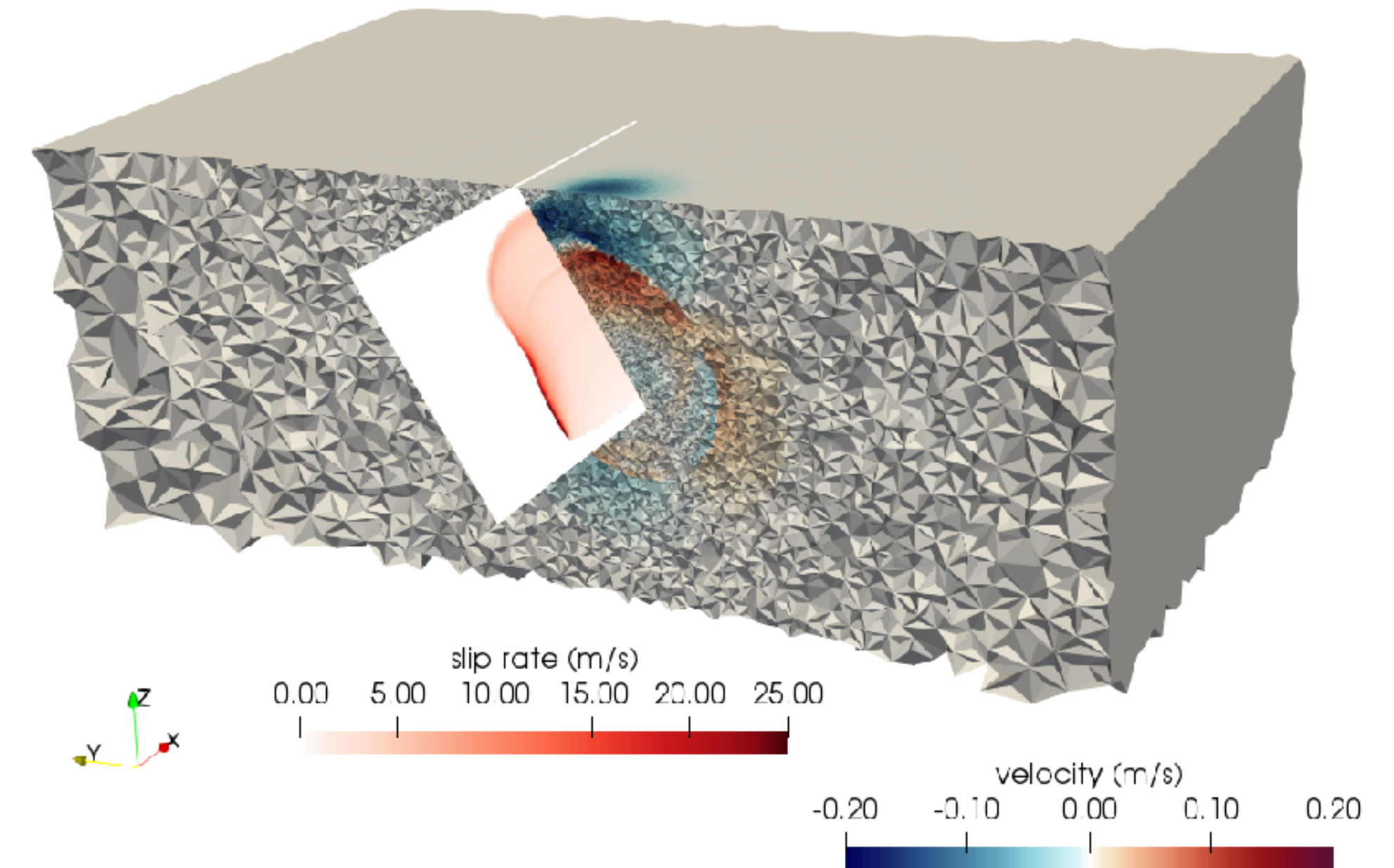
tpv12_13_material.yaml

tpv13_faultreceivers.dat

tpv13_receivers.dat

Example mesh for SCEC tpv13, 250m on fault resolution.

<http://scecddata.usc.edu/cvws/>



Asymmetric ground motion in the surrounding of a dipping fault

Our input file

- using easi

<https://github.com/SeisSol/easi/>

easi design philosophy

1. Write general and reusable functions $f : \mathbb{R}^m \rightarrow \mathbb{R}^n$. E.g.
 - Constant map: $f(\mathbf{x}) = \mathbf{c}$
 - Affine map: $f(\mathbf{x}) = A\mathbf{x} + \mathbf{c}$
 - Polynomial map: ($m = 1$): $f(x) = \sum_{i=0}^n \mathbf{a}_i x^i$
 - JIT compilation map: $f(\mathbf{x}) = \text{run-time compiled C-like function}$
 - ASAGI map: Trilinear interpolation from structured grid

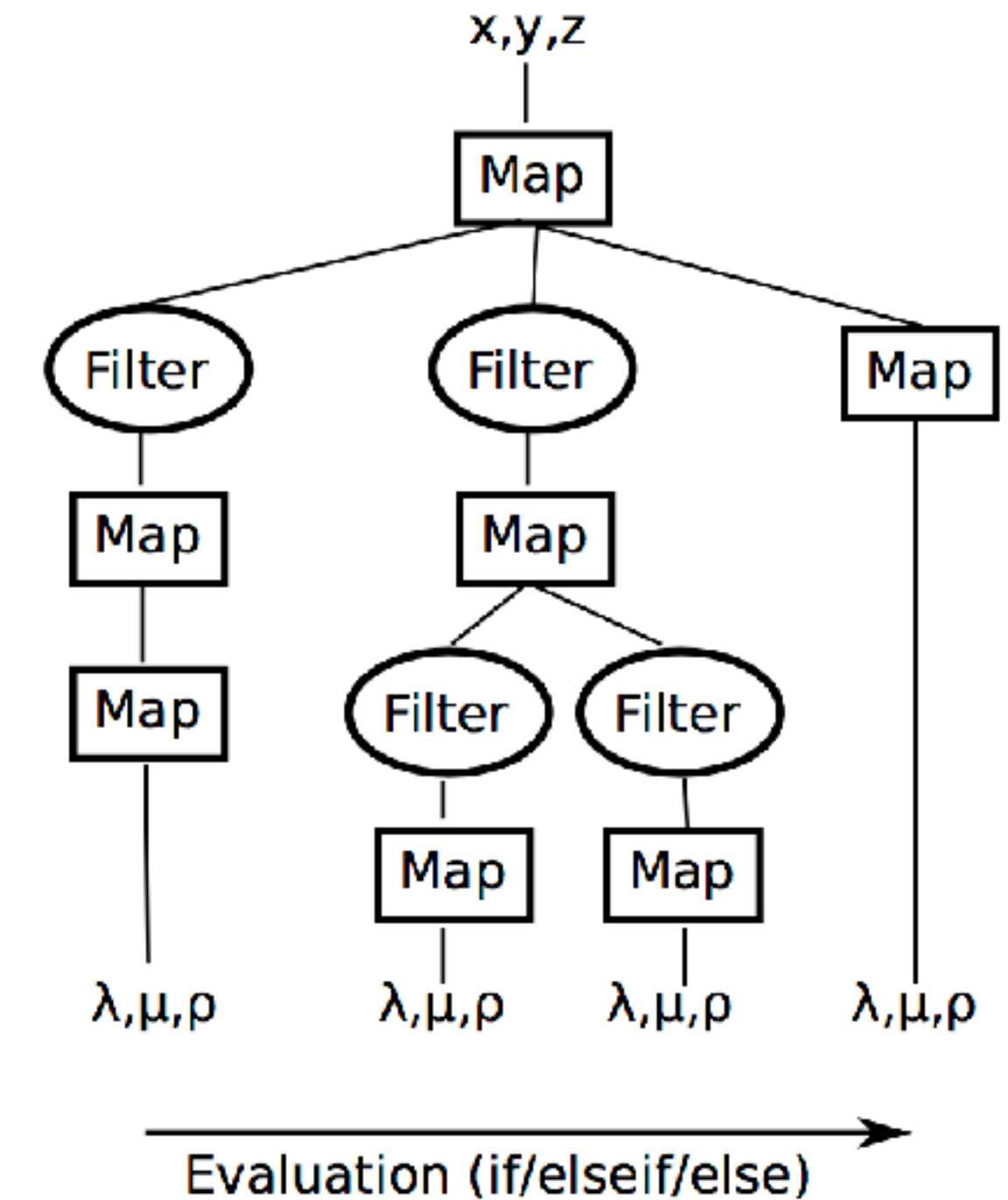
2. Powerful expressions through composition:

$$f = f_1 \circ \dots \circ f_N$$

3. Everything is specified through human readable configuration files (YAML).

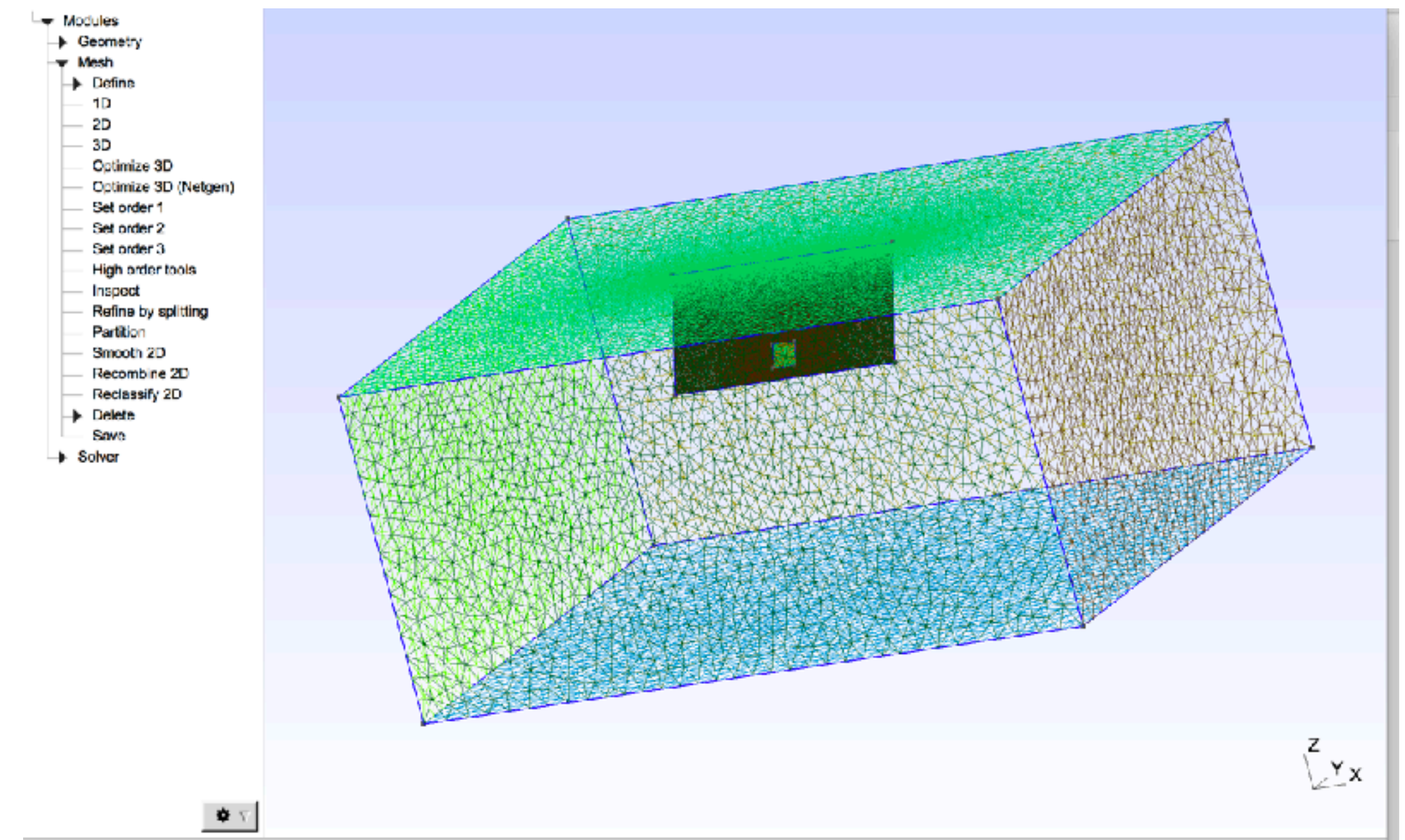
We are able to replace more than 5000 lines of Fortran code with easi.

easi composition principle

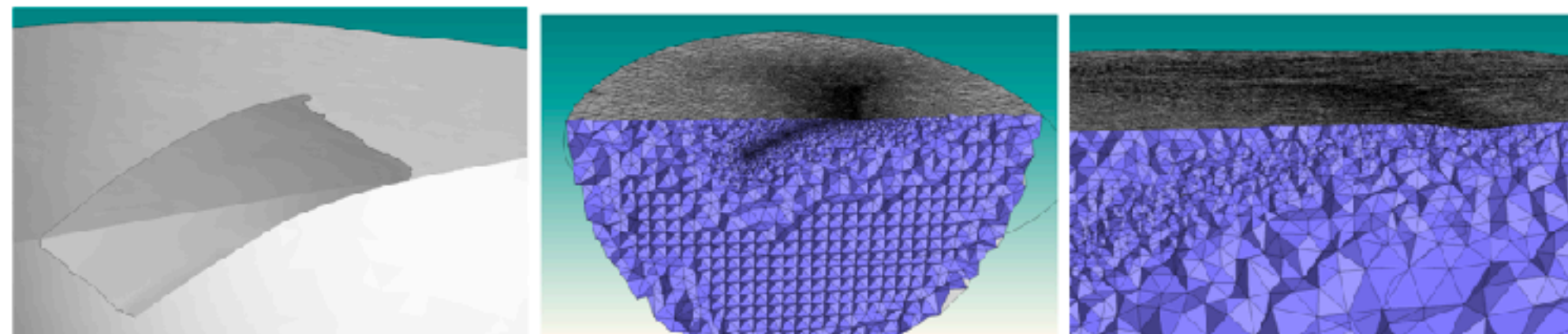


Geometry and meshing

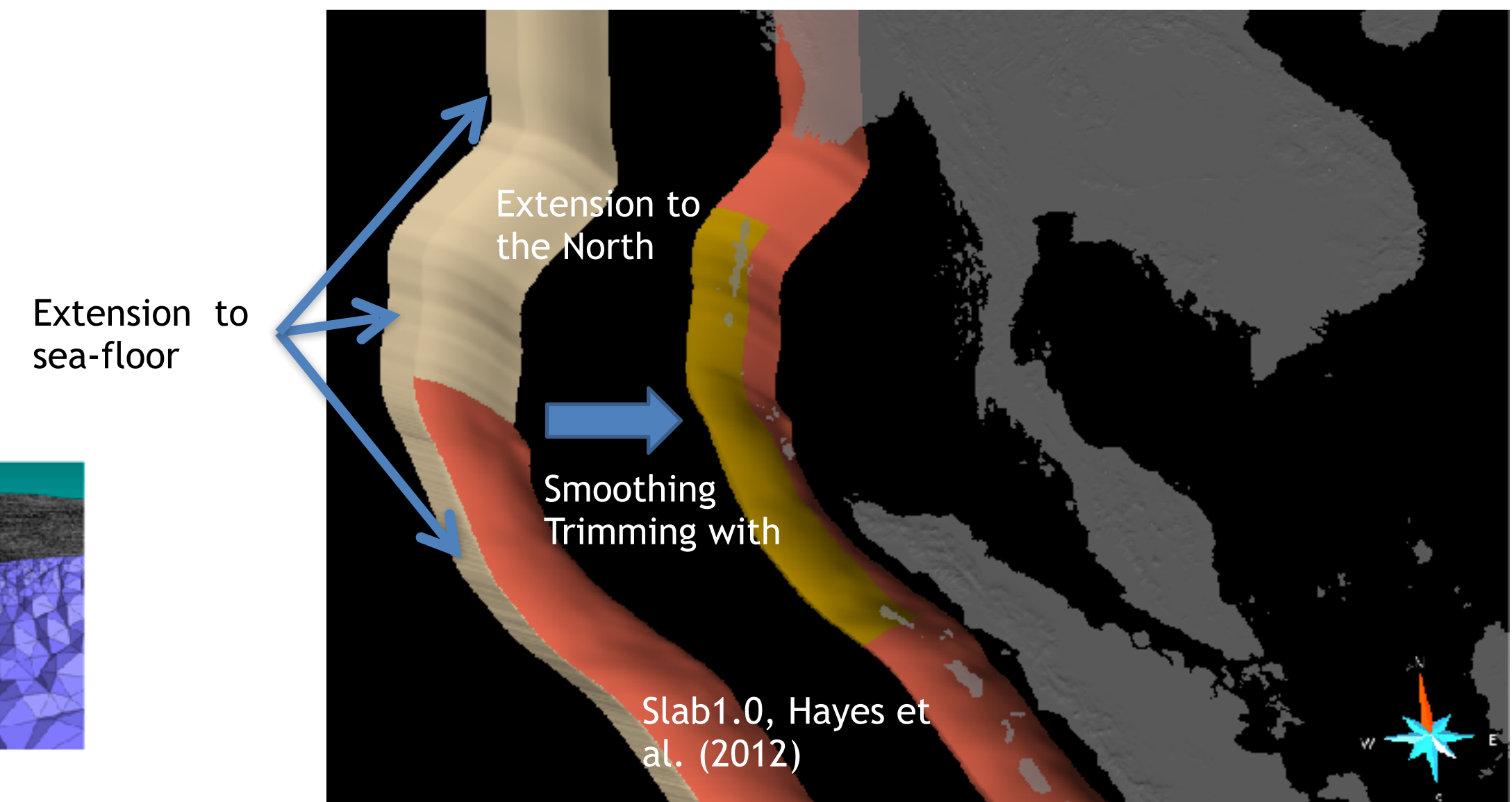
- **Gmsh** (<http://gmsh.info>, open source) for most simple geometries and every-day mesh sizes, many tutorials, limited in terms of geometry
- **Simmodeler** (Simmetrix, **free for academics**) for large meshes / complex geometries: customised GUI for SeisSol, pumgen library for parallel meshing on Clusters
- Mesh is provided in parallel data format - code does internal **partitioning**



Gmsh interface for example geometry and 2D mesh



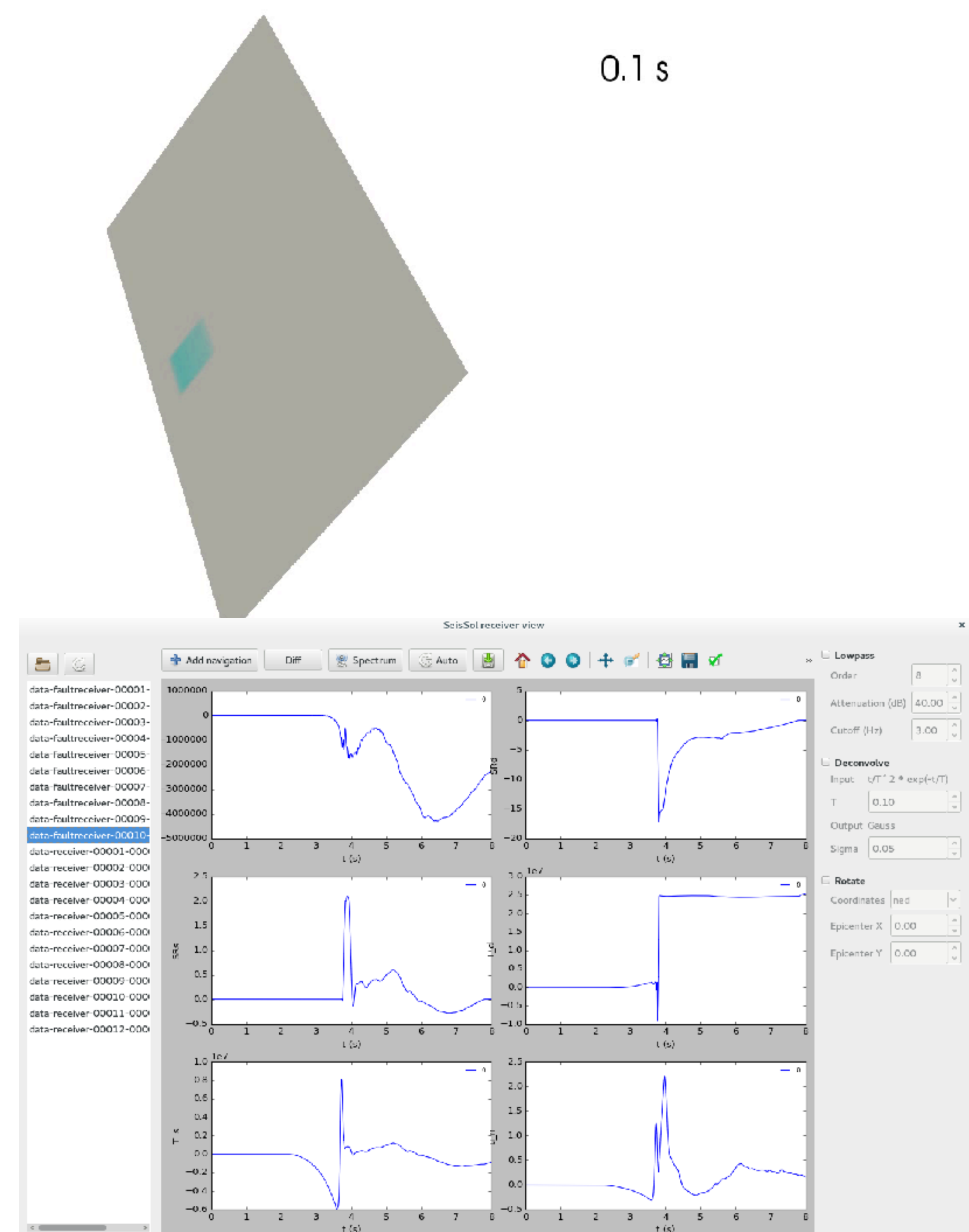
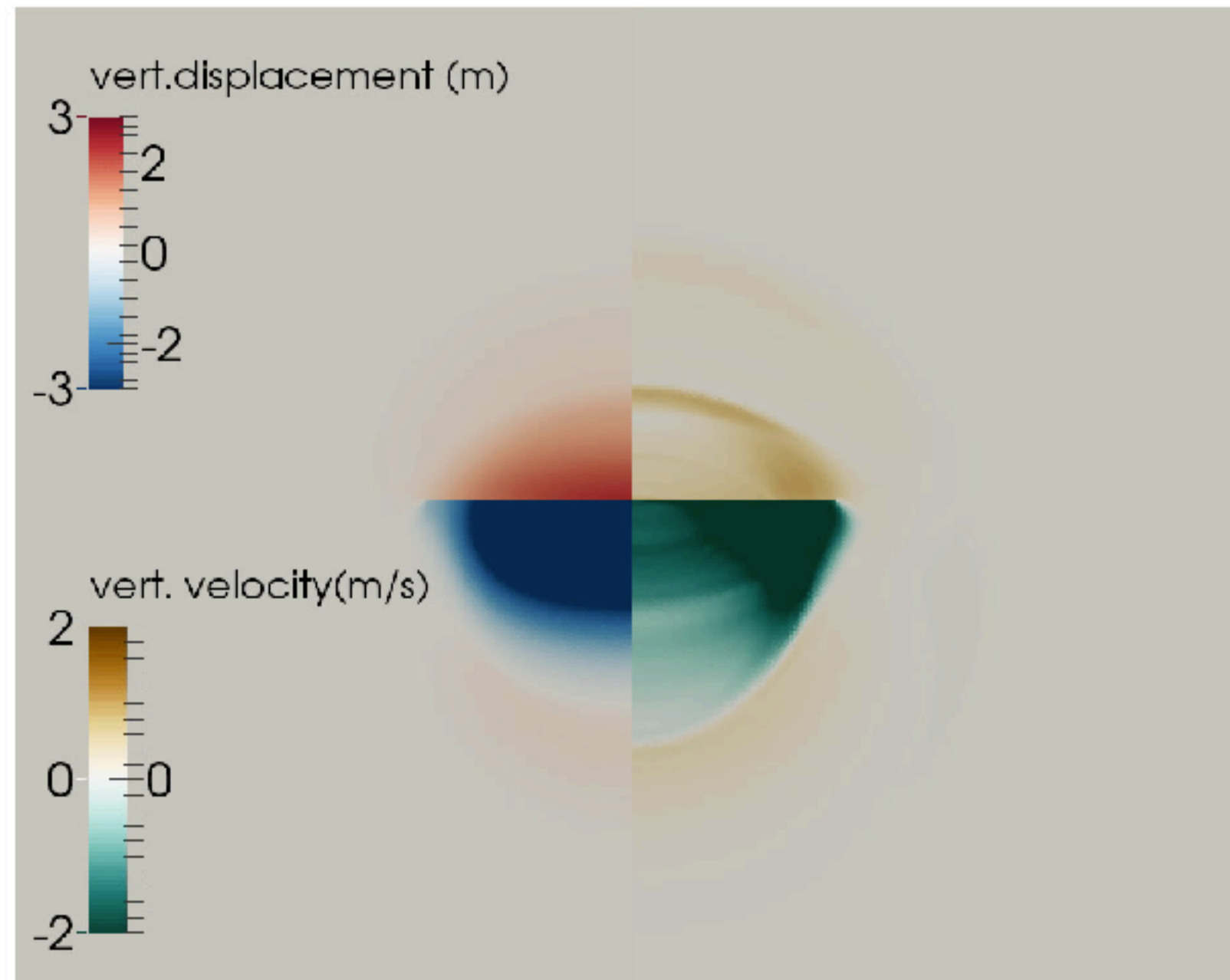
<http://www.simmetrix.com/index.html>



GoCAD interface for complex geometries

Output/Visualization

- **Paraview:** on-fault fields, wavefield, surface and plastic strain
- Seismograms via viewrec from SeisSol/postprocessing/visualization/receiver/bin/



EXAMPLE 2

RAPID EARTHQUAKE/Tsunami RESPONSE –

THE 2018, PALU-SULAWESI EVENT

Coupled, Physics-based Modeling Reveals Earthquake Displacements are Critical to the 2018 Palu, Sulawesi Tsunami

T. Ulrich¹, S. Vater², E. H. Madden^{1,3}, J. Behrens⁴, Y. van Dinther⁵, I. van Zelst⁶, E. J. Fielding⁷, C. Liang⁸, and A.-A. Gabriel¹



RAPID EARTHQUAKE/Tsunami RESPONSE - THE 2018, PALU-SULAWESI EVENT

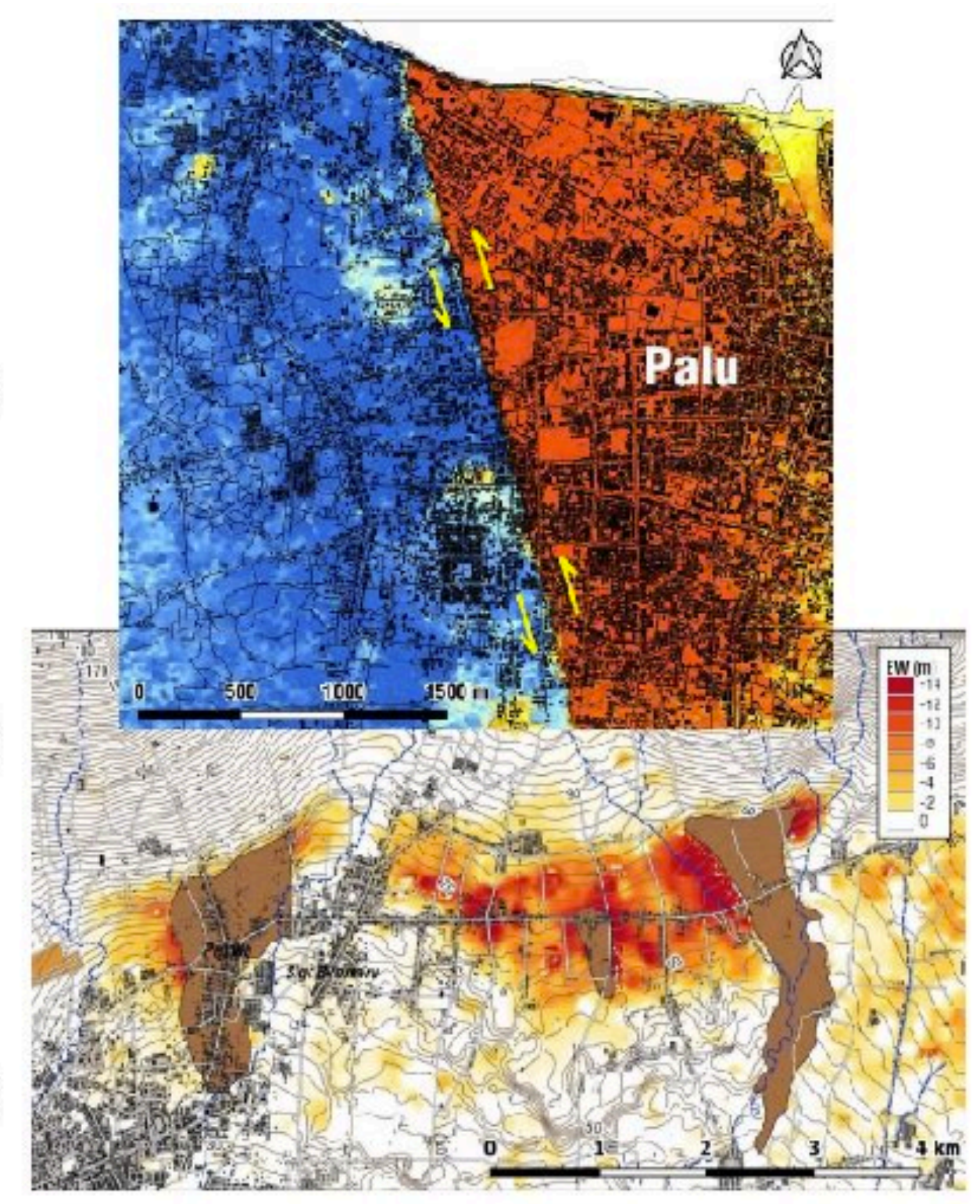
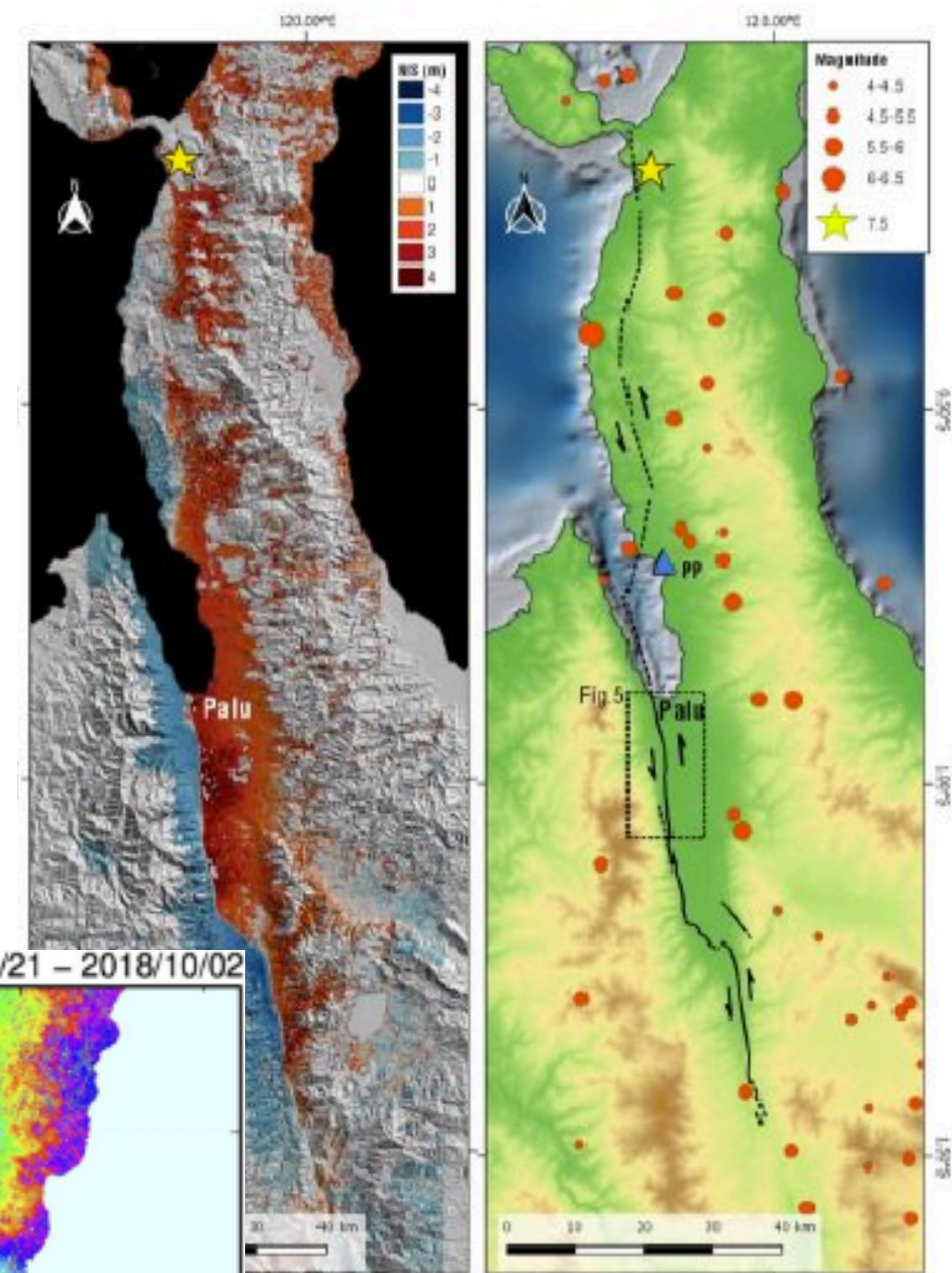
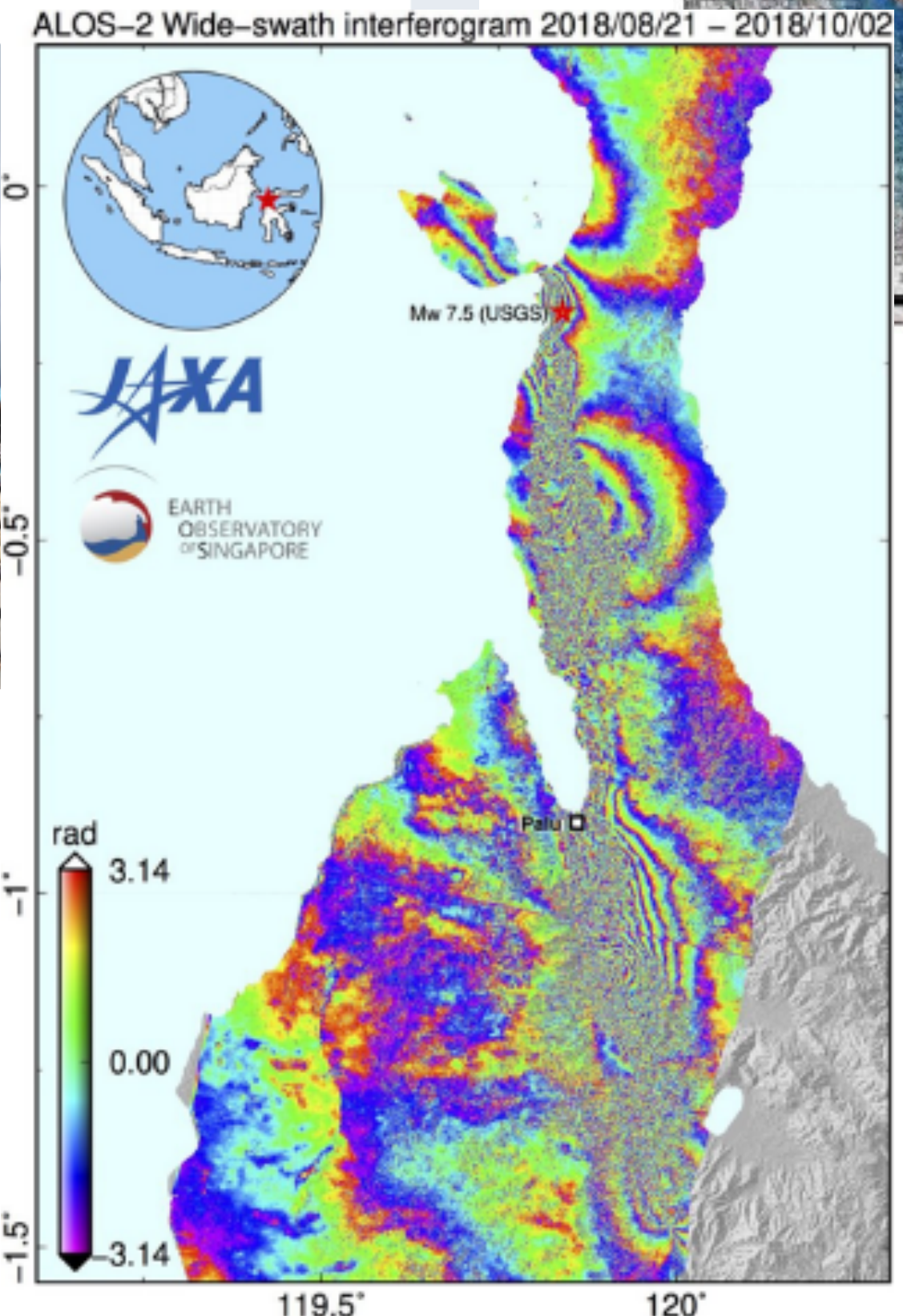
#sulawesi

Top Latest People Photos Videos News Broadcasts

Search filters · Show



Kristalina Georgieva @KGeorgieva · Oct 19
Just one week ago I was in #Palu #Sulawesi to see first hand the destruction caused by the earthquake and tsunami. My thoughts remain with the people I met, and we have mobilized our support to get to the affected areas as soon as possible. [worldbank.org/en/news/press-...](https://www.worldbank.org/en/news/press-...)



PHYSICS-BASED EARTHQUAKE-TSUNAMI MODELING

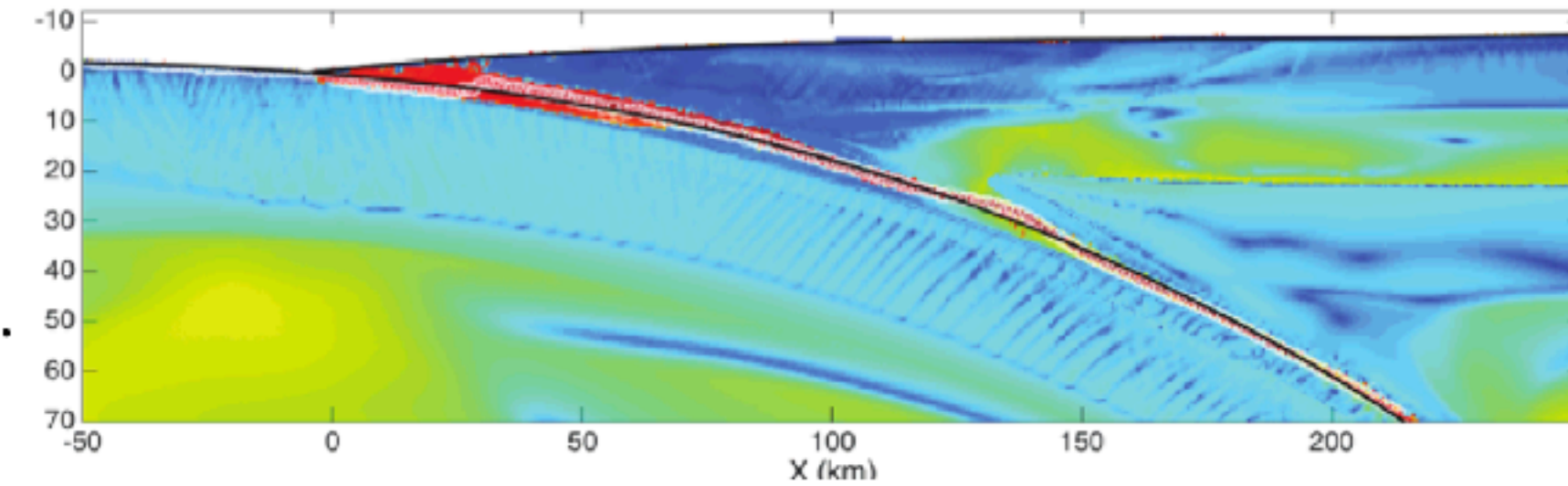
- THE ASCETE FRAMEWORK

www.ascete.de

DEFORMATION

ETH zürich

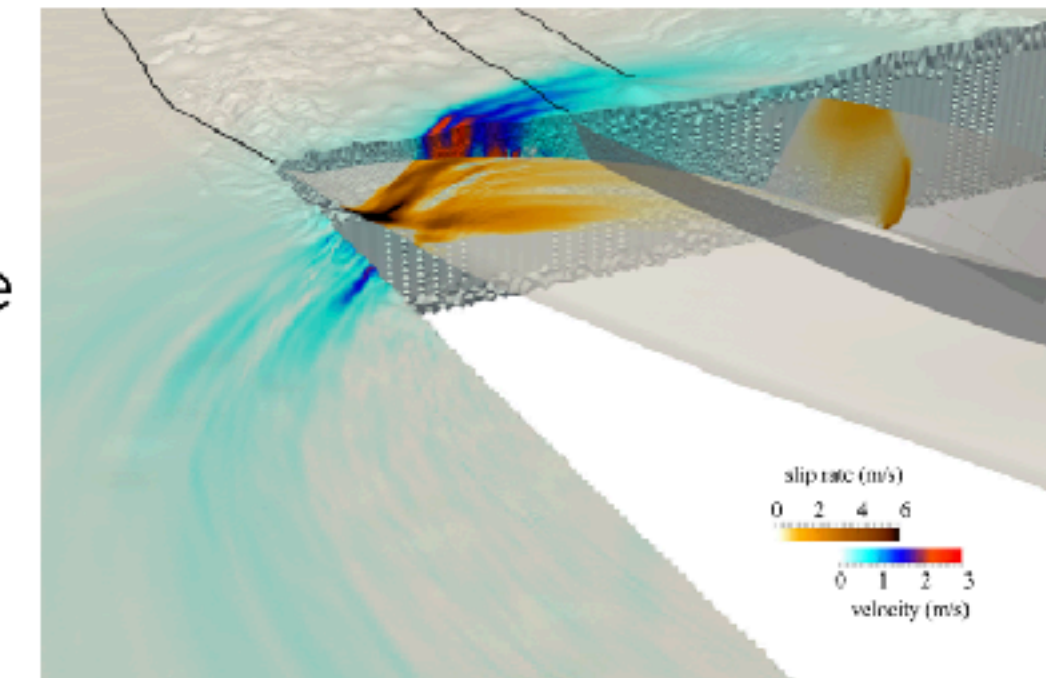
Seismo-thermal-mechanical model captures geodynamics & seismic cycling.
Provides initial conditions for the earthquake model.



EARTHQUAKE

LMU
LUDWIG-MAXIMILIANS-UNIVERSITÄT MÜNCHEN

Rupture model of a single earthquake with seismic wave propagation.
Provides time-dependent, coseismic seafloor displacements for the tsunami model.



TUM
TECHNISCHE UNIVERSITÄT MÜNCHEN

SCIENTIFIC COMPUTING

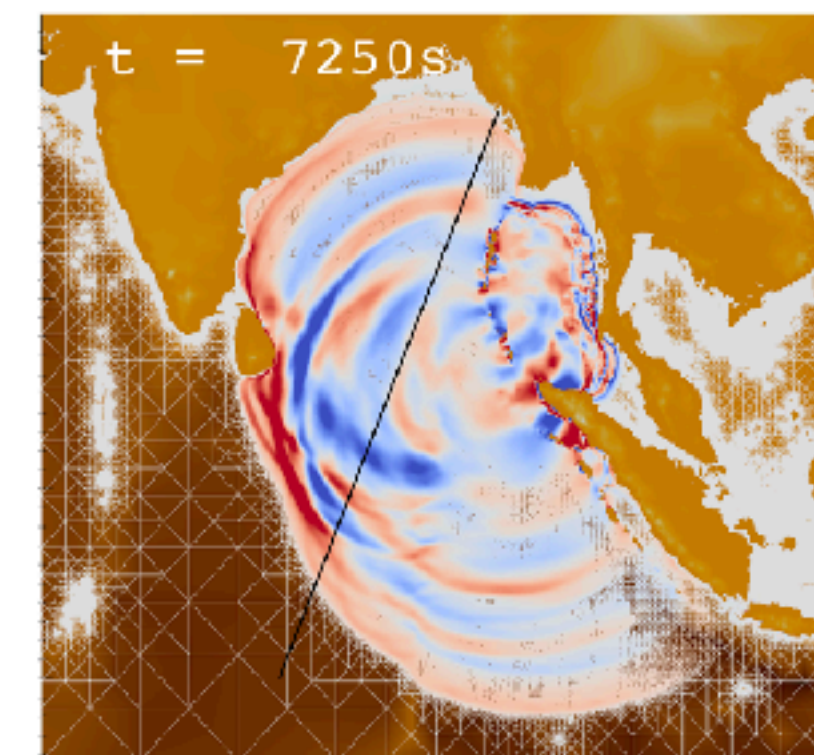
Physics-based models of the necessary scale require highly optimized parallel algorithms and software.



TSUNAMI

UH

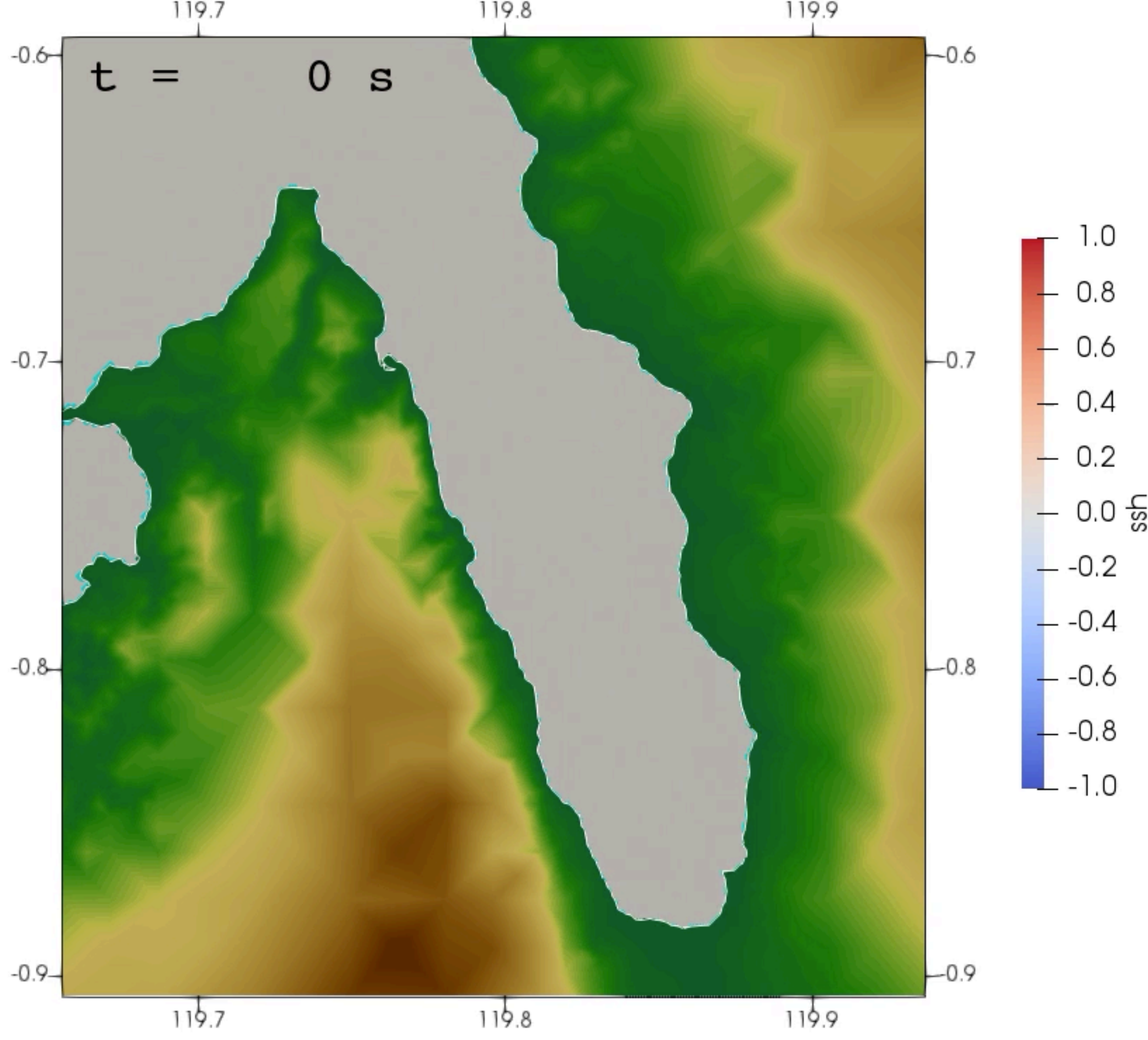
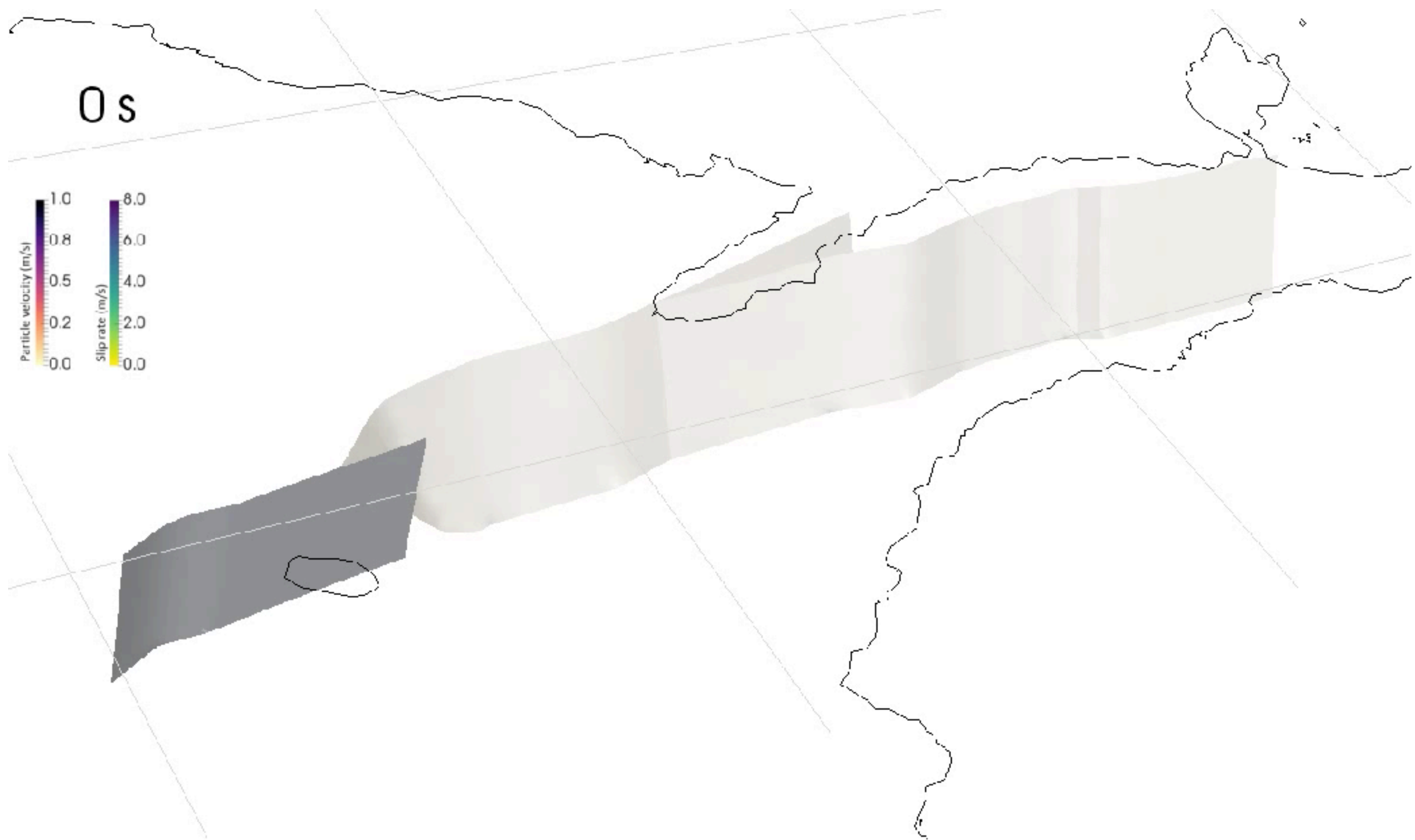
Non-linear, hydrostatic wave propagation and inundation model.



RAPID EARTHQUAKE/Tsunami RESPONSE -

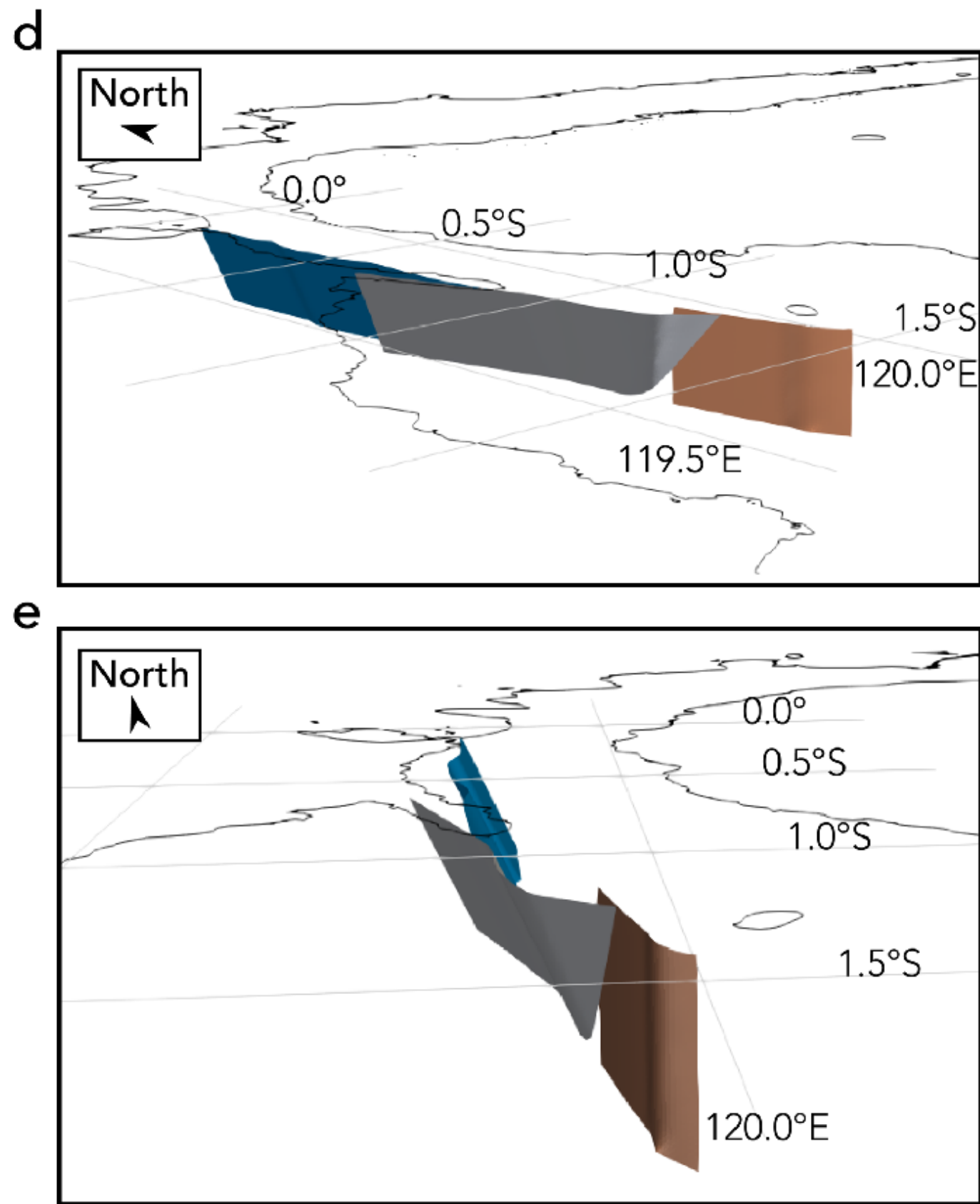
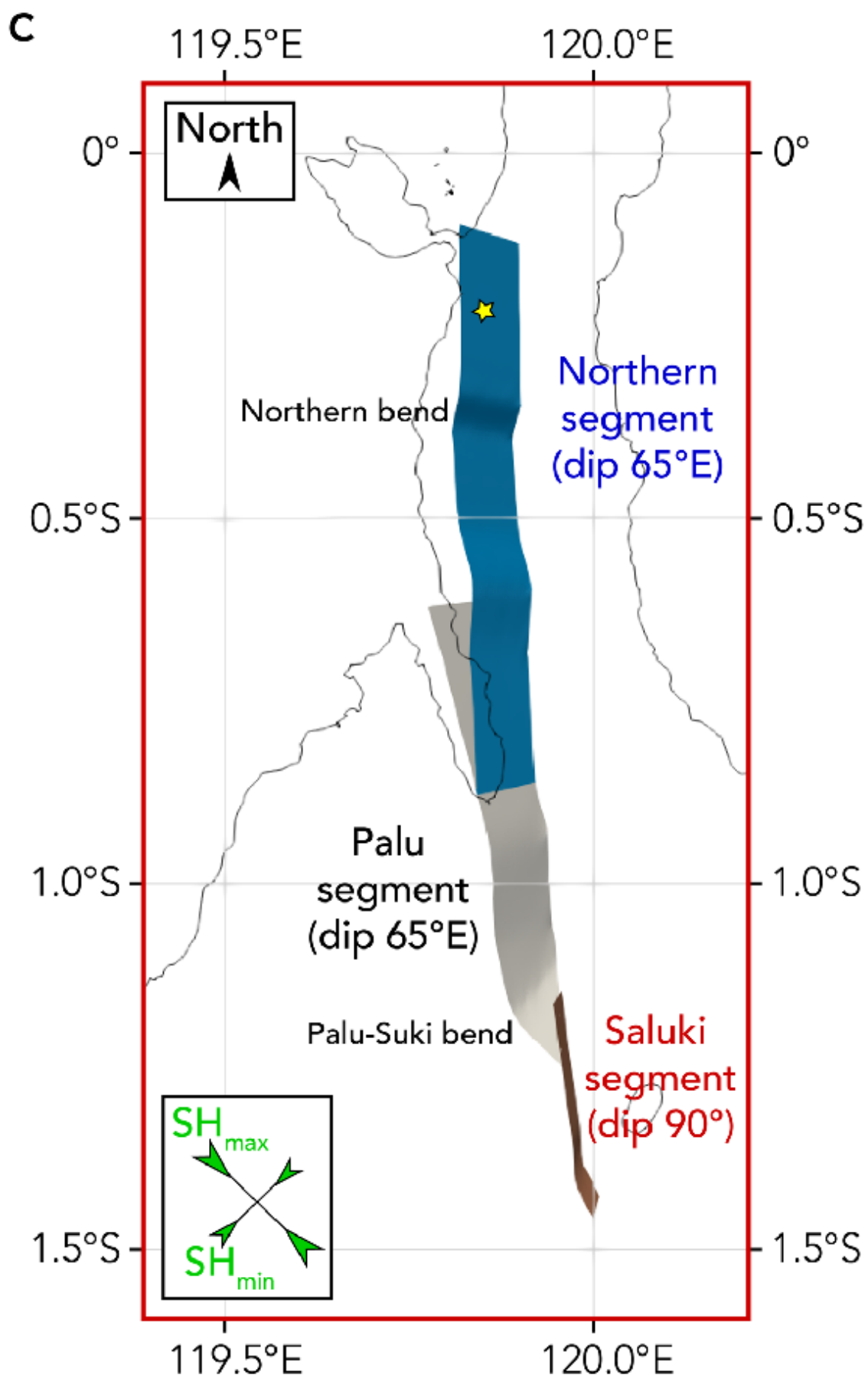
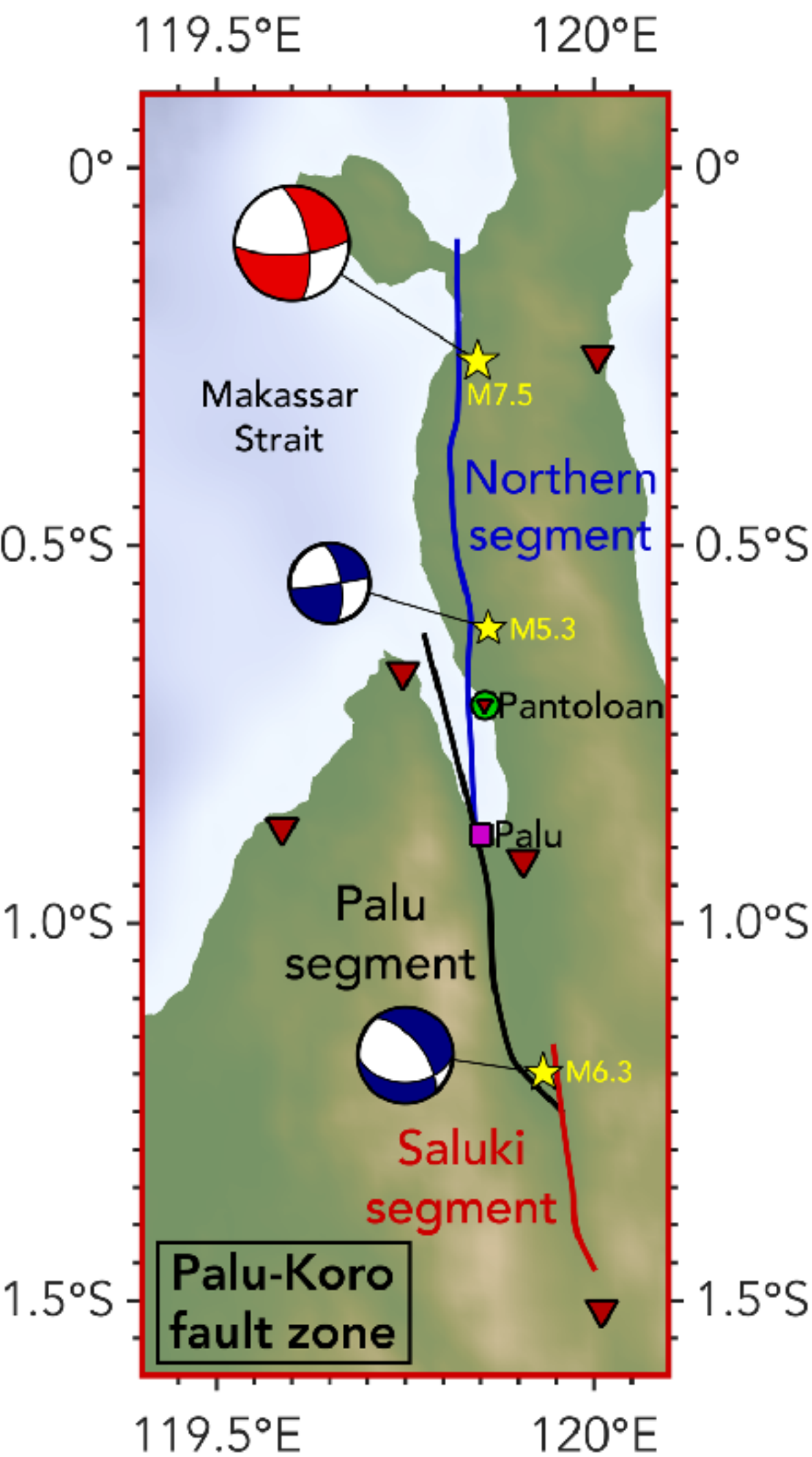
THE 2018, PALU-SULAWESI EVENT

Earthquake ground displacements accounting for transtension, dipping faults and bathymetry cause sufficient vertical displacements within Palu Bay to generate a tsunami comparable to available data



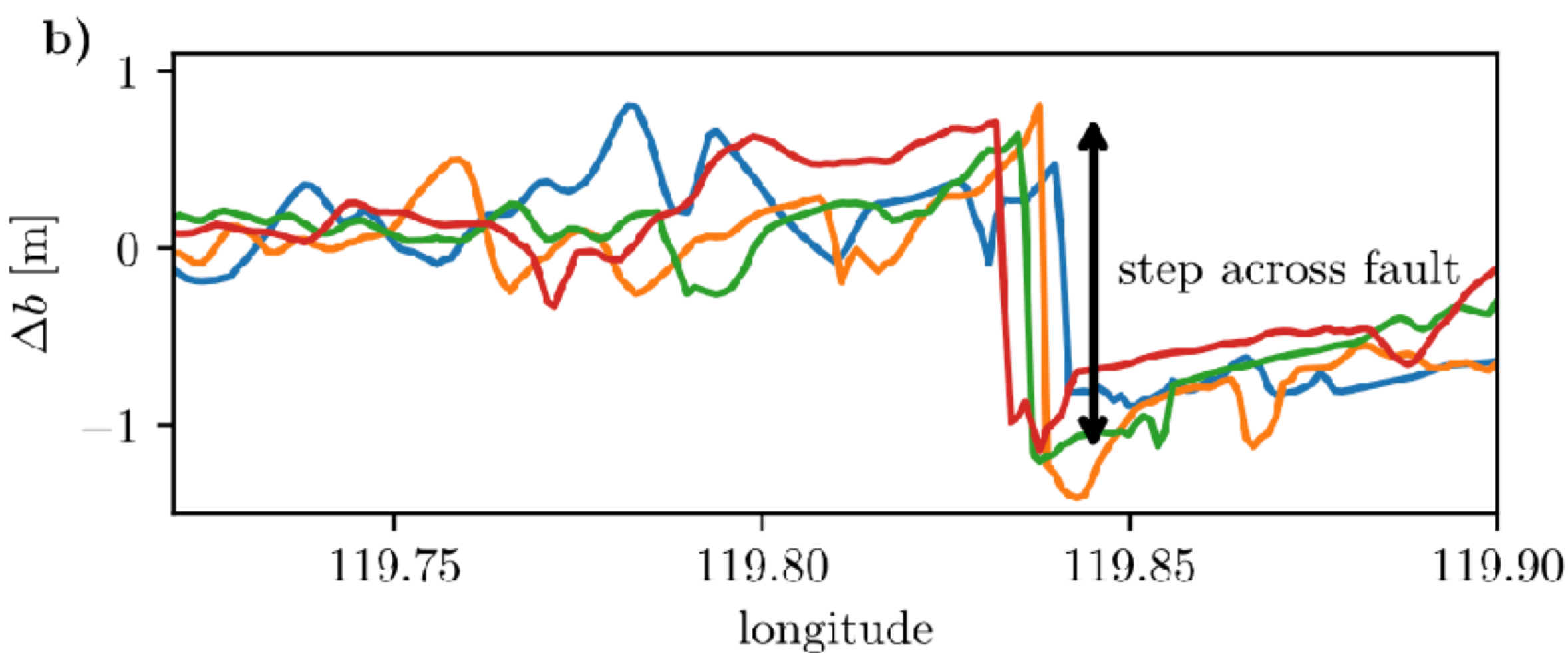
MODEL SETUP FROM SPARSE DATA

- 3D fault system from Sentinel-2, SAR data, regional seismicity
- Stress and strength based on World stress map; transtensional regime; high fluid pressure, maximising the ratio of shear / normal stresses; aligning shear traction with ground deformation and focal mechanisms; dynamic rupture across the fault system's geometric complexities.
- Dynamics constrained by teleseismics and moment rate release

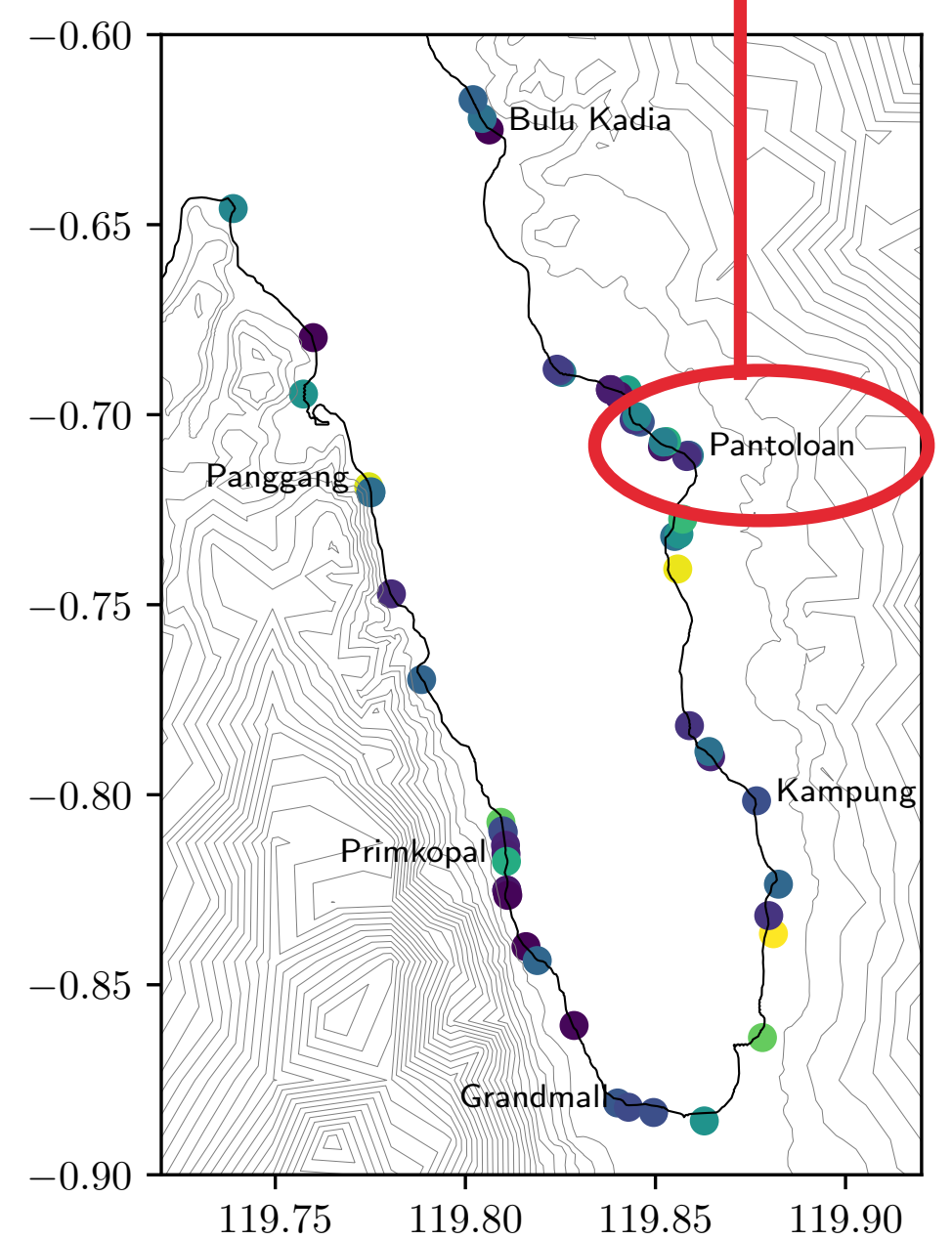
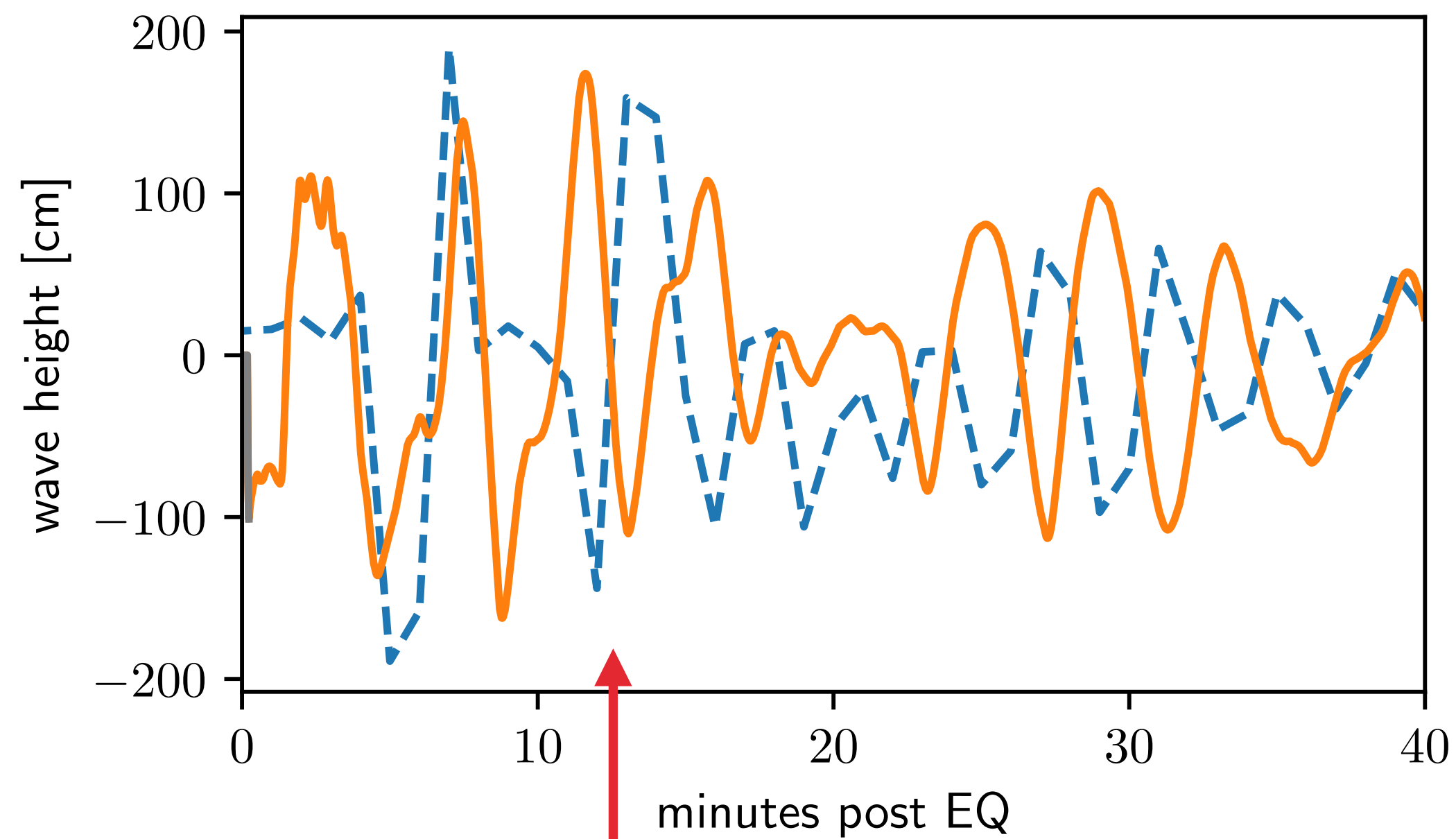


A CO-SEISMIC TSUNAMI

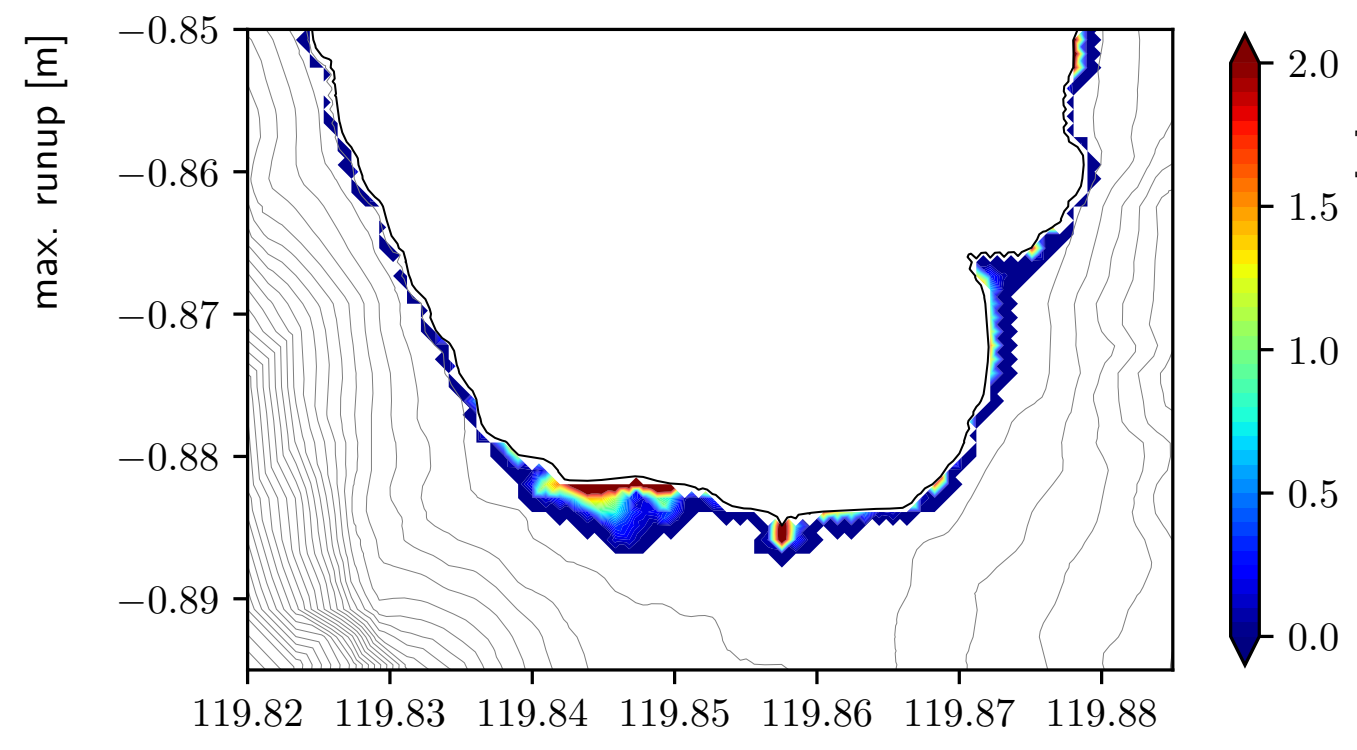
- Step of 1.5m across fault due to normal faulting component, additional effects of bathtub-like bathymetry



Model results compared with data at Pantoloan wave gauge

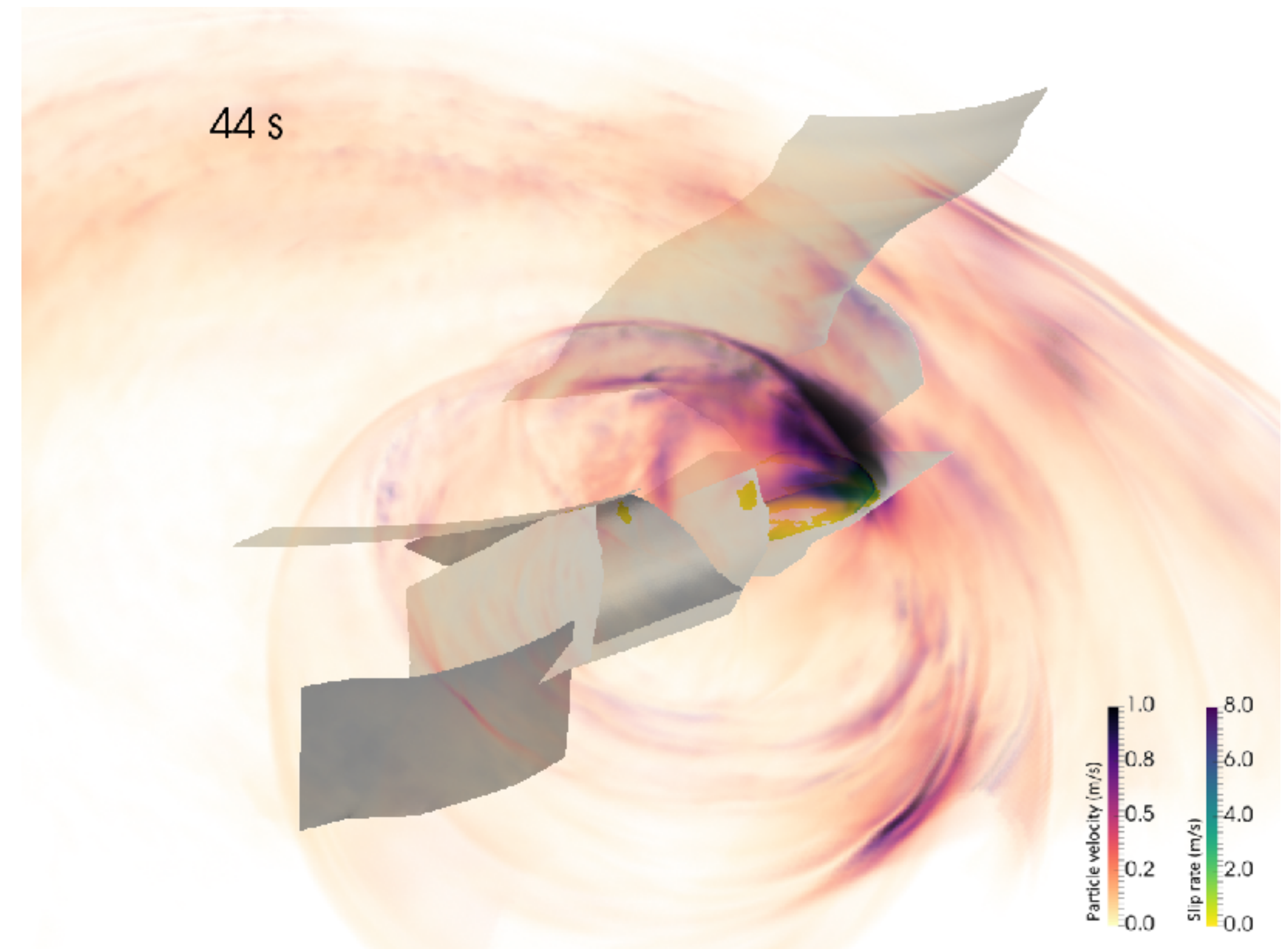


Model maximum inundation map



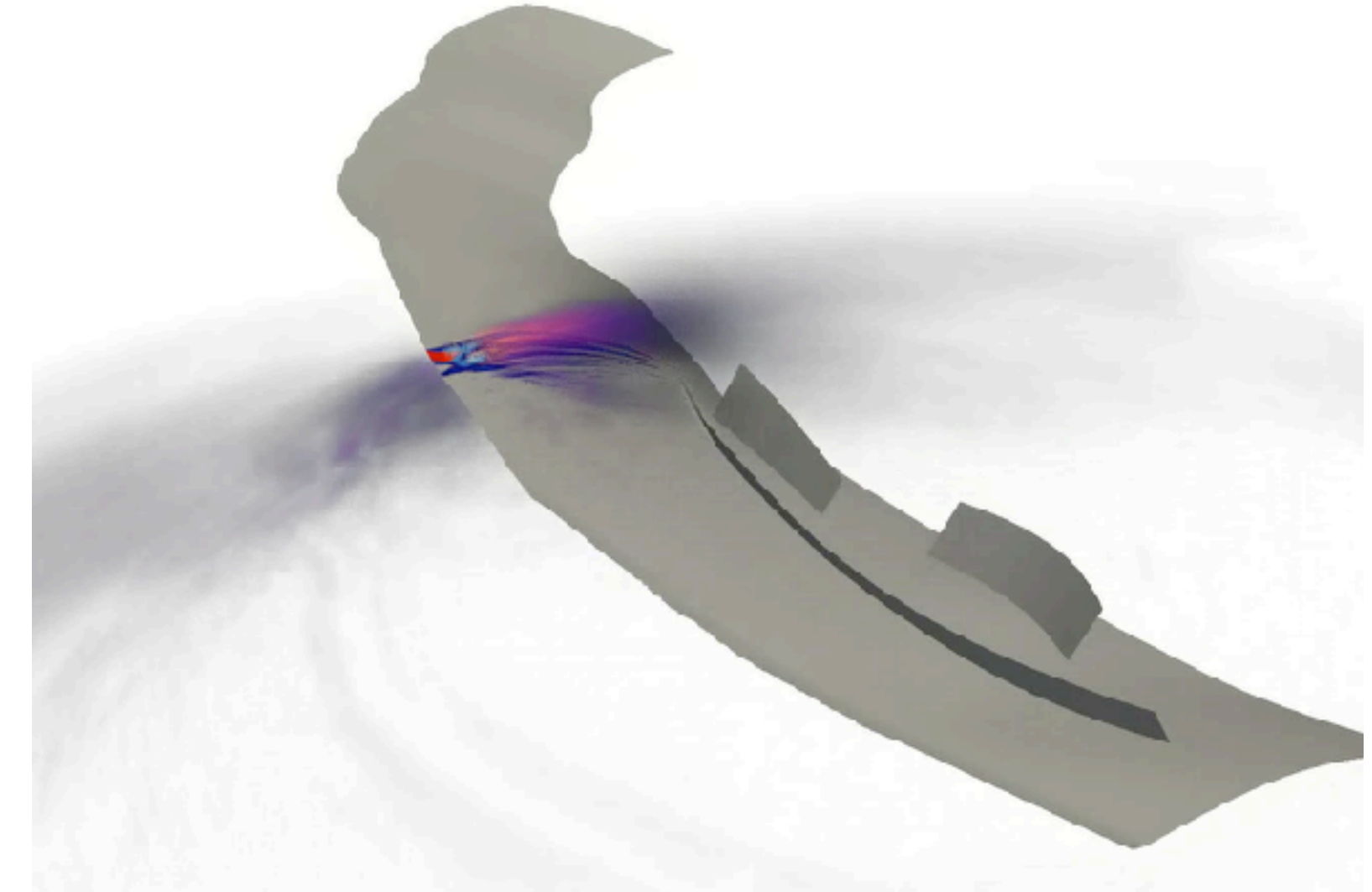
Conclusions (I):

- **Physics-based modeling provides mechanically viable insight into the physical conditions that allow rupture on complex fault systems and helps constraining competing views on earthquake sources**
- **Observational constraints, specifically community models, can be routinely included; Observational methods can themselves be constrained**
- **Bridging scales by coupling of rupture dynamics, seismic cycling, tsunami, global seismic wave propagation, intermediate and long-term geodynamic modelling**
- **Advances in high-performance computing and dense observations allow us to go beyond scenario-based analysis, aiming for urgent response quickly after an event occurs, ensemble simulations, dynamic inversion and uncertainty quantification**



Conclusions (II):

Our science is reproducible and open



- A setup including a mesh with over 3 million elements for the 2004 Sumatra-Andaman earthquake can be obtained from Zenodo <https://dx.doi.org/10.5281/zenodo.439946>.

```
$ git clone --recursive https://github.com/SeisSol/SeisSol
$ git checkout 201703
$ git submodule update

$ scons order=6 compileMode=release \ generatedKernels=yes
arch=dhsw \ parallelization=hybrid commThread=yes \ netcdf=yes

$ export OMP_NUM_THREADS=<threads >
$ mpiexec -n <processes > ./SeisSol parameters.par

# SuperMUC Phase 2
$ export OMP_NUM_THREADS =54
$ export KMP_AFFINITY=compact ,granularity=thread
```

see also: <http://www.studentclustercompetition.us/>

A ARTIFACT DESCRIPTION: EXTREME SCALE MULTI-PHYSICS SIMULATIONS OF THE 2004 SUMATRA MEGATHRUST EARTHQUAKE

A.1 Abstract

This artifact description contains information about the complete workflow required to set up simulations with the Shaking Corals version of SeisSol. We describe how the software can be obtained and the build process as well as necessary preprocessing steps to generate the input dataset for the node level performance measurements. Input datasets for the scaling and production runs are not publicly available due to their size. In addition, the artifact description outlines the complete workflow from the raw input data to the final visualization of the output.

ACKNOWLEDGEMENTS



www.geophysik.uni-muenchen.de/Members/gabriel

Follow me on twitter [@inSeismoland](https://twitter.com/inSeismoland)

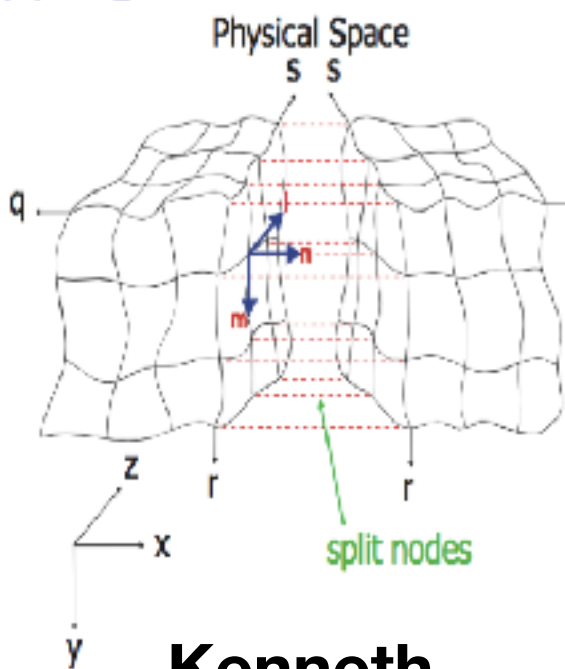
The earthquake source physics team at LMU:



Duo Li



Bo Li



Kenneth Duru
(now at ANU)



Betsy Madden
(now at University of Brasilia)



Stephanie Wollherr
(now graduated)



Thomas Ulrich



Sebastian Anger

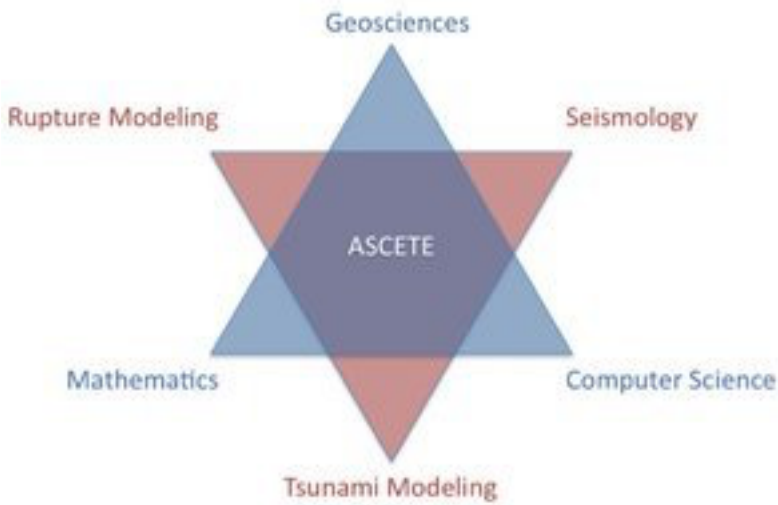


Taufiqurrahman



Aniko Wirp

Current projects:



Collaborators:



CHARLES UNIVERSITY



CoCoReCS
BAIES



Competitive Research Funds